Mediators of pre-mRNA splicing regulate sister chromatid cohesion in mammalian cells

Sriramkumar Sundaramoorthy

University College London

and

Cancer Research UK London Research Institute

PhD Supervisor: Dr. Mark Petronczki

A thesis submitted for the degree of

Doctor of Philosophy

University College London

January 2014

Declaration

I Sriramkumar Sundaramoorthy confirm that the work presented in this thesis is my own. Where information has been derived from other sources, I confirm that this has been indicated in the thesis.

Abstract

The ‘endless forms most beautiful’ that populate our planet rely on the process of cell division to ensure equal segregation of the cellular content including the DNA to the two daughter cells. The accurate segregation of chromosomes in eukaryotes relies on connection between replicated sister chromatids, a phenomenon known as sister chromatid cohesion. Sister chromatid cohesion is mediated by a conserved ring-like protein complex known as cohesin. Defects in this process can promote aneuploidy and contribute to meiotic segregation errors with adverse consequences for developing embryos. Despite numerous advances into understanding cell division at the molecular level, we still lack a comprehensive list of the participating proteins and complexes. The aim of this thesis was to use available functional genomic and proteomic data to identify novel regulators of mitosis in human cells. Using an RNAi approach, we identified a set of factors involved in pre-mRNA splicing whose depletion prevents successful cell division. Loss of these splicing factors leads to a failure in chromosome alignment and to a protracted mitotic arrest that is dependent on the spindle assembly checkpoint. This mitotic phenotype was accompanied by a dramatic loss of sister chromatid cohesion that we could show happens as soon as DNA replication. While depletion of pre-mRNA splicing mediators had no effect on cohesin loading onto chromatin, it prevented the stable association of cohesin with chromatin. Immunoblotting revealed that the depletion of splicing factors caused a 5-fold reduction in the protein levels of Sororin, a protein required for stable association of cohesin with chromatin in post-replicative cells. Further analysis suggests erroneous splicing of Sororin pre-mRNA upon depletion of splicing factors. Importantly, the sister chromatid cohesion loss caused by depletion of splicing factors could be suppressed by a Sororin transgene that lacks introns. Our results suggest that that pre-mRNA splicing of Sororin is a rate-limiting step in the maintenance of sister chromatid cohesion in human cells. Our work reveals that a primary cellular pathology of compromised pre-mRNA splicing is a mitotic arrest accompanied by split sister chromatids. Our work linking splicing and sister chromatid cohesion has implications for the pathology of Chronic Lymphocytic Leukemia (CLL). One of the splicing factors that we implicate in sister chromatid cohesion is SF3B1, whose gene is one of the most frequently mutated genetic drivers found in CLL patients.

Acknowledgement

At the outset, I would like to thank my supervisor Mark Petronczki for providing me not just with an opportunity to work with him but also to share his knowledge and experience about working in cell biology. I am deeply grateful to Mark for having taught me the importance of both doing science with integrity and passion while equally importantly being able to present your ideas and work in as lucid a form as possible. I would also like to thank him for instilling in me the importance for any experiment either in the lab or in life in general to have controls.

I am thankful to the people in the Cell Division and Aneuploidy (CDA) lab for all their help and guidance over the years. It was a privilege to be surrounded by people smarter than myself so that I could learn as much as I have. I would like to thank Lola for being a great sounding board for all my ideas about science, theology, politics etc. and also for all her help with the many experiments. I would like to thank Sergey 'Tovarich' Lekomtsev for introducing me to the dark room 4 years ago and less importantly for helping me with my screen and for all the help over the past 4 years. I am grateful to Kuan-Chung for his thoughts about experiments, science, life and his 'inspiring views' about life and the food in London. Thanks go out to Tohru for his great guidance and for having had to endure my umpteen questions when I started out in the lab. I would also like to thank Laurent for being a brilliant 'lab elder brother', pointing out when I was doing wrong to make me a better researcher but also being among the first to compliment me on my rare good days. Special thanks go to Kristyna for all her help in and out of the lab over the past couple of years and for sharing all the wonderful stories about the 398 buses. I would also like to thank Murielle for her constant encouragement, help with experiments and for all the rides to Potters Bar.

I am thankful to Peter Parker and Mike Howell for spending time away from their busy schedule on my thesis committee providing their valuable guidance and suggestions at every stage of my PhD at the LRI. Special thanks go to Mike and the members of the High Throughput Screening lab for their help in performing my screen

I am also indebted to all the people in Clare hall for making it a wonderful place to work in. Special thanks go to Marco for his help with the RT-PCR experiments, Nicola and Katharina for their help and guidance when I was starting out at Clare Hall. I am also grateful to the research administrators and assistants both at Clare hall and Lincoln's inn fields for their excellent help in terms of my umpteen requests for visas, letters and accommodation etc. Without their help, the PhD would have easily been a much more arduous experience.

I would also like to thank my friends and family for their steadfast support not just through my PhD years but also throughout my life.

I am thankful to the Breast Cancer Campaign for providing me with a PhD grant for the duration of my PhD and for the special opportunity to visit the British houses of Parliament.

Finally, I would like to thank Prof. Richard Dawkins for having fostered in me a sense of curiosity and wonder about the natural world and for instilling in me the perseverance to question dogmas and blind faith.

Table of Contents

Table of figures

List of tables

Abbreviations

AB	Antibody
AcGFP	*Aequora coerulesc*ens GFP
AIM-1	Aurora and Ipl1-like midbody-associated protein
APC/C	Anaphase promoting complex
ARL5A	ADP ribosylation factor like 5A
ATP	Adenosine triphosphate
Cdc	Cell division cycle
CDC5L	Cell division cycle 5 like
CDK	Cyclin dependent kinase
CdLS	Cornelia de Lange syndrome
CEP55	Centrosomal protein 55
CHMP	Charged multivesicular body proteins
CKI	Cdk inhibitor
CPC	Chromosome passenger complex
DNA	Deoxyribonucleic acid
dNTP	Deoxyribonucleotide triphosphate
ER	Endoplasmic reticulum
ECT2	Epithelial cell transforming sequence 2
ESE	Exonic splicing enhancers
ESS	Exonic splicing silencers
FRAP	Fluorescence recovery after photobleaching
FRET	Förster resonant energy transfer
GFP	Green fluorescence protein
hnRNP	Heterogeneous nuclear small nuclear ribonuclear proteins
iFRAP	Inverse fluorescence recovery after photo bleaching
INCENP	Inner centromere protein
ISE	Intronic splicing enhancers
ISS	Intronic splicing silencers
MFAP1	Microfibrillar associated protein 1
mRNA	Messenger RNA
NBD	Nucleotide binding domain
NHP2L1	Non histone chromosome protein 2-like protein 1
PLK1	Polo-like kinase 1
PPT	Polypyrimidine tract
Pre-mRNA	Precursor mRNA
RAD21	Radiation sensitive 21

RhoA	Ras homolog family member A
RNA	Ribonucleic acid
RNAi	RNA interference
S	Serine
SAC	Spindle assembly checkpoint
SART1	Squamous cell carcinoma antigen recognized by T cells
SCC	Sister chromatid cohesion
SCC1	Sister chromatid cohesion 1
SCF	Skp, Cullin, F-box containing complex
SDS	Sodium Dodecyl Sulfate
siRNA	Small interfering RNA
SMC	Structural maintenance of chromosomes
snRNA	Small nuclear RNA
snRNP	Small nucleotide ribonucleic particles
SSC	Saline-sodium citrate
T	Threonine
TTC19	Tetratricopeptide repeat domain 19
WB	Western blot
WT	Wild Type
Y	Tyrosine

Chapter 1. Introduction

All living organisms, irrespective of their status in evolution, consist of the same elementary unit; the cell. In 1858, espousing Theodore Schwann and Mathias Schleiden's views on life, Rudolph Virchow is famous to have declared, 'Omnis cellula e cellula' or that all cells arise from pre-existing cells (Tan and Brown, 2006). Over 150 years later, we are still unsure about many of the molecular mechanisms that allow a cell to dutifully duplicate itself. Organisms, no matter the number of cells they possess, arise from a single cell that undergoes repeated cycles of cell division during which the genetic material is accurately partitioned into the two daughter cells. Defects in cell division therefore have adverse consequences not just for the cell but also for the organism as a whole. Deciphering the intriguing mechanisms that underpin cell division is important not only for decrypting one of the many mysteries of the cell but also for developing therapeutic tools to combat cancer.

1.1 The cell cycle

The cell reproduces by firstly duplicating its contents and then by redrawing its boundaries. In the process, it passes though a carefully regulated cycle of events called the cell cycle. This process of duplication of cellular content followed by division must be carried out with an extraordinary amount of precision, which is why a number of checks and balances exist along a cell's journey to divide itself.

1.1.1 Cell cycle phases and checkpoints

The cell cycle in eukaryotes consists of two morphologically distinct phases: Interphase and M phase (Figure 1). Interphase in turn is made up of three sub phases; the first gap phase (G_1-phase), synthesis phase (S-phase), and second gap phase (G_2-phase). The length of the different phases while tightly controlled, can be varied by a number of internal and external stimuli. Interphase, seemingly a period of stupor for the cells is actually a period of intense activity wherein the cell readies itself for division by duplicating its genetic material (DNA replication) and various cellular organelles. In G_1-phase, cells restart among others, the transcription, translation and transport machinery that had been shut off during the preceding mitosis. Having laid the ground work to duplicate itself in the subsequent

phases, cells pass through a restriction point that provides a binary decision system based on an assessment of whether the cells are ready to pass through to the next stage or if they need to pause in the cell cycle. In case conditions are unfavourable for the cell to progress through, it either pauses in G_1-phase or it enters a prolonged quiescent phase termed G_0-phase. Under favourable conditions, cells initiate S-phase during which the genomic DNA is replicated (Masai et al., 2010). This process is initiated at specific locations within chromosomes termed the origins of replication. At these sites, the DNA double helix is opened up to accommodate a number of accessory proteins and enzymes that lead to DNA synthesis in a bidirectional and semi conservative manner (Masai et al., 2010). As soon as the DNA is replicated, the 'sister' DNA molecules are held in place together through a tight linkage termed cohesion (Nasmyth and Haering, 2009). This cohesion is vital for the cell division process and will be discussed in more detail later.

After having duplicated the DNA and the various cellular organelles in S-phase and the subsequent G_2-phase, cells enter mitotic phase or M phase. M phase of the cell cycle is visually more dynamic with the cell undergoing rapid changes in morphology over a relatively short period of time (Flemming, 1882). Through a series of choreographed steps, the cell first condenses the DNA to form the chromosomes following which the cell segregates them to opposite ends. The physical force required for the above essential process is provided by one of the cytoskeletal components of the cell; the microtubules. These polymers of the tubulin protein, help by attaching to the kinetochores that link the sister chromatids of the chromosomes and begin to pull them to opposite poles. A counteracting force is exerted by the cohesion machinery, which is the linkage between the sister chromatids. This tug of war results in tension that is sensed by the cells. When and only when tension is detected across all the chromosomes, a number of signalling cascades fire up within the cell, one of which serves to sever the cohesion between the sister chromatids that leads to the segregation of the DNA towards the opposite poles (Musacchio and Salmon, 2007) (Figure 4).

The other organelles in the cell such as the centrosome, the ER, the Golgi etc would now have segregated through distinct mechanisms (Lowe and Barr, 2007). Subsequently, the cell undergoes a series of morphological changes in between

the separated chromosomal masses that results in the division of the cell. This process is referred to as cytokinesis and completes cell division. The story ends differently depending on the cell type but in essence, a barrier is brought in between the two nascent cells and the cell is said to have divided into its two daughter cells (Barr and Gruneberg, 2007, Green et al., 2012).

Progression through the cell cycle is controlled by a series of checkpoints (Figure 1). The first of these checkpoints that the cell encounters is the G1/S checkpoint or Start. The presence of favourable conditions activates G1/S and S phase cyclins (See section 1.1.2) resulting amongst other events in the phosphorylation of proteins that are required for initiating DNA replication.

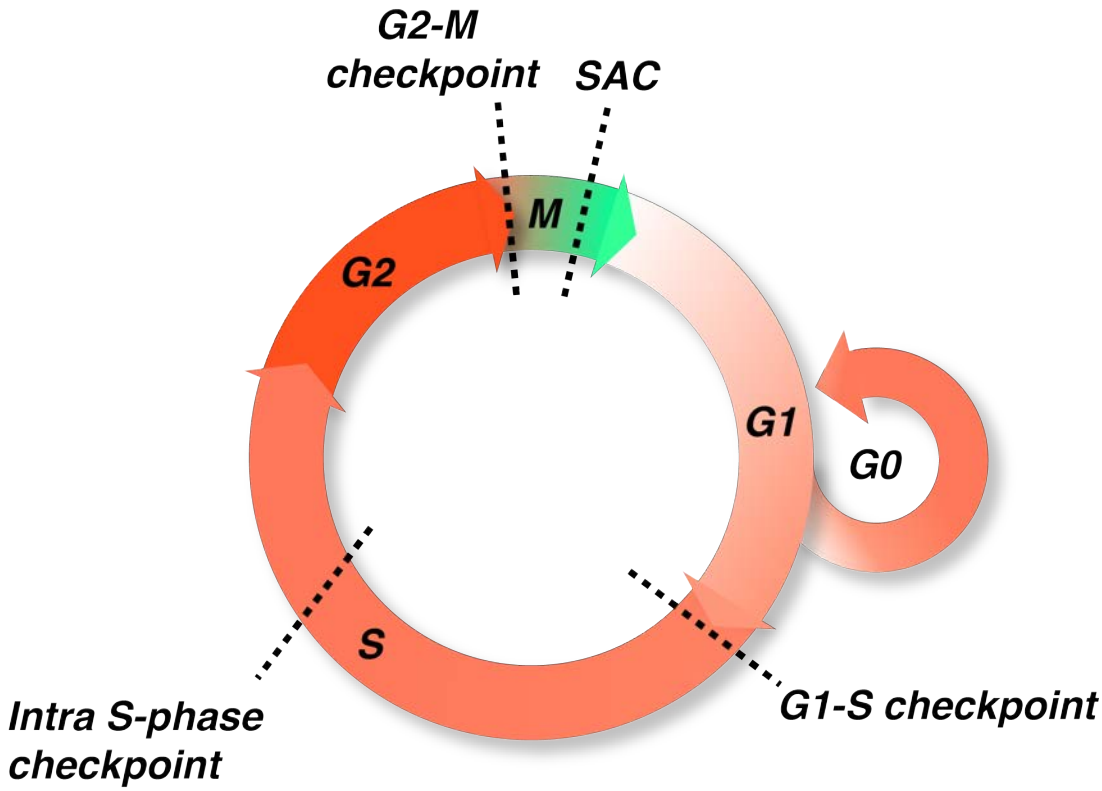

Figure 1 The eukaryotic cell cycle

The eukaryotic cell cycle is divided into distinct phases that include interphase (made up of G_1, S and G_2-phases, shown in increasing intensities of Red) and M phase or mitotic phase. Within the cell cycle, cells face a number of regulatory hurdles or checkpoints that ensure a successful passage of the cell through the cell cycle. These checkpoints include the G1-S checkpoint that monitors cell growth and growth signals, the intra-S phase checkpoint that monitors DNA replication, the G2-M checkpoint that monitors completion of DNA replication and repair processes and the Spindle assembly checkpoint (SAC) in mitosis that monitors the error free attachment of kinetochores to microtubules. (Adapted from: The cell cycle: Principles of control by David Morgan).

A different checkpoint exists within S phase that ensures that the DNA replication is error free. This checkpoint can also sense damage to the DNA and can regulate the replication fork progression in response to damage (Gottifredi and Prives, 2005, Jones and Petermann, 2012). In addition to this, DNA damage sensing checkpoints exist between the G1/S and the G2/M transitions to assess if there have been any damage inflicted upon the DNA and if so, the checkpoint pauses the cell cycle to allow the cells time to repair the damage. This checkpoint is crucial to avoid transmission of damaged DNA to daughter cells during mitosis leading to genomic instability (Harrison and Haber, 2006) Additionally, the transition from G2 phase into mitosis is also carefully monitored. Cyclin B-Cdk1 (M phase cyclins), phosphorylate key proteins thereby regulating the irreversible entry into mitosis. The cell encounters yet another checkpoint during the metaphase to anaphase transition in mitosis. This checkpoint, also known as the spindle assembly checkpoint (SAC), ensures that cells are allowed to segregate their chromosomes and exit mitosis if and only if they have achieved bi-orientation or the stable engagement of both the kinetochores of every one of their chromosomes with either of the two spindle poles. Unattached kinetochores can send out a signal that can delay the segregation of chromosomes until bi-orientation is achieved across the board. Upon satisfying the SAC, the anaphase promoting complex or cyclosome (APC/C), which initiates the destruction of cyclins and the cleavage of the cohesin ring that holds the sister chromatids together, triggers chromosome segregation and anaphase onset. The SAC is important because it helps trigger a synchronized splitting of sister chromatids globally within the cell in an irreversible manner. Concurrently, the destruction of the cyclins along with the activity of phosphatases leads to the inactivation of CDKs and the dephosphorylation of CDK substrates. This in turn causes leads to the completion of mitosis (mitotic exit) and sets the stage for cytokinesis.

1.1.2 Regulation of the cell cycle

Considering that fact that the fate of the organism as a whole depends of repeated rounds of cell division happening accurately and at a precise time, a number of regulatory mechanisms have evolved to control progression through different stages of the cell cycle. Failure to follow this pattern of regulated cell growth and division could have disastrous consequences for the stability of the genome and

the overall viability or fitness of the organism. A number of regulatory pathways in the cell cycle function through checkpoints which are one way transitioning sentries along the cell cycle that act as decision points for the cell to proceed to the next phase provided it has passed through the preceding phase successfully (Hartwell and Weinert, 1989).

Cellular factors that help the cells in traversing between the different stages of the cell cycle had been postulated a long time ago. Using cell hybrid experiments, it was demonstrated that fusing a cell in S-phase with another in G_1-phase induced DNA replication in the fusion. It was also shown that fusing a G_1 cell with one that was in G_2-phase (about to enter mitosis), prevented mitotic entry (Rao and Johnson, 1970). These experiments suggested the existence of physical entities or factors that when transferred from one cell to another could influence cell cycle progression in the latter. In 1971, Yasuo Masui and Clement Markert identified Maturation Promoting Factor (MPF Aka Mitosis Promoting Factor) that in frog oocytes induced meiosis even in the presence of protein synthesis inhibitors (Masui and Markert, 1971). It was further demonstrated that MPF oscillated through the cell cycle suggesting that it might be linked to a cell cycle clock within the cell (Masui, 1982). Following this, MPF was shown not only to initiate mitosis in other eukaryotes and but also to have an enzymatic activity and that this enzymatic activity was sufficient to induce mitosis (Gerhart et al., 1984). In 1983, Tim Hunt, while studying protein synthesis in post fertilized frog oocytes, discovered that although several proteins accumulated after fertilization of the oocyte, one of them disappeared abruptly at the time of cell division. Upon correlating with the cell cycle phase, it was shown that the disappearance of the protein occurred at mitosis. The protein was named Cyclin after its cyclical pattern of appearance and disappearance in the oocytes (It was named Cyclin ostensibly after the favourite hobby of the head of the study at that time; cycling) (Evans et al., 1983). The existence of cyclins in multiple species was then demonstrated amid the observation that addition of cyclins to mitotic extracts led to its disappearance in a short span of time implying its degradation through proteolysis. This discovery coupled with the finding that the activation of MPF required synthesis of new proteins raised the interesting possibility that cyclins were probably linked to MPF. After a number of discoveries over the years including the Cyclin Dependent

Kinase 1 (*cdk1* or *cdc2*) in fission yeast (Nurse, 1990) and its regulation in higher eukaryotes (Morgan, 1995, Bloom and Cross, 2007), it has now been established that indeed cyclins form a complex with cyclin dependent kinase to form MPF, to define specific stages in the cell cycle. It was also discovered that even though CDK protein levels remained constant through the cell cycle, its activation required association with its partner, Cyclin, whose levels fluctuated through the cell cycle. In a testament to the indispensable requirement and evolutionary conservation of CDKs, replacing the *S. cerevisiae CDC2* kinase, a key regulator of mitosis, with its human counterpart remarkably supported cell viability and growth (Lee and Nurse, 1987). As their name indicates, CDKs are a family of catalytic serine threonine kinase proteins that require association with cyclins, the regulatory subunit of the complex to be functional. The binding of cyclins induces a conformational change in the kinase that allows it to bind to ATP and a substrate to catalyse the transfer of the γ phosphate to the target serine or threonine residue on the substrate.

In budding and fission yeast, there is only one critical cell cycle CDK protein and binding to a diverse range of cyclins generates specificity for each cell cycle phase. Different cyclin proteins dominate at different phases of the cell cycle and are thought to be crucial for specifying target specificity for CDK based phosphorylation (Ubersax et al., 2003, Loog and Morgan, 2005, Jeffrey et al., 1995, Kitagawa et al., 1996).

In higher eukaryotes, cells contain a range of cyclin-CDK complexes that regulate distinct stages of the cell cycle.

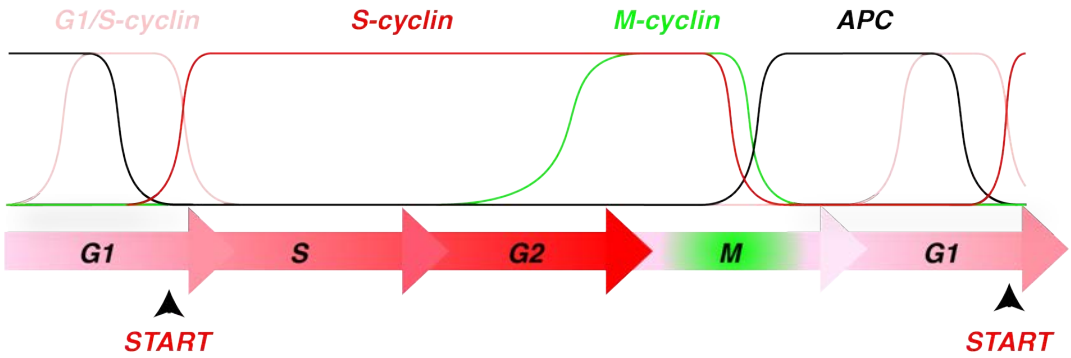

Figure 2 Major transition events of the cell cycle and the cyclins that mediate them

A schematic diagram depicting the major classes of cyclins in the vertebrate cell cycle and their abundance. Also shown is the activity level of the anaphase promoting complex or cyclosome (APC/C) that targets proteins for proteolytic degradation

inducing irreversible cell cycle transitions. (Adapted from: The cell cycle: Principles of control by David Morgan)

Firstly, the G_1-phase cyclins (cyclin D1, D2 and D3 in vertebrates), in association with CDKs (CDK4 and CDK6 in vertebrates) coordinates extracellular factors and cell growth with entry into the cell cycle. The levels of these cyclins rise in response to cell growth and other extracellular growth signals. G_1/S Cyclins (cyclin E1 and E2 in vertebrates) on the other hand, accumulate in G_1-phase and drop precipitously during entry into S-phase. The START or the restriction point is a checkpoint and is a point of no return in the transition from the G_1-S-phase. The restriction point in mammalian cells is regulated by the Rb pathway, so named because mutations in the primary effector of the pathway, pRb (retinoblastoma protein) led to the retinoblastoma (Weinberg, 1995). The primary function of the G_1/S cyclins seem to be to overcome the restriction point and initiate the programme for entry into S-phase. These cyclins form complexes with CDK proteins (CDK2 in vertebrates). Cyclin D-CDK4/6 and Cyclin E-CDK2 together phosphorylate and inactivate the pRB pathway thereby activating E2F to allow transcription of its target genes and promote G_1/S transition. Chief among these targets include DNA replication factors, proteins required in the nucleotide synthesis pathways among others (Tanaka and Araki, 2010, Talluri and Dick, 2012).

S-phase cyclins (cyclin A1 and A2 in vertebrates) also accumulate along with G_1/S cyclins and complex with CDK1 and CDK2 in vertebrates. Even though these cyclins are produced in G_1-phase, they remain inactive because of inhibitory binding to Sic1 protein in yeast (Schneider et al., 1996) and to proteins of the CIP/KIP family namely p21 and p27 in mammals (Nakayama and Nakayama, 1998). Activation of G_1/S cyclins leads to the phosphorylation of these inhibitors that eventually leads to their ubiquitylation and degradation by the SCF (Skp, Cullin & F box containing complex) pathway (Verma et al., 1997, Koivomagi et al., 2011). This results in the activation of the S-phase cyclins that in turn switch on the DNA replication machinery. The levels of these cyclins remain high in S-phase through to mitosis.

M-phase cyclins (cyclin B in vertebrates) form complexes with CDK1 in all eukaryotes. Their levels rise in G_2 phase, but the activity of these complexes are

suppressed by both inhibitory phosphorylations on CDK1 and also through binding to CDK inhibitors (CKIs) (Harper et al., 1993). The M-phase cyclins peak at metaphase and preside over the dramatic scheme of events during mitosis. Once bi-orientation of all chromosomes is complete, the mitotic cyclins are targeted for proteolytic degradation by the APC/C.

1.1.3 Mitosis in mammalian cells

The mitotic phase of the cell cycle albeit smaller in duration, is visually much more dramatic than the interphase. In the late 1880s, Wilhelm Waldeyer introduced the term chromosome to 19th century cytologists (Zacharias, 2001). About 10 years earlier, Walther Flemming, the father of cytogenetics, was studying cell division in cells derived from the fins and gills of salamanders. He observed the process of cell division and made detailed sketches of the process. He named the nuclear material that was being distributed between the two daughter cells, chromatin (Greek for coloured substance) and he called the process of division, Mitosis (Mito being Greek for threads) (Flemming, 1882, Mitchison and Salmon, 2001). Mitosis, the process of cellular division, has been studied extensively over the past 100 years or so and can be divided into distinct stages that differ dramatically in cellular morphology.

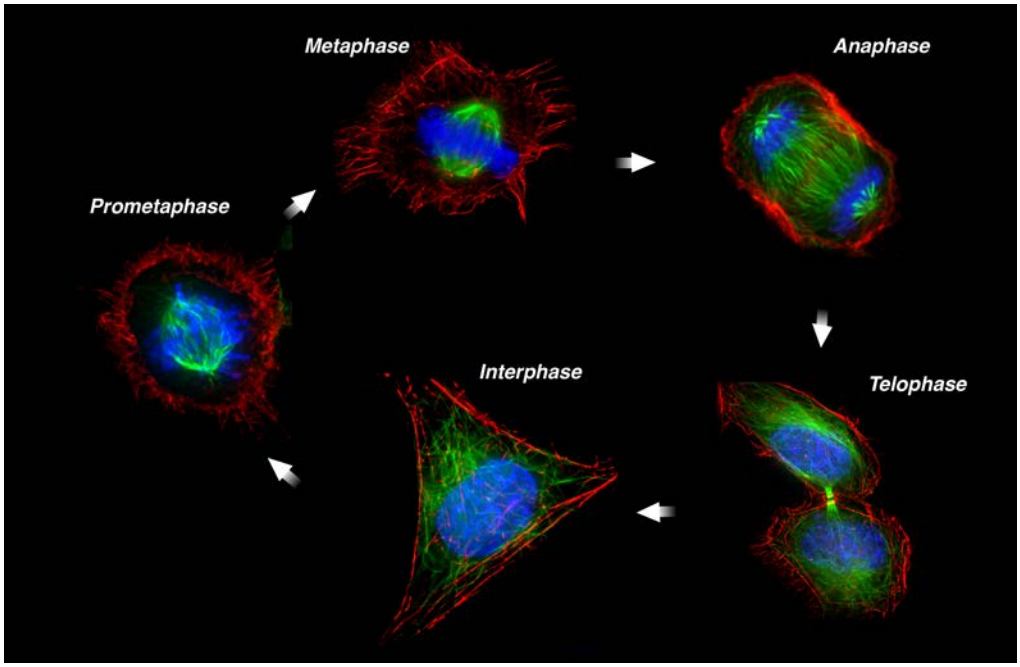

Figure 3 Mitotic phases in a mammalian cell

Images of HeLa cells depicting the various stages of mitosis in animal cells with tubulin stained in green, the actin cytoskeleton in red and the DNA (DAPI) in blue. Cells enter mitosis with a replicated pairs of sister DNA molecules and cellular contents. As cells enter prophase and prometaphase, the nuclear envelope breaks down and the mitotic spindle starts attaching to the chromosome through their kinetochores. Attachment of the kinetochores of all the chromosomes in the cell leads to their plate-like arrangement in the equator of the cell in metaphase. Upon satisfying the SAC, cells transit from metaphase to anaphase wherein the sister chromatids separate by being pulled towards opposite poles. Subsequently, a plasma membrane driven cleavage furrow forms and ingresses in the middle of the cell to cleave the cell into two daughter cells.

The different stages of mitosis in mammalian cells are outlined in Figure 3 and will be discussed in detail below. Upon entry into mitosis, cells pass through prophase. In this phase, the nucleus, which contains the replicated DNA, undergoes an extensive process of condensation (Hirano and Mitchison, 1994). Concurrently, the centrosomes, the microtubule organizing centres of the cells, begin to disengage and migrate towards the opposite ends of the cell to form the spindle poles and setup the mitotic spindle (Rusan et al., 2001, Tanenbaum and Medema, 2010). At the end of prophase and towards the beginning of prometaphase, the nuclear envelope breaks down and the kinetochores of the chromosomes begin to attach themselves to the microtubules that are emanating from the spindle poles (Cheeseman and Desai, 2008). Both the copies of the replicated chromosomes, called sister chromatids, are held together by the cohesin ring complex (Nasmyth and Haering, 2009) (See section 1.2)

The attachment of the pair of kinetochores on each chromosome to microtubules from the opposites poles attempts to pull the sister chromatids apart and this force is resisted by a phenomenon called sister chromatid cohesion (Nasmyth and Haering, 2009, Peters and Nishiyama, 2012). This opposition of the forces exerted by the microtubules is critical for successful segregation of chromosome to the two daughter cells. During metaphase, the force exerted by the microtubules aligns the chromosome at the equator of the cell and leads to tension at the kinetochores. Lack of tension at the kinetochores and unattached kinetochores contribute to the engagement of the SAC (Figure 4). The SAC subsequently inhibits the activity of the APC/C to prevent mitotic progression. Once all chromosomes have achieved bi-orientation, the SAC components dissociate away from the kinetochores and the SAC is turned off. The cell is now ready to perform nuclear division. This is set in

motion by the activity of the APC/C. The APC/C being an E3 ubiquitin ligase, mediates the ubiquitylation and the proteasome mediated destruction of a number of critical substrates in the cell including cyclin and securin leading to anaphase onset and exit from mitosis (Pines, 2011).

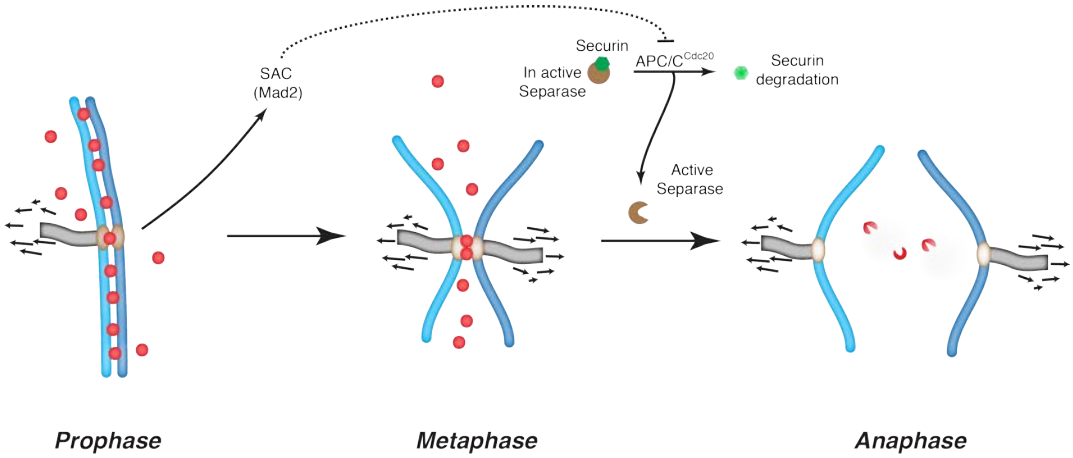

Figure 4 Sister chromatid cohesion and chromosome segregation in vertebrates

A successful segregation of sister chromatids to opposite poles requires concerted action of a number of players. The cohesin ring holds the sister chromatid together from DNA replication until they are ready to separate in anaphase. Cohesin is present both at the centromere and along the arms of the chromosomes and its removal of happens in two waves. In the first step, during prophase, the bulk of cohesin is removed from the arms while centromeric cohesion is retained until anaphase. The kinetochores of each sister chromatid has to be attached to microtubules from opposite spindle poles for them to be segregated. The presence of unattached kinetochores triggers the spindle assembly checkpoint (SAC) that prevents the onset of anaphase by inhibiting APC/C. Upon acheivement of 'bi-orientation', the SAC is turned off and the APC/C is activated. APC/C causes the degradation of securin, which liberates separase. The activated separase being a protease can cleaves the Scc1 subunit of cohesin at the centromeres and triggers the segregation of sister chromatids towards opposite poles. (Adapted from (Petronczki et al., 2003))

Securin is an inhibitor of the protease separase (Funabiki et al., 1996, Ciosk et al., 1998). Upon removal of securin, separase is activated and it catalyses the cleavage of the SCC1 subunit of the cohesin ring, allowing the sister chromatids to be pulled away towards the spindle poles (Uhlmann et al., 1999, Peters and Nishiyama, 2012). In the early stages of anaphase, also known as anaphase A, the sister chromatids are pulled towards the spindle poles by the rapid shortening of the microtubules attached to the kinetochores. In the second stage of anaphase, anaphase B, the mitotic spindle elongates by increasing the pole-to-pole distance and this ensures the segregation of the chromosomes away from the equator of the

cell. Simultaneously, the cell prepares to physically cleave the mother cell into two daughter cells. In animal cells, the mitotic spindle, including the spindle midzone and the astral microtubules, specifies the site of cytoplasmic division ensuring tight coordination between nuclear and cytoplasmic division. A subset of spindle pole derived microtubules different from the kinetochore microtubules, overlap at the equator of the cell. Further bundling and crosslinking of these microtubules by a number of microtubule binding and bundling proteins leads to the formation of the tightly bundled microtubule rich structure called the central spindle or the spindle midzone (Glotzer, 2005, Glotzer, 2009). The central spindle acts as the scaffold for a number of signalling proteins including kinases, structural proteins, regulators of RhoA GTPase and other proteins that are required to orchestrate the process of cytokinesis. In the final stage of mitosis, called telophase, the nuclear envelope begins to reform around the segregated DNA masses. The cell physically divides by initially forming membrane invaginations called cleavage furrows brought about by a contractile ring made of actin and myosin (Green et al., 2012, Balasubramanian et al., 2012). The ingression of the cleavage furrow proceeds until a dense remnant of the central spindle called the midbody remains at the narrow cytoplasmic bridge between the two daughter cells. The final severing of the connection between the two daughter cells happens a little while after telophase and involves the recruitment of microtubule severing proteins, membrane vesicles and membrane sculpting proteins around the midbody in a process called abscission (Guizetti and Gerlich, 2010).

1.1.4 Multiple supervisory mechanisms regulate mitosis

The successful execution of mitosis involves the accurate segregation and transmission of the genetic material to the daughter cells and the precise division of the cytoplasm into the two daughter cells. Strict regulatory mechanisms are in place to ensure that these processes occur at the right place and at the right time. The bulk of the regulatory mechanisms rely on modifications of the proteins involved in executing the processes. These modifications include a number of posttranslational processes such as phosphorylation by mitotic kinases such as Cdk1, Aurora Kinases and Polo-like kinase1, dephosphorylation of the substrates of these kinases by a variety of phosphatases and also other mechanisms like ubiquitin mediated proteolysis of specific targets. The phosphorylation and

dephosphorylation of specific targets provides the cell with a method to rapidly activate and deactivate a specific process or pathway during mitosis. Ubiquitin-mediated proteolysis of substrates on the other hand gives directionality to the cells by providing an irreversible pathway towards mitotic exit. These regulatory mechanisms and their role in mediating specific aspects of mitosis will be discussed below.

1.1.4.1 Phosphorylation and dephosphorylation based regulation of mitosis

Multiple kinases and phosphatases carry out the posttranslational modification or adding or removing a phosphate group to specific residues on the substrate. Given the key role of cell proliferation in cancer, mitotic kinases are a promising cancer target and inhibitors against these kinases are in various stages of development (Perez de Castro et al., 2008). Chief among these kinases involved in regulating mitosis in mammalian cells are Cyclin dependent kinase 1, Aurora kinases family and Polo-like kinase 1 (PLK1) and they will be discussed further

CDK1

CDK1, controls entry into mitosis by targeted phosphorylation of a number of substrates. Phosphorylation by Cdk1-cyclin B complex is known to be required for a number of cellular changes during mitosis including but not limited to cell rounding, nuclear envelope breakdown, chromatin condensation, formation of bipolar spindle, dispersal of organelles etc. The levels of Cyclin B1, the principle mitotic Cyclin in vertebrates, rises through G_2-phase and M-phase (Gavet and Pines, 2010) and associates with Cdk1 thenceforth. These complexes have an intricate localization pattern. Upon the formation of these complexes, they remain in the cytoplasm and show a marginal localization to the centrosomes in early prophase and remain there until late prophase, when they are abruptly translocated to the nucleus where it is involved in nuclear envelope breakdown. After the disintegration of the nuclear envelope however, Cyclin B-Cdk1 localizes to the cytoplasm. In spite of the fact that these complexes are present in G_2-phase, they are kept inactive by the inhibitory phosphorylation on T14 and Y15 residues of Cdk1 by two kinases of the Wee1 related kinase family, *wee1* and *myt1*(Piwnica-Worms et al., 1991, McGowan and Russell, 1993, Mueller et al., 1995). *myt1* is the key inhibitory kinase as it can phosphorylate both T14 and Y15 whereas *wee1* can

only phosphorylate Y15. In addition to the inhibitory phosphorylation of Cdk1, Myt1 binds to Cyclin B and prevents its translocation into the nucleus thereby preventing its activity in two different ways (Liu et al., 1999, Wells et al., 1999). At the beginning of mitosis, the phosphatase Cdc25 is activated by Cyclin B-Cdk1 whereby it removes the inhibitory phosphorylations (T14 and Y15) resulting in a feedback loop of Cyclin B-Cdk1 activation that in turn leads to a hyper phosphorylation of *wee1* and *myt1* inactivating these kinases (Watanabe et al., 1995, Nakajima et al., 2003). The combined action of these phosphorylation and dephosphorylation snowballs into a rapid increase in active CyclinB-Cdk1 complexes during prophase. In mammalian cells, three variants of CDC25 namely CDC25A, CDC25B and CDC25C exist and they are all implicated in the activation of Cyclin B-CDK1. CDC25B is the first to be activated. Its levels increase at late S phase and remains high until prometaphase. CDC25B is thought to be involved in the initial activation of Cyclin B-CDK1 when the latter is still at the centrosomes and excluded form the nucleus (Lammer et al., 1998, De Souza et al., 2000). CDC25A and CDC25C are relatively inactive in G_2-phase and gain activity in prophase. CDC25A levels increase in prophase due to drop in the rate of its degradation. While CDC25C levels remain constant throughout the cell cycle, the proportion of active CDC25C increases dramatically in prophase. Activation of CDC25A and CDC25C lead to a further activation of Cyclin B-CDK1 to the levels that are sufficient to drive the cell into mitosis (Izumi et al., 1992, Hoffmann et al., 1993, Strausfeld et al., 1994, Mailand et al., 2002). True to its status as a master regulator of mitosis, Cyclin B-Cdk1 phosphorylates a variety of effectors that each has roles in hundreds of pathways during mitosis (Holt et al., 2009, Dephoure et al., 2008). These include mitotic cell rounding (Matthews et al., 2012), nuclear envelope breakdown and reformation (Guttinger et al., 2009), mitotic spindle assembly (Nigg et al., 1996, Wheatley et al., 1997), segregation of organelles in the secretory pathway (Lowe et al., 1998, Preisinger and Barr, 2005) among others.

Recent observations indicate that for mitotic entry of cells and for the continued maintenance of the phosphorylated state of Cyclin B-CDK1 substrates, in addition to the activation of Cyclin B-CDK1, it is necessary to inhibit the activity of PP2A, the phosphatase that dephosphorylates CDK1 substrates. These reports demonstrated that during mitosis, PP2A activity is inhibited by ARPP19 and alpha-endosulfine,

proteins that are activated by a kinase called greatwall (Gharbi-Ayachi et al., 2010, Mochida et al., 2010)

Once the cell initiates chromosome segregation and the Cyclin B-CDK1 complex has achieved its objectives of phosphorylating and modulating the activity of its substrates, Cdk1 is inactivated by the proteolytic degradation of Cyclin B that is induced by the APC/C. The APC/C bound to its activator Cdc20, recognizes a D box domain (See section1.1.4.2) in cyclin B and targets it for ubiquitylation and subsequent degradation (Pines, 2011). However, in order to exit mitosis, it is not just sufficient that cells inactivate Cyclin B-CDK1, the many substrates of Cyclin B-CDK1 also have to be dephosphorylated for the rapid reversal of processes that aided in mitotic entry (Wurzenberger and Gerlich, 2011, Guttinger et al., 2009, Moser and Swedlow, 2011). Cytokinesis is one such process that requires the inactivation of Cdk1 and the dephosphorylation of its substrates (Niiya et al., 2005, Potapova et al., 2006).

The identity of the protein phosphatase that dephosphorylates the substrates of CDK1 in animal cells has not been fully elucidated. In budding yeast, it has been shown that the activity of a phosphatase called Cdc14 is essential for mitotic exit (Stegmeier and Amon, 2004). However, Cdc14 phosphatase activity was shown not to be essential for mitotic exit in *C.elegans* (Saito et al., 2004) and knockouts of Cdc14A and B in chicken and human cells had no effect on mitosis although a modest increase in sensitivity to DNA damage was demonstrated (Mocciaro et al., 2010). Evidence indicates that two phosphatases belonging to the phosphoprotein phosphatase (PPP) family of proteins could be the enzymes that dephosphorylate Cdk1 substrates. Evidence for PP1 to be a Cdk1 specific phosphatase comes from studies in multiple model organisms. In Drosophila cells, it was shown that mutations in one of the four PP1 genes lead to abnormalities in anaphase and errors in chromosome segregation (Axton et al., 1990). In frog egg extracts it was demonstrated that either immunodepletion or inhibition of PP1 resulted in reduced dephosphorylation of known Cdk1 substrates like Cdc27 (Wu et al., 2009). Additionally, it was shown in mice that increasing PP1 activity reduced Cdk1 phosphorylation of its substrates (Manchado et al., 2010). On the other hand, there is also evidence to suggest that the phosphatase responsible for dephosphorylating Cdk1 substrates in human cells is PP2A. *In-vitro* experiments revealed that

synthetic peptides that carried phosphorylated version of Cdk1 consensus sites were the preferred targets for PP2A mediated dephosphorylation (Agostinis et al., 1992). In addition, an siRNA screen based on time-lapse imaging in Hela cells revealed that depletion of PP2A and its regulatory subunit B55α led to delays in nuclear envelope reformation, chromosome decondensation, spindle disassembly and golgi reassembly, thus an overall delay in mitotic exit (Schmitz et al., 2010). In summary, PP1 and PP2A enzymes are likely to collaborate for the removal of CDK1 substrate phosphorylation during mitotic exit.

Polo like Kinase 1 (PLK1)

Apart from CDK1, PLK1 is a kinase that also plays critical roles in executing the process of mitosis. PLK1 is well conserved across eukaryotes and at least a single homolog of PLK1 is present in all eukaryotes. During early mitosis, PLK1 localizes to the centrosomes and the localization pattern switches to the kinetochores during the later stages of mitosis. In anaphase, PLK1 is seen to localize at the central spindle (Barr et al., 2004). The N terminus of PLK1 contains a kinase domain and the C terminus contains a polo box domain that is composed of a pair of polo box sequences called PB1 and PB2. The polo box domain is responsible for binding of PLK1 to specific substrates or structures and to localize to specific locations within the cell. The polo box domain has a higher affinity for proteins that are phosphorylated on a serine or threonine residue in the Polo box-binding region. Even though CDK1 is thought to usually provide the priming phosphorylation for these proteins (Elia et al., 2003), in late anaphase, a time when Cdk1 has been turned off, PLK1 has been shown to self-prime its targets (Neef et al., 2007, Burkard et al., 2009). Like CDK1, PLK1 mediated phosphorylation is important for a number of cellular processes during mitosis and loss of its function either through mutations or through the use of small molecule inhibitors leads to aberrant monopolar spindles and a potent mitotic arrest (Sunkel and Glover, 1988, Lenart et al., 2007). PLK1 is involved in mitotic entry (Qian et al., 1998), assembly of mitotic spindle (Sumara et al., 2004), maturation of the centrosomes (Lane and Nigg, 1996, Santamaria et al., 2007, Oshimori et al., 2006) dispersal of secretory organelles (Sutterlin et al., 2001, Barr, 2002), resolution of sister chromatid cohesion at chromosome arms in prophase (Sumara et al., 2002), control of cytokinesis (Bastos and Barr, 2010, Petronczki et al., 2007, Burkard et al., 2007, Brennan et al.,

2007) among other processes in the cell (Barr et al., 2004, Petronczki et al., 2008). The essential role of PLK1 in early mitotic events precluded the discovery of its critical function in cytokinesis until chemical genetic tools to inactivate PLK1 acutely and specifically at anaphase became available (Petronczki et al., 2007, Burkard et al., 2007, Brennan et al., 2007, Santamaria et al., 2007). Upon completion of mitosis, the KEN box domain in PLK1 is recognized by Cdh1, an activator of APC/C^{Cdh1} and PLK1 is targeted for ubiquitylation and proteolytic degradation in late mitosis and early G_1-phase (Lindon and Pines, 2004)

Aurora kinase

Another important group of kinases that regulate mitosis is the aurora family of kinases (Carmena et al., 2009, Carmena and Earnshaw, 2003, Ruchaud et al., 2007). In metazoans, three different members of this family exist namely Aurora A, Aurora B and Aurora C. Aurora C is found exclusively in mammalian germ cells and its functions are presently unknown. All members of the Aurora kinase family have a catalytic kinase domain and varying lengths of other non-catalytic domains. The levels of Aurora A and B increases in mitosis and it appears that activation loop phosphorylation of these kinases is required for their activity. Aurora A localizes to the centrosome in and to the mitotic spindle and it has been shown to be required for centrosome maturation and for the proper assembly of the mitotic spindle (Barr and Gergely, 2007, Glover et al., 1995, Marumoto et al., 2005). Aurora A is also known to be important for the activation of PLK1 by phosphorylation of its regulatory T loop (Macurek et al., 2008). This is reversed by the activity of the phosphotase PP6 (Zeng et al., 2010).

Aurora B on the other hand forms a complex with INCENP, Survivin and Borealin proteins, called the Chromosome Passenger Complex (CPC). Aurora B acts as the catalytic subunit of the CPC (Ruchaud et al., 2007). As cells enter mitosis, the CPC associates with chromatin and phosphorylates histone H3 at Ser10, a key mitotic marker. Additionally, the CPC through Aurora B, promotes the condensation of DNA, a process essential for mitosis by helping to recruit condensin, a protein complex that is known to be required for DNA condensation (Collette et al., 2011, Lipp et al., 2007). Additionally, the CPC is required for correcting erroneous microtubule-kinetochore interactions such as merotelic or syntelic attachments and is also required for proper functioning of the SAC (Cheeseman et al., 2002, Hauf et

al., 2003, Tanaka et al., 2002, Carmena et al., 2012). Although it was suggested that the localization of Aurora B to the centromeres of chromosomes in early mitosis was essential towards its function of preventing erroneous microtubule-kinetochore attachments (Cheeseman and Desai, 2008), recent evidence suggests that its centromeric localization may be dispensable (Campbell and Desai, 2013). During the later stages of mitosis, as the cell transits from metaphase to anaphase, the CPC shifts in its localization from centromeres to the spindle midzone (Ruchaud et al., 2007) where it forms a phosphorylation gradient (Fuller et al., 2008). This translocation is crucial for a number of reasons. Firstly, Aurora B acts a regulator of the cytokinesis (Adams et al., 2000, Hauf et al., 2003, Kaitna et al., 2000, Schumacher et al., 1998). Second, it ensures that the mitotic checkpoint components do not re-associate with kinetochores at anaphase onset (Vazquez-Novelle and Petronczki, 2010). Recent reports have also proposed a novel role for Aurora B in the 'Nocut' checkpoint whereby the process of abscission is delayed until the chromatin is cleared away (Norden et al., 2006, Mendoza et al., 2009). Aurora B was shown to phosphorylate and activate CHMP4C, a key inhibitor of the process of abscission (Steigemann et al., 2009, Carlton et al., 2012).

1.1.4.2 Regulation of mitotic exit by APC mediated proteolysis

As mentioned above, ubiquitin mediated proteolysis of substrates gives directionality to the cell cycle during mitosis by providing an irreversible pathway towards mitotic exit based on degradation of key targets (Potapova et al., 2006). This process is mediated by the anaphase promoting complex/cyclosome (APC/C) (Pines, 2011). The APC/C is an E3 ubiquitin ligase that targets proteins for degradation through ubiquitylation and subsequent proteolysis through the 26S proteasome. There are two distinct activators whose function confers specificity to the activity of the APC/C. These are Cdc20 and Cdh1. Cdc20 is active during the metaphase to anaphase transition whereas Cdh1 is not active until late mitosis and G_1-phase. The binding of APC/C to its activator Cdc20 requires phosphorylation of APC/C by Cdk1 and PLK1 (Shteinberg et al., 1999, Kramer et al., 2000, Golan et al., 2002, Kraft et al., 2003, Eytan et al., 2006). The APC/C^{Cdc20} targets proteins for degradation during the critical metaphase to anaphase transition to initiate mitotic exit. The activity of the APC/C^{Cdc20} is inhibited by the SAC (Musacchio and Salmon, 2007). Substrates of the APC/C^{Cdc20} possess amino acid motifs that are recognized

by Cdc20 and these are called destruction box motif (D box). The most important substrates of APC/C^{Cdc20} in mitosis are the cyclins and securin. The destruction of Cyclin A precedes the destruction of Cyclin B which happens only after the satisfaction of the SAC (Clute and Pines, 1999). APC/C^{Cdh1} on the other hand, does not require prior activation through phosphorylation in order to bind its effector Cdh1. However, Cdh1 is kept inactive by inhibitory phosphorylation by Cdk1 (Kotani et al., 1999, Kramer et al., 2000, Reber et al., 2006). The removal of Cdk1 activity at the metaphase to anaphase transition by APC/C^{Cdc20} activates Cdh1 by dephosphorylation of the inhibitory phosphorylation (Hagting et al., 2002, Kraft et al., 2005). Cdh1 therefore is active from late mitosis until early G1 phase and it binds to the APC/C to form the APC/C^{Cdh1} that is now free to bind its effectors through their KEN box domains and target them for destruction (Pfleger and Kirschner, 2000). The rise of the G1/S cyclins that are not subject to regulation by the APC/C causes the eventual phosphorylation of Cdh1 and the inactivation of the APC/C in yeast (Zachariae et al., 1998, Jaspersen et al., 1999) and in mammalian cells (Lukas et al., 1999). The once in cell cycle directionality provided by the specific degradation of substrates at the right time by the APC/C is instrumental for cells to undergo a successful mitotic exit.

1.2 Sister chromatid cohesion

One of the key requirements for the accurate and timely segregation of the duplicated chromosomes during mitosis is sister chromatid cohesion (Guacci et al., 1994). The pulling forces of the kinetochore microtubules at the centromeres of the chromosomes is counteracted by the linkage between the sister chromatids not just at the centromeres but also along the entire length of the chromosome. These counteracting forces lead to a stretching of the chromatids towards opposite poles and their alignment at the equator of the cell also known as ‘bi-orientation’ (Tanaka et al., 2000). Loss of cohesion between the sister chromatids at the metaphase to anaphase transition allows the kinetochore microtubules to pull the sister chromatids to opposite poles and complete mitosis successfully. Crucial to this process is the fact that the cohesion between the sister chromatids must remain effective until all the chromosomes have achieved bi-orientation. Defects in sister

chromatid cohesion can promote aneuploidy in cancer (Solomon et al., 2011) and are likely to contribute to meiotic segregation errors with deleterious consequences for embryos and fertility (Hunt and Hassold, 2010).

In addition to its indispensible role in cell division, Sister chromatid cohesion (SCC) plays a vital role in DNA double strand break repair. Double strand breaks can be repaired by an error prone non-homologous end joining mechanism or through an error free homologous recombination based mechanism (Chapman et al., 2012). Crucial for the homologous recombination repair process is the presence of the undamaged sister chromatid that can be used a template for homologous recombination and this is ensured by sister chromatid cohesion (Bannister et al., 2004, Xu et al., 2005, Ellermeier and Smith, 2005, Klein et al., 1999, Sonoda et al., 2001, Potts et al., 2006, Strom et al., 2004, Strom et al., 2007, Watrin and Peters, 2006).

Furthermore, mutations or deletions of genes involved in sister chromatid cohesion can lead to a number of congenital developmental disorders such as Cornelia de lange syndrome and Roberts syndrome (Mannini et al., 2010b, Mannini et al., 2010a).

1.2.1 Sister chromatid cohesion is mediated by a protein complex called cohesin

One of the first hypotheses regarding the interesting phenomena of sister chromatids being linked together until anaphase was that the physical concatenation between the sister chromatids was not resolved by topoisomerase enzymes until the chromosomes were bi-oriented. Also, it was suggested that bi-orientation followed by the complete deconcatenation of the sister chromatids triggered anaphase onset. Douglas Koshland and Leland Hartwell tested this idea in their seminal work in 1987. They introduced a circular plasmid DNA into *S. cerevisiae* cells and observed that under conditions that could preserve catenated DNA molecules but not protein-DNA interactions, cells that had passed through S phase could not hold the sister DNA molecules together arguing against DNA catenations being the primary factor holding the sister chromatids together. The authors postulated the existence of ‘one or more interesting proteins that function to hold sister chromatids together’ (Koshland and Hartwell, 1987)

A few years later, scientists working with genetic screens in budding yeast, identified *MCD1* (SCC1/RAD21 in vertebrates) to be not only associated with chromosomes but also to be important for sister chromatid cohesion and chromosome segregation (Guacci et al., 1997). Importantly, *MCD1* (SCC1) also dissociated from chromosomes at the time of anaphase onset when the connection between sister chromatids is lost (Michaelis et al., 1997). Following this, a number of other discoveries were made into identifying the genes that mediate sister chromatid cohesion. Based on these studies, an evolutionarily conserved protein complex composed of a number of subunits as detailed below was postulated and the complex was christened cohesin. It consists of

1. A core cohesin complex that is composed of a tripartite ring made up of two Structural Maintenance of chromosomes (SMC) proteins called SMC1 and SMC3, a non-SMC subunit *MCD1* (SCC1 or Rad21 in humans) along with *SCC3* (SA1/2 in humans) (Anderson et al., 2002, Haering et al., 2002). In addition to these 4 core cohesin subunits that are indispensible for cohesion in cells, there are a number of other accessory factors that play vital roles in sister chromatid cohesion. These include:
2. The accessory factor Pds5 (PDS5A and PDS5B in vertebrates),
3. A cohesin loading complex (Also known as Kollerin or Adherin) composed of *SCC2* protein (NIPBL in mammals) and *SCC4* (MAU4 in mammals) that is essential for loading cohesin but is dispensable for cohesin's continued association with chromatin,
4. An acetyl transferase Eco1 (ESCO1 and ESCO2 in mammals) that is also required for cohesion establishment for not for its maintenance on chromatin.
5. And finally, Sororin and WAPL that are accessory proteins that play counteracting roles in controlling the dissociation of cohesin from chromatin and the maintenance of cohesion after its establishment from S-phase through to mitosis.

1.2.2 Cohesin structure

At the core of sister chromatid cohesion lies the tripartite ring structure made up of a heterodimer of SMC proteins, SMC1 and SMC3 along with the non SMC protein SCC1/Rad21. The tripartite structure of cohesin was revealed by biochemical

experiments (Haering et al., 2002) (Figure 5) have also been confirmed by electron micrograph images (Anderson et al., 2002)

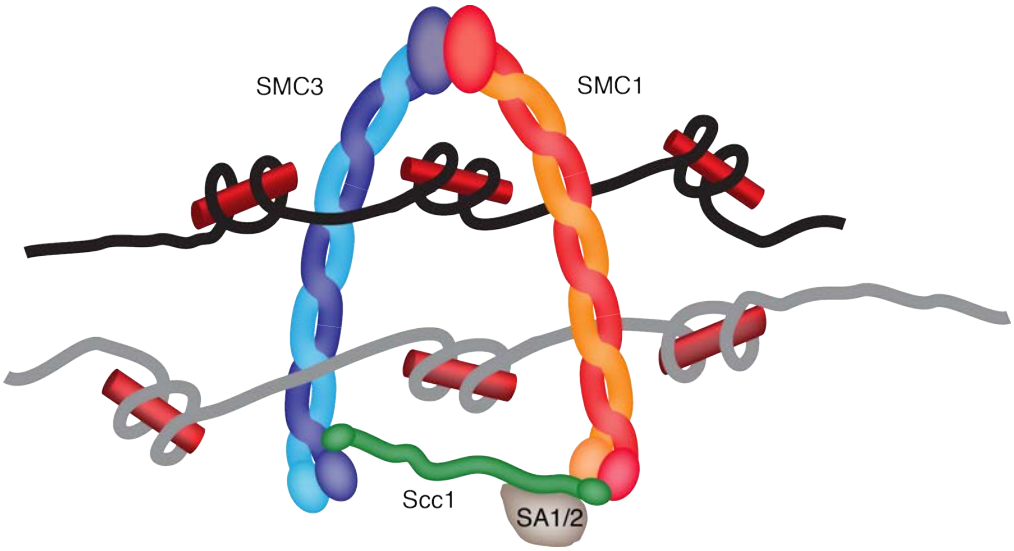

Figure 5 Structure of the cohesin ring complex
The cohesin complex is made up of a tripartite ring structure formed by an SMC1-SMC3 heterodimer along with an SCC1 subunit binding the two SMC subunits. In addition to the ring, the core cohesin complex contains a fourth component called SA2 (Aka Stag2). The cohesin ring is thought to function by physically embracing the two sister DNA strands and hold them together until it is time for them to separate in mitosis. (Adapted from (Nasmyth and Haering, 2009))

The integrity of this core ring structure has been shown to be essential for cohesin function in cells (Gruber et al., 2003). The SMC subunits of the cohesin ring each form an approximately 50 nm long rod shaped protein harbouring intramolecular antiparallel coiled-coil regions that fold back on themselves. The proteins have a globular hinge domain at one end and a nucleotide binding 'head' domain at the other end (Haering et al., 2002). Since the protein is wound around itself in an antiparallel fashion, the ATP nucleotide binding domain or the ATPase domain is made up of both termini of the protein and the hinge domain is made up of the amino acids in the middle of the protein. The two nucleotide binding domains (NBDs) of SMC1 and SMC3 proteins are connected by the third component of the cohesin ring, SCC1, with the N terminus of SCC1 binding to SMC3 and the C terminus binding to SMC1.

Considering that the main component of the protein complex that mediates sister chromatid cohesion in cells is a tripartite ring, it was postulated that the mechanism of sister chromatid cohesion involves a topological link with chromatin being

embraced by the cohesin ring. Kim Nasmyth and colleagues tested this hypothesis using a circular yeast mini chromosome that contained a centromere. Upon isolating the mini-chromosomes from cells, the authors observed that they were associated with cohesin. They further discovered that both proteolytic cleavage of the cohesin ring using either TEV cleavable forms of SCC1 or SMC1 and linearization of the mini-chromosome using a site-specific nuclease released cohesin from chromatin. This strongly suggested that the link between cohesin and chromatin was purely topological (Ivanov and Nasmyth, 2005). Additionally, the authors could also demonstrate the same finding by isolating cohesed mini-chromosomes and showing that cleavage of either the DNA or cohesin caused the loss of cohesion between sister mini-chromosomes (Ivanov and Nasmyth, 2007).

The nucleotide binding domains (NBD) of SMC1 and SMC3, similar to the NBD of ABC transporter superfamily proteins (Smith et al., 2002), have a bi-lobed arrangement with a helical domain that is attached to a set of β sheets that contain nucleotide binding Walker A and Walker B residues. One molecule of Mg2+ ATP is bound to the Walker A and Walker B motifs in the NBD of one SMC subunit and simultaneously to the ABC signature motif in the other subunit.

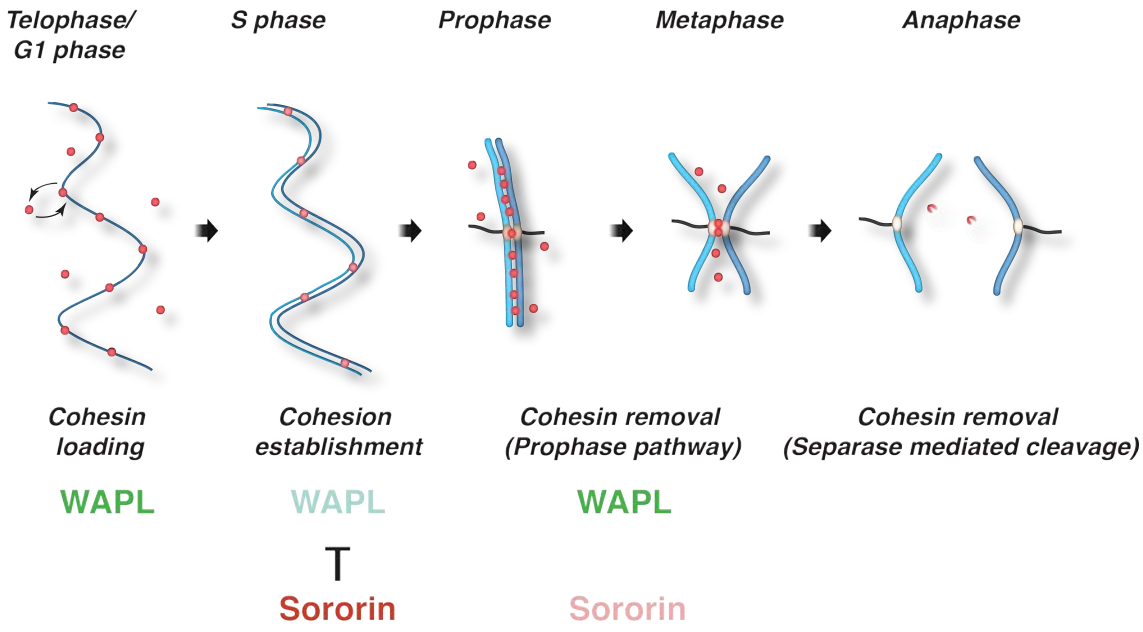

Figure 6 Sister chromatid cohesion along the cell cycle

Schematic diagram depicting the different states of interaction between cohesin and chromatin. Cohesin loading happens in telophase or the G1 phase of the subsequent

of the cell cycle. Cohesin is dynamically associated with chromatin due to the anti-establishment effect mediated by WAPL. Stable establishment of cohesion happens only after DNA replication and acetylation of the SMC3 subunit of cohesin. This coupled with the activity of Sororin, which helps to offset the anti-establishment effect of WAPL in S- and G_2-phases of the cell cycle. In mitosis, removal of cohesin from chromatin happens in two steps: the first step involves the return of the anti-establishment effect of WAPL due to the inactivation of Sororin and results in removal of over 90% of cohesin from chromosome arms. Centromeric cohesion is removed only at anaphase onset and involves the proteolytic cleavage of the SCC1 subunit of cohesin. (Adapted from (Peters et al., 2008))

This arrangement wherein the NBDs of the two SMC subunits co-operate to bind a single ATP molecule is supported by the fact that the SMC heterodimers cooperate to hydrolyse the bound ATP (Arumugam et al., 2006). Though ATP hydrolysis has been shown to be critical for cohesin loading onto chromatin (Arumugam et al., 2003), the molecular effects of ATP binding or hydrolysis on cohesin function have not been fully elucidated. It is possible that the binding of ATP cooperatively by the two SMC subunits forces them to come together whereas the hydrolysis of the bound ATP causes the NBDs of the two SMC subunits to dissociate.

The third component of the cohesin ring is SCC1 or Rad21. It is part of the kleisin family of proteins (Schleiffer et al., 2003) and acts as a bridge between the two SMC proteins with the N terminus of SCC1 binding close to the NBD of SMC3 and the C terminus of SCC1 binding to the NBD of SMC1. The crystal structure of the junction between SMC1 and SCC1's C terminus has been solved and it was shown that the C terminus of SCC1 forms a winged helical domain that binds to the NBD of SMC through hydrophobic interactions (Haering et al., 2004). It was further demonstrated that this interaction between SMC1 NBD and SCC1 C terminus is instrumental in ATP binding and hydrolysis (Arumugam et al., 2006). The interaction between SCC1's N terminus and the NBD of SMC3 though less well studied and less important for the ATPase activity of SMC3 is nevertheless crucial for cohesin function. (Arumugam et al., 2006, Gruber et al., 2006). In addition to the interaction with SMC3 and SMC1 at its N and C termini respectively, SCC1 also contains the two target cleavage sites for the protease separase, which is crucial for the removal of cohesion during the metaphase to anaphase transition (Uhlmann et al., 1999) (Hauf et al., 2001)

The fourth subunit of the core cohesin complex is the SCC3 protein (SCC3 in yeast and Stromal Antigen or SA1/2 or STAG1/2 in higher eukaryotes). It is known to bind directly to SCC1 at a region downstream of the separase cleavage site of SCC1 and is essential for sister chromatid cohesion (Haering et al., 2002, Nishiyama et al., 2010). In vertebrate cells, cohesin exists as a complex of the trimeric ring with either SA1 or SA2 protein (Losada et al., 2000, Sumara et al., 2000). Interestingly, depletion of SA1 and SA2 separately affect telomeric and centromeric cohesion respectively suggesting that different types of cohesin complexes can regulate different functions within the cell (Canudas and Smith, 2009, Peters, 2012).

In addition to the above mentioned core cohesin subunits, there are a number of other proteins that play specific roles in the different stages though which cohesin exerts its effect in cells and will be discussed in accordance with their specific roles in the cohesin cycle.

1.2.3 Models for cohesin mediated sister chromatid cohesion

Over the years, a number of models have been proposed to explain the ability of cohesin to enforce sister chromatid cohesion in cells. Consistent with the observation that the link between cohesin and chromatin is topological rather than physical (Gruber et al., 2003, Ivanov and Nasmyth, 2005, Ivanov and Nasmyth, 2007, Haering et al., 2008), the predominant models that seek to explain sister chromatid cohesion favour the enveloping of the chromatin by the cohesin complex. These ‘ring’ models have at least 3 variants as illustrated in Figure 7. The strong ring model (Figure 7A) postulates that the sister DNA molecules are trapped within a monomeric cohesin ring. The weak ring models on the other hand (Figure 7B and C), predict the existence of inter-cohesin complexes in addition to the topological link between chromatin and cohesin.

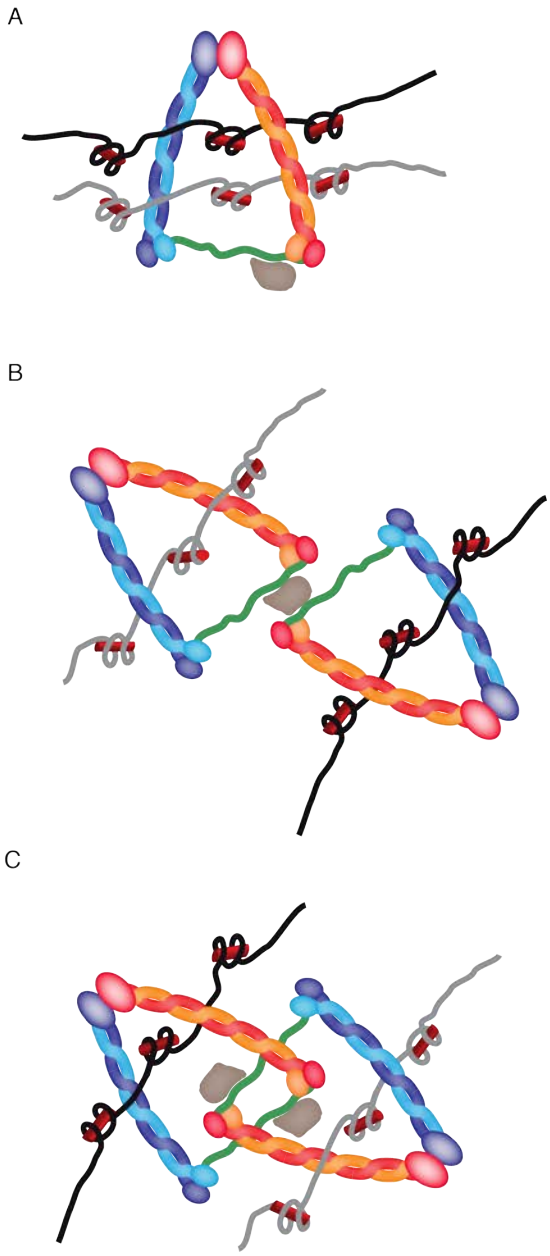

Figure 7 Models for cohesin mediated sister chromatid cohesion

Schematic diagrams depicting (A) strong ring model where both sister chromatids are enclosed by one cohesin ring and (B) handcuff model 1 where a pair of cohesin rings each enclosing one of the two sister chromatids, held together by a common SA2 subunit and (C) handcuff model 2 wherein two cohesin rings are intertwined with each harbouring a sister chromatid. (Adapted from (Nasmyth and Haering, 2009))

Even though experiments have been performed to investigate this hypothesis, little evidence seems to support the existence of inter cohesin complex interactions. Tagging the same cohesin subunit differently and probing its ability to co-precipitate yielded little support for the hypothesis (Haering et al., 2002). Förster Resonant

Energy Transfer sensor (FRET sensor) based experiments also revealed no significant evidence for inter cohesin complex formation (Mc Intyre et al., 2007). In conclusion, even though the strong ring model cannot at the moment explain how cohesin associates with specific areas along the genome if the link with chromatin is purely topological, there is no evidence to suggest that multimeric forms of cohesin as postulated by the handcuff models exists.

1.2.4 Cohesin loading onto chromatin involves the Adherin complex, the opening of the SMC1-SMC3 hinge and cohesin's ATPase activity

The primary step for sister chromatid cohesion to occur is the association between cohesin and chromatin. Cohesin loading onto chromatin is known to happen much earlier than when sister chromatid cohesion becomes apparent. In vertebrate cells, it happens in the telophase of the preceding mitosis. More than 90% of the cohesin complexes that associate with chromatin during interphase dissociate from chromatin during prophase thereby generating a large pool of soluble cohesin that could associate with chromatin in the next interphase (Waizenegger et al., 2000, Gerlich et al., 2006, Peters et al., 2008). Experiments in HeLa cells using Inverse Fluorescence Recovery After Photobleaching (iFRAP) have revealed that in addition to the soluble pool of cohesin, a population of chromatin-associated cohesin exists that dissociates from chromatin in less than 25 minutes in pre-replicative cells. After replication though, about one third of the chromatin bound cohesin associates much more stably with chromatin and persists through S-phase through to mitosis. (Gerlich et al., 2006).

One of the main predictions of the ring model with respect to cohesin-chromatin association is that since chromatin is trapped topologically inside the cohesin ring, at some point either the ring is assembled de-novo around chromatin, or double starnds breaks induced in specific regions in the DNA allow the cohesin ring to pass through or that the cohesin ring is opened at any of the three junctions within the ring structure to accommodate the chromatin. The first possibility could be ruled out because cohesin is known to exist as a trimeric ring even when it is not associated with chromatin (Gruber et al., 2003). While there is no evidence against the second possibility of DNA being excised at specific locations to allow cohesin entry, there is mounting evidence to suggest that cohesin association with

chromatin involves the transient opening of the cohesin ring. Kim Nasmyth and colleagues tested this possibility by artificially closing the different junctions within the cohesin ring in order to decipher the 'entry gate' for chromatin to enter cohesin. They found that fusing either the N or C terminus of SCC1 with SMC3 and SMC1 NBDs respectively did not prevent the association of cohesin with chromatin. Subsequently, they replaced the hinge region of SMC1 and SMC3 with p14 and MP1 proteins that formed a pseudosymmetric heterodimer. While these hybrid proteins could associate with SCC1, form the ring structure and also hydrolyse ATP, they could not associate with chromatin indicating that the opening of the SMC1-SMC3 hinge regions is necessary for cohesin loading onto chromatin (Gruber et al., 2006). Additionally, the scientists also introduced sequences that encoded for human FRB and FKBP12 proteins into the hinge regions of SMC1 and SMC3 respectively. FKBP12 and FRB proteins are known to bind each other tightly if and only if FKBP12 binds to rapamycin (Choi et al., 1996). These hybrid protein complexes were then shown to associate with chromatin only in the absence and not in the presence of rapamycin, again indicating that the entry gate for chromatin to get into the cohesin ring is the SMC1-SMC3 hinge region (Gruber et al., 2006).

The process of cohesin loading onto chromatin is also known to require the ATPase activity of cohesin as mutations in SMC1 or SMC3 that affect ATP binding or hydrolysis abolished cohesin association with chromatin (Arumugam et al., 2003, Weitzer et al., 2003). In addition to the ATPase activity of cohesin, a conserved cohesin loading complex also known as adherin or kollerin plays an essential role in cohesin loading onto chromatin (Ciosk et al., 2000, Seitan et al., 2006, Watrin et al., 2006). Adherin is a protein complex composed of two subunits, the larger of which is called SCC2 (NIPBL in mammals) and the smaller subunit being SCC4 (MAU2 in mammals). Mutations in either SCC2 (Michaelis et al., 1997) or SCC4 (Ciosk et al., 2000) affect sister chromatid cohesion. Though an association of the adherin complex with the pre-replicative (pre-RC) complexes was shown to recruit adherin to chromatin (Takahashi et al., 2004, Gillespie and Hirano, 2004), the exact mechanism through which adherin loads cohesin onto chromatin is unknown. The loading of cohesin does not just require adherin, but also the ATPase activity of cohesin and the transient opening of the SMC hinge region of the cohesin ring. This leads to speculation that adherin could be an enzymatic regulator of cohesin's

ATPase activity or of hinge disengagement and that this activity might lead to the opening of cohesin's entry gate (Peters and Nishiyama, 2012).

1.2.5 Establishment of sister chromatid cohesion happens during DNA replication

Even though the association between cohesin and chromatin happens prior to DNA replication, functional sister chromatid cohesion is established only during S phase (Uhlmann and Nasmyth, 1998). It has been speculated that cohesion establishment goes hand in hand with the replication fork progression. The physical proximity of sister chromatids following passage of the replication fork may promote the establishment of cohesion. Consistent with this idea, a number of components of the replication fork are required for sister chromatid cohesion including the PCNA clamp loader CTF8 (Terret et al., 2009), the replication fork stabilizing TIM1-Tipin complex (Errico et al., 2009). Considering that cohesin is loaded onto chromatin much before replication, it is interesting to ponder about the fate of cohesin at replication. The possibilities are either that cohesin dissociates from the chromatin and then re-associates after the replication fork has passed or that the fork passes through the cohesin ring. Experiments that were done to assess the role of sister chromatid cohesion in cells that have sustained DNA damage have revealed that cohesion can be established in the absence of bulk replication suggesting that fork passage through the cohesin ring can not be the sole mechanism through which cohesion is established (Strom and Sjogren, 2005, Strom et al., 2007, Strom and Sjogren, 2007). iFRAP experiments that were done as described in the section above (Gerlich et al., 2006) revealed that even though cohesin is bound to chromatin before replication, the residence time of a chromatin bound pool of cohesin lasted just a few minutes in pre-replicative cells and this residence time increased dramatically to up to a few hours in cells that had undergone DNA replication. From this and other experiments, it is prudent to conclude that the stabilization of cohesin on chromatin happens simultaneously with cohesin's ability to perform the essential function of mediating sister chromatid cohesion. The ability of cohesin to strongly associate with and therefore hold together sister chromatids for long periods assumes significance especially in the case of oocytes where cohesion, once established during pre-meiotic S-phase in females has to be

maintained for the entire reproductive period, up to several decades in humans (Hunt and Hassold, 2010).

In addition to these observations, it has been shown that an acetyltransferase called Eco1 (ESCO1 and ESCO2 in humans) is essential for establishment of sister chromatid cohesion in yeast (Toth et al., 1999, Tanaka et al., 1999, Ivanov et al., 2002), Drosophila (Williams et al., 2003) and human cells (Hou and Zou, 2005) . While Eco1 is indispensible for cohesion establishment during DNA replication, it is neither needed for cohesin loading nor for the continued maintenance of cohesion (Toth et al., 1999). Thus, an Eco1-dependent event plays a key role in the establishment of sister chromatid cohesion. Subsequent work showed that Eco1 acetylates cohesin's SMC3 subunits at either K112 & K113 in yeast (Rolef Ben-Shahar et al., 2008, Unal et al., 2008) or K105 & K106 in humans (Zhang et al., 2008b). The major deacetylase that reverses SMC3 acetylation in yeast cells is Hos1 (Beckouet et al., 2010, Borges et al., 2010, Xiong et al., 2010) and its counterpart in human cells is HDAC8 (Deardorff et al., 2012).

While it has been demonstrated that the acetylation of SMC3 is a critical step for turning cohesin cohesion competent, the exact mechanism by which acetylation helps with this process is not well understood. One possibility is that since the acetylated lysine residues are close to the NBD of SMC3, it could regulate the ATP binding and hydrolysis cycles of cohesin so that once cohesin is loaded onto replicated DNA, acetylation could prevent fresh binding and hydrolysis of ATP so as to prevent cohesin dissociation from chromatin.

An alternate explanation for how acetylation of SMC3 could contribute to cohesion establishment is based on experiments that suggest that the acetylation function of ECO1 becomes unnecessary if two cohesin associated proteins Wpl1 (WAPL in humans) and PDS5 (PDS5A and PDS5B in humans) are deleted (Tanaka et al., 2001, Rolef Ben-Shahar et al., 2008, Unal et al., 2008, Zhang et al., 2008a, Rowland et al., 2009, Sutani et al., 2009). There are two distinct possibilities that could explain the role of SMC3 acetylation on cohesion establishment based on these new data. One possibility is that since WAPL causes cohesin removal from chromatin, SMC3 acetylation by Eco1 directly blocks WAPL's cohesin removal activity (Rolef Ben-Shahar et al., 2008, Unal et al., 2008). Data from structural studies in yeast suggest that Wpl1 might be involved in regulating the ATPase

activity of cohesin and that this may be subject to the acetylation status of Smc3 (Chatterjee et al., 2013). An alternate hypothesis is that there exists an anti-establishment activity contributed towards by WAPL, PDS5, SMC3 and SCC3 and that acetylation of SMC3 by ECO1 serves to overcome this anti-establishment effect (Rowland et al., 2009). There is mounting evidence to support the idea that acetylation of SMC3 helps establish cohesion by preventing cohesin dissociation from chromatin. Recently it has been shown in human cells that acetylation of SMC3 is required for the recruitment of Sororin, a factor that is required for sister chromatid cohesion throughout interphase (Rankin et al., 2005, Nishiyama et al., 2010, Lafont et al., 2010, Song et al., 2012)

1.2.6 Sororin plays a very important role in maintenance of cohesion in post-replicative cells

Sororin (Aka CDCA5) was discovered in a proteomic screen for novel substrates of Cdh1 activated anaphase promoting complex or cyclosome (APC/C^{Cdh1}) using the Xenopus egg extract system (Rankin et al., 2005). It was subsequently shown to associate with cohesin in the nuclei of interphase cells. Importantly, depletion of sororin caused severe defects in sister chromatid cohesion. Conversely, overexpression of the protein lead to ectopic cohesion or 'over-cohesion'. With reference to its crucial role in sister chromatid cohesion, the protein was named Sororin after the Latin word 'soror' which means sister. Although initial experiments suggested that Sororin was conserved only in vertebrates, recent work has demonstrated that orthologs of this protein exist in other species for e.g., depletion of Dalmatian, a 95 kDa protein in Drosophila resulted in sister chromatid cohesion defects (Nishiyama et al., 2010).

Sororin is a 27 KDa basic protein with an electrophoretic mobility of 35 KDa on SDS PAGE (Rankin et al., 2005). The KEN box domain that is present in the centre of the protein is responsible for targeting Sororin for cell cycle dependent degradation induced by the action of the APC/C^{Cdh1} (Rankin et al., 2005). Soon after its discovery, Sororin was demonstrated to associate with cohesin through its C terminus (Wu et al., 2011) and to be essential for the stabilization of cohesin on chromatin after cohesion establishment in S-phase (Schmitz et al., 2007). As mentioned in the previous section, it was further observed that Sororin recruitment to chromatin was induced by SMC3 acetylation along with DNA replication

(Nishiyama et al., 2010, Lafont et al., 2010). Based on experiments carried out so far, it appears that the primary function of Sororin is to oppose the 'anti-establishment' activity mediated by WAPL. Evidence for this comes not only from the fact that depletion of Sororin and WAPL has opposite phenotypes in terms of sister chromatid cohesion status but also because the essential function of Sororin becomes dispensable if WAPL is also removed from cells (Nishiyama et al., 2010).

In trying to investigate the mechanism by which Sororin could help overcome the 'anti-establishment' activity of WAPL-PDS5, it was observed that Sororin and WAPL both contain a Phenylalanine-Glycine-Phenylalanine motif (FGF motif) that could be shown to bind to PDS5 (Nishiyama et al., 2010). It is therefore conceivable that competition between Sororin and WAPL in order to bind to PDS5 dictates the status of cohesin association with chromatin. This is supported by the observation that mutating the FGF motif on Sororin disrupts its ability to interact with PDS5 and causes sister chromatid cohesion defects without affecting Sororin's ability to interact with cohesin in Xenopus egg extracts (Nishiyama et al., 2010). At odds with this report, experiments performed in HeLa cells suggest that Sororin FGF mutants can still rescue the loss of sister chromatid cohesion caused by depletion of endogenous Sororin (Wu et al., 2011). Irrespective of the discrepancies between the reports, it can be hypothesised that Sororin competes with WAPL for binding to PDS5 and that it helps to modulate WAPL mediated 'anti-establishment' activity at the cohesin-chromatin interface. This hypothesis could explain how Sororin helps to stabilize cohesin-chromatin interactions while WAPL seeks to do the opposite. The exact molecular basis for this regulation has not been resolved yet. While Sororin was shown *in vitro* to displace WAPL from a complex with PDS5, there is no evidence to suggest that it can do so in the cell (Nishiyama et al., 2010). Another possibility as to how Sororin could influence the stability of cohesin-chromatin association rests of the hypothesis that Sororin binding to PDS5 through the FGF motif could confer a conformational shift in the interaction between the PDS5-WAPL complex and cohesin preventing WAPL from dissociating cohesin off chromatin thereby inducing a stable association between cohesin and chromatin.

1.2.7 Cohesin removal from mitotic chromosome happens in two distinct steps in higher eukaryotes

The presence of sister chromatid cohesion is essential for chromosome bi-orientation in cells and therefore for successful cell division. The timely retention followed by dissociation of cohesin at chromatin is paramount to achieving this objective. As explained above, sister chromatid cohesion mediated by the cohesin complex is established in S-phase along with DNA replication and holds the replicated sister chromatids together until it is time for them to separate in anaphase (Guacci et al., 1994). In higher eukaryotic cells but not yeast, the dissociation of cohesin from chromatin takes place in two distinct steps (Losada et al., 1998, Sumara et al., 2000, Waizenegger et al., 2000). The two waves of cohesin removal in cells confers the characteristic X shape to the chromosomes in chromosome spread preparations and will be discussed in more detail below.

1.2.7.1 The prophase pathway of cohesin removal

The first step of cohesin dissociation from chromatin takes place in prophase and prometaphase. During this step, about 90% of the cohesin dissociates form the chromatids although cohesin still persists in the centromeres (Waizenegger et al., 2000, Peters et al., 2008). In addition to the core cohesin ring components, accessory factors such as WAPL, PDS5A, Sororin, Adherin (SCC2 & SCC4) also dissociate form chromatin (Sumara et al., 2000, Rankin et al., 2005, Gandhi et al., 2006, Kueng et al., 2006, Watrin et al., 2006, Wendt et al., 2008). The process is different in yeast as a majority of cohesin persists on chromosomes until metaphase and the adherin complex is chromatin bound throughout the cell cycle (Ciosk et al., 2000).

The removal of cohesin through the prophase pathway does not rely on the proteolytic cleavage of the SCC1 subunit and instead relies on the anti-establishment activity of WAPL (Gandhi et al., 2006, Kueng et al., 2006) along with a series of phosphorylation-based processes. Polo like kinase (PLK1) a kinase that is active in mitosis, phosphorylates the SCC1 and SA2 subunits of cohesin and causes the dissociation of cohesin from chromatin (Losada et al., 2002, Sumara et al., 2002, Gimenez-Abian et al., 2004, Lenart et al., 2007). This observation was further supported by the fact that replacing the SA2 subunit of cohesin with a non-

phosphorylatable form leads to reduced dissociation of cohesin from chromatin in prophase and prometaphase (Hauf et al., 2005). In order to understand how PLK1 is targeted to SA2, scientists tried to identify cohesin subunits that could bind to PLK1 through its polo box domain. In the course of this investigation, Sororin was identified to be a candidate for PLK1 binding. The consensus sequence for a polo box binding domain is [S(S/T)P] and Sororin harbours such a site [^{157}TSTP^{160}] that once activated by a Cdk1 priming phosphorylation at the threonine residue immediately before proline, can bind to PLK1 through its the Polo Box Domain (PBD). It was demonstrated that mutation of the threonine to alanine (T159A) in sororin not only abolished PLK1 binding but also prevented the removal of cohesin through the prophase pathway (Zhang et al., 2011). These observations collectively suggest that PLK1 promotes the prophase pathway by phosphorylating the SA2 subunit of cohesin.

Even though SA2 phosphorylation by PLK1 is required for the prophase pathway of cohesin dissociation from chromatin, there are other factors that are involved in regulating the process. First indications for this came from observations that depletion of WAPL prevented the prophase dissociation of cohesion from chromatin even though SA2 phosphorylation by PLK1 was unaffected and the intensity of the phenotype was much more dramatic than one caused by inhibition of PLK1 activity (Gandhi et al., 2006, Kueng et al., 2006). Conversely, overexpression of WAPL led to a precocious loss of sister chromatid cohesion even though SA2 phosphorylation was unaffected. Since it was shown that Sororin played an antagonistic role to WAPL in terms of cohesin-chromatin association, it was postulated that mitotic phosphorylation of Sororin could destabilize the Sororin-PDS5A complex or conversely, stabilize WAPL-PDS5A complex that would now be able to dissociate cohesin from chromatin (Nishiyama et al., 2010, Zhang et al., 2011, Dreier et al., 2011). Jan-Michael Peters and colleagues have recently performed experiments wherein they identified Aurora Kinase B (AURKB) and Cdk1 phosphorylation sites in Sororin that upon phosphorylation affected Sororin's ability to interact with cohesin. This mitotic phosphorylation of Sororin by AURKB and Cdk1 was further demonstrated to lead to a stabilization of the WAPL-PDS5 complex thereby causing the removal of cohesin from chromatin through the prophase pathway independent of SA2 phosphorylation by PLK1 (Nishiyama et al.,

2013). In addition to the phosphorylation of Sororin by AURKB and Cdk1, its degradation by APC/C^{Cdh1} mediated proteolysis ensures that there is no premature sister chromatid cohesion being formed before the subsequent S-phase.

In conclusion, the prophase pathway of cohesin removal from chromatin involves:

1. The PLK1 dependent phosphorylation of SA2 and SCC1
   and independently,
2. The AURKB and Cdk1 mediated phosphorylation of Sororin that leads to a stabilization of WAPL-PDS5 mediated anti-establishment activity
3. And possibly the mitotic phosphorylation of WAPL and PDS5

In order to achieve chromosome bi-orientation, sister chromatid cohesion has to be maintained at least at the centromere, the DNA sequence upon which the kinetochores assemble. Until bi-orientation is achieved, the onset of anaphase is prevented by the spindle assembly checkpoint (SAC) that blocks the activity of the anaphase promoting complex (APC/C). If and only if all chromosomes have achieved bi-orientation can anaphase onset be triggered. Two interesting questions here are: (1) How does cohesin at the centromere resist dissociation through the prophase pathway? (2) Why is the majority of cohesin removed from mitotic chromosomes through the prophase pathway

1.2.7.2 The prophase pathway exit gate for DNA in cohesin is the SMC3-SCC1 interface

The molecular details behind the removal of a bulk of chromatin bound cohesin during prophase are still being uncovered. Unlike the anaphase-specific separase mediated cleavage that acts by cleaving the SCC1 subunit, the prophase pathway is known not to require separase-mediated cleavage of SCC1 (Sumara et al., 2002) (Waizenegger et al., 2000) (Kueng et al., 2006). These observations led to hypothesis that the removal of cohesin from chromatin through the prophase pathway must involve a transient opening of the cohesin ring. A clue as to the location of the exit gate of cohesin comes from work performed recently in budding yeast *S.* cerevisiae (Chan et al., 2012). In order to decipher the exit gate used by the prophase pathway, the researchers created fusions of either SMC3's NBD with the N terminus of SCC1 or the NBD of SMC1 with the C terminus of SCC1 neither

of which were shown to be lethal in yeast cells (Gruber et al., 2006). Since the SMC3 acetylating activity of ECO1 is necessary for overcoming the anti-establishment effect mediated by WAPL and also since the WAPL mediated anti-establishment effect is thought to underly the prophase pathway, the researchers reasoned the lethality of *eco1* mutants could be suppressed by the artificial closure of the prophase pathway DNA exit gate. They discovered that fusion of Smc3's head to the N terminus of SCC1 rescued the loss of Eco1 whereas fusion of SMC1's head to the C terminus of SCC1 did not. This strongly suggested that the anti-establishment effect mediated by WAPL involves the opening of the SMC3-SCC1 junction (Chan et al., 2012). In addition to the study in budding yeast, the authors also reported similar results in Drosophila cells where they discovered that WAPL dependent release of cohesin from drosophila polytene chromosome is perturbed by introducing an artifical fusion at the interface between SMC3' head and Scc1 (Eichinger et al., 2013). Furthermore, a recent study reported experiments performed in human cells where researchers used the FRB-FKBP12 system (Choi et al., 1996, Gruber et al., 2006) (Also see page 40), creating rapamycin inducible fusions of each of the 3 junctions within the cohesin ring. They observed that fusion of the SMC3-SCC1 interface but not the SMC1-SCC1 or SMC1-SMC3 junction prevented the dissociation of cohesin from chromatin (Buheitel and Stemmann, 2013). Altogether, these experiments strongly suggest that the prophase pathway removes cohesin rings from chromatin by opening cohesin's SMC3-SCC1 interface.

1.2.7.3 Functions of the prophase pathway

The prophase pathway removes cohesin from the chromosome arms of mitotic cells between the prophase and prometaphase stages of mitosis while cohesin at the centromere is not subjected to this process. The loss of arm cohesion is dependent on the activity of a number of players such as SA2, Sororin, WAPL, PLK1, AURKB and Cdk1. The characteristic X-shape of mitotic human chromosomes is a result of the differential ability cohesin to dissociate from the arms of the chromosomes but not at the centromeres (Waizenegger et al., 2000). It was observed that the lack of resolution of arm cohesion upon loss of the prophase pathway while delaying mitosis is nevertheless not lethal to cells (Kueng et al., 2006). It is possible that separase mediated cleavage at anaphase is sufficient to

dissociate cohesin from centromeres and the arms of chromosomes in the absence of the prophase pathway. Moreover, cohesin dissociation through the prophase pathway is largely absent in yeasts. Therefore, it is interesting to ponder about the function that the prophase pathway fulfils in higher eukaryotes. There are a number of possible reasons for the prophase pathway to exist. Firstly, its is thought that the removal of arm cohesion could help the deconcatenation of the chromosome arms by Topo II and could therefore help in timely and accurate disjunction during anaphase. Another possibility is that the prophase pathway creates a large pool of soluble and more importantly intact cohesin rings whose SCC1 subunit is untouched by separase. A substantial fraction of this pool could readily re-associate with chromatin in the subsequent cell cycle. It has been shown cohesin has an important role in gene regulation in G_1-phase, much before the establishment of sister chromatid cohesion (Wendt et al., 2008). If all cohesin associated with chromosomes were to be removed through separase mediated cleavage, re-association of cohesin with chromatin would have to await the new synthesis of SCC1 subunits to replace the ones that have been cleaved by separase. Presumably this process while seemingly feasible in budding yeast, may not be favoured in higher eukaryotes.

1.2.7.4 Protection of centromeric cohesion from the prophase pathway

The removal of cohesin from chromatin during mitosis proceeds in two waves. The first step, called the prophase pathway removes most of the arm cohesin while centromeric cohesion is retained until anaphase. What makes the centromeric cohesion immune to the prophase pathway? One of the first observations that served to solve this conundrum was that the depletion of Sgo1 (SGOL1 in humans) gene led to a precocious loss of even centromeric sister chromatid cohesion in prometaphase (Salic et al., 2004, Kitajima et al., 2004, Watanabe and Kitajima, 2005, McGuinness et al., 2005). This premature loss of centromeric cohesion upon loss of Sgo1 led to the conclusion that Sgo1 protected centromeric cohesion from being targeted by the prophase pathway thereby maintaining sister chromatid cohesion until anaphase onset. Subsequently it was demonstrated that Sgo1 could interact with and could recruit PP2A, a phosphatase to the centromere. Consistent with this observation, PP2A, similar to Sgo1, localizes to the centromere and is

required for maintenance of centromeric cohesion (Kitajima et al., 2006, Riedel et al., 2006, Tang et al., 2006). The Sgo1-PP2A complex has been shown *in vitro* to be able to dephosphorylate the SA2 subunit of cohesin (Kitajima et al., 2006). It was further demonstrated in human cells that that the loss of centromeric sister chromatid cohesion caused by depletion of SGOL1 could be rescued by the expression of a non-phosphorylatable form of SA2 (McGuinness et al., 2005). Recently, Jan-Michael Peters and colleagues showed that the SGOL1-PP2A complex can dephosphorylate Sororin that is phosphorylated in mitosis by AURKB and Cdk1 thereby protecting centromeric cohesion from WAPL mediated dissociation in prophase and prometaphase. The authors could further demonstrate that the phosphorylation of SA2 and Sororin in mitosis contributed independently to the prophase pathway but that they could both be silenced by SGOL1-PP2A mediated dephosphorylation (Nishiyama et al., 2013). Thus, sister chromatid cohesion at centromeres is protected from prophase pathway removal by the Sgo1-PP2A complex which antagonizes mitotic phosphorylation of cohesin and Sororin (Liu et al., 2012).

1.2.7.5 Separase mediated cleavage of SCC1 removes cohesin from centromeres during anaphase onset

The prophase pathway helps to dissociate about 90% of cohesin from chromatin during the early stages of mitosis. However, cohesin at the centromeres is retained until anaphase onset when cleavage of its SCC1 subunit by the protease separase removes it. It has been known that while removal of separase from cells prevents resolution of sister chromatid cohesion (Waizenegger et al., 2002), the expression of a non-cleavable variant of SCC1 slows down but does not block the resolution of centromeric cohesion (Hauf et al., 2001) suggesting that in addition to the known sites, there are cryptic cleavage sites in SCC1 that are also cleaved by separase or that separase has additional targets. Separase is normally held in a complex with a protein called securin that prevents separase from acting on its substrates before anaphase onset possibly by blocking access to separase's active site (Ciosk et al., 1998, Hornig et al., 2002, Waizenegger et al., 2002). In addition to securin based inactivation, separase in vertebrate cells is held inactive by spatial confinement with cyclin B induced by Cdk1 phosphorylation on S1121 (Stemmann et al., 2001, Gorr et al., 2005). Therefore separase activity is controlled by two distinct checks within

cells in order to prevent premature loss of cohesion. Once all the chromosomes have achieved bi-orientation, the spindle assembly checkpoint is inactivated and the APC/C becomes active through the liberation of its activator protein Cdc20 (Musacchio and Salmon, 2007). The APC/C subsequently catalyses the ubiquitylation and degradation of a number of substrates including cyclin B and securin. The removal of securin and cyclin B activates separase, which undergoes an autocatalytic cleavage that may not be necessary for its subsequent activity (Waizenegger et al., 2000). Subsequently, it acts by cleaving SCC1 thereby leading to the destruction of centromeric cohesion (Uhlmann et al., 1999, Uhlmann et al., 2000, Waizenegger et al., 2000, Hauf et al., 2001, Sun et al., 2009). Even though separase normally performs SCC1 cleavage of centromeric cohesin, it is capable of removing arm cohesion in case the prophase pathway is suppressed (Kueng et al., 2006). The separase mediated cleavage of SCC1 (also known as kleisin which is Greek for closure) during anaphase onset facilitates the removal of the cohesin ring from chromatin and thereby dissolves sister chromatid cohesion. Furthermore, It has been demonstrated in yeast and Drosophila that artificial cleavage of SCC1 by the introduction of TEV cleavage sites that can be cleaved by the TEV protease is sufficient to trigger disjunction of sister chromatids and the pole ward movement of chromosomes (Uhlmann et al., 2000, Pauli et al., 2008, Oliveira et al., 2010).

1.2.8 Roles of cohesin beyond sister chromatid cohesion

In addition to its canonical role in mediating sister chromatid cohesion, cohesin plays important roles in other areas of cell physiology. These include but are not limited to DNA damage repair, chromatin organization and transcriptional control. These will be discussed in more detail below.

1.2.8.1 Cohesin and DNA damage repair processes in somatic cells

Cohesin is known to be involved in regulating DNA damage repair processes both in mitotic cells (Cortes-Ledesma and Aguilera, 2006, Sjogren and Nasmyth, 2001) and in meiotic cells (van Heemst et al., 1999, Klein et al., 1999, Ellermeier and Smith, 2005). In human cells, cohesin, in addition its role in regulating repair of DNA damage also plays a role as a DNA damage G2/M checkpoint-signaling platform that is independent of cohesion (Kim et al., 2002, Watrin and Peters, 2009). DNA damage, when it happens, can be repaired by an error prone non-

homologous end joining mechanism or through an error free homologous recombination based mechanism (Chapman et al., 2012). Crucial for the homologous recombination repair process is the presence of the undamaged sister chromatid that can be used as a template for homologous recombination during S-phase and G_2-phase. It is thought that sister chromatid cohesion ensures close physical proximity of the template for homologous recombination. In mitotic cells, it is not only the cohesin complexes that have established cohesion in S-phase that mediate in the repair process but also the new cohesin complexes that are recruited onto the chromatin in response to DNA damage (Strom et al., 2004, Strom and Sjogren, 2005, Unal et al., 2008). New functional cohesin complexes can be recruited not just at the site of DNA damage but globally on the chromosome in response to DNA damage (Unal et al., 2007). However, this was only possible if the cohesion that was established during DNA replication was maintained (Sjogren and Nasmyth, 2001). It was further demonstrated that the formation of DNA damage induced cohesion required not only adherin (Strom et al., 2004) but also modulation of its SCC1 subunit by phosphorylation at Ser83 by Chk1 kinase and acetylation at K84 and K210 by Eco1 in yeast (Heidinger-Pauli et al., 2008, Heidinger-Pauli et al., 2009).

1.2.8.2 Cohesin and DNA damage repair processes in meiotic cells

In meiotic cell division, two rounds of chromosome segregation has to follow a single round of DNA replication to achieve the reductional division necessary for distributing each of the 4 chromatids (2 each from the maternal and paternal chromosomes) to 4 haploid nuclei (Petronczki et al., 2003). Key to achieving this process is the dissolution of cohesin from the chromatids in two distinct steps. Firstly, the cohesin from the arms is removed by separase mediated cleavage in meiosis I. Centromeric cohesin is preserved until meiosis II where it is used to bi-orient and segregate chromatids (Klein et al., 1999, Toth et al., 2000, Watanabe and Nurse, 1999). In addition to generating cross-overs and join homologous chromosomes during meiosis, cohesin in involved in mediating programmed double strand break repair (PDBR) wherein the repair process favours using the homologous chromatid as template for the repair process rather than the sister chromatid (Petronczki et al., 2003). This process, leads to the physical exchange of segments of non-sister chromatids and the formation of the chaismata. This

process depends on the substitution of the SCC1 subunit of the cohesin ring with a meiosis specific version of the kleisin subunit called Rec8, that is required for chaismata formation (Klein et al., 1999, Bannister et al., 2004, Xu et al., 2005). Apart from the experiments described above that used budding yeast, the role of cohesin in meiotic DNA damage repair has been demonstrated in fission yeast (Ellermeier and Smith, 2005) and in higher eukaryotes (Llano et al., 2012).

1.2.8.3 Cohesin in chromatin organization and transcription control

Among the first indication that cohesin functions beyond sister chromatid cohesion came from experiments in Drosophila cells where it was shown that a mutant carrying a mutation in Nipped-B gene (SCC2 component of adherin), was deficient in activation of homeobox genes (Rollins et al., 2004). This was also observed in cells from the human patients suffering from Cornelia de Lange syndrome (CdLS), a disease that leads to mental retardation and upper limb malformations (Tonkin et al., 2004). Mutations in the human counterpart of SCC2, NIPBL is known to cause CdLS (Krantz et al., 2004, Tonkin et al., 2004). Cohesin associated with the nucleus of post mitotic cells where no sister chromatid cohesion is possible (Wendt et al., 2008). Inactivation of cohesin in Drosophila post-mitotic mushroom body γ-neurons resulted in axon pruning defects caused partially by loss of expression of the ecydysone receptor revealing the role of cohesin as a regulator of the expression of the receptor (Pauli et al., 2008, Schuldiner et al., 2008). In addition to the above-mentioned experiments, subsequent studies demonstrated the role of cohesin in transcription control in zebrafish (Horsfield et al., 2007), fission yeast (Gullerova and Proudfoot, 2008) and trypanosomes (Landeira et al., 2009).

Even though, a role for cohesin in chromatin organization and transcription control is evident in a number of species, its precise role in regulating these processes remains hazy. Recent reports have begun to shed light into these activities of cohesin. Firstly chromatin immunoprecipitation (ChIP) experiments in a number of species have demonstrated that cohesin preferentially binds to specific locations within the chromatin. In budding and fission yeast, cohesin is predominantly found to associate with centromeres and pericentric regions with small amounts also associating with Cohesin Attachment Regions (CARs) (Blat and Kleckner, 1999, Megee et al., 1999, Tanaka et al., 2001). Surprisingly, cohesin binding sites in chromatin were different from adherin binding sites suggesting that cohesin is

loaded at adherin loading sites and subsequently translocated to the centromere and the CARs (Lengronne et al., 2004, Schmidt et al., 2009, Hu et al., 2011). Although how cohesin achieves this translocation is unknown, it is known that cohesin translocates to regions of convergent transcription and that induction of genes removes cohesin to the end of that particular transcription unit (Lengronne et al., 2004). This raises the possibility that the cohesin distribution seen in yeast is a consequence of gene transcription activity and not a specific pattern that is related to controlling transcription (Peters and Nishiyama, 2012). In spite of this it is still thought that cohesin helps specify the boundary to restrict the spreading of transcriptional silencing at the silent mating type loci in budding yeast (Donze et al., 1999) and is also thought to regulate transcription termination in fission yeast (Gullerova and Proudfoot, 2008)

In Drosophila cells, contrary to the situation in yeast, cohesin binding sites on chromatin completely overlap with adherin binding sites and they localize along the entire length of actively transcribed genes (Misulovin et al., 2008). A yet another situation prevails in mammalian cells where although cohesin can be found bound to chromatin at NIPBL binding sites (Kagey et al., 2010), there are far more cohesin binding sites than NIPBL (Schmidt et al., 2010) suggesting that similar to yeast, cohesin loading might occur at a site that is different from the eventual accumulation site. In contrast to yeast cells however, the pattern of cohesin binding to chromatin in mammalian cells is thought to be specified by DNA sequences that are recognized by the CTCF protein (CCCTC binding factor) (Parelho et al., 2008, Rubio et al., 2008, Stedman et al., 2008, Wendt et al., 2008). CTCF is a protein that binds to DNA using one or more of its 11 zinc finger domains and is thought to delineate the border between active and inactive regions of the chromatin (Ohlsson et al., 2010). Depletion of CTCF reduces cohesin binding at these specific sites without reducing overall cohesin levels along the chromatin suggesting that in mammalian cells, CTCF is not required for cohesin loading onto the chromatin but is required for its subsequent distribution to specific locales (Wendt et al., 2008, Parelho et al., 2008, Stedman et al., 2008).

As of now, there is no evidence to suggest that recruitment of cohesin to sites specified by CTCF is essential for its function in sister chromatid cohesion because depletion of CTCF does not cause premature loss of SCC (Wendt et al., 2008).

However depletion of cohesin in mammalian cells leads to defects in gene expression that resemble defects caused by depletion of CTCF. For instance, depletion of cohesin and CTCF leads to similar decrease in levels of H19 and igf2 proteins (Nativio et al., 2009, Wendt et al., 2008). Based on these experiments, it has been hypothesized that cohesin regulates gene expression by arbitrating long range intra-chromatid interactions between distant CTCF binding sites through the formation of chromatin loops. This postulation relies on the observation that CTCF functions through formation of chromatin loops (Splinter et al., 2006, Majumder et al., 2008) and on the idea that gene expression driven by the activity of enhancers and silencers depends on proximity between these elements that can be afforded through chromatin loops produced through topological links between distant regions of the chromatin (Nativio et al., 2009, Peters and Nishiyama, 2012). In spite of these advances into understanding cohesin's role in gene expression, the importance of cohesin's interaction with CTCF in regulating gene expression and the precise molecular mechanism through which it acts remains to be understood.

1.2.9 Cohesinopathies and cohesin in cancer

Defects in cohesin function leads to a number of human pathologies that are collectively known as Cohesinopathies (Remeseiro et al., 2013). Many of these are monogenic human diseases that have been linked exclusively to loss of cohesin subunits. Cornelia de Lange syndrome (CdLS) is one such disorder that leads to developmental defect and mental retardation (Dorsett and Krantz, 2009). About 60% of patients with CdLS have a heterozygous mutation in NIPBL (Adherin) with 5% harbouring mutations in SMC3 and 1% in SMC1 (Krantz et al., 2004, Tonkin et al., 2004, Liu and Krantz, 2009, Musio et al., 2006, Deardorff et al., 2007). Furthermore, it was recently shown that ablation of SA1 subunit in mice led to CdLS like phenotype (Remeseiro et al., 2012). Irrespective of the cohesin subunit implicated, it was observed that most patients did not have defects in sister chromatid cohesion suggesting that the function of cohesin in gene expression may cause CdLS pathologies. In support of this hypothesis, it was recently reported that SMC3 acetylation defects caused by loss of HDAC8, the deacetylase antagonizing SMC3 acetylation by ESCO1/2 leads to CdLS (Deardorff et al., 2012). It remains to be identified whether the role of cohesin in gene expression or sister chromatid

cohesion or a combination of both is responsible for the developmental defects observed in CdLS.

Roberts syndrome and SC phocomelia are genetically recessive disorders that are characterized by slow growth, mental retardation and limb malformation similar to CdLS (Van den Berg and Francke, 1993, Herrmann and Opitz, 1977, Jackson et al., 1993). Even though they were initially classified as distinct disorders, later studies reported that both the syndromes were characterized at the cellular level by gross chromosomal abnormalities and this was confirmed recently by the observation that patients from either disorders had mutations in ESCO1 (ECO1 in yeast) (Vega et al., 2005, Schule et al., 2005). Patient cells from both Roberts syndrome and SC phocomelia share defects in centromeric cohesion that is consistent with the fact that ESCO1, a factor required for cohesion establishment, harbours the mutations (Tomkins et al., 1979, German, 1979). While it has long been postulated that both RS and SC phocomelia are results of protracted mitosis caused by faulty cohesion in cells (Tomkins and Sisken, 1984), it has also been suggested that perturbations in cohesin binding to heterechromatin regions of the chromatin could influence gene expression of hetereochromatic genes (Dorsett, 2007) and that this could be a possible reason for the growth and developmental abnormalties that are characteristic of RS /SC phocomelia. Whether the disease results out of loss of cohesion or if it is a result of a different function mediated by ESCO1/cohesin remains to be determined.

Meiotic aneuploidy is the most common known cause of developmental disorders and mental retardation (Hunt and Hassold, 2010). Loss of cohesin function could contribute to trisomies caused by irregular chromosome segregation during meiosis. Down's syndrome is one such example where sister chromatid non-disjunction of chromosome 21 leads to its irregular inheritance in the progeny (Gilliland and Hawley, 2005, Hassold and Hunt, 2001, Hunt and Hassold, 2010). Although non-disjunction events involving other chromosomes are also reported, with the exception of chromosome 13 and 18, they are embryonically lethal. The non disjunction of chromatids appear to increase with maternal age and since there is a correlation between increased maternal age and precocious sister chromatid cohesion loss in oocytes, the non-disjunction events are thought to be due to faulty cohesin function (Angell, 1995, Wolstenholme and Angell, 2000, Pellestor et al.,

2003, Pellestor et al., 2006). Mutation of the meiosis specific SMC1β in mice lead to age related oocyte defect that are similar to human diseases lending credence to the above mentioned hypothesis (Hodges et al., 2005). Although there is no definitive evidence to link loss of cohesin function with down's syndrome, it is plausible that cohesion established during DNA replication has to be maintained for months and years in case of human oocytes and this probably explains why incidences of non-disjunction increases with maternal age (Peters et al., 2008).

In addition to these developmental disorders that are caused by faulty cohesin function in cells, there is mounting evidence to suggest the cohesin malfunction may contribute to aneuploidy and chromosomal instability that is a hallmark of human tumours. Firstly, elevated levels of WAPL were found in a number of cervical cancers and it was also demonstrated that down regulation of WAPL inhibits the growth of tumour derived from cervical cancer tissues (Oikawa et al., 2004, Oikawa et al., 2008). Since WAPL plays a critical role in the timely removal of arm cohesion, perturbations in its levels in cells could cause non-disjunction events that lead to aneuploidy. Secondly, elevated levels of one of the two acetyltransferases required for cohesion establishment, ESCO2, has also been implicated in melanomas (Ryu et al., 2007). Thirdly, mutations that inactivate the function of STAG2, a component of the core cohesin ring structure were shown to cause sister chromatid cohesion defects that lead to aneuploidy in a near diploid human cell line. It was also demonstrated that targeted correction of faulty endogenous STAG2 alleles in human glioblastoma cells led to increased fidelity in chromosome segregation (Solomon et al., 2011). Finally, mutations in SMC1, SMC3, NIPBL and SA2 were implicated in colorectal cancer patent cells based on a mutational study. The authors also postulated that loss of sister chromatid cohesion through somatic mutations could lead to the chromosomal instability that is observed in cancer cells (Barber et al., 2008).

1.3 Pre-mRNA splicing

The primary aim of my PhD project was to identify novel regulators of mitosis and cytokinesis in animal cells. Recently, a number of studies have reported on the role of pre-mRNA splicing factors in regulating mitosis. A brief introduction into the mechanism of pre-mRNA splicing, the composition of the spliceosome; the protein

complex responsible for pre-mRNA splicing and the current understanding of the role of pre-mRNA splicing in mitosis is presented below. This is intended to facilitate the interpretation of the results that we have obtained through our studies.

1.3.1 The spliceosome and pre-mRNA splicing

One of the critical steps in the expression of eukaryotic genes is the removal of the non-coding introns from the precursor mRNAs (pre-mRNAs) to form the mature mRNA. A multi-megadalton complex called the spliceosome mediates the process of pre-mRNA splicing. The vast majority of human genes contain introns that span about 1000 base pairs or more on average and dwarf the average eukaryotic exon by a factor of 10 to 1 (Lander et al., 2001). Removal of these non coding introns with pinpoint accuracy is the function of the spliceosome, arguably the most complex macromolecular complex within the cell (Nilsen, 2003). Even though some exons seem to be present in every variant of the mature mRNA produced from the pre-mRNA, also referred to as constitutively spliced, some exons are skipped by the splicing machinery, or alternatively spliced to grant the cell the ability to generate the multiple protein variants from the same pre-mRNA (Nilsen and Graveley, 2010). Understanding the intricacies involved in the pre-mRNA splicing process is important not only for a better comprehension of gene expression but also for developing therapies against diseases known to stem from splicing defects (Wang and Cooper, 2007, Ward and Cooper, 2010). In eukaryotes, two unique forms of the spliceosome exist. The U2-dependent spliceosome which catalyses the splicing of the U2-introns whereas the U12-dependent spliceosome catalyses the splicing of the more rare form of U12-introns (Patel and Steitz, 2003).

1.3.2 Models of pre-mRNA splicing and cis-acting pre-mRNA elements in splicing

Short sequences in the pre-mRNA contribute towards differentiating an intron from an exon. These include the 5’ splice site (ss), the 3’ splice site (ss) and the branch site (Figure 8). The branch site is usually located about 30-40 base pairs upstream of the 3’ss and is immediately followed by a polypyrimidine tract (PPT). In addition this, there are a number of Exonic and intronic splicing enhancers (ESEs and ISEs) and silencers (ESSs and ISSs). These enhancers and silencers can act on constitutive as well as alternative splicing and act by binding to cognate regulatory

factors to control the assembly and disassembly of the spliceosome (Smith and Valcarcel, 2000, Wang and Burge, 2008). There are also other factors that help to differentiate between an intron and an exon. While a group of well conserved proteins called the SR proteins helps in splice site recognition by binding to ESEs, a different group of factors called heterogeneous nuclear small nuclear ribonuclear proteins (hnRNP proteins) bind to ESSs and are involved in intron skipping (Graveley, 2000, Caputi and Zahler, 2002, Martinez-Contreras et al., 2007, Long and Caceres, 2009)

The removal of the introns from the pre-mRNA involves two trans-esterification reactions (Moore and Sharp, 1993).Firstly, the 2'OH group of the branch site adenosine performs a nucleophilic attack on the 5'splice site. This leads to the cleavage of the intron at this site and joining of the cleaved 5'ss with the branch site adenosine. This reaction forms the characteristic lariat structure, an intermediate in the splicing reaction. During the second reaction, the 3'ss is subjected to a nucleophilic attack by OH group of the 5' exon, thereby leading to the ligation of the exons together and the release of the intron lariat. While the above scheme of the two catalytic reactions acting to remove the introns from the pre-mRNA is widely accepted, there are competing models that seek to explain how the spliceosome goes about performing its functions and these will be described below briefly.

1.3.2.1 Classical model of spliceosome assembly and pre-mRNA splicing

The classical model of spliceosome assembly envisages a step-wise and ordered assembly of individual components of the spliceosome along the pre-mRNA junction as and when the transcription machinery is generating it (Figure 8). The U2-spliceosome is composed of 5 snRNP (small nuclear ribonucleic particle) molecules namely U1, U2, U5 and U4/U6 snRNPs and a large number of other non-snRNP proteins that associate either transiently or stably with the snRNPs. Each snRNP moiety is composed of an snRNA (small nuclear RNA), a common set of 7 Sm proteins (B, D1, D2, D3, E, F and G) and number of other proteins specific for each snRNP (Will and Luhrmann, 2011).

In the first step of spliceosome assembly, the U1 snRNP recognizes the 5'ss by virtue of the base pairing between the intron and the snRNA component of the U1 snRNP following which non-snRNP proteins such as SF1 and U2AF interact with

the branch site and the PPT respectively forming the E complex (Berglund et al., 1997, Berglund et al., 1998). This engagement of the branch site leads to the recruitment of the U2 snRNP to the branch site which analogous to the U1 snRNP recruitment is dependent on base pairing between the U2 snRNA and the intron and forms what is known as the A complex or the prespliceosome. In a subsequent step, the U5, U4/U6 tri snRNP which is assembled from the U5 and U4/U6 snRNPs, is recruited along with a large number of non snRNP proteins including the nineteen containing complex to the prespliceosome leading to the formation of the B complex (Makarova et al., 2001). Conformational rearrangements occur within the B complex which leads to the dissociation of the U1 and U4 snRNPs forming the activated form of the spliceosome also known as the B* complex. The first catalytic step of the splicing reaction happens now and results in the excision of the intron at the 5'ss. The spliceosome is now converted into the C complex which after a few structural rearrangements is ready to the second step of catalysis in which the 5' exon is ligated with the 3' exon and the intron is removed as a lariat with the 5'ss bonded to the 2'OH group of the branch site. The spliceosome is then disassembled and reassembled onto any other nascent transcript being produced (Jurica, 2008, Valadkhan, 2007, Smith et al., 2008, Makarov et al., 2002, Makarova et al., 2004, Wahl et al., 2009, Will and Luhrmann, 2011). Meanwhile, a protein complex called the exon junction complex marks the mature mRNA at the splice site to indicate a successful splicing event. This mark is important for the export and subsequent stability of the spliced mature mRNA in the cytoplasm where it will then be engaged by the translational machinery (Le Hir et al., 2000, Tange et al., 2004, Giorgi and Moore, 2007, Le Hir and Seraphin, 2008)

1.3.2.2 Alternative spliceosome assembly pathways

In addition to the canonical stepwise spliceosome assembly pathway as described above (Figure 8), other methods of spliceosome assembly seem to exist in cells. For instance, a spliceosome complex containing all 5 snRNPs but without a pre-mRNA was isolated from yeast cells and this complex, when added to a pre-mRNA, was shown to be able to form an active spliceosome without first undergoing disassembly (Stevens et al., 2002). This led to the postulation of the holospliceosome model wherein a single recruitment of a fully formed penta-snRNP complex onto the nascent transcript is assumed (Rino and Carmo-Fonseca, 2009).

This complex is thought to then undergo rapid conformational changes as the splicing reaction proceeds.

Additionally, at least in metazoans, a phenomenon termed exon definition also seems to operate. Exon definition is the idea that in cases where the intron size exceeds ~200 bases, the spliceosome initially forms across an exon rather than along an intron (Robberson et al., 1990, Sterner et al., 1996, Fox-Walsh et al., 2005). This phenomena, more common in mammals than in other metazoans (Xiao et al., 2007), involves binding of the U1 snRNP to the 5'ss downstream of the exon but the ensuing respective binding of the SF1 and U2AF to the 3'ss and the PPT upstream of the said exon. The subsequent binding of the U2 snRNP to the branch site upstream of the exon along with the recruitment of SR proteins by the Exon Splicing Enhancers (ESEs) leads to the formation of the spliceosome across the exon (Hoffman and Grabowski, 1992, Reed, 2000). The subsequent catalytic steps of splicing require a switch from the exon defined complex assembly to an intron defined one. The mechanism for this switch is poorly defined. However, an exon defined spliceosome complex can be directly converted into an intron defined B complex (Schneider et al., 2010). This phenomenon is important for regulation of exon inclusion or skipping during alternative splicing events (House and Lynch, 2006, Bonnal and Valcarcel, 2008, Sharma et al., 2008).

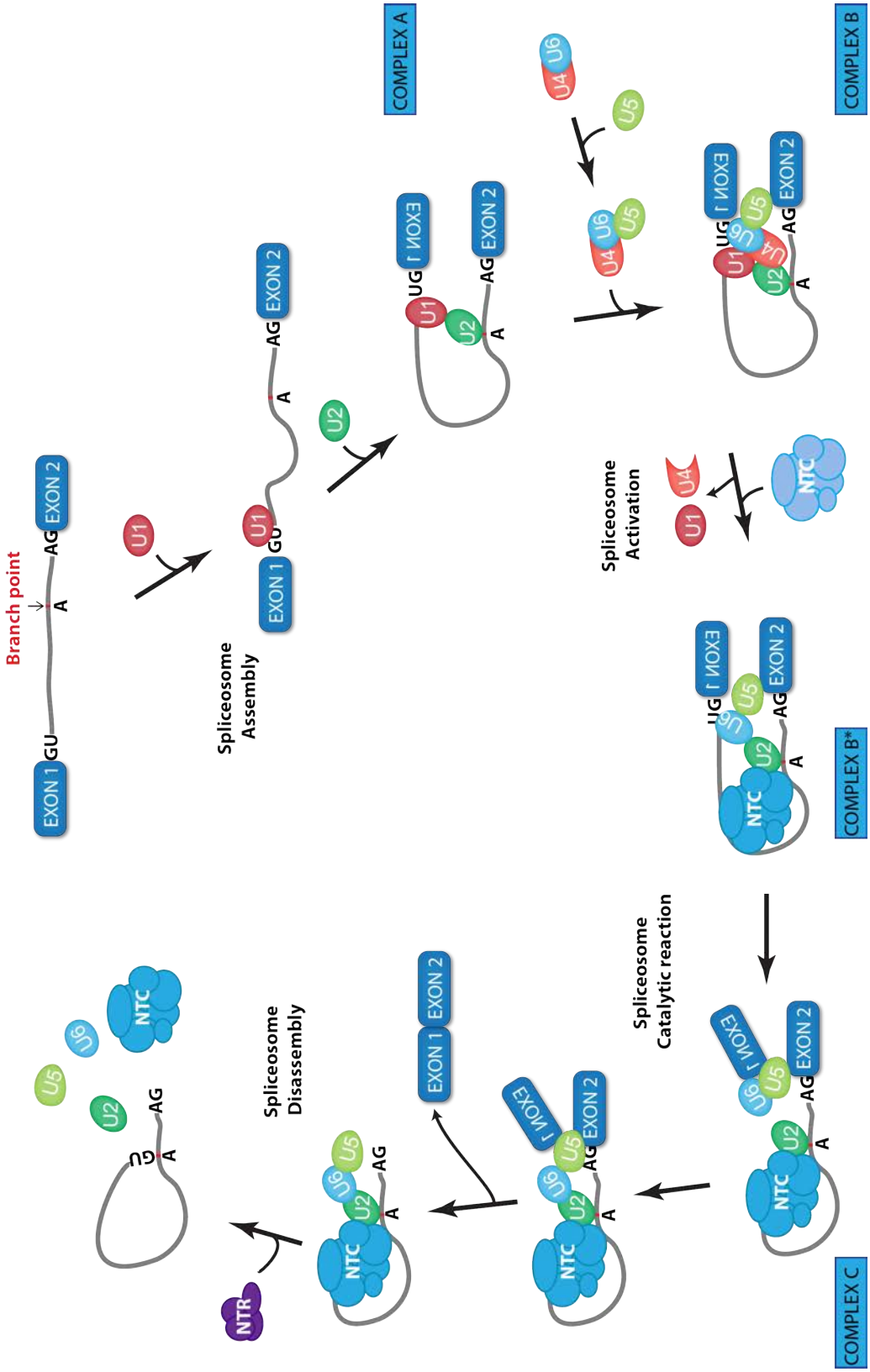

Figure 8 Schematic diagram depicting the classical spliceosome assembly and splicing pathway

1.3.3 The protein composition of the mammalian spliceosome

The eukaryotic spliceosome is a giant multi megadalton protein that relies not just on snRNPs but also on a number of other non-snRNP proteins that associate either transiently or stably with the snRNPs. These proteins play important roles in splice site recognition, facilitating interaction between various subunits of the spliceosome, and in linking splicing with other post transcriptional activities such as mature mRNA export to the cytoplasm. Proteomic studies employing mass spectrometry have managed to uncover the components of the mammalian spliceosome to varying extents (Jurica and Moore, 2003). Since most of the transitions of the spliceosomal complex between different states are rapid and very transient, initial proteomic studies to identify proteins that are part of the spliceosome relied on purifying the spliceosome as a mixture of different stages along the splicing process (Neubauer et al., 1998, Rappsilber et al., 2002, Zhou et al., 2002). Subsequently, purification and mass spectrometry analysis, *in vitro,* of three individual complexes along the splicing pathways including complex A (Hartmuth et al., 2002), complex B* (Makarov et al., 2002) and complex C (Jurica et al., 2002) were reported. In addition to these studies carried out *in vitro* using human cell extracts, a penta-snRNP complex that was formed without a pre-mRNA attached to it was also isolated from yeast cells raising the possibility of a completely assembled spliceosome being able to bind to and mediate splicing of a pre-mRNA without first undergoing disassembly (Stevens et al., 2002). Another *in-vivo* analysis (Ohi et al., 2002) led to the isolation of spliceosome complexes from both budding and fission yeast that corresponded with complex C isolated *in-vitro* from human cells (Jurica et al., 2002). These complexes were found to contain U2, U5 and U6 snRNAs along with splicing factors involved in the second catalytic step suggesting that unlike the *in vitro* experiments where the pre-splisosomal complexes predominate, *in vivo*, the second step of catalysis is rate limiting (Ohi et al., 2002). Ranging from just over 17 proteins identified in the first mass spectrometry study (Neubauer et al., 1998) to between 150-300 using later *in-vitro* studies (Rappsilber et al., 2002, Zhou et al., 2002), the spliceosome emerged to be one of the largest assembly of nuclear proteins in the cell. Recent analysis of spliceosomal complexes from Drosophila, human cells (Herold et al., 2009) and budding yeast (Fabrizio et al., 2009) combined with the more refined analysis of the

human spliceosome at distinct stages (Behzadnia et al., 2007, Deckert et al., 2006) has led to a broad agreement of the spliceosome to contain about 170 proteins.

In summary, about 45 proteins are packaged in the spliceosome in the form of snRNPs whereas non-snRNP proteins make up the rest of the protein complement of the spliceosome. While there are about 110 proteins associated with the pre-catalytic B complex in metazoans including the components of the U1 snRNP, U2 snRNP, the tri snRNPs and the nineteen containing complex (NTC), there are only 60 in the same complex in yeast. Similarly, while there are approximately 110 proteins associated with metazoan C complexes, yeast C complexes have only 50 associated proteins. It is possible that the proteins found exclusively in metazoans might play important roles in alternative splicing which is not of significance to yeast cells (Bartels et al., 2002). As mentioned above, the spliceosome undergoes rapid conformational changes through the process of splicing and a variable number of proteins associate and dissociate from the spliceosome at each stage of the splicing process. In spite of this, the fact that the same homologous proteins associate and dissociate from the spliceosome at a specific step in both metazoans and yeast goes on to suggest the conservation of the spliceosome and its action across phyla and also is testament to the effectiveness of various experiments performed in different species to isolate the components of the spliceosome (Deckert et al., 2006) (Fabrizio et al., 2009, Herold et al., 2009).

1.3.4 Role of splicing proteins in mitosis and the cell cycle

In one of the first siRNA based screens to identify novel regulators of the cell cycle, Frank Buchholz and colleagues used siRNAs to target over 5000 human genes in HeLa cells and identified about 37 genes with novel roles in mitosis (Kittler et al., 2004) of which 7 were known components of the spliceosome. Subsequently the authors expanded their analysis using siRNAs to a genome level and performed similar assays as above (Kittler et al., 2007) and estimated that about 1351 genes were involved in regulating different stages of the cell cycle of which about 18 genes were previously known to be associated with the spliceosome (Zhou et al., 2002, Hofmann et al., 2010)

More recently, the European consortium MitoCheck, published the results form their genome wide screen for cell cycle regulatory genes using time-lapse

imaging(Neumann et al., 2010). Of the ~150 genes thought to be part of the human spliceosome, based on the time lapse recoding available in the MitoCheck database, we estimate about 30 genes to have mitotic phenotypes when depleted. Our estimate is in agreement with a literature discussion regarding the potential role of splicing factors in mitosis (Hofmann et al., 2010) in which the authors pinpointed 27 spliceosome-associated genes with a mitotic phenotype within the MitoCheck dataset(Neumann et al., 2010, Hofmann et al., 2010). These findings suggest that a surprising number of splicing factors contribute to the successful execution of mitosis in human cells in an as yet undefined manner.

In addition to these large-scale screens identifying novel roles for spliceosome factors in mitosis, a number of studies have reported the role of individual spliceosomal genes in mitosis. Firstly, Kathy Gould and colleagues described mutants of Cdc5 in fission yeast to be defective in G2-M transition (Ohi et al., 1994). The authors then found that fission yeast Cdc5 associated with the U2, U5 and U6 snRNPs and was essential for pre-mRNA splicing (McDonald et al., 1999). Subsequently, the authors established that mutants without cdc5 were defective in nuclear division because they failed to form a functional spindle which was a result of faulty pre-mRNA splicing of α-tubulin mRNA. They also demonstrated that these defects could be rescued by removing the single intron in α-tubulin mRNA although the cells still suffered from global loss of splicing (Burns et al., 2002).

Additionally, it was reported that mutants of budding yeast lacking *cdc40* (PRP17 in humans), a gene known to be part of the yeast spliceosome, arrested in mitosis. It was also subsequently shown that these defects in mitosis stemmed from a loss of pre-mRNA splicing of *anc1* mRNA, *anc1* being an important transcription factor for a number of cell cycle regulatory genes (Dahan and Kupiec, 2004). The authors could also demonstrate that the mitotic defects sustained by loss of *cdc40* could be rescued by replacing the genomic *anc1* with a cDNA variant that lacked the introns.

Thirdly, drosophila cells lacking dprp38 and MFAP1, components of the tri snRNP were shown to arrest in G2/M transition (Andersen and Tapon, 2008). The authors observed that this correlated with a reduction of mature mRNA levels of cdc25, a known regulator of mitosis. This finding was similar to finding in HeLa cells where knockdown of U2AF1, a known component of the U2snRNP, was shown to cause

cells to arrest in mitosis. This was also accompanied by a reduction in mature mRNA levels of many genes including CDC25 (Pacheco et al., 2006)

Finally, it was shown that a protein belonging to the SR family of splicing regulators, SRm160 (Serine/Arginine repeat related nuclear matrix protein of 160 KDa) was associated with factors involved in sister chromatid cohesion such as SMC1, SMC3, SCC1 and SA2 (McCracken et al., 2005). Supplementing the above-mentioned work, while we were performing our experiments, a report was published that investigated the role of an RNA binding protein RBMX in sister chromatid cohesion in HeLa cells. RBMX belongs to the hnRNP family of proteins, a group of proteins that are important regulators of pre-mRNA splicing. The authors discovered that depletion of RBMX led to a potent mitotic arrest and that this arrest was caused by premature loss of sister chromatid cohesion. Based on co-depletion experiments with Sororin and WAPL, the authors concluded that RBMX is involved, in addition to Sororin, in removing the anti-establishment effect mediated by WAPL (see section 1.2.6)(Matsunaga et al., 2012).

In addition to the effects of splicing factors on mitosis, a number of genes involved in processes downstream of pre-mRNA splicing have also been implicated in regulating cell division. Illustratively, a report on the depletion of UAP56 and URH49, members of the TREX family of proteins in HeLa cells was published. The TREX family of proteins are involved in coupling transcription and pre-mRNA splicing to mRNA export (Masuda et al., 2005, Reed and Cheng, 2005, Strasser et al., 2002). In the study, the authors depleted UAP56 and URH49 and observed its effects on gene expression at a genome level (Yamazaki et al., 2010). Additionally, the authors noticed mitotic defects in cells depleted of these genes. They further demonstrated that the mitotic progression defects in the case of UAP56 was caused by a premature loss of sister chromatid cohesion. The authors further showed that depletion of additional components of the TREX family led to similar defects in sister chromatid cohesion.

In summary, loss of a variety of splicing factors has been shown to affect cell division in a number of different ways. It is possible that the defects in cell division observed upon loss of spliceosome components could arise through indirect ways (i.e. loss of mature mRNA levels of known cell division regulator through loss of splicing factor) or through direct effects (direct role of splicing factors in mitosis) or

a combination of both. While there have also been reports highlighting the role of splicing-associated factors in specific processes within mitosis, the mechanism and the precise targets of the splicing factors remain to be discovered.

1.3.5 Splicing defects in disease and cancer

Splicing factors have been reported to have either a causative role in disease, or act as modulator of disease severity or susceptibility in humans. Splicing associated diseases can arise as a result of either cis-acting factors (mutations within the gene that is the target of the splicing machinery) that affect the expression of a specific gene or due to trans-acting factors (mutations in subunits of the spliceosome machinery) that affect the expression a large number of genes (Wang and Cooper, 2007). Cis-acting factors include mutations that either affects splice site specification or the activity of exon and intron splicing enhancers (ESEs & ISEs) or exon and intron splicing suppressors (ESSs and ISSs) to affect the expression the protein concerned. It has been postulated that up to 60% of all mutations that cause disease do so by affecting splicing of the gene concerned (Lopez-Bigas et al., 2005). Of all the mutations in the human gene mutation database (HGMD), 78% are single nucleotide substitutions in exons (Stenson et al., 2003). While at first glance most of these mutations could be predicted to alter the protein code and thereby function, it is also possible that splicing defects caused by alteration in ESE or ESS sequences could result in the reported pathogenicity. For instance, based on a mutational study in exon 9 and 12 of CFTR, the gene implicated in cystic fibrosis, it was reported that a quarter of even synonymous substitutions resulted in an altered splicing pattern (Pagani et al., 2005). In addition to these factors, the role of alternative splicing in generating a number of splice variants of the same protein further complicates the issue as a large fraction of splice variants thus generated remain to be identified. For instance, in a recent study it was revealed that out of a set of 50 well characterized genes, two third were found to express novel isoforms that in 40% of the cases were found to be the predominant variant in normal cells (Roy et al., 2005).

In addition to cis-acting mutations, trans-acting mutations that target the spliceosome leading to a disruption of the splicing machinery are also known to result in human pathologies. Since the spliceosome is a gigantic protein complex containing over 150 proteins, it is easily susceptible to defects. Spinal muscular

dystrophy (SMA) is caused by mutations in genes involved in snRNP assembly. SMA is an autosomal recessive disorder that is caused by loss of Survivor of Motor Neuron-1 (SMN) gene specifically in motor neurons (Winkler et al., 2005). Retinitis pigmentosa is caused by mutations that disrupt snRNP function (Briese et al., 2005, Mordes et al., 2006, Tanackovic et al., 2011). Retinitis pigmentosa is a retinal degeneration disorder that specifically affects photoreceptor cells. Three genes that are dominant for the disease namely PRPF31, PRPF8 and HPRP3 are involved in the assembly of the tri snRNP, a complex required for proper functioning of the spliceosome (See section 1.3.2.1) (McKie et al., 2001, Vithana et al., 2001, Makarova et al., 2002, Chakarova et al., 2002).

The role of splicing abnormalities in tumorigenesis is also well established (Bonnal et al., 2012, Skotheim and Nees, 2007, Srebrow and Kornblihtt, 2006, Venables, 2006). Cis-acting mutations in known tumour suppressor such as LKB1 (Hastings et al., 2005), KLF6 (Narla et al., 2005), BRCA1 (Pettigrew et al., 2005) and oncogenes such as KIT (Chen et al., 2005) have been known to lead to tumorigenesis. Additionally there is growing evidence to suggest that changes in trans-acting splicing elements could cause cancer. Firstly there are reports that demonstrate that phosphorylation of SR proteins is increased in cancers (Ghigna et al., 2005, Karni et al., 2007) and a report also highlighted that in a sequenceing based screen, out of 189 genes identified to be mutated in breast and colon cancers, one of them was an SR protein SRP55 (Aka SFRS6) (Sjoblom et al., 2006). More recently, a number of studies report that sequencing of DNA from abnormal blood cells of patients suffering from leukemia and pre-leukemeic syndromes revealed that a high proportion of these cases were linked to mutation in genes that were part of the spliceosome (Papaemmanuil et al., 2011, Visconte et al., 2012, Wang et al., 2011). These diseases include chronic lymphocytic leukemia (CLL), chronic myelomonocytic leukemia (CMML), myelodysplastic syndrome (MDS) and acute myeloid leukemia (AML). The spliceosomal genes associated with these disorders have all been shown to be part of the early prespliseosomal U2 snRNP complex. One of these, SF3B1, is among the most frequently mutated genes in CLL patients (Wang et al., 2011, Rossi et al., 2012, Quesada et al., 2012, Landau and Wu, 2013). Similarly, while 43% of CMML patients had single amino acid mutations in SRSF2 (Meggendorfer et al., 2012), 10% of MDS patients had

mutations in U2AF1 (U2AF35) (Graubert et al., 2012). Furthermore, other splicing factors such as ZRSR2 (URP), SF1, PRPF40B, U2AF2 (U2AF65) and SF3A1 were also mutated in myeloid neoplasms (Papaemmanuil et al., 2011, Visconte et al., 2012, Wang et al., 2011, Yoshida et al., 2011). Despite the overwhelming association of mutations of these spliceosomal components with myeloid neoplasms and leukemias, the mechanisms by which these mutations contribute to pathogenesis at the cellular level and the specific targets of these splicing factors that are perturbed remain unclear.

1.4 Functional genomics in cell cycle research

With the emergence of the RNAi technology in mammalian cells, it is now possible to not only study the function of a gene in a particular biological process, but also to perform a search for all the genes in the genome that are involved in a specific biological phenomenon. By performing a high throughput genome-wide siRNA screen, it is now possible to construct maps of protein coding genes that are involved in biological processes. The cell cycle is one such area of research where functional genomics can help throw light on the role of novel genes in known biological processes. A number of genome wide screens have been reported in *Drosophila* cells and *C.elegans* (Sonnichsen et al., 2005, Eggert et al., 2004, Kamath et al., 2003). Three genome-wide screens have been performed in mammalian cells aiming to identify genes involved in the cell cycle (Neumann et al., 2010, Kittler et al., 2007, Mukherji et al., 2006). Alternatively, a proteomics approach has also been used to investigate the protein complement of structures important for the cell division process (Skop et al., 2004).

Rebecca Heald and colleagues performed a proteomic study on the mammalian midbody, the microtubule remnant that is thought to play an important role in the final separation of the two cells (Skop et al., 2004). The authors isolated midbodies from mammalian cells and identified the proteins using multidimensional protein identification technology (MudPIT). About 160 novel proteins were found to be associated with the midbody. Following this, the authors assessed protein function in *Caenorhabditis elegans* using siRNA-based depletion of 172 homologs of the proteins identified in the mammalian midbody proteomic study. While 38 of these

genes were known to have a role in cell cycle progression, depletion of approximately 58% of the rest of the genes displayed defects in cytokinesis. It is also interesting to note that 14% of the genes identified to have a role in cytokinesis are also implicated in diseases including leukemia, Huntington's disease among others.

The first genome-wide screen for cell cycle regulators targeted 95 % of the protein-coding genes in the human genome (Mukherji et al., 2006) and used DNA staining, automated microscopy, and image analysis to produce a list of cell cycle regulatory genes. The authors used siRNA pools against 24000 predicted human genes and also 10000 siRNAs against 5000 druggable human genes. Approximately 2 million images were acquired and automated image segmentation analysis was performed. It was demonstrated that cell cycle progression was affected by depletion of 1,152 genes that could be classified into eight different phenotypic classes based on specific phase of arrest, nuclear shape and area etc. Out of the 1,152 genes identified, the authors tested the reproducibility by transfecting siRNAs against 57 targets and assessing the phenotypic penetrance. Following this, they performed a deconvolution analysis wherein the siRNAs that made up the pool were transfected individually and the ability of the siRNAs to reproduce the phenotype produced by the pool was tested. Out of 24 randomly chosen genes tested, 19 of them displayed the phenotype in at least 2 out of the 4 siRNAs that made up the pool thereby suggesting that at least among the genes tested, the majority of the hits were not a result of siRNA off-target effects.

In a second study, Frank Buchholz and colleagues used *in vitro* transcribed endonuclease prepped siRNAs (esiRNAs) for gene silencing followed by DNA content analysis to identify genes that controlled cell cycle progression in human cells (Kittler et al., 2007). As a pilot experiment the authors performed a study with a subset of 5,305 human genes and had identified 37 genes that upon depletion led to defects in cell division or cell cycle progression (Kittler et al., 2004). Subsequently, the authors targeted about 17,828 genes in the human genome esiRNAs in HeLa cells for a genome wide analysis. The cells were stained with propidium iodide to visualize the DNA after 72 h of esiRNA treatment. DNA content analysis was subsequently used to identify genes that regulated cell cycle progression. The authors also performed validatory assays using a stringent nine

parameter fingerprint to assign genes to specific functions. Based on their study, the authors estimated around 1351 genes to be involved in cell cycle regulation.

Finally, MitoCheck, a European consortium, has accomplished the challenging task of performing a genome-wide screen for cell cycle regulatory genes using high content time-lapse microscopy (Neumann et al., 2010). Prior to performing the genome-wide screen, the authors performed extensive optimization experiments. The authors also optimized the process of reverse transfecting cells on arrays in an approach that would be conducive for high-content live cell imaging (Erfle et al., 2007).The authors performed a proof-of-principle screen for 49 genes involved in chromosome segregation in HeLa cells expressing histone H2B (histone subunit) fused to GFP (green fluorescent protein) (Neumann et al., 2006). The siRNAs targeting the candidate genes were spotted as arrays on microscopic slides, thereby facilitating high throughput live imaging. 42 of the genes targeted (85%), showed visible defects in chromosome segregation whereas no defects were observed in non-targeting control siRNA treated cells. Using this approach, the authors were able to obtain a time-resolved phenotypic profile for each of the genes targeted. Extending this screen to a genome-wide scale, in 2010 the authors published the results of their screen where they targeted 21,000 protein-coding human genes (Neumann et al., 2010). Based on the automated analysis similar to their screen before, they identified a list of 1249 genes that were potentially involved in mitosis. Following this, the authors performed validation using multiple siRNAs against individual genes to narrow down the list of mitotic genes to about 572. In addition to the validation experiments, complementation assays were carried out on a fraction of the hits. Even though 21 genes were targeted for the analysis, only 12 were successfully complemented by mouse transgenes suggesting that many of the hits generated by the siRNAs were probably false positives . The data generated by this screen is publicly available at the MitoCheck website (www.mitocheck.org).

The above screens provide a rich source of information regarding the genes involved in the cell cycle. However, genome-wide screens often use generic readouts and do not focus on a particular process, and therefore lack the detailed level of analysis necessary. For this reason, the above-mentioned screens suffer from a lack of specificity and it is difficult to assign particular functions to many

novel genes. Intriguingly, the percentage overlap between at least two different screens referred to above was only about 10% (Kittler et al., 2007, Mukherji et al., 2006). Yet all the siRNA screens mentioned above produced a list of over 1000 candidate cell cycle regulatory genes.

1.5 Goal of this research

The high throughput cell cycle screens as detailed above are useful data resources for further studies that focus on individual processes within the cell cycle. Although large-scale screens are useful in assigning a putative role in a process for a specific protein, these screens as such are not capable of solving important biological questions. Reviews that accompanied the report from the MitoCheck consortium (Swedlow et al., 2010) and others (Conrad and Gerlich, 2010) stress the necessity for more focussed and targeted approaches to better understand individual processes that make up the cell cycle. Thus, cell division research has to move from screens covering a multitude of processes to screens scrutinizing a specific process using new and targeted assays. The aim of this study is to use the data from existing genome wide genomic and proteomic screens to identify novel regulators of mitosis and upon identification of such genes, to characterize them functionally and understand their role in executing mitosis.

Chapter 2. Materials & Methods

2.1 Cells and growth conditions

HeLa Kyoto cells, HEK 293FT and HCT116 used in this study were grown in Dulbecco's Modified Eagle Medium, DMEM (Invitrogen 41965) supplemented with 10% FCS (Sigma) and 1% Pen Strep (Invitrogen). In order to establish stable cell lines, media supplemented with either 0.35 µg/mL puromycin (Sigma) or 500 µg/mL G418 (Invitrogen) was used. Cells were grown in an incubator that was maintained at 37^{O}C along with 5% CO_2.

2.2 siRNA screen and siRNA transfection

2.2.1 siRNA screen

To perform the siRNA screen, Dharmacon siGENOME smartpool siRNAs were obtained for the 718 genes selected for the screen in 0.1 nmole quantities in 96 well plate format. Each well in a 96 well plate contained a pool of 4 siRNAs against a gene and were distributed across ten 96 well plates along with positive controls (known mitotic regulators such as ECT2, MgcRacGAP, AurKB etc.) and non-targeting negative controls (scrambled siRNA, RISC free siRNA etc.). HeLa Kyoto cells were seeded at a concentration of about 2,500 cells per well in clear bottomed 96 well plates (Falcon, Beckton Dickinson). Prior to cell seeding, siRNA pools at a final concentration of 37.5 nM, and the transfection reagent, Lipofectamine RNAiMax (Invitrogen 13778-150) at a final concentration of 1:600 (0.167µl/well), were deposited and mixed in the wells. Cells were grown for 52 hrs at 37^{O}C and 5% CO_2 in DMEM and then processed for fixation with ethanol at -20^{o}C overnight. Following the fixation, the cells were stained with Cellomics Whole cell stain (Thermo Scientific 8403402) at a final concentration of 1:75 and the DNA was visualized by DAPI (4',6-Diamidino-2-Phenylindole,Dihydrochloride, Invitrogen) at a final concentration of 1 µ/mL. The screen was performed in triplicate and was performed in collaboration with Dr. Michael Howell's High Throughput Screening lab (HTS) at the Lincoln's Inn Fields branch (LIF) of the London Research Institute (LRI) where automated image acquisition was performed using an ArrayScan ATI microscope (Thermo Scientific) equipped with a 10X objective. 20 images per well were captured and subsequently processed using imageJ software. The processed

images were visually scored for the percentage of cells containing abnormally shaped nuclei (including multilobed or fragmented nucleus) or multiple nuclei. The three biological plates were scored independently and the median value (the percentage of cells with abnormal nuclei) was calculated and plotted.

2.2.2 siRNA sequences and transfection protocol

The siRNA duplexes listed below were used at a final concentration of 37.5 nM. The siRNA duplexes highlighted in bold were used a reference for generating siRNA resistant transgenes of the respective genes. Control siRNA (Thermo Scientific siGENOME Non-Targeting siRNA #1 and #4 D-001210-01 D-001210-04 and RISC free siRNA D-001220-01). Smartpool siRNAs against ECT2 (M-006450-00), MgcRacGAP (M-008650-00), AurKB (M-003326-08), ESCO1 (M-023413-01), ESCO2 (M-025788-01) were used. siGENOME individual siRNAs were used against ARL5A (D-012408-01, D-012408-02, D-012408-03, D-012408-04), MFAP1 (D-020071-01, D-020071-02, **D-020071-03**, D-020071-17), SART1 (D-017283-01, **D-017283-02**, D-017283-03, D-017283-04), NHP2L1 (D-019900-01, **D-019900-02**, D-019900-03, D-019900-04), CDC5L (D-011237-01, D-011237-02, D-011237-03, D-011237-04), Sororin (**D-015256-06**), Sgol1 (D-015475-17) and Scc1 (D-006832-03). siRNA against Scc4 (ACACAUUGCUGGGCCUGUAUU) was obtained from Sigma Aldrich. The candidate genes for the primary screen are listed in Table 1 below. The full list of siRNAs used in the primary siRNA screen and the spliceosome chromosome spread screen is available in the appendix.

1	AAK1
2	ABLIM1
3	ABTB1
4	ACOT4
5	ADAM19
6	ADAM33
7	AIFM3
8	AKAP5
9	AKR1C4
10	ALDH9A1
11	AMPD3
12	ANKFN1
13	ANKRD5
14	ANXA11
15	ARL13B
16	AVPR2
17	ABC1
18	ACAD9
19	ACTL6A
20	ACTR3B
21	ACTRT2
22	ACVR1C
23	AGXT2L1
24	AKAP12
25	AKT3
26	ALOX15B
27	AMIGO
28	ANK2
29	ANKRD2
30	ANKRD7
31	ANXA5
32	ANXA6
33	ANXA7
34	AP1G1
35	AP2M1
36	ARHGAP17
37	ARHGEF11
38	ARL4A
39	ARL5A
40	ARPC2

41	ASB12
42	ATXN2
43	B3GALTL
44	BAHCC1
45	BARD1
46	BAZ2B
47	BCAS2
48	BFAR
49	BLES03
50	BMP2
51	BMPR1A
52	BTBD14A
53	BTN3A2
54	C10ORF45
55	C10ORF53
56	C11ORF24
57	C11ORF38
58	C12ORF39
59	C13ORF23
60	C14ORF121
61	C14ORF177
62	C14ORF4
63	C14ORF54
64	C14ORF94\HAUS4
65	C18ORF24
66	C19ORF35
67	C19ORF54
68	C19ORF7
69	C1GALT1
70	C1ORF102\OSCP1
71	C1ORF109
72	C1ORF125
73	C1ORF156
74	C1ORF178
75	C1ORF210
76	C1ORF50
77	C1ORF71\CNST
78	C1QTNF2
79	C20ORF77
80	C21ORF91

81	CLASP1
82	CLCNKB
83	COG7
84	COTL1
85	COX7A2L
86	CRABP1
87	CRISP2
88	CSN3
89	CTLA4
90	CTNNBL1
91	CXORF58
92	CYC1
93	C2ORF17
94	C2ORF25
95	C3F
96	C3ORF14
97	C3ORF52
98	C4B
99	C4ORF23
100	C6ORF110
101	C6ORF167
102	C6ORF51
103	C7ORF47
104	C8ORF44
105	C9ORF16
106	C9ORF167
107	CA12
108	CABP7
109	CACNG4
110	CACYBP
111	CALR
112	CAMK1
113	CAMK2B
114	CAMKV
115	CANX
116	CAPZA1
117	CASC5
118	CASP2
119	CBX7
120	CCDC108

121	CCDC17
122	CCDC56
123	CCDC70
124	CCDC8
125	CCDC89
126	CCDC9
127	CCL28
128	CCT4
129	CDC5L
130	CDC6
131	CDK4
132	CDK8
133	CDKL2
134	CDKL5
135	CDT1
136	CDYL2
137	CENP E
138	CENP T
139	CEP192
140	CHRDL1
141	CHRNA5
142	CKAP2
143	**CKAP5**
144	CKS2
145	CLDN16
146	CLIP1
147	CLK1
148	CLPB
149	CMBL
150	CNTFR
151	CNTNAP1
152	COL10A1
153	COPA
154	COPB1
155	CORO1B
156	CORO1C
157	CPA5
158	CRADD
159	CRYGN
160	CSK

161	CSNK2B
162	CTDSPL
163	CTNND1
164	CTRC
165	CTRL
166	CUL1
167	CYP2C19
168	DARC
169	DBN1
170	DBNL
171	DCLRE1C
172	DCTN1
173	DCTN2
174	DDX24
175	DEPDC7
176	DGAT2
177	DGKI
178	DHPS
179	DHX8
180	DKFZP434P0316
181	DKFZP564C186
182	DKFZP686L1814
183	DMRTC1
184	DNCL1
185	DNM1L
186	DOCK2
187	DOCK9
188	DOPEY2
189	DPEP3
190	DRD1
191	DSE
192	DTL
193	DUSP19
194	DUSP8
195	DYNC1H1
196	DYRK2
197	EDA2R
198	EDC4
199	EEA1
200	EFCAB4B

201	EGFL7
202	EGLN1
203	EGLN2
204	EHD1
205	EIF2AK3
206	ELA3B
207	ELAC2
208	ELMOD1
209	ENAH
210	ENPP5
211	ERH
212	EXOC1
213	EXOC3
214	F2RL2
215	FAM101A
216	FAM101B
217	FAM118B
218	FAM131A
219	FAM136A
220	FAM38A
221	FAM47B
222	FAM76B
223	FAM82B
224	FANCC
225	FANCE
226	FANCI
227	FATE1
228	FBLN5
229	FBXL21
230	FBXO5
231	FCRL6
232	FFAR3
233	FGF12
234	FGFR2
235	FKBP6
236	FLJ10276
237	FLJ20397
238	FLJ22318
239	FLJ23657
240	FLJ25084

241	FLJ33008
242	FLJ46041
243	FLOT1
244	FOSL2
245	FZD8
246	GABRR1
247	GALNT5
248	GALR3
249	GAS1
250	GDF9
251	GDI1
252	GEM
253	GIMAP5
254	GIPC1
255	GJA5
256	GJB1
257	GJB3
258	GJE1\ GJC3
259	GLRX
260	GLT1D1
261	GLT8D1
262	GNA14
263	GNAI2
264	GNAS
265	GNB2
266	GNB2L1
267	GNG5
268	GOLPH3L
269	GORASP1
270	GORASP2
271	GOSR2
272	GPATC1
273	GPR19
274	GPR55
275	GPR68
276	GPRIN1
277	GPX5
278	GRK5
279	GTPBP1
280	GUCY1B3

281	GZMA
282	HAVCR2
283	HAX1
284	HCFC1
285	HDX
286	HEXA
287	HHIP
288	HIP2
289	HISPPD2A
290	HIST1H2AJ
291	HIST3H2A
292	HLA-DQA1
293	HNMT
294	HOOK1
295	HOXD1
296	HP1BP3
297	HSD17B7
298	HSPA14
299	HSPA5
300	HSPBAP1
301	HTF9C
302	HTR5A
303	IBSP
304	IFNK
305	IFNW1
306	IK
307	IKIP
308	IL4R
309	INHBA
310	IQUB
311	IRAK4
312	ITGB1
313	ITSN2
314	JAG2
315	JAK1
316	JUP
317	KALRN
318	KCNAB3
319	KCNJ6
320	KCNK18

321	KCNK5
322	KCNK6
323	KCNN4
324	KCNT2
325	KCTD13
326	KCTD5
327	KEAP1
328	KIAA0350
329	KIAA0368
330	KIAA0649
331	KIAA0895
332	KIAA1166
333	KIAA1267
334	KIF12
335	KIF18B
336	KIF22
337	KIF2A
338	KIF2C
339	KIF5B
340	KIFC1
341	KIFC3
342	KLC2
343	KLK1
344	KRT28
345	KY
346	LAD1
347	LCE1B
348	LCK
349	LCN9
350	LGALS1
351	LIMA1
352	LIMD1
353	LIMK1
354	LIMS1
355	LIN54
356	LIN9
357	LMNA
358	LMNB1
359	LOC147645
360	LOXL3

361	LRP1
362	LRP10
363	LRP5
364	LRTM2
365	LY86
366	LYPLAL1
367	M6PR
368	MAGOH
369	MAOA
370	MAP2K5
371	MAP4K2
372	MAPK15 (ERK7/8)
373	MAPKSP1
374	MASTL
375	MC3R
376	MC5R
377	MCP
378	MCPH1
379	MEGF11
380	MFAP1
381	MFI2
382	MFSD4
383	MGAT4B
384	MGC11061
385	MGC13125
386	MGC15763
387	MGC20398
388	MGC3036
389	MGC4707
390	MGLL
391	MICAL3
392	MKLN1
393	MLL5
394	MMP12
395	MS4A1
396	MSN
397	MTBP
398	MTP_18 HUMAN
399	MYD88
400	MYH9

401	MYO6
402	MYOF
403	MYOZ1
404	MYST1
405	MZF1
406	NAGS
407	NCOA6
408	NCOR2
409	NDUFB10
410	NDUFS3
411	NEDD1
412	NEDD4
413	NEDD4L
414	NEGR1
415	NEK10
416	NEK3
417	NEU1
418	NEURL
419	NFKBIE
420	NHP2L1
421	NIPSNAP1
422	NKTR
423	NMNAT1
424	NOD1
425	NOD27
426	NOG
427	NOX4
428	NP_001007190.1
429	NP_001008271.1
430	NP_001010866.1
431	NP_277022.1
432	NP_689812.2
433	NP_689919.1
434	NP_981947.1
435	NPM1
436	NPM3
437	NR5A1
438	NRIP3
439	NSF
440	NSG2_HUMAN

441	NSUN5C
442	NSUN7
443	NTRK3
444	NUP214
445	NUTF2
446	ODZ3
447	OGG1
448	OIP5
449	OPRS1
450	OR51E1
451	OR51T1
452	OR52E4
453	OSM
454	P2RY10
455	PAEP
456	PAFAH1B1
457	PALM
458	PAPPA
459	PARP14
460	PCDH8
461	PCLO
462	PDE4B
463	PDE4C
464	PDK1
465	PDK1
466	PDK2
467	PDLIM7
468	PDXP
469	PDZD4
470	PEX10
471	PEX13
472	PHACTR2
473	PHPT1
474	PI4KB
475	PICALM
476	PINK1
477	PIP
478	PIP5K2C
479	PJA2
480	PLCB2

481	PLCE1
482	PLEC1
483	PLK3
484	PLRG1
485	PLXNA1
486	PML
487	PNUTL2
488	POLG
489	POP5
490	POU2F2
491	PP1A
492	PPAP2C
493	PPIH CYCLOPHILIN H
494	PPIL5
495	PPM1L
496	PPP1CB
497	PPP1R12A
498	PPP2R2A
499	PPP2R2B
500	PPP5C
501	PPP6C
502	PRG2
503	PRICKLE2
504	PRKAB1
505	PRMT1
506	PRMT5
507	PRMT6
508	PRTN3
509	PTAFR
510	PTGER2
511	PTGS2
512	PTPDC1
513	RPA1
514	GJD4
515	OR4D1
516	RAB22A
517	RAB24
518	RAB37
519	RAB4A
520	RAB7A

521	RAB8A
522	RABGAP1L
523	RABGGTB
524	RAC2
525	RAPGEF3
526	RASL11A
527	RBBP9
528	RBM10
529	RBM41
530	RCN3
531	RCN3
532	RDH10
533	RDH11
534	REEP4
535	RGMA
536	RGS11
537	RHBDL1
538	RHOT2
539	RNASE4
540	RNASE4
541	RNF141
542	RNF215
543	RP6-213H19.1
544	RPAIN
545	RPS6KA2
546	RSAD1
547	RSU1
548	RXFP2
549	RYK
550	RYR2
551	S100A10
552	S100A2
553	S100A6
554	SAP30BP
555	SART1
556	SCCPDH
557	SCGB1D1
558	SCGB2A2
559	SCN11A
560	SCN1B

561	SCN5A
562	SCYL1
563	SDK1
564	SDK2
565	SEC23A
566	SEC23B
567	SEC31
568	SEMA4B
569	SEPP1
570	SGK196
571	SH2D4A
572	SH3GLB2
573	SIGLEC1
574	SIGLEC11
575	SIGMAR1
576	SIPA1
577	SLAMF1
578	SLC22A12
579	SLC25A5
580	SLC30A8
581	SLC35D2
582	SLC37A4
583	SLC5A2
584	SLC5A3
585	SLCO4A1
586	SLK
587	SMC2
588	SMTN
589	SMU1
590	SNFT
591	SNRPG
592	SNX4
593	SON
594	SPAG4L
595	SPATC1
596	SPCS2
597	SPP1
598	SPRY4
599	SRBD1
600	SRP14

601	ST14
602	ST6GAL2
603	STAU1
604	STK33
605	STK39
606	STRN
607	STS
608	SVOPL
609	SYP
610	SYT8
611	TAAR1
612	TAS1R2
613	TBC1D17
614	TBL1X
615	TCTN3
616	TDG
617	TDO2
618	testis serine protease 1 precursor
619	TFIP11
620	TGFBR1
621	THEG
622	TIMELESS
623	TIPARP
624	TJP2
625	TLR1
626	TLR2
627	TM2D1
628	TMEM129
629	TMEM185A
630	TNFAIP3
631	TNIP2
632	TNKS
633	TNP2
634	TNPO1
635	TOMM22
636	TOR1A
637	TOR1AIP1
638	TOR1B
639	TREML4
640	TRIM21
641	TRIM63
642	TRMT1
643	TRPA1
644	TRPC3
645	TRPV1
646	TRUB2
647	TSP50
648	TSPYL1
649	TTLL12
650	TTYH2
651	TTYH3
652	TUBA4A
653	TUBB2C
654	TXNDC3
655	TXNL4A
656	UBE2M
657	UBL5
658	UBQLN2
659	UBQLNL
660	UCK1
661	UCN
662	UCP3
663	UGT3A2
664	UNC93A
665	UNQ3033
666	USE1
667	USP1
668	USP29
669	USP30
670	USP52
671	USPL1
672	UTP11L
673	UTS2
674	VAMP1
675	VAPA
676	VCL
677	VCX
678	VPS35
679	VRK1
680	VRK2
681	VTI1A
682	WDR5B
683	WDR61
684	WDR81
685	WDR85
686	WDR89
687	WFDC2
688	WNK1
689	WNK4
690	WNT4
691	WTIP
692	XAGE2
693	XP_498354.1/ MAGEB16
694	XPO1
695	YEATS4
696	YPEL5
697	ZBED4
698	ZBTB40
699	ZC3H8
700	ZFP3
701	ZFP42
702	ZHX2
703	ZNF114
704	ZNF189
705	ZNF362
706	ZNF479
707	ZNF511
708	ZNF549
709	ZNF561
710	ZNF575
711	ZNF579
712	ZNF641
713	ZNF664
714	ZNF688
715	ZNF750
716	ZNF85
717	ZSCAN2
718	ZSCAN5

Positive controls	
1	ANLN
2	AURKB
3	CEP55
4	CIT
5	ECT2
6	INCENP
7	KIF20A
8	KIF23
9	KIF23
10	PLK1
11	PRC1
12	RACGAP1

Negative controls	
1	siGENOME NTC
2	RISC free NTC

Table 1 List of candidate genes in functional genomic screen

The siRNA transfections were performed using a reverse transfection protocol with Lipofectamine RNAiMax (Invitrogen 13778-150) as per the manufacturer's instructions. Briefly, siRNA at 37.5 nM was diluted with OptiMEM (GIBCO 31985-047) and mixed with appropriate volume of RNAiMax as per surface area of the wells as (indicated in Table 2). After incubating for 15 minutes at room temperature, the mixture was added to appropriate number of cells, as per the culture vessel, in DMEM medium. Cells were then incubated for 24, 36, 48 or 52 h and processed for downstream experiments as applicable.

Plate	OptiMEM	RNAiMax	siRNA (stock =20uM)	Cell number	Final volume
10 cm plate	1 ml	15 ul	11.25 ul	800,000	6 ml
6 cm plate	1 ml	10 ul	7.5 ul	300,000	4 ml
12 well	175 ul	2.6 ul	3.75 ul	40,000	2 ml
24 well	100 ul	1 ul	0.9375 ul	25,000	500 ul

Table 2 siRNA transfection in Hela Kyoto cells across various cell culture surfaces

2.3 Plasmids and cell lines

2.3.1 List of plasmids used in the study

The plasmids used in the study are listed in Table 3 below.

	Name	DNA id	Description	Source
1	pIRES puro 3 AcFL	dna0049	AcFL tag (AcGFP-FLAG) at the N terminus of an MCS (Multiple Cloning Site)	(Su et al., 2011)
2	pIRES puro 3 AcFL MFAP1 siRes	dna0428	SiRNA resistant MFAP1 transgene with AcFL tag at N terminus	This study
3	pIRES puro 3 AcFL SART1 siRes	dna0429	SiRNA resistant SART1 transgene with AcFL tag at N terminus	This study
4	pIRES puro 3 AcFL NHP2L1 siRes	dna0430	SiRNA resistant NHP2L1 transgene with AcFL tag at N terminus	This study
5	pLVX puro-AcFL	dna0431	AcFL tag (AcGFP-FLAG) at the N terminus of an MCS. Vector for Lentiviral expression system	This study
6	pLVX puro-AcFL Sororin siRes	dna0433	SiRNA resistant Sororin transgene with AcFL tag at N terminus. Vector for lentiviral expression system	This study
7	pSPAX2	dna0435	2nd generation packaging vector for lentiviral expression system	Addgene
8	pMD2.G	dna0436	Envelope vector for lentiviral expression system	Addgene
9	pEGFP-M27-RNaseH1	dna0434	RNase H1 variant that localizes specifically to nucleus, tagged at the C terminus with EGFP	(Cerritelli et al., 2003)

Table 3 List of plasmids used in this study

2.3.2 Preparation of stable cell lines using plasmid transfection

To create tagged alleles of the genes used in the study (MFAP1, NHP2L1, SART1) for expression in human cells, AcGFP (Aequorea coerulescens GFP) was amplified from pAcGFP-N1 (Clontech) and inserted into pIRESpuro3 (Clontech). During amplification, a Kozak sequence (CGCCACC) and a FLAG epitope (DYKDDDDK) were added to AcGFP before the start codon and after the last amino acid, respectively. The coding sequences of the above mentioned genes were obtained (Source Biosciences) and introduced into this pIRES puro 3-AcFL vector using the restriction enzymes AgeI and EcoRI. To create siRNA-resistant variants of the genes the following sequences were mutated using Quikchange II site directed mutagenesis kit (Stratagene #200523). Highlighted in yellow are the single

nucleotide substitutions that were performed. For MFAP1, the sequence aagtgaaggtaaagcgtta was mutated to aggttaaagtgaaacgcta, for NHP2L1, the sequence ttgaaaggctcttagtcta was mutated to ttgagagactgttggtgta, for SART1, the sequence gcaagagcatgaacgcgaa was mutated to gcaaaagtatgaatgccaa. The plasmids were transfected into HeLa Kyoto cells using FuGENE 6 transfection reagent (Roche 11815091001) for the generation of stable cell lines. Briefly, HeLa Kyoto cells were pre seeded at appropriate density at 37°C and 5% CO2 in DMEM (Invitrogen) medium with 10% FCS (Sigma). On the day of the transfection, the cell confluence was visually confirmed to be about 50% following which the plasmid and Fugene 6 were mixed at the ratio of 1 µg plasmid : 3 µl FuGENE 6 transfection reagent and diluted with OptiMEM. After incubating the mixture at room temperature for no more than 10 min, the mixture was added to cells along with fresh DMEM. The cells were grown for 24 h after which the medium was supplemented with 0.35-0.4 µg/ml puromycin (Sigma) to selectively maintain cells expressing pIRESpuro3-AcFL tagged alleles of the genes concerned. Clonal cell lines were then generated after two weeks of antibiotic selection and were characterized by immunofluorescence microscopy and immunoblotting. HeLa Kyoto cells were also transfected as above with a plasmid coding for RNase H1-EGFP (a generous gift from Dr. Robert Crouch (Cerritelli et al., 2003) following which the GFP positive cells were enriched by fluorescence activated cell sorting (FACS) at the FACS facility at the LRI.

2.3.3 Preparation of stable cells lines using Lentiviral infection

To create tagged alleles of Sororin for expression in human cells, the coding sequence of Sororin was introduced into pIRES-puro 3-AcFL vector using the restriction enzymes AgeI and EcoRI. To create siRNA-resistant variant of sororin the sequence cgcaggagccctaggattt was mutated to agaagatccccagaatct using Quikchange II site directed mutagenesis kit (Stratagene #200523). After this, the entire AcFL-Sororin sequence was excised from pIRES-puro3 vector using the restriction enzymes ClaI and EcoRI and cloned into pLVX-puro (Clontech). HEK 293FT cells were pre seeded and grown to about 50% confluency before being transfected with a combination of three plasmids containing pLVX-puro-Sororin (WT or siRNA resistant) and second generation packaging system: psPAX2 (Addgene, 12260) and pMD2.G (Addgene, 12259) using Lipofectamine 2000

(11668-019) according to the manufacturer's instructions. Viral particles were then collected 48 hrs after transfection by harvesting the supernatant and filtering it through a 0.45µm PVDF filter unit (Millex HV SLHV033RS). Cycling HeLa Kyoto cells were infected with various titres of the viral particles in presence of 8 µg/ml polybrene (Sigma 107689). The cells were grown for 48-60 h in the presence of the viral particles after which the medium was supplemented with 0.35-0.4 µg/ml puromycin (Sigma) to selectively maintain cells expressing pIRES-puro3-AcFL tagged alleles of sororin. After passaging the cells for 3 generations, clonal cell lines were generated by picking individual colonies of cells using a cloning ring and growing the cells so isolated for two weeks with antibiotic selection. The cell lines were characterized by immunofluorescence microscopy and immunoblotting.

2.3.4 Other transgenic cell lines used in the study

Cells expressing H2B-mCherry were kindly provided by Dr. Kuan Chung-Su (Su et al., 2011) and were grown in DMEM media supplemented with 500 µg/ml G418 (Invitrogen). Cells stably expressing SMC1-EGFP were used for Inverse Fluorescence Recovery After Photobleacing (iFRAP) experiments and were a kind gift from Dr. Jan-Michael Peters (Schmitz et al., 2007).

2.3.5 List of cell lines used in this study

The cell lines used in this study are listed in Table 4 below.

No.	Cell line name	Description	Source/ Reference
cl017	AcFL tag	Tag only cell line	(Su et al., 2011)
cl132	AcFL MFAP1 siRes	Cell line expressing siRNA resistant MFAP1 tagged with AcFL	This study
cl133	AcFL SART1 siRes	Cell line expressing siRNA resistant SART1 tagged with AcFL	This study
cl134	AcFL NHP2L1 siRes	Cell line expressing siRNA resistantNHP2L1 tagged with AcFL	This study
cl135	AcFL tag (viral)	Tag only cell line made by lentiviral expression system	This study
cl136	AcFL sororin siRes	Cell line expressing siRNA resistant Sororin tagged with AcFL made by lentiviral expression system	This study
cl137	RNaseH1 M27	RNaseH1 M27 (nucleus only) with EGFP tag at C terminus	This study. Plasmid from: (Cerritelli et al., 2003)

Table 4 List of cell lines used in the study

2.4 Cell synchronization and drug treatments

To synchronize cells in S phase, 2.5 mM of thymidine (T9250 Sigma) was added to cells either at the time of transfection or 24 h later. At the time of release, cells were rinsed twice with DMEM and fresh medium was added. To synchronize cells for performing chromosome spreads, asynchronously growing HeLa Kyoto cells that were grown for 24, 44 or 52 h following siRNA transfection were treated with 330 nM nocodazole (M1404 Sigma) for 4 h. To score for the ability of the cells to form a metaphase plate (See Figure 15) HeLa Kyoto cells were synchronized in metaphase by treatment for 3 h with the proteasome inhibitor MG132 at a final concentration of 10 μM.

2.5 Western blotting (WB)

2.5.1 Preparation of whole cell lysates

Cells were grown until the indicated time point and then harvested either by trypsinization or by mitotic shake off as appropriate. Cells were then spun down at 3000 rpm for 3 minutes (Eppendorf desktop centrifuge 5434) and subjected to a PBS wash (4^{o}C). Following pelleting of the cells and removal of PBS, lysates were prepared by direct resuspension of cells in Laemmli buffer (12.5 mL 4x SDS-PAGE stacking buffer (0.5 M Tris-Cl pH 6.8, 0.4% SDS w/v), 10 mL glycerol (anhydrous), 20 mL SDS (10% w/v), 2.5 mL ß-mercaptoethanol, 2.5 mL bromophenol blue (1% w/v)). Lysates were boiled at 95^{o}C for 5 minutes and subsequently sonicated at 10 Amp microns in a sonicator (Soniprep, Sanyo).

2.5.2 SDS PAGE and Western blotting

Following the preparation of whole cell lysates, the protein concentration was measured by Bradford's assay using the Bradford's reagent (BioRad) and subsequently 30 ug each of the samples were loaded per well in an SDS-PAGE (sodium dodecyl sulphate poly acrylamide gel electrophoresis) gel in a criterion cassette (BioRad) and subjected to electrophoresis. Following this, the proteins were transferred onto an Immobilon PVDF membrane (Millipore) using a semi dry transfer procedure. Subsequently, the membrane was blocked with 5% milk for 30 min and incubated with the primary antibody as indicated at 4^{O}C overnight and then

with the appropriate secondary antibody conjugated with HRP for 1 h at RT. The detection of the protein was then carried out using an ECL chemiluminescence reaction (GE Healthcare).

2.5.3 Fluorescent detection of western blotting

For performing fluorescent detection of western blotting, the procedure similar to the one above (Section 2.5.2) was used except that the membrane used, Immobilon FL PVDF (Miilipore), exhibits low autofluorescence activity. Moreover the secondary antibody used was coupled to a fluorescent tag (Anti rabbit IgG conjugate (Dylight R 680) and anti mouse IgG conjugate (Dylight R 800) (Cell signalling). Both the secondary antibodies were used a final concentration of 1:15,000. The proteins on the membrane were subsequently detected using an Odyssey Imaging System (LI-COR Biosciences).

2.6 Real time PCR for measurement of mRNA levels

The following primers were used for the quantitative real Time PCR (qRT-PCR) experiments. ARL5A (Fwd: ttgggctggataatgcaggg, Rev: ttttcttaggtcctcatgcgct), CEP55 (Fwd: tggaacaacagatgcaggca, Rev: tgagtgcagcagtgggactt), Sororin Intron1 (Fwd: acgcagtccggtgaaagat, Rev: agcgagaagattcccaaaca), Sororin Exon 2 (Fwd: agggccccatctcctactaa, Rev: gccagatttcagggaggatg), Sororin Exon1-Exon2 (Fwd: atgtctgggaggcgaacg, Rev: acctccgcagaggcttagta), GAPDH (Fwd: cctcccgcttcgctcct, Rev: ctggcgacgcaaaagaaga). HeLa Kyoto cells were reverse transfected with the indicated siRNAs along with thymidine either added at the time of transfection or added 6 or 24 h post transfection. Cells were released from thymidine after 24 h and allowed to proceed though the cell cycle. 5 h after release, the cells were harvested and lysed in RLT plus buffer (Qiagen RNeasy Plus kit) + β-Mercaptoethanol (Sigma). RNA was extracted from the cells using the RNeasy plus MiniKit (Qiagen) according to the manufacturer's instructions. After measuring the RNA concentration in a nanodrop spectrophotometer, 1.5 µg of total RNA was reverse transcribed with random hexamers using the TaqMan reverse transcription kit (Applied Biosystems). Pre-mRNA and mature mRNA levels were assessed by quantitative real time PCR (qRT-PCR) performed using the indicated primer pairs using iQ-SYBR Green Supermix and CFX96 Real-Time System (BioRad) using the following reaction conditions.

Reagent	Volume (µL)
cDNA	1
H_2O	3.6
Primer 1 (10 µM stock)	0.2
Primer 2 (10 µM stock)	0.2
Sybr Green SuperMix	5
Total	**10**

Table 5 qRT-PCR reaction constituents

No.	Step	Time (Secs)
1	95^{O}C	180
2	95^{O}C	10
3	58-65^{O}C (as appropriate)	30
4	Plate read	
5	**Go to step No.2 40 times**	
6	Melt curve 60-95 ^{O}C	
7	Plate read	
8	End	

Table 6 Program for qRT-PCR reaction

The relative percentage mRNA was calculated using the ΔΔCT method as described earlier (Winer et al., 1999) and the GAPDH gene was chosen for normalization of the mRNA measurements.

2.7 Immunofluorescence microscopy (IF)

Cells grown on coverslips with a diameter of 18 mm and thickness 1 (Assistent) were fixed overnight with methanol at -20°C or for 10 min at 37°C in 4%

formaldehyde (Thermo Scientific, 16% PFA stock diluted with PBS). After fixation, samples were washed thrice in 0.01% Triton X-100 in PBS for 5 minutes each and then permeabilized with 0.2% Triton X-100 in PBS for 10 minutes. Following three more washes in 0.01% Triton X-100 in PBS, the coverslips were incubated with the blocking solution of 3% BSA in PBS containing 0.01%TritonX-100 for 1 h. Samples were incubated with the primary antibody in the blocking solution at $4^{O}C$ overnight after which three washes with 0.01% Triton X-100 in PBS was done and the coverslips were incubated with appropriate secondary antibody in the blocking solution at room temperature for an hour along with 1µg/mL DAPI. Following three more washes with 0.01% Triton X-100 in PBS, the coverslips were mounted onto microscopic slides with ProLong Gold (Molecular Probes) and left to dry overnight. Images of the samples as processed above were acquired on Zeiss Axio Imager M1 or M2 microscopes using a Plan Neofluor 40x/1.3 oil objective lens or 63X/1.4 Apochromat oil objective lens (Zeiss) equipped with an ORCA-ER camera (Hamamatsu) and controlled by Volocity 6.1. software (Improvision). Images were deconvolved using Volocity's iterative restoration function.

2.8 Antibodies and dyes

The following primary antibodies were used in this study for Western blotting (WB) and Immunofluorescence (IF) experiments: mouse monoclonal anti-AcGFP (JL8, Clontech, IF & WB 1:2000), rabbit anti-AcGFP (Clontech, IF & WB 1:2000), mouse monoclonal anti-α-tubulin (B512, Sigma, IF & WB 1:10000), rabbit monoclonal anti-β-tubulin HRP Conjugate (9F3, Cell Signaling, WB 1:2000), mouse monoclonal anti-Aurora B (AIM-1, 611083 BD Transduction Laboratories, IF: 1:500), mouse monoclonal anti-SMC1 (6892, Cell signalling, WB 1:1000), rabbit polyclonal anti-SMC3 (ab9263, Abcam, WB 1:2000), goat polyclonal anti-SA1 (A300-157A, Bethyl labs, WB 1:1000), rabbit monoclonal anti-SA2 (5882, Cell signalling, WB 1:1000), rabbit polyclonal PDS5A (A300-089A, Bethyl labs, WB 1:10000), rabbit polyclonal PDS5B (A300-537A, bethyl labs, WB 1:2000), rabbit polyclonal anti-MFAP1 (SAB2104903, Sigma, WB 1:2000), rabbit polyclonal anti-NHP2L1 (95958, Abcam WB 1:5000), rabbit polyclonal anti-SART1 (SC376460, Santa Cruz, WB 1:1000). Dr. Jan Michael Peters (IMP, Vienna) kindly provided the following antibodies: rabbit polyclonal anti-Sgol1 (#975, WB 1:500), rabbit polyclonal anti-Sororin (#953, WB 1:2000), rabbit polyclonal anti-Scc4 (#974, WB 1:1000), rabbit polyclonal anti-Scc1

(#890, WB 1:1000). Dr. Katsuhiko Shirahige (University of Tokyo) kindly provided a monoclonal mouse antibody against acetylated SMC3 (WB 1:1000). Secondary antibodies conjugated to either Alexa Fluor 488 or 594 (Molecular Probes) at a final concentration of 1:1000 were used for IF detection. DNA was stained with 1 µg/ml DAPI (Molecular Probes). HRP-conjugated secondary antibodies at a concentration of 1:5,000 were used to detect proteins on immunoblots using chemiluminescence (GE Healthcare). For fluorescent detection of western blotting, anti rabbit IgG conjugate (Dylight R 680) and anti mouse IgG conjugate (Dylight R 800) (Cell signalling) at a final concentration of 1:15,000 were used for detection with Odyssey Imaging System (LI-COR Biosciences).

2.9 Time-Lapse microscopy

To quantify mitotic duration and cell division status in Figure 17 & Figure 26, HeLa Kyoto cells were seeded in 12 well plates (Nunc). An hour prior to imaging the media was switched to CO_2 independent media without phenol red (Invitrogen). Phase contrast images of cells were acquired every 5 min, as indicated at 37^{o}C using a Zeiss Axio Observer Z1 microscope controlled by SimplePCI software (Hamamatsu) equipped with an Orca 03GO1 camera (Hamamatsu) and a Plan-Apochromat 10x/0.45 objective. The images so acquired were processed using ImageJ software and analysed using the mitotic duration plugin (Lenart et al., 2007). For higher resolution imaging as in Figure 38, cells were seeded in Labtek chambered borosilicate coverglass chambers (Nunc, Thermo Scientific) and imaged with the microscope as above at intervals of 3 or 5 min as indicated but with a 40x/1.3 DIC H oil objective. The images so acquired were then processed using ImageJ software.

2.10 Flow cytometry

To quanity cell cycle progression for thymidine-synchronized cells in (Figure 32), flow cytometry analysis was performed as below. HeLa Kyoto cells were synchronized in thymdine for 24 h and were released for 3 h after which they were trypsinized, fixed in 75% EtOH and stored at –20ºC until analysis. For analysis, 50 µL of FBS was added to each sample. The cells were then centrifuged, washed in PBS and re-suspended in 300 µL of PBS containing 200 µg/ml of RNase (Sigma)

and 5 µg/ml of propidium iodide (Sigma). Samples were incubated 15 min. at 37°C and analyzed using a FACScalibur (Becton Dickinson), using doublet discrimination to gate single cells. Cell cycle profiles were analyzed with FlowJo (Tree Star softwares).

2.11 Chromosome spreads, interphase and mitotic Fluorescence In-Situ Hybridization (FISH)

2.11.1 Chromosome spreads

Chromosome spreads of HeLa Kyoto and HCT116 cells treated with siRNA duplexes were performed as follows. Cells were reverse transfected with the indicated siRNAs at a final concentration of 37.5 nM following which they were grown at 37^{o}C for 24, 48 or 52 h as indicated. To enrich for mitotic cells, the medium was supplemented with 330 nM nocodazole for 4 hrs. Following this cells were harvested by mitotic shakeoff and centrifugation. Subsequently, cells were incubated in a hypotonic solution (DMEM: filtered deionized water at 1:2) for 6 min at room temperature (RT). Subsequently, cells were fixed with freshly made Carnoy's buffer (1:3 Glacial acetic acid:methanol) for 15 min at RT and spun down. This fixation step was repeated thrice. The suspension of cells in Carnoy's buffer (final volume: 100-200 µl depending on cell density) was then dropped onto a clean slide from a distance of about 2 feet and left to dry overnight at RT. The dried slides were washed in PBS solution containing 1µg/ml DAPI and was then mounted using Prolong Gold mounting solution.

2.11.2 Interphase Fluorescence *In-Situ* Hybridization (FISH)

Interphase FISH experiments were performed on cells treated as shown before (Schmitz et al., 2007). Briefly, cells were reverse transfected with siRNA onto coverslips with a diameter of 18 mm and thickness 1 (Assistent). 2.5 mM thymidine added either at the time of transfection or 24 h later. Following 24 h of thymidine arrest, cells were released from the thymidine arrest by rinsing twice in DMEM and allowed to proceed through the cell cycle. 5 h after release, they were fixed with Carnoy’s buffer (15 min at RT) and left to dry overnight.

BAC clone RP11-113F1 corresponding to the human tff1 gene was kindly provided by Dr. Erwan Watrin (University of Rennes). The BAC was used to produce FISH probes labeled with PrimeIt II Random primer labeling kit (Stratagene) and Cy3-dCTP (Amersham Biosciences) as per the manufacturer's instructions. Briefly, the about 100 ng of the BAC was denatured at 95^{O}C for 2 min and then incubated with 10 µl of random hexamers, denatured again at 95^{O}C for 2 min and mixed with 1 µl of Klenow polymerase, 1 µl cy3 labelled dCTP and 10 µl of 5X dCTP buffer and incubated in the dark at 37^{O}C overnight. After performing a DNA cleanup using Qiaquick gel extraction kit (Qiagen 28704), 20 µg Human cot-1 DNA (Invitrogen; to avoid probe binding to repetitive sequences) and 10 µg salmon sperm DNA (Invitrogen; to avoid non specific probe binding) were added to the probes. Ethanol precipitation was then performed for concentrating the probe following which the probes were resuspended in 50 µl MilliQ. Just before use, the probes were diluted in hybridization buffer (Cytocell aquarius) to a final ratio of 1:10. The probe was added to the fixed coverslips. The coverslip, now with the probes were denatured for 3 min at 75^{o}C. Subsequently, they were incubated in a humidified chamber at 37^{o}C overnight. After the incubation, the coverslips were washed fbriefly in 0.4X SSC made from a stock of 20X (3M NaCl + 300 mM $Na_3C_6H_5O_7$) at 72^{o}C for 3 min and then in 2X SSC with 0.05% Tween 20 at RT for 30 secs. Following this, DNA was counterstained with 1 µg/ml DAPI and the coverslips were mounted with ProLong Gold (Molecular Probes). Images were acquired on a Zeiss Axio Imager M1 microscope using a Plan Neofluor 40x/1.3 oil objective lens equipped with an ORCA-ER camera (Hamamatsu) and controlled by Volocity 6.1. software (Improvision). Images were deconvolved using Volocity's iterative restoration function. Distance measurements were performed in Volocity by locating the centres of each of the pair of centroids manually and measuring the distance along a straight line between the two centroids. In control and Sgol1 depleted cells, since the distances were often difficult to resolve because of the proximity of the dots. As a consequence, only cells where at least 2 out of the 3-centroid pairs were resolvable were considered for the analysis. In Sororin, MFAP1, NHP2L1 and SART1 depleted cells, the vast majority of paired signals were clearly resolved and could be measured.

2.11.3 Mitotic FISH experiment*

To analyse the status of sister chromatid cohesion in intact mitotic cells without subjecting them to the harsh chromosome spread and synchronization processes, we performed mitotic FISH experiments on asynchronous cells. Cells were reverse transfected with indicated siRNAs onto 18 mm coverslips and grown for 24 or 48 hrs. Subsequently, the cells on the coverslips were fixed with Carnoy's buffer for 15 min at RT. FISH probes for the centromeres of chromosomes 6 (LPE 06G) and chromosome 8 (LPE 08R) (Cytocell aquarius) were used to probe the status of sister chromatid cohesion status. The FISH probes were diluted with hybridization buffer (Cytocell aquarius) at a ratio of 1:10 and subsequently added to the fixed coverslips. Denaturation was performed for 3 min at 75^{o}C, and the slide was left to hybridize overnight at 37^{o}C in a humidified and lightproof chamber. Following this, the coverslip was washed in 0.25 x SSC for 3 min at 73^{o}C and subsequently in 2 x SSC with 0.05% Tween 20 for 30 secs at RT. The coverslips were then incubated in PBS containing 1µg/ml DAPI to counterstain DNA. Finally the coverslips were mounted using Prolong Gold mounting solution. Images were then acquired on a Zeiss Axio Imager M2 microscope using a Plan Neofluor 40x/1.3 oil objective lens equipped with an ORCA-ER camera (Hamamatsu) and controlled by Volocity 6.1 software (Improvision). Distance measurements were performed in Volocity by locating the centres of each of the pair of centroids manually and measuring the distance along a straight line between the two centroids. Since HeLa Kyoto cells are trisomic for chromosome 6 and chromosome 8, three pairs of dots for each chromosome was present. The distance between each of the six paired FISH signals was estimated and if it was longer than 2 µm, they were considered not to be paired anymore. The value of 2 µm was used because this was the average distance between the centroids in metaphase of a control cell, where the centroids would be expected to be the furthest apart and still be paired.

*Experiment performed in collaboration with
Dr. Maria Dolores Vasquez Novelle

2.12 Inverse Fluorescence Recovery After Photobleaching (iFRAP) and image quantification

iFRAP experiments were performed based on experiments described previously (Gerlich et al., 2006, Schmitz et al., 2007). Cells stably expressing SMC1-EGFP were obtained from Dr. Jan-Michael Peters (Schmitz et al., 2007) and were reverse transfected with the indicated siRNA duplexes at a final concentration of 37.5 nM in Labtek 2 chambered borosilicate coverglass chambers (Nunc, Thermo Scientific). 2.5 mM thymidine was added either at the time of seeding or 24 h post seeding. Cells were released from thymidine arrest after 24 h by rinsing twice in DMEM and allowed to proceed through the cell cycle for 5 h. An hour before imaging, the medium was changed to CO_2 independent medium without phenol red (Invitrogen) supplemented with 10% FCS, 0.2 mM L-glutamine, PenStrep, and 1 mM Na-pyruvate (all Invitrogen). 1 mg/ml cycloheximide (Sigma) was added to avoid new synthesis of SMC1-EGFP. The imaging and bleaching was performed at 37 °C using a Olympus FV1000D (InvertedMicroscopeIX81) laser confocal scanning microscope equipped with a PlanApoN ×60/1.40 NA Oil Sc objective lens and controlled by FV10-ASW software (Olympus). One half of the nuclear region was bleached leaving the other half intact. Repeated bleaching was performed every 10 secs for 5 iterations in order to remove the soluble and dynamically bound pool of Smc1-EGFP. This resulted in a reduction in the fluorescence intensity of the unbleached nuclear area as well. The first post bleach frame used for the downstream analysis was acquired 2 min after photobleaching to allow for complete equilibration of bleached soluble SMC1-EGFP across the nucleus. ImageJ software (http://rsbweb.nih.gov/ij/) was used for the intensity measurements. EGFP intensities were measured by drawing a rectangular area of the same dimensions in the bleached and unbleached area followed by subtraction of the mean background signal outside of the cell. The iFRAP ratio was calculated as the ratio of the background corrected mean fluorescence intensity of the bleached versus unbleached area normalized to the first post bleach frame. The IFRAP ratio was plotted over time for the different siRNA treatments.

Chapter 3. Results 1- A functional genomic screen to identify novel regulators of mitosis

Mammalian tissue culture cells are a very good model system to understand a number of biological processes. With the optimization of the RNAi technology, it is now possible to perform a comprehensive analysis of all the genes in the genome to assess their roles in specific biological processes. Genome-wide screens aiming to identify cell cycle and cell division factors have been reported in *Drosophila* cells and *C.elegans* (Kamath et al., 2003, Eggert et al., 2004, Sonnichsen et al., 2005) and in mammalian cells. Proteomic studies have also been performed to identify novel components of the mammalian midbody, a structure that is crucial for the completion of cytokinesis by abscission (Skop et al., 2004, Guizetti and Gerlich, 2010). The aim of my PhD project was to utilize existing genome-wide screening and proteomic datasets to identify novel regulators of cell division and upon identification of novel genes, to further characterize their biological roles.

3.1 Establishing and optimizing an siRNA based screen to identify new genes that regulate mitosis

The starting point for my project was to combine available functional genomics data to shortlist genes to be investigated for novel roles in regulating mitosis. We selected 851 genes that were either identified as causing mitotic failure upon depletion according to the genome wide screens or genes that were identified as midbody associated by the proteomics approach (Skop et al., 2004). Subsequently, a set of criteria was used to eliminate genes that were either well-characterized regulators of cell division, pseudogenes, ribosomal proteins and annotation mistakes. Based on this winnowing process, we ended up with a shortened candidate list of 718 genes as shown in Figure 9, that we went on to study in our screen (See section 2.2.1 and the appendix for a list of all the genes screened)

Before ordering the siRNAs against the candidate genes that we selected, we proceeded to optimize the assay and the conditions that we would use for the screen. Firstly, regarding choice of the cell line to be used for the screen, we chose to use HeLa Kyoto cells, which is a human cervical cancer cell line derived from a patient who suffered from an aggressive adenocarninoma of the cervix (C, 1974).

HeLa Kyoto cells have been widely used for studying the cell cycle for a variety of reasons; they are easy to maintain and propagate and more importantly they are amenable to high throughput microscopic imaging and are an excellent for RNAi based depletion of genes, which were the mainstay of the project. However, it is worth noting that HeLa Kyoto cells suffer from chromosomal instability and are thus aneuploid thereby necessitating careful interpretation of the results obtained.

We performed a series of optimization experiments wherein the effect of a number of parameters such as the choice of siRNA transfection reagent, its concentration, the concentration of siRNA, cell passage number, seeding density and method of cell fixation among others on the phenotypic penetrance and image quality were tested. As shown in Figure 10, we used siRNAs targeting known mitotic regulators such as Aurora Kinase B, ECT2 and RacGAP1 to test the assay firstly in 12-well plates. We used a liposome-based reverse transfection protocol to introduce the siRNA duplexes into HeLa Kyoto cells at a final concentration of 37.5 nM of the siRNA duplexes in the culture medium. 52 h post transfection, we fixed the cells and stained them with a whole cell stain for visualizing the cytoplasm and DAPI for the nucleus. Transfection with siRNAs targeting positive control genes led to the efficient depletion of the target protein and caused a penetrant nuclear morphology phenotype, as shown by DAPI staining (Figure 10). The presence of bi-nucleated or multi-nucleated cells indicated the requirement of the gene in cytokinesis whereas the presence of lobed or abnormally shaped nuclei indicated the requirement of the gene concerned in chromosome segregation. Based on these test results, we chose to use abnormalities in nuclear morphology in fixed interphase cells as the indicator for defective mitosis or cytokinesis and hence as a readout for our screen.

Following this, we also optimized the assay in 96 well plates, which was the format that would be used for the screen. This was performed in collaboration with Dr. Michael Howell's High Throughput Screening lab (HTS lab) at the London Research Institute (LRI). We obtained optimal results with a cell number of about 2500 per well in a 96 well plate. We also decided to perform automated cell seeding and transfection using liquid handling robots at the HTS lab. Based on the optimization experiments, we further decided to use siGENOME smartpool siRNAs from Dharmacon that were arrayed in a 96 well plate format for the screen. The 21

nucleotide long siGENOME siRNAs carry ON-TARGET modifications in the sense strand that prevent its processing by the RISC complex thereby reducing off-target effects. In addition, the use of smartpools (4 different siRNAs against each gene) instead of individual duplexes reduces the effective concentration of individual duplex and is thought to further reduce chances of off-target effects.

3.2 Primary siRNA screen for identifying novel mitotic genes

After optimizing the assay for the screen, we performed the screen as follows, siRNA pools targeting the 718 genes were distributed across ten 96 well plates along with positive controls (known mitotic regulators such as AurKB, ECT2, MgcRacGAP, PRC1 etc.) and non-targeting negative controls (scrambled, RISC free siRNA etc.) as shown in Figure 11. We performed the screen in triplicate as shown in Figure 12. At 52 h post transfection, we fixed the cells in 100% ethanol at -20^{O}C overnight, stained them and subjected them to automated image acquisition using an ArrayScan ATI microscope equipped with a 10X objective. The images were subsequently scored manually for abnormal nuclear morphology with over 300 cells being counted for each well. Subsequently, the median value of the three biological repeats was determined for each siRNA pool. The screen result is displayed in graph form in Figure 12. The negative controls used in the screen such as the scrambled control and the RISC free control scored less than 8% in terms of nuclear abnormalities. All positive control genes were detected with top scores ranging between 75-99% indicating that the screening assay had been successful. Based on visual confirmation and the feasibility of downstream processing, we selected genes that scored above an arbitrary cut-off of 23% for further analysis.

3.3 Deconvolution screen for hits identified in primary reveal multiple off target hits

Based on the primary screen data, we selected 50 genes for a subsequent deconvolution analysis. Since the primary screen was performed with smartpools of 4 individual siRNAs targeting different regions within the same gene, we reasoned that performing a deconvolution analysis using the individual siRNAs that make up the pool would serve to determine how many and which individual siRNA duplex reproduces the phenotype observed in the original screen. This can give

indications as to whether a hit is more or less likely to be caused by depletion of the intended target. It serves to increase the confidence level in assigning a particular phenotype to the depletion of the gene concerned. While hits with only one siRNA producing the effect are more likely to be caused by off-target effects, genes for which two or more (out of 4) siRNA duplexes reproduce the phenotype observed with the pools are strong candidates for a causal link between the effect and loss of gene product. A definite test for phenotype-gene linkage requires RNAi-resistant transgenes (see later) or an inactivation of the candidate gene by gene targeting or genome editing.

We performed the deconvolution analysis in three 96 well plates with positive (ECT2, MgcRacGAP, PRC1 etc.) and negative (scrambled RISC free) control siRNA duplexes distributed across the plates. Image acquisition and the subsequent manual scoring were done as described for the primary screen. The results from the deconvolution experiments are summarised in

Gene	% Abnormal nuclei (siRNA Smartpools)	Number of siRNAs scoring > 20% abnormal nuclei
MFAP1	24.63	**4**
SNRPG	50.89	**3**
DHPS	23.44	**3**
ECT2	99.00	**3**
CACNG4	46.71	**2**
DPEP3	36.13	**2**
MGC3036	38.26	**2**
NEDD1	24.03	**2**
RPAIN	36.76	**2**
SDK2	61.22	**2**
SON	49.22	**2**
ARL5A	22.64	**2**
C14ORF177	26.68	**2**
TNP2	20.29	**2**
CCDC17	20.76	**2**
AKAP12	41.00	**1**
BLES03	24.18	**1**
CAMK2B	34.56	**1**
FAM38A	21.24	**1**
GPR19	27.43	**1**
MFSD4	63.33	**1**

MGC4707	29.82	**1**
NEURL	35.89	**1**
OR51T1	17.47	**1**
PDE4C	22.69	**1**
SLCO4A1	20.73	**1**
SMU1	33.55	**1**
SNFT	46.69	**1**
SVOPL	65.05	**1**
TUBA4A	35.24	**1**
CORO1C	41.24	**1**
FAM101A	54.57	**1**
P2RY10	26.50	**1**
PRG2	35.46	**1**
np_981947.1	67.90	**1**
TSPYL1	26.43	**1**
AAK1	4.00	**1**
CCL28	4.00	**1**
CXORF58	22.62	**1**
TJP2	7.00	**0**
FAM131A	19.24	**0**
ITSN2	18.23	**0**
PDK2	25.89	**0**
TAS1R2	24.72	**0**
ZBTB40	24.16	**0**
TREML4	18.11	**0**
PDK1	18.38	**0**
USP52	18.49	**0**
DGAT2	21.00	**0**
STRN	20.50	**0**
CORO1B	22.68	**0**

Table 7 Results of secondary deconvolution siRNA screen.
Highlighted in green are the genes that could reproduce the screen phenotype in at least 2 out of the 4 siRNAs tested

We observed that while 14 out of the 50 genes showing a nuclear morphology phenotype for at least two out of the four siRNAs tested (Table 7), we could reproduce the screen (Smartpool phenotype) in only 7 out of the 50 genes suggesting that about 90% of the hits that emerged from the screen are likely to be caused by off-target effects linked to one of the pool's siRNA duplexes.

Based on the deconvolution experiments, we observed that MFAP1 (4 out of 4 oligos positive) represented the strongest hit. Also, we observed that depletion of ARL5A (3 out of 7 oligos positive) led to an interphase phenotype that was reminiscent of an abscission defect (Persistence of tubulin bridges between

interphase cells) and therefore we decided to focus our attention on ARL5A for a start.

3.4 The cytokinesis defect observed upon transfection of ARL5A siRNAs is an off-target effect

One of the top hits to emerge from the siRNA screen was ARL5A or ADP ribosylation factor-like 5A. ARLs belong to a subfamily of ARF-like proteins that are Ras related GTPases (Tamkun et al., 1991). ARL5A is a member of the ARL family of proteins and while its crystal structure has been solved (Wang et al., 2005), its function within the cell remains unknown. Transfection of two siRNA duplexes targeting ARL5A resulted in a penetrant and interesting phenotype; we observed more than 55% multi-nucleated cells indicating a defect in undergoing cytokinesis (Figure 13). Excitingly, we observed that even cells with a single nucleus were often connected to their neighbouring cells by tubulin bridges indicating a severe defect in cytokinetic abscission (Figure 13). Tubulin bridges exist in normal cells in the 1 to 2 h time window between cleavage furrow ingression and abscission. However, a higher proportion of cells with tubulin bridges was apparent upon transfection of ARL5A siRNAs retained a tubulin bridge. Closer inspection revealed that the staining pattern of tubulin in the intercellular bridges that we observed was different for ARL5A siRNA (Figure 13). Because the dense midbody structure that forms in the centre of the intercellular bridge acts as an impermeable barrier for the tubulin antibody, control cells usually present a staining pattern where the tubulin bridge is visualized with a small gap in the middle (Matuliene and Kuriyama, 2002, Zhao et al., 2006). This gap was absent in about 88% of anaphase and telophase cells treated with ARL5A siRNAs suggesting that midbody integrity was affected in cells devoid of ARL5A. We confirmed this by staining cells for the kinesin MKLP1, a component of the Centralspindlin complex and a key part of the midbody in animal cells (Matuliene and Kuriyama, 2002). The MKLP1 staining was significantly diminished in cells depleted of ARL5A (Figure 13) again suggesting that the midbody structure was poorly formed if cells were treated with siRNAs targeting ARL5A.

Because of the proclivity of siRNA screens to produce off target effects, we decided to perform quantitative real time PCR (qRT-PCR) experiments to assess the

correlation between the phenotype observed and the depletion efficiency of the target mRNA. We performed the qRT-PCR experiment using primers that were specific for ARL5A and used GAPDH primers as controls for the assay. Based on our imaging experiments, we observed the multi-nucleation and tubulin bridge phenotype in 2 out of the 6 siRNAs used against ARL5A. However, qRT-PCR results revealed that all 6 siRNAs were able to reduce ARL5A mRNA levels to a similar extent (Figure 13). Thus, the cellular phenotype of ARL5A siRNAs does not appear to correlate with the depletion efficiency of ARL5A mRNA. Closer inspection of the sequences of the two ARL5A siRNA duplexes that caused defective cytokinesis revealed a sequence overlap. This finding combined with the lack of correlation between depletion efficiency and the cellular phenotype strongly indicated that the observed cytokinesis phenotype was the result of an off-target effect.

We subsequently compared the sequence of the two effective ARL5A against the sequence of genes that were already known to regulate abscission. We observed that both ARL5A siRNAs that caused a cytokinesis defect (ARL5A siRNA 1 and 2) had sequence complementarity with the mRNA encoding CEP55 (Figure 14A). CEP55 is a midbody-associated protein that is required for midbody integrity and for recruiting the ESCRT machinery for abscission (Fabbro et al., 2005, Zhao, 2006, Lee et al., 2008, Bastos and Barr, 2010). Depletion of CEP55 causes late cytokinesis failure and strikingly causes midbody defects including the absence of the gap in tubulin staining. Thus, it is possible that the two ARL5A siRNA duplexes that cause cell division defects target CEP55 in addition to ARL5A. We tested this possibility by performing qRT-PCR using CEP55 specific primers for cells treated with all 6 siRNAs that were designed to target ARL5A. We observed that the 2 siRNAs that were causing the multi-nucleation and tubulin bridge phenotype in cells reduced CEP55 mRNA levels while the other 4 siRNAs did not (Figure 14B). We subsequently obtained similar results by performing immunoblotting for CEP55 protein levels (Figure 14C). Based on these data, we conclude that the cytokinesis phenotype that we observed after transfection of ARL5A siRNA duplexes is caused by an off-target effect, namely the depletion of the known cytokinesis regulator CEP55.

3.5 Depletion of MFAP1 causes abnormal nuclear morphology in interphase cells

Another hit to emerge from the primary siRNA screen was MFAP1, Microfibrillar Associated Protein 1. MFAP1 is protein that was found to be part of the tri-snRNP complex of the spliceosome (See section 1.3.2.1)(Jurica and Moore, 2003). Drosophila MFAP1 was shown to be essential for pre-mRNA splicing and interestingly, for G2/M transition (Andersen and Tapon, 2008). Depletion of MFAP1 resulted in fragmented and multilobed interphase nuclei indicating a defect in mitotic chromosome segregation (Figure 15). All 4 siRNA duplexes targeting MFAP1 efficiently depleted the protein as evidenced by qRT-PCR experiments using MFAP1 specific primers and also by immunoblotting experiments using MFAP1 antibodies and caused a cellular phenotype (Figure 15). These data strongly suggest that, unlike ARL5A above, the phenotype observed is caused by the loss of MFAP1 protein.

To decisively test the hypothesis that loss of MFAP1 causes nuclear morphology defects, we decided to develop a genetic complementation system using an siRNA-resistant transgenic allele of MFAP1. We obtained the cDNA coding for MFAP1 (Source Bioscience) and introduced the silent mutations in the target sequence of siRNA3 (See section 2.2.2 and 2.3.2 for methodology used) creating MFAP1-r. We also added a tandem N-terminal AcGFP-FLAG (Aequorea coerulescens Green Fluorescent Protein-FLAG, referred to as AcFL henceforth) tag to MFAP1-r. Using the resulting transgene, we generated a clonal stable cell line that expressed the transgene in more than 95% of the cells and at a level comparable to the endogenous counterpart (Figure 16). Subsequently, we tested the ability of the transgene to rescue the nuclear morphology defect upon depletion of the endogenous protein by siRNA transfection. Depletion of endogenous MFAP1 disrupted nuclear morphology in more than 50% of cells expressing only the AcFL tag. Expression of the RNAi-resistant MFAP1 transgene potently suppressed the interphase phenotype (Figure 16). Interestingly, we also observed that the level of endogenous MFAP1 is reduced in the MFAP1 transgenic cell line indicating the action of protein copy number or stability control mechanisms. Our experiments establish that loss of MFAP1 causes an interphase nuclear morphology defect.

This finding prompted us to investigate the underlying reason for this cellular defect and to probe the function of MFAP1 in maintaining nuclear integrity.

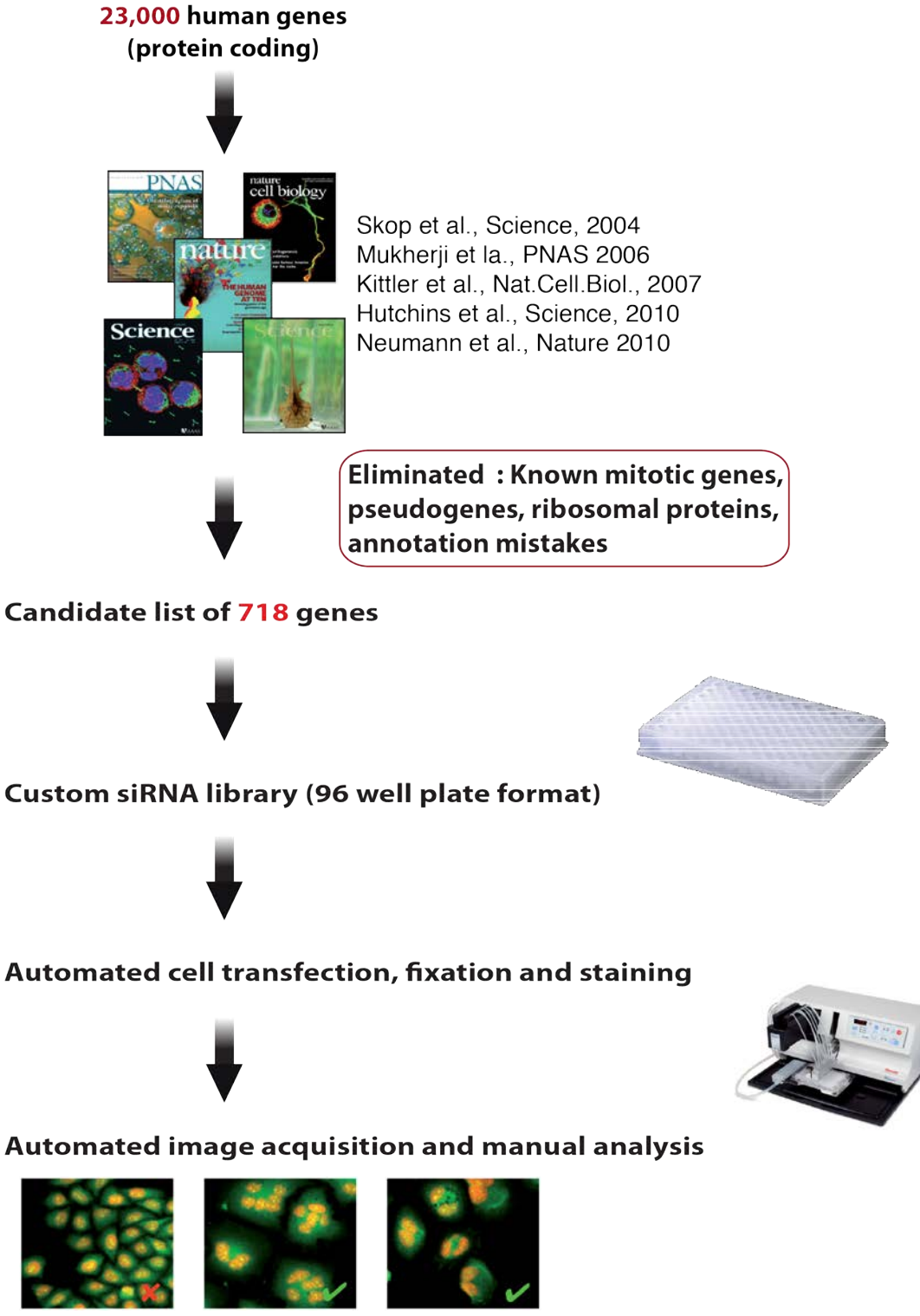

Figure 9 Workflow scheme for the functional genomic screen using genome-wide screens and proteomic datasets as a starting point

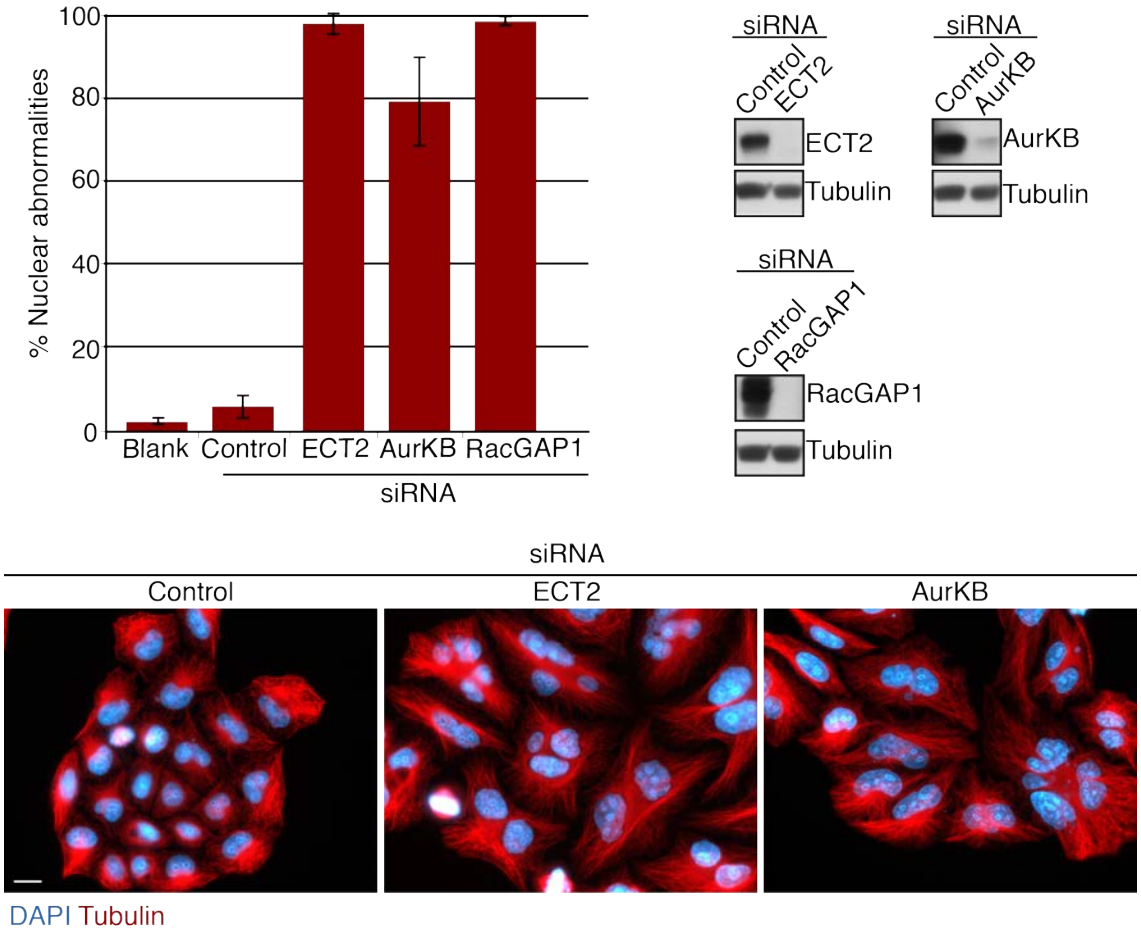

Figure 10 Penetrant mitotic defects in HeLa Kyoto cells transfected with siRNAs targeting known cell division factors

HeLa Kyoto cells transfected with indicated siRNA duplexes (37.5 nM) were analyzed 48 h post transfection. Quantification of the percentage of nuclear abnormalities (upper left panel) (n > 200 cells, error bars represent mean ± SD of 3 independent experiments). Whole cell extracts were analyzed by immunoblotting using the indicated antibodies (upper right panel). Immunofluorescence image of mono-nucleate control cells and ECT2-depleted multinucleated cells (lower panel, scale bar = 16 µm).

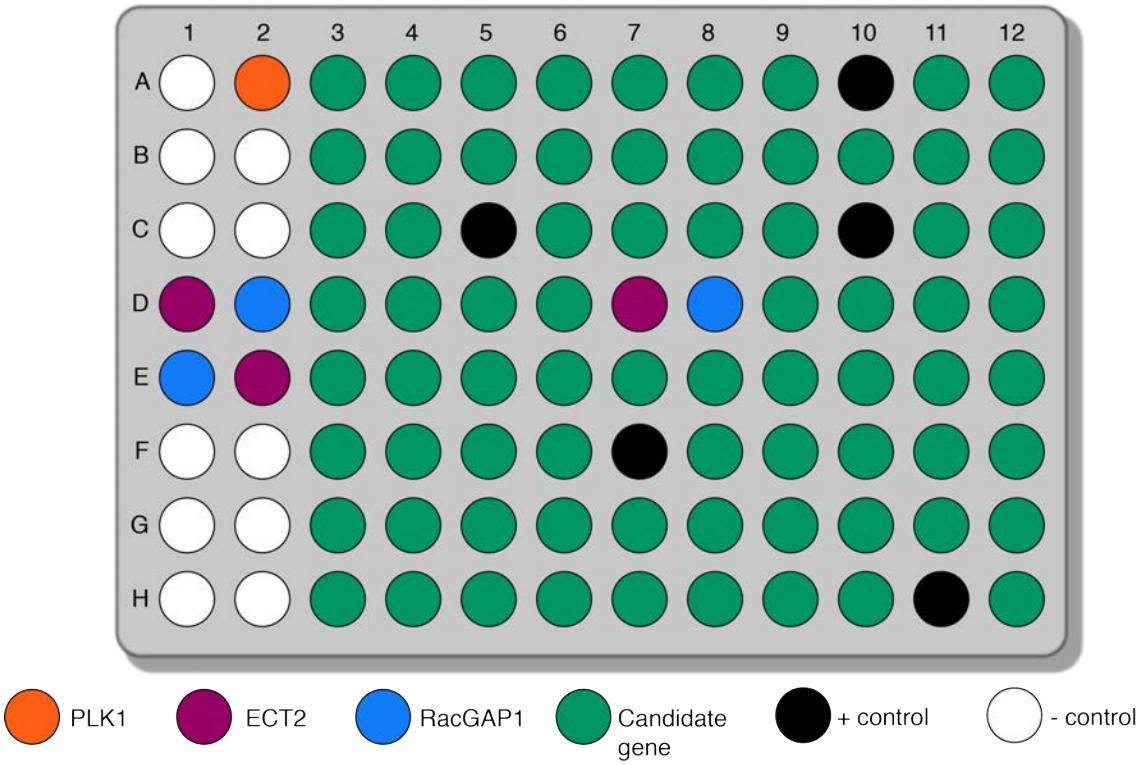

Figure 11 Arrangement of candidate genes for siRNA screen

Illustrative plate arrangement map used in the siRNA screen. siRNA smartpools directed against the 718 genes were distributed across ten 96-well plates (in green). Positive controls against known regulators of mitosis and cytokinesis were randomly distributed across all ten plates (shown here in black). Also, the positions D7 and D8 were reserved for siRNA smartpools against ECT2 and RacGAP1 respectively in all ten plates. During the dilution of the master siRNA plate and the subsequent aliquoting process, the liquid handling robot deposited siRNA smartpools in all the wells except for the first two columns, which were left blank. At the time of transfection, siRNA duplxes against Plk1 (well A2, in orange), ECT2 (wells D1 and E2, in purple), RacGAP1 (wells D2 and E1, in blue) and non-targeting control siRNAs (either RISC free or SiGENOME control siRNAs, in white), were added manually.

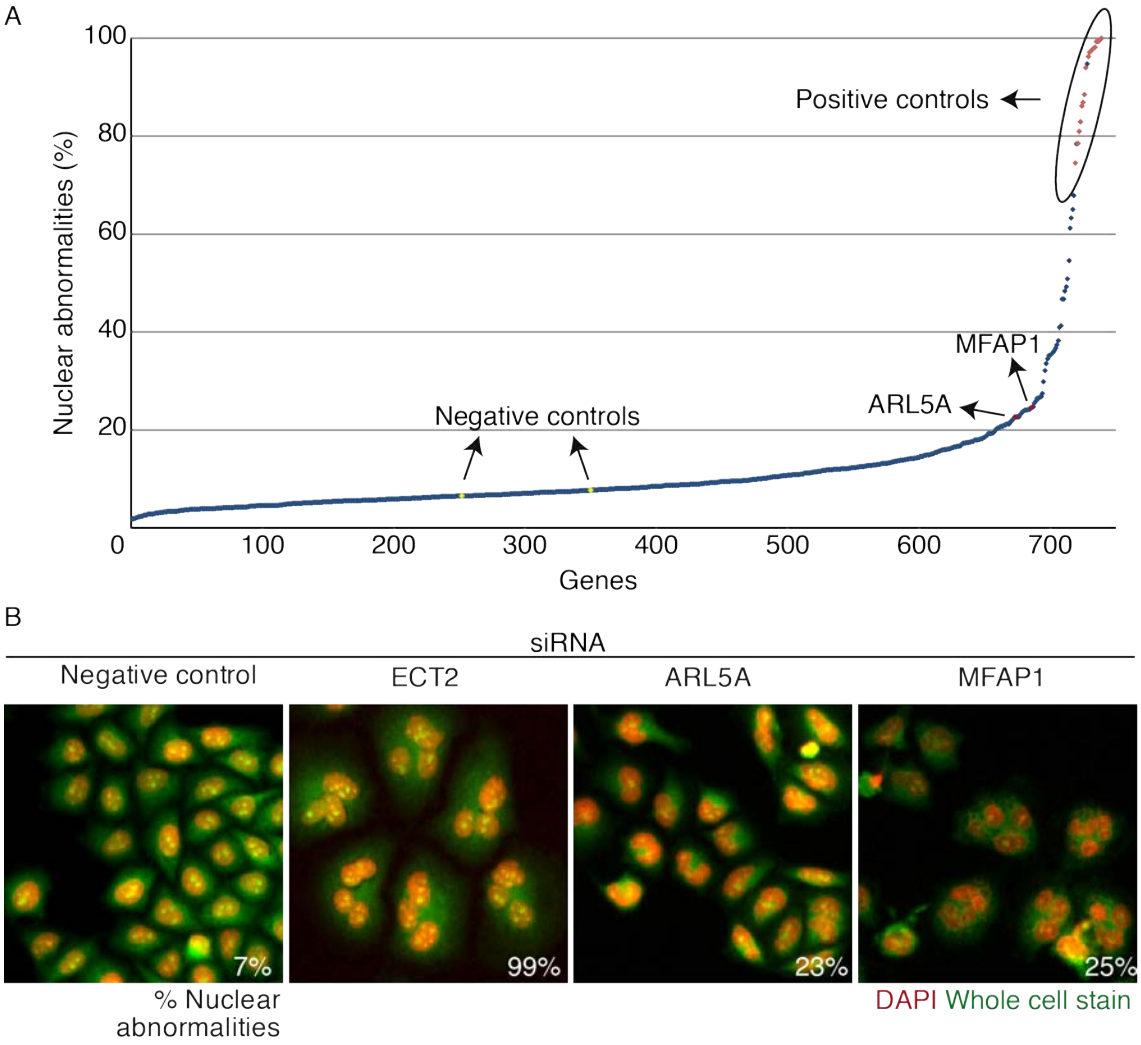

Figure 12 Primary siRNA screen results

(A) HeLa Kyoto cells were seeded onto 96 well plates pre-spotted with the siRNA duplexes (37.5 nM) and transfection reagent. Cells were grown for 52 h and then analyzed by fluorescence microscopy. Quantification of the percentage of multinucleate cells or cells with abnormal nuclei (n > 300 cells. Data points represent the median value from three independent experiments). For a detailed list of genes targeted and phenotypic penetrance, please refer to the appendix. (B) Representative images from the screen shows mononucleate control cells, ECT2-depleted positive control cells as well as cells treated with siRNAs against ARL5A and MFAP1.

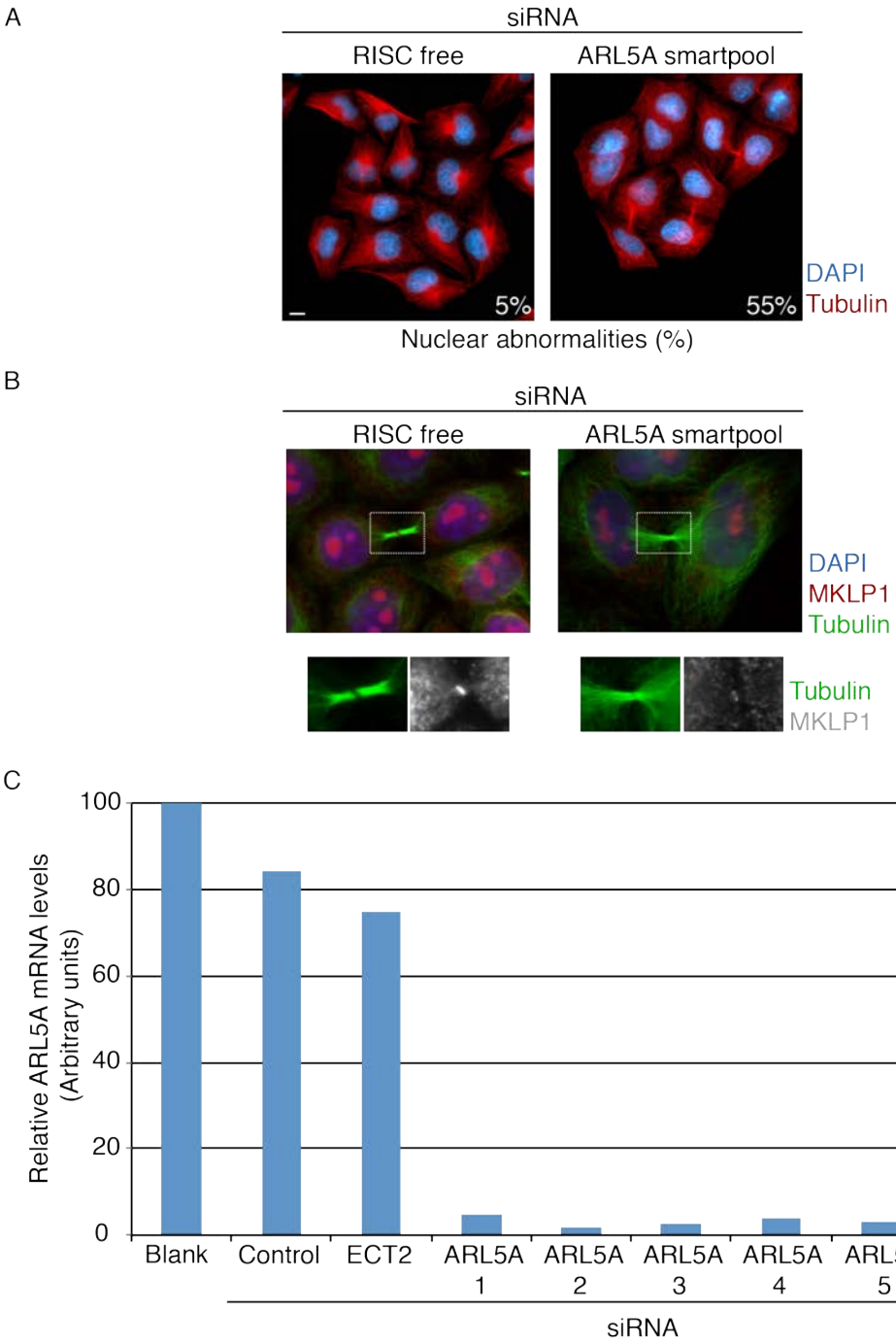

Figure 13 Depletion of ARL5A leads to multinucleation and cells connected by tubulin bridges

(A) HeLa Kyoto cells transfected with indicated siRNA duplexes (37.5 nM) were analyzed 52 h post transfection. Immunofluorescence images. Scale bar = 10 µm. (B) Cells treated as above were stained for a midbody marker MKLP1, tubulin and DAPI to assess midbody stability. (C) HeLa Kyoto cells treated with indicated siRNAs were grown for 52 h and processed for qRT-PCR analysis. Quantification of the mRNA levels as assessed using ARL5A specific primers. ARL5A siRNAs1 and 2 but not 3-6 show cytokinesis defect

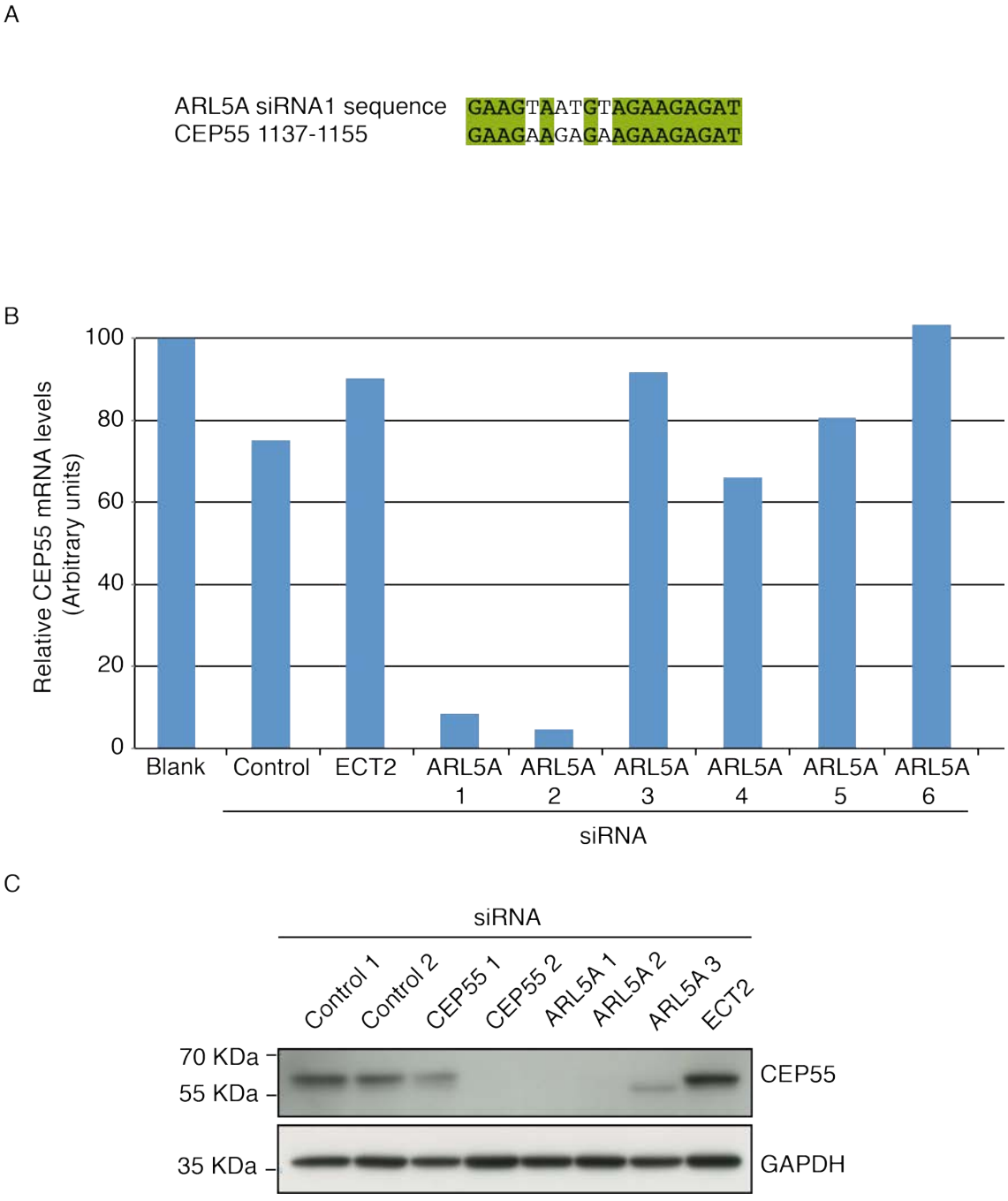

Figure 14 ARL5A siRNAs1 and 2 also deplete CEP55.

(A) Sequence alignment of the recognition sequence of ARL5A siRNA1 with CEP55 reveals strong similarity between the two raising the possibility of an off-target effect. (B) HeLa Kyoto cells transfected with indicated siRNA duplexes (37.5 nM) were grown for 48 h and then processed for qRT-PCR analysis. CEP55 mRNA levels were quantified using CEP55 specific primers. (B) Cells were treated with the indicated siRNAs and after 48 h, were treated with 50 nM of nocodazole overnight to synchronize them in mitosis. Whole cell extracts of mitotic cells so isolated were analyzed by immunoblotting using the indicated antibodies.

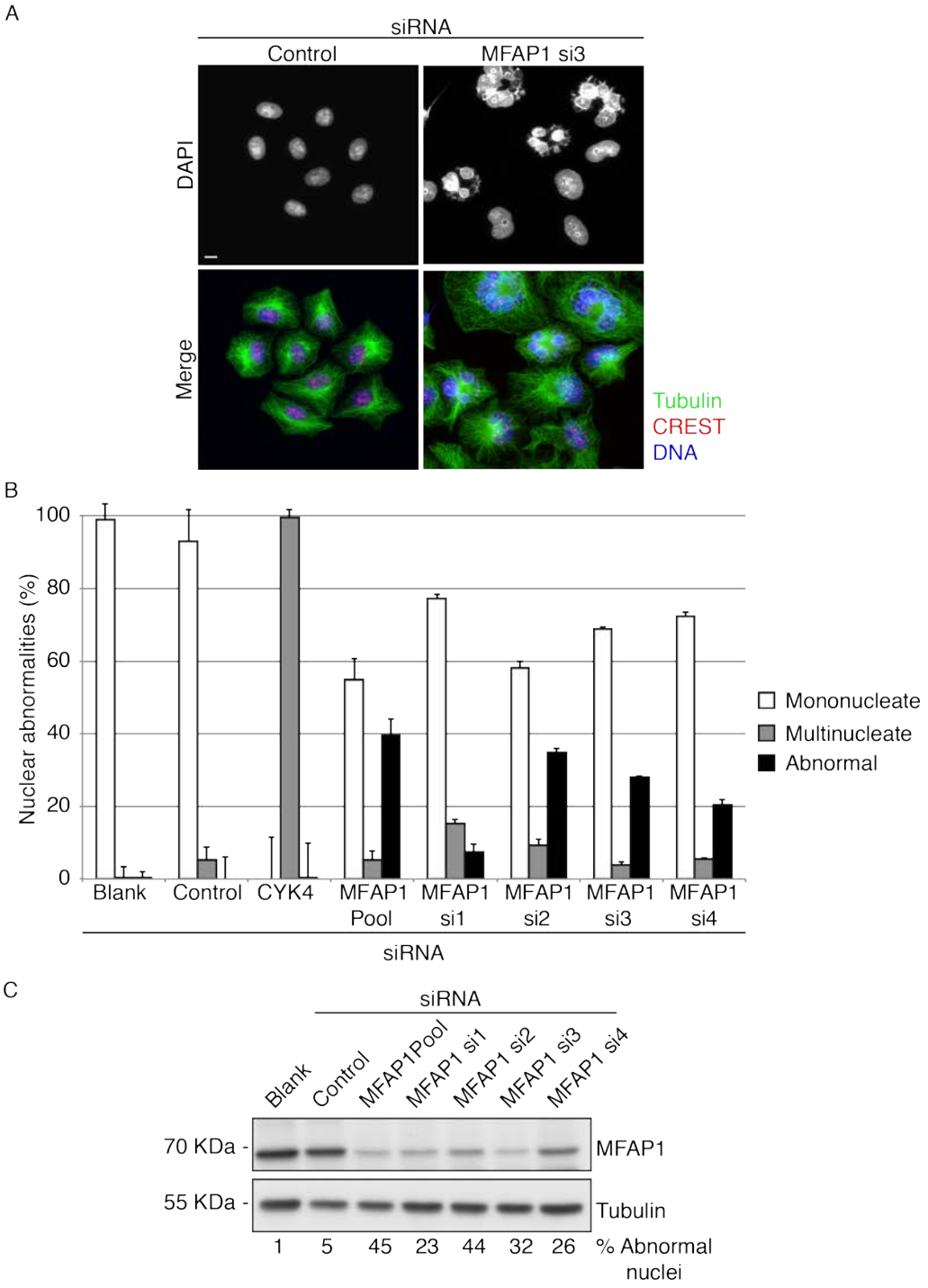

Figure 15 Depletion of MFAP1 results in abnormal nuclear morphology in interphase cells

(A) HeLa Kyoto cells transfected with indicated siRNA duplexes (37.5 nM) were analyzed 72 h post transfection. Immunofluorescence image of mono-nucleate control cells and MFAP1 depleted cells. Scale bar = 10 µm. (B) Quantification of the percentage of nuclear abnormalities of cells treated as above (n > 200 cells, bars represent mean ± SD of 3 independent experiments). (C) Whole cell extracts of cells treated as in (A) were analyzed by immunoblotting using the indicated antibodies 72 h post transfection of the indicated siRNAs.

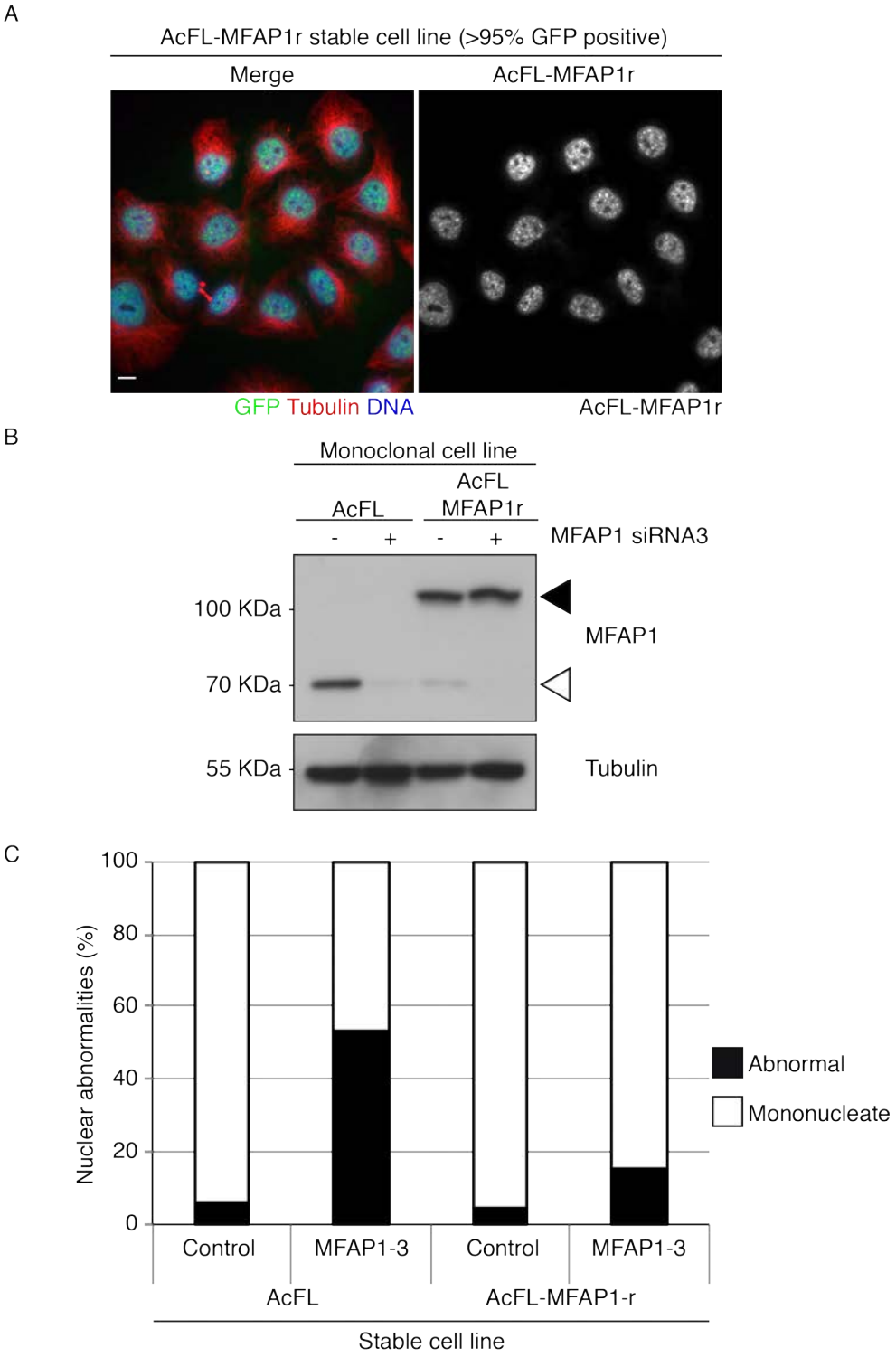

Figure 16 A genetic complementation system for MFAP1

(A) A clonal cell line stably expressing a siRNA resistant transgenic copy of MFAP1 was generated by introducing silent mutations within the MFAP1 siRNA 3 recognition sequence of MFAP1 cDNA. After transient transfection into HeLa Kyoto cells, a clonal cell line was generated through selection with puromycin (0.4 µg/mL). Immunofluorescence image of the above mentioned cell line fixed and stained for GFP to reveal percentage of cells expressing transgene (n> 200 cells, scale bar = 10 µm).

(B) The clonal cell lines expressing either the tagged MFAP1 transgene or the tag alone were transfected with indicated siRNA duplexes (37.5 nM) for 48 h after which they were treated with 50 nM of nocodazole overnight to synchronize them in mitosis. Whole cell extracts of mitotic cells so isolated were analyzed by immunoblotting using the antibodies against MFAP1 and β-tubulin as a loading control (middle panel). Endogenous MFAP1 and transgenic AcGFP-FLAG tagged MFAP1 are indicated by open and filled arrowheads respectively. (C) Quantification of the percentage of nuclear abnormalities in the clonal cell lines treated with the indicated siRNAs cells (n > 200 cells, N=3 independent experiments).

Chapter 4. Results 2- Elucidating the mitotic consequences of MFAP1 loss

4.1 Depletion of MFAP1 causes a spindle assembly checkpoint dependent mitotic arrest

The striking interphase nuclear morphology defect observed upon depletion of MFAP1 indicates that errors during mitotic chromosome segregation could be the underlying cause. To test this hypothesis, we decided to investigate the timing and the dynamics of mitosis in cells lacking MFAP1. We recorded HeLa Kyoto cells that were transfected with either individual siRNAs targeting MFAP1 or control siRNA duplexes using bright-field time-lapse microscopy. Cells that were treated with control siRNA entered mitosis and exited successfully with an average duration of 45 min (Figure 17B). Cells transfected with siRNA against MFAP1 on the other hand spent over 12.5 h on average in mitosis. Accompanying the long mitotic arrest, most cells depleted of MFAP1 either underwent cell death during mitosis or an abnormal mitotic exit characterized by a failure to separate daughter cells (Figure 17B). The latter is likely the result of mitotic slippage (Brito and Rieder, 2006). These results demonstrate that MFAP1 is required for the timely execution of mitosis and that loss of the protein causes cells to arrest in mitosis for long periods of time. The corollary of these observations is that the interphase defect observed in MFAP1-depleted cells in our screen, could be the consequence of mitotic defects.

Progression through mitosis and mitotic exit requires the proteolytic destruction of cyclin B that is initiated by the E3 ubiquitin ligase APC/C (Golan et al., 2002, Kramer et al., 2000, Pines, 2011) (Also See section 1.1.4.2). APC/C activity is controlled by the spindle assembly checkpoint (SAC), that inhibits the complex's activity in response to chromosomes that have to establish bipolar attachment to the mitotic spindle (Musacchio and Salmon, 2007). Defects in several processes and pathways during mitosis, e.g. spindle formation, kinetochore function and sister chromatid cohesion, can trigger a SAC response and arrest cells in mitosis. The mitotic arrest in MFAP1-depleted cells could be caused by compromised APC/C activity and maybe due to the engagement of the SAC. To test this hypothesis, we depleted MFAP1 in combination with a key component of the SAC, Mad2.

Depletion of Mad2 alone reduced the average duration of mitosis from 45 min in control cells to less than 20 min (Figure 17C). Importantly, co-depletion of MFAP1 and Mad2 reduced the average duration in mitosis from 12.5 h to less than 20 min (Figure 17A and Figure 17C). This demonstrates that the mitotic arrest in cells lacking MFAP1 is dependent on the SAC. Furthermore, this observation suggests that the underlying aberration in cells lacking MFAP1 is a potent trigger for the engagement of the SAC.

4.2 Loss of MFAP1 abrogates chromosome alignment at the metaphase plate.

Given the SAC-dependent mitotic arrest observed upon depletion of MFAP1 (Figure 17), we tested the ability of MFAP1-depleted cells to align their chromosomes at the metaphase plate. While a failure to align chromosomes at the metaphase plate could arise because of a number of reasons, it can often act as a potent inducer of an SAC response. We transfected HeLa Kyoto cells with either control or MFAP1 siRNA and tested their ability to form a metaphase plate using immunofluorescence microscopy (Figure 18). Control cells were distributed at prometaphase, metaphase and anaphase, as judged by staining for DNA, Aurora-B kinase and the kinetochore/centromere marker CREST (Figure 18). Strikingly, MFAP1 siRNA treated cells were trapped in prometaphase and never managed to progress through to metaphase or anaphase (Figure 18). We could reliably distinguish between prometaphase and anaphase stages based on the localization pattern of Aurora B that shifts from the centromeres in prometaphase to the midzone in anaphase (Gruneberg et al., 2004).

Prior to fixation, a subset of cells were also treated with the proteasome inhibitor MG132, which traps cells at metaphase due the inability to degrade mitotic APC/C substrates such as cyclin B and securin (Pines, 2011). MG132 addition to control cells caused an accumulation of metaphase cells with aligned chromosomes (Figure 18). However, no such enrichment was evident in MFAP1 siRNA-treated cells, in which chromosome remained scattered throughout the mitotic cell (Figure 18). These results suggest that cells lacking MFAP1 were unable to align their chromosomes at the metaphase plate, even when provided with ample time by blocking mitotic progression using MG132. We speculate that this could be the

reason for triggering the spindle assembly checkpoint culminating a prominent mitotic arrest.

4.3 Depletion of MFAP1 causes precocious loss of sister chromatid cohesion

The inability of MFAP1 depleted cells to align their chromosomes at the metaphase plate suggested to us that either the mitotic spindle was malformed or that integrity of the chromosomal or kinetochore architecture was affected. Sister chromatid cohesion is essential for chromosome bi-orientation and alignment at the metaphase plate (Nasmyth and Haering, 2009, Peters and Nishiyama, 2012). To scrutinize the state of sister chromatid cohesion, we decided to perform metaphase chromosome spreads in control siRNA and MFAP1 siRNA-transfected cells (Figure 19). HeLa Kyoto cells were grown for 52 h after siRNA transfection and treated with 330 nM of nocodazole for 4 h prior to processing for chromosome spreads. An siRNA targeting Sgol1, a protein known to protect centromeric sister chromatid cohesion in mitotic cells (Salic et al., 2004, McGuinness et al., 2005, Goulding and Earnshaw, 2005, Wang and Dai, 2005, Watanabe and Kitajima, 2005, Tang et al., 2006) was used as a positive control for loss of sister chromatid cohesion (Figure 19). The vast majority of cells that were transfected with control siRNAs displayed the characteristic X-shaped chromosome structure, in which the sister chromatids remain physically connected at the centromeres (Figure 19). In contrast, depletion of Sgol1 potently abrogated sister chromatid cohesion (Figure 19). Interestingly, depletion of MFAP1 using four different siRNA duplexes led to severe defects in sister chromatid cohesion (Figure 19). More than half of spreads originating from cells transfected with MFAP1 siRNA duplexes 1 and 3 showed individualized sister chromatids that have lost the characteristic chromosomal X-shape (Figure 19). The fact that 4 independent siRNA duplexes resulted in a cohesion phenotype and the correlation between depletion efficiency and phenotypic penetrance (Figure 15) suggests that MFAP1 is required for sister chromatid cohesion. Our data furthermore indicates that the loss of sister chromatid cohesion could be the

underlying cause for the mitotic arrest and chromosome alignment phenotype of MFAP1-depleted cells.

4.4 FISH in mitotic cells confirms loss of sister chromatid cohesion following depletion of MFAP1

In order to complement the chromosome spread assays, we decided to test the status of sister chromatid cohesion by performing fluorescent *in situ* hybridization (FISH) in intact fixed mitotic cells. HeLa Kyoto cells were treated with negative control siRNA or siRNAs targeting MFAP1, Sgol1 and also Sororin, a gene required for sister chromatid cohesion maintenance in mammalian cells (Rankin et al., 2005, Schmitz et al., 2007, Nishiyama et al., 2010). FISH probes recognizing the centromeres of chromosome 6 and 8 were used for assessing the status of cohesion. Since HeLa Kyoto cells are trisomic for chromosome 6 and 8, control siRNA treated cells displayed 3 pairs of dots for each of the 2 probes used. In more than 84% of control cells, paired sister chromatid signals were never more than 2 µm apart even at metaphase, the stage where they were likely to be farthest apart due to the tension exerted by the mitotic spindle (Figure 20A). FISH analysis of cells transfected with Sororin and Sgol1 siRNA duplexes revealed that most sister centromeres were separated by more than 2 µm (Figure 20), indicative of a loss of sister chromatid cohesion. Similarly, depletion of MFAP1 also led to a majority of cells to displaying sister centromeres separated by more than 2 µm (Figure 20). These results confirm our observations made by chromosome spreading analysis (Figure 19) and suggest the loss of MFAP1 disrupts cohesion between sister chromatids also in intact mitotic cells.

4.5 An siRNA resistant MFAP1 transgene can rescue loss of sister chromatid cohesion caused by loss of endogenous MFAP1

As shown in Figure 16, we developed a genetic complementation system for MFAP1, wherein we could demonstrate that a cell line stably expressing a siRNA-resistant transgene of MFAP1 could rescue the abnormal nuclear morphology in interphase cells lacking endogenous MFAP1. Having identified a severe loss of sister chromatid cohesion in cells lacking MFAP1, we tested the ability of the

siRNA-resistant transgene to suppress this phenotype. Expression of siRNA-resistant AcFL-MFAP1-r but not the AcFL tag alone reduced substantially but not completely restored sister chromatid cohesion in cells transfected with siRNA targeting endogenous MFAP1 (Figure 21). Together with our finding that 4 independent siRNA duplexes targeting MFAP1 disrupt cohesion (Figure 19), this result strongly suggests that the loss of sister chromatid cohesion is caused by depletion of MFAP1 and not by an off-target effect. The failure of the transgene to completely restore the state of sister chromatid cohesion (Figure 21) could be due to the AcFL tag interfering with protein functionality.

4.6 Conclusions: Results 2- Elucidating the mitotic effect of MFAP1 depletion

Based on the experiments discussed above, we have established that the loss of MFAP1 in HeLa Kyoto cells can cause a spindle assembly checkpoint-dependent mitotic arrest that eventually leads to cell death or to cells exiting mitosis in an abnormal manner. The abnormal mitotic exit could explain the irregular interphase nuclear morphology observed in these cells. We have further deciphered that the prolonged mitotic arrest is accompanied by the inability of MFAP1 depleted cells to form a metaphase plate. Our chromosome spreads and FISH analysis suggest that a precocious loss of sister chromatid cohesion is likely to be responsible for this phenomenon. Through our experiments, we have uncovered a novel regulator of sister chromatid cohesion in mammalian cells. Further work described in the subsequent sections led us to an in-depth investigation and analysis of the molecular mechanism underlying this novel finding.

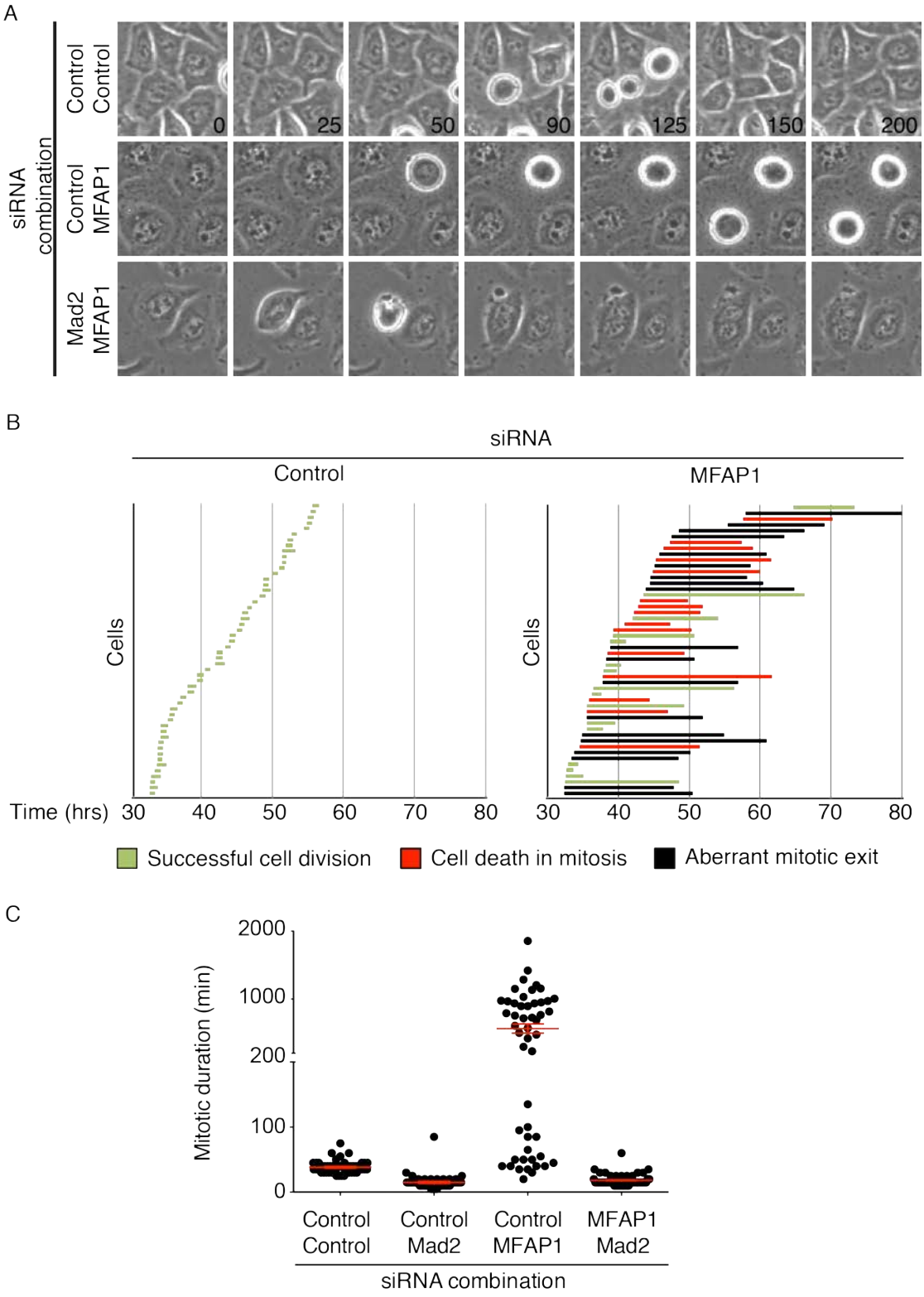

Figure 17 Depletion of MFAP1 leads to SAC-mediated mitotic arrest

(A) HeLa Kyoto cells treated with the indicated combination of siRNAs for 24 h were subjected to low-resolution time-lapse microscopy (time in min). The images so acquired were analysed using the mitotic duration plugin in ImageJ. (B) Cells were scored for duration between mitotic cell rounding and anaphase onset (middle panel).

The x-axis of the graph represents time (h) after siRNA transfection. In the graph, the cells are arranged according to their time of mitotic entry. Each bar in the graph represents one cell and the length of the bar denotes the duration that each cell spends in mitosis. Green bars = successful division, black bars = unsuccessful and abnormal mitotic exit) and red bars = cell death. (n=50 cells, N=1) (C) Cells that were treated with a combination of siRNAs against MFAP1, Mad2 and control were recorded over time and analysed with the mitotic duration plugin as above. Each dot represents mitotic duration in one cell (Lower panel, n=50 cells, N=1. Bars represents mean ± SD).

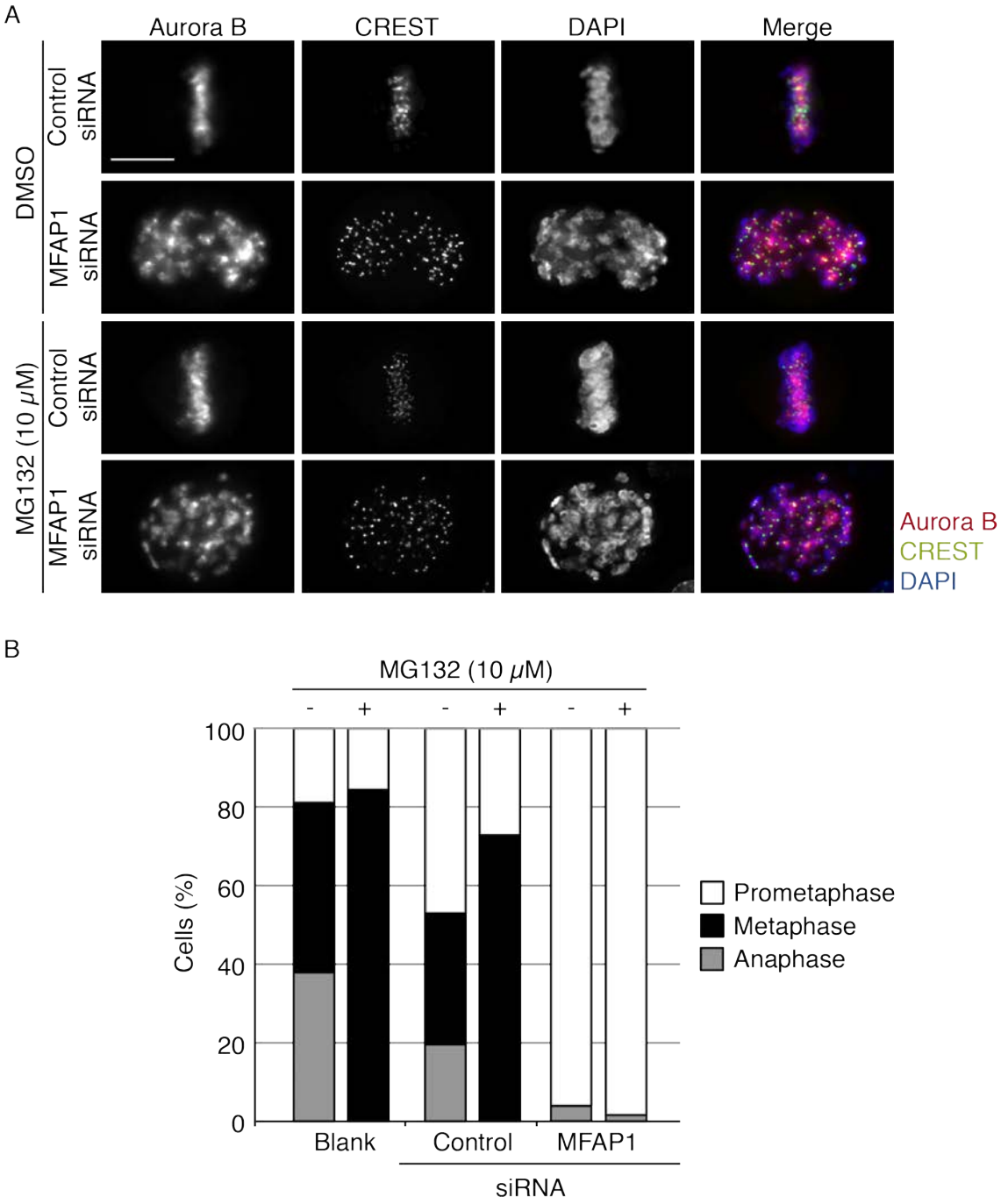

Figure 18 MFAP1 depletion prevents chromosome alignment at the metaphase plate

(A) In order to test the ability of siRNA treated cells to form a metaphase plate, HeLa Kyoto cells transfected with indicated siRNAs were grown for 48 h following which they were treated with either DMSO or MG132 (10 μM) for 3 h, fixed and stained for Aurora B kinase, CREST and DAPI. Immunofluorescence images of cells treated with control or MFAP1 siRNA with or without MG132 treatment are shown. Scale bar = 10 μm. (B) Samples treated as above were scored for proportion of cells in different mitotic phases as indicated (lower panel, n> 50 cells, N=1)

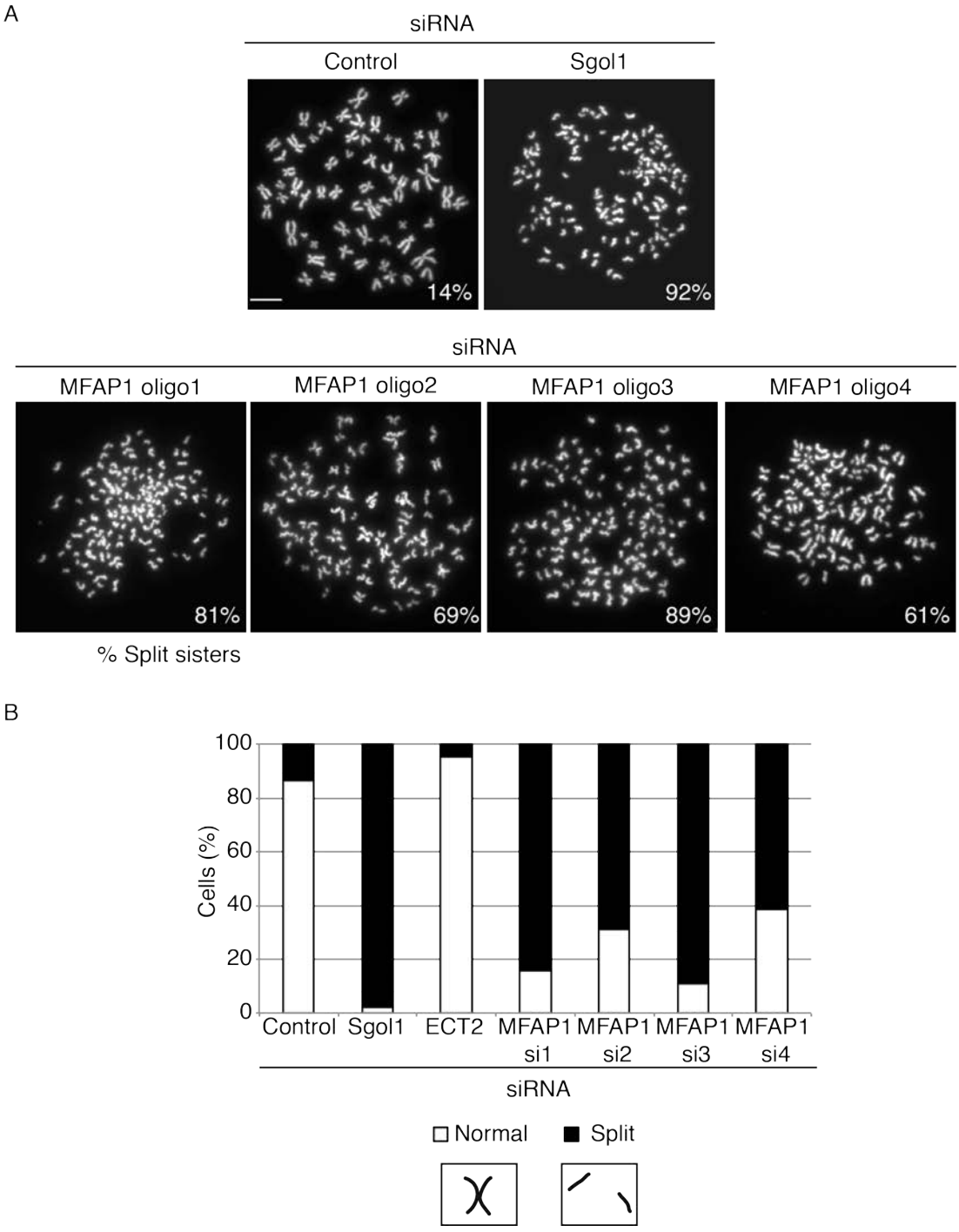

Figure 19 Precocious loss of sister chromatid cohesion is evident upon loss of MFAP1

(A) Hela Kyoto cells transfected with the indicated siRNAs were grown for 52 h and then treated with nocodazole (330nM) for 4 h prior to processing them for chromosome spreads. Images of DAPI stained chromosome spreads from cells treated with the indicated siRNAs are shown. Scale bar = 10 µm. (B) Samples treated as above were scored for the proportion of cells in different states of sister chromatid cohesion. Sgol1 was a positive control for loss of sister chromatid cohesion while ECT2 was a control for transfection efficiency (n> 100 cells, N=1)

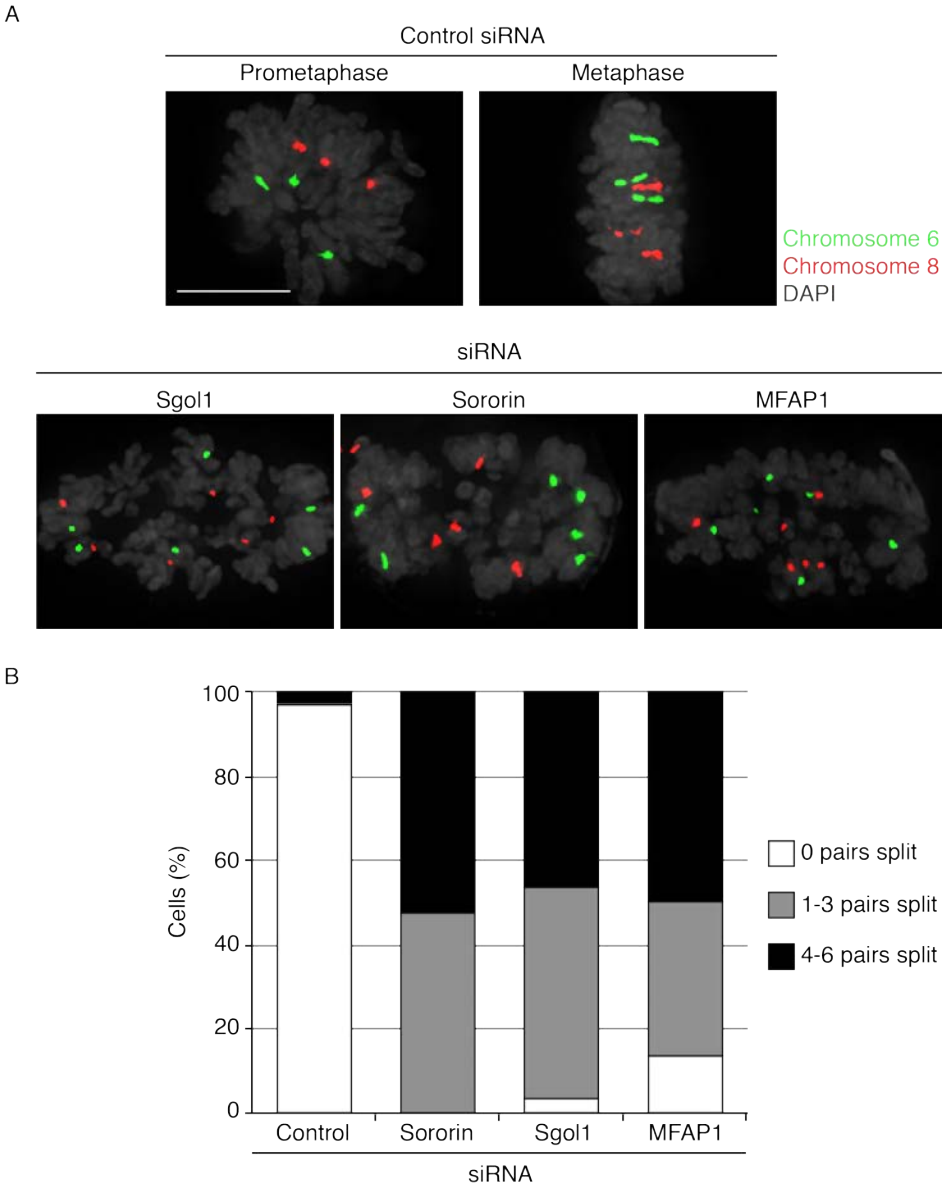

Figure 20 Mitotic FISH confirms the loss of sister chromatid cohesion in MFAP1 depleted cells

(A) HeLa Kyoto cells were transfected with the Control and MFAP1 siRNA3 (37.5 nM) for 48 hrs and with Sgol1 and Sororin (37.5 nM) for 24 hrs following which they were fixed and processed for fluorescence *in situ* hybridization (FISH). Centromeric probes against chromosomes 6 and 8 and DAPI as a counterstain for the DNA were used. Images of cells treated as above were acquired. Scale bar = 10μm. (B) Images so acquired were scored for proportion of cells in different states of sister chromatid cohesion using the number of paired FISH signals as proxies. More than 84% of control cells exhibited a distance no more than 2 μm between paired FISH signals even in metaphase, where they are likely to be farthest apart. Cells wherein the distance between FISH signals was longer than 2 μm were considered to have split sisters. This criteria was applied to cells treated with the indicated siRNA duplexes and the proportion of split sisters in each treatment condition was plotted as shown (n> 30 cells, N=1).

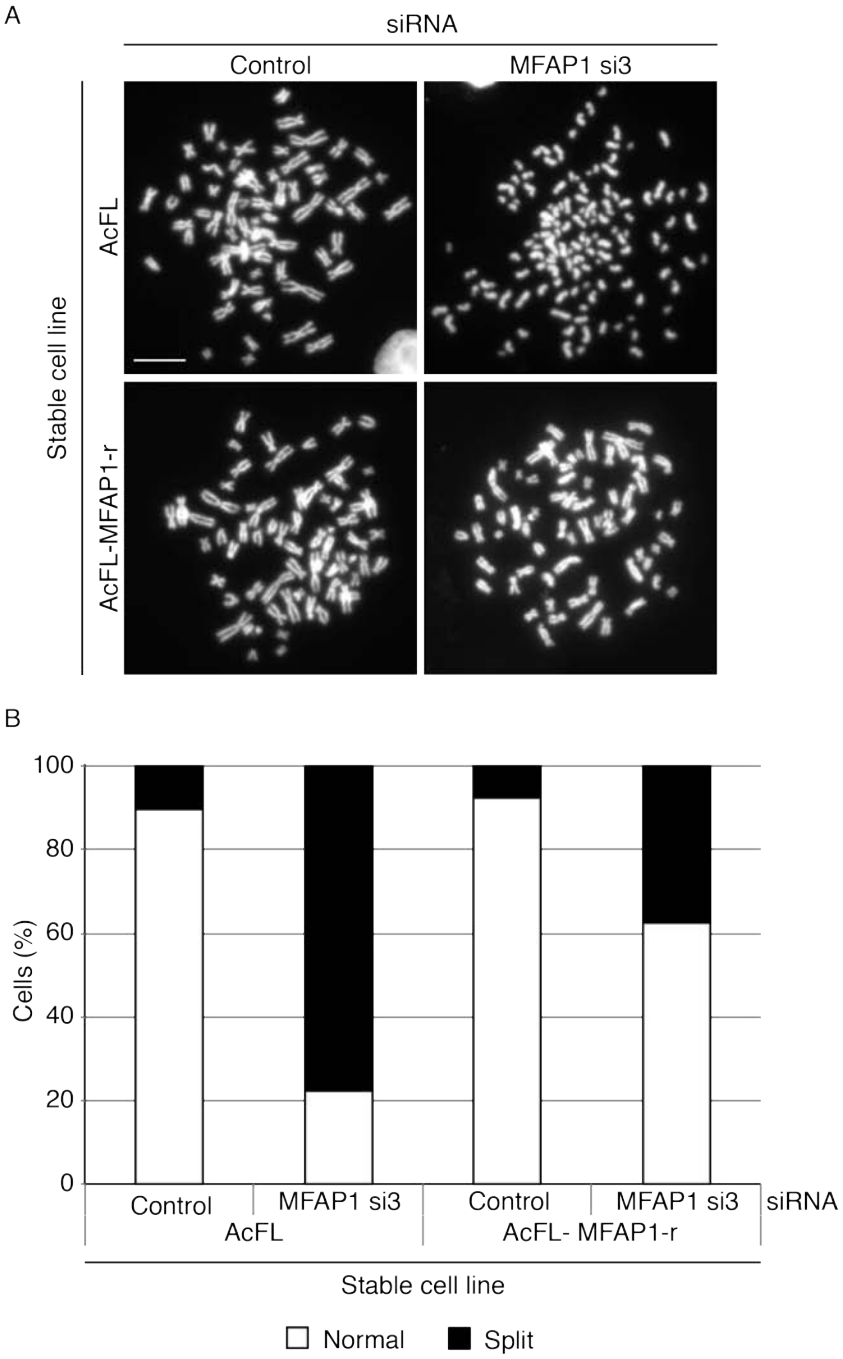

Figure 21 An siRNA-resistant transgene of MFAP1 suppresses the loss of sister chromatid cohesion in cells lacking endogenous MFAP1

(A) Stable cell lines expressing either an AcGFP-FLAG (AcFL) tagged siRNA resistant MFAP1 (AcFL-MFAP1-r) or the AcFL tag alone were transfected with the indicated siRNAs at a final concentration of 37.5 nM. Following transfection, they were grown for 52 h and then treated with nocodazole (330nM) for 4 h and then processed for chromosome spreads. Images of DAPI-stained chromosome spreads from cells treated with the indicated siRNAs (upper panel, scale bar = 10 μm). (B) Samples treated as above were scored for the state of sister chromatid cohesion. (n> 100 cells, Bars represent mean from 3 independent experiments).

Chapter 5. Results 3- Subset of genes regulating pre-mRNA processing also regulate sister chromatid cohesion

Based on the experiments described before, we have uncovered a novel role for MFAP1 in regulating sister chromatid cohesion in human cells. MFAP1 is known to be a key part of the tri-snRNP complex that is required for the formation of the spliceosomal B complex (Jurica and Moore, 2003, Zhou et al., 2002) and was also shown to regulate pre-mRNA splicing and G2-M transition in drosophila cells (Andersen and Tapon, 2008). Interestingly, a large number of splicing components have been identified in the Mitocheck genome-wide analysis of cell division as genes, which cause mitotic abnormalities, in particular a mitotic arrest, when depleted (Neumann et al., 2010). This has led to speculations as to the underlying molecular defect and function of splicing components during cell division (Hofmann et al., 2010). Our finding that depletion of MFAP1 disrupts sister chromatid cohesion raised the possibility that additional spliceosome-associated factors control mitosis through sister chromatid cohesion. This could provide an explanation for their prevalence as hits in mitotic screens. Based on these considerations, we decided to test whether spliceosome components other than MFAP1 are required for cohesion by expanding our analysis to a bigger set of splicing factors. The components of the spliceosome have been uncovered by using mass spectrometry techniques (Zhou et al., 2002). After comparing the list of splicing factors identified by mass spectrometry with the data from the Mitocheck screen, we compiled a list of 33 splicing factors of interest (Neumann et al., 2010, Hofmann et al., 2010). Initial characterization of these genes and detailed characterization of a subset of these genes will be described in the following sections.

5.1 Chromosome spread screen identifies a further group of splicing factors that regulate sister chromatid cohesion in human cells

Based on the list of 33 splicing factors that we generated, we used siGENOME smartpool siRNAs to deplete the corresponding proteins and investigated the state of sister chromatid cohesion by chromosome spread analysis (Figure 22). Known regulators of sister chromatid cohesion such as Sgol1 (Kitajima et al., 2004, Salic et al., 2004, Goulding and Earnshaw, 2005, McGuinness et al., 2005, Watanabe and Kitajima, 2005) and the core cohesion subunit Scc1 (Sonoda et al., 2001, Uhlmann et al., 1999, Gruber et al., 2003, Adachi et al., 2008, Nasmyth and Haering, 2009, Peters and Nishiyama, 2012) were used as positive controls for the assay. Strikingly, depletion of all but 3 of the 33 spliceosome-associated proteins led to significant loss of sister chromatid cohesion (Figure 22 and Figure 23). Our results using siRNA smartpools suggest a widespread requirement of splicing factors in sister chromatid cohesion. The phenotypic penetrance of many gene depletions was comparable to the loss of a core cohesin subunit, such as Scc1 (Figure 22). This further emphasizes the importance of investigating the role of these genes and splicing in general in sister chromatid. Additionally we observed that the splicing factors whose depletion affected sister chromatid cohesion were not restricted to a particular sub-complex of the spliceosome and were not involved in a specific step of spliceosome assembly. Instead, they were distributed throughout the spliceosome assembly process and were each part of multiple snRNP complex. This suggests the requirement of not only a specific complex but generally of pre-mRNA splicing in sister chromatid cohesion (Figure 24).

5.2 Deconvolution analysis supports the role of a number of splicing factors in sister chromatid cohesion

The chromosome spread screen of spliceosome components as described above revealed that the majority of the splicing factors that we selected and tested, disrupted the connection between sister chromatids. Next, we decided to use deconvolution analysis to evaluate whether the observed phenotypes were likely

caused by depletion of the intended target than an off-target effect. In that direction, we first classified the genes that we identified based on the particular step of the pre-mRNA splicing that they were thought to be a part of (Figure 24). Based on the distribution and the relative phenotypic penetrance of the hits, we selected the top 2 hits from each spliceosome sub complex (shown in Figure 24) for further analysis. Using the individual siRNA duplexes that make up the smartpool mixture for the 10 genes selected as per the criteria set above, we performed chromosome spread analyses. We observed that for 9 out of the 10 genes tested two or more out of the 4 siRNA duplexes caused defects in sister chromatid cohesion (Figure 25). This suggests a causal relationship between the observed chromosomal phenotype and the loss of the intended target. Subsequently, we selected NHP2L1, SART1 and CDC5L to be further analysed using assays similar to MFAP1 as they represented the top 3 hits in terms of phenotypic penetrance. NHP2L1 (non histone chromosome protein 2-like1) and SART1 (Squamous cell carcinoma Antigen Recognized by T cells 1) are known, along with MFAP1, to be part of the U4/U6, U5 tri-snRNP complex of the spliceosome (Jurica and Moore, 2003, Will and Luhrmann, 2011). CDC5L is a component of the nineteen containing complex which is crucial for the conversion of the active spliceosome from the B* complex to the C complex (Ajuh et al., 2000, Ajuh et al., 2001, Grote et al., 2010).

5.3 Depletion of NHP2L1 & SART1 causes a SAC-dependent mitotic arrest

In addition to the chromosome spread experiments, we performed time-lapse microscopy to test the effect of depletion of SART1 and NHP2L1 on mitotic progression and duration in these cells. Cells were transfected with siRNAs targeting SART1 or NHP2L1. In addition, the essential SAC component Mad2 was co-depleted with SART1 or NHP2L1. While control siRNA treated cells spent on average about 45 mins between cell rounding and anaphase onset, cells treated with Mad2 siRNA alone required less than 25 mins for progression through mitosis (Figure 26). Cells transfected with SART1 or NHP2L1 siRNAs alone spent more than 7.5 hr and 18 hr in mitosis, respectively, and often underwent mitotic cell death or an abnormal division (Figure 26 and data not shown). Co-depletion of

Mad2 along with either SART1 or NHP2L1 reduced the average duration of mitosis to less than 25 minutes. Consistent with a role for SART1 and NHP2L1 in sister chromatid cohesion, these result show that depletion of the two proteins causes a SAC-dependent arrest in mitosis.

5.4 A genetic complementation system for NHP2L1 and SART1

In addition to performing deconvolution experiments to test for off target effects (Figure 25), we decided to develop a genetic complementation system for NHP2L1 and SART1 similar to the one that we developed for MFAP1 (Figure 16). To this end, generated stable clonal cell lines expressing AcFL-tagged siRNA-resistant transgenes of NHP2L1 or SART1. Following depletion of the endogenous counterparts, the ability of these siRNA-resistant transgenes to restore sister chromatid cohesion was tested by chromosome spread analysis (Figure 27). While depletion of SART1 and NHP2L1 caused the splitting of sister chromatids only in cells expressing the tag AcFL but not in cells expressing RNAi-resistant transgenes (Figure 27). The SART1 and NHP2L1 transgenes potently restored sister chromatid cohesion to a normal status in cells lacking the endogenous proteins. This experiment eliminates off-target concerns and firmly establishes that SART1 and NHP2L1 are required for sister chromatid cohesion.

5.5 The splicing factors MFAP1, SART1 and NHP2L1 are required for sister chromatid cohesion in HCT116 cells

Before embarking on deciphering the molecular mechanism for the unusual observation that loss of splicing factors affects sister chromatid cohesion, we tested whether this phenomenon was restricted to chromosomally unstable and aneuploid HeLa Kyoto cells. To do this, we performed a chromosome spread analysis following depletion of splicing factors in HCT116 cells, a diploid human colon cancinoma cell line (Figure 28). Transfection of siRNA duplexes targeting NHP2L1, MFAP1 and SART1 caused a strong increase in the fraction of cells with split sister chromatids in HCT116 cells (Figure 28). The phenotypic penetrance that we observed for depletion of the same gene in HCT116 cells was lower than in HeLa

Kyoto cells (Figure 25). Although the reason for this difference is currently unclear, transfection efficiency, protein endurance or differential protein requirements in different cell types are likely candidate causes. Nevertheless, the occurrence of approximately 40 to 60% of HCT116 cells with split sister chromatids upon depletion of splicing factors compared to the control cells suggests that the requirement of splicing components for sister chromatid cohesion is not restricted to aneuploid HeLa Kyoto cells but also found in diploid cells.

5.6 Conclusions: A subset of genes regulating pre-mRNA splicing is required for sister chromatid cohesion

Based on the experiments that I have described in this section, we have concluded that the depletion of not just MFAP1 but a whole subset of splicing factors leads to a loss of sister chromatid cohesion. Transgenic rescue experiments revealed that the defects in cohesion are not the result of siRNA off-target effects. The effect of pre-mRNA splicing genes on sister chromatid cohesion is not a HeLa Kyoto cell specific phenomenon but also observed in HCT116 cells. Furthermore, the splicing genes that we show to mediate cohesion are not restricted to any particular step in the spliceosome assembly process but are distributed throughout the assembly pathway. This raises the possibility that pre-mRNA splicing in general is directly or indirectly required for sister chromatid cohesion. It also argues against a specific second function of a particular spliceosome complex in sister chromatid cohesion. Further work in the upcoming sections will lead to a better understanding of the molecular basis behind these observations.

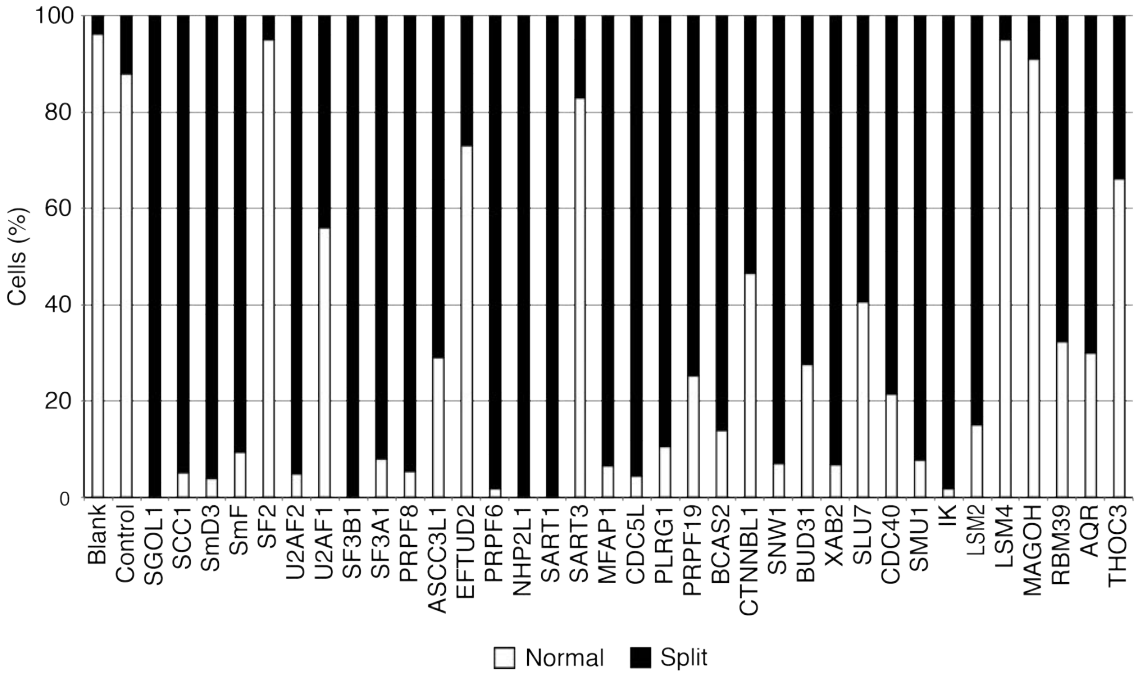

Figure 22 Chromosome spread analysis identifies a role for mediators of pre-mRNA splicing in sister chromatid cohesion

HeLa Kyoto cells transfected with the indicated siRNA smartpools were grown for 52 h and then treated with nocodazole (330nM) for 4 h and processed for chromosome spread analysis. Samples were scored for proportion of cells in different states of sister chromatid cohesion. Sgol1 and Scc1 were positive controls for loss of sister chromatid cohesion (n> 100 cells for each condition).

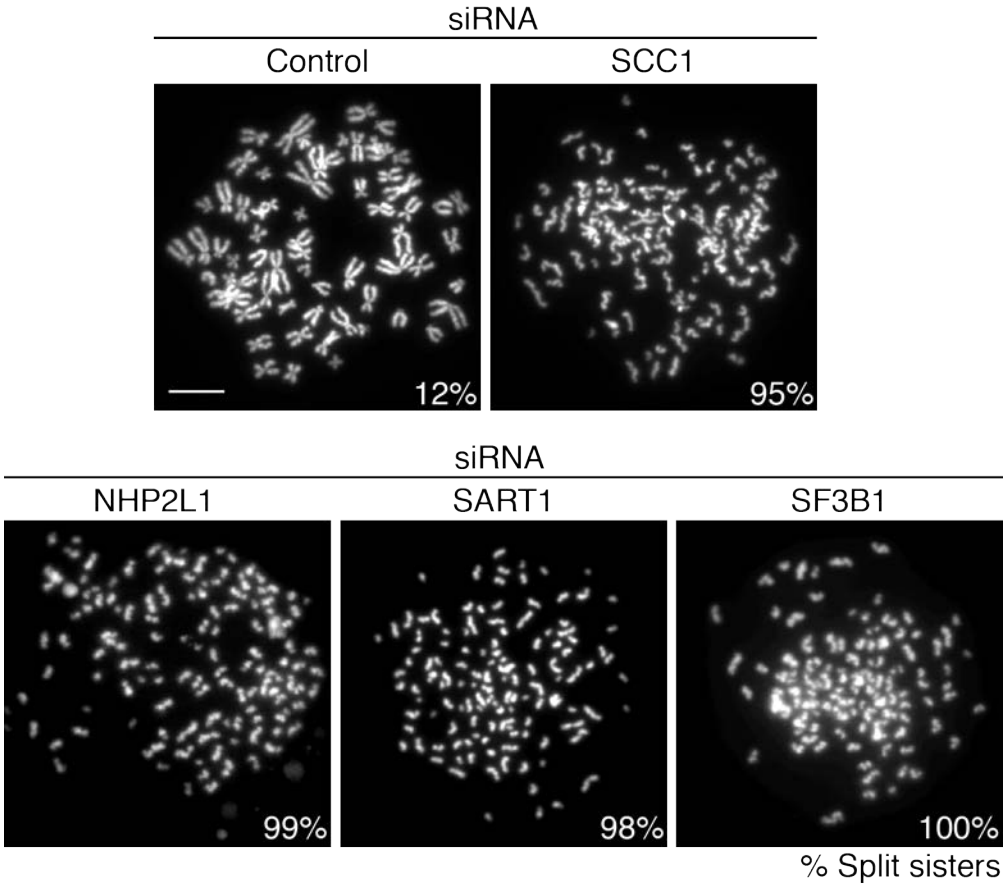

Figure 23 Representative images from the chromosome spread analysis of pre-mRNA splicing genes required for sister chromatid cohesion

HeLa Kyoto cells transfected with the indicated siRNAs were grown for 52 h and then treated with nocodazole (330nM) for 4 h following which they were processed for chromosome spreads and stained for DAPI. Samples treated as above were scored for proportion of cells with split sister chromatids Scc1 was a positive control for loss of sister chromatid cohesion. Representative images from chromosome spread screen with the positive and negative controls along with a few of the hits from the screen are displayed (scale bar = 10 µm, n> 100 cells)

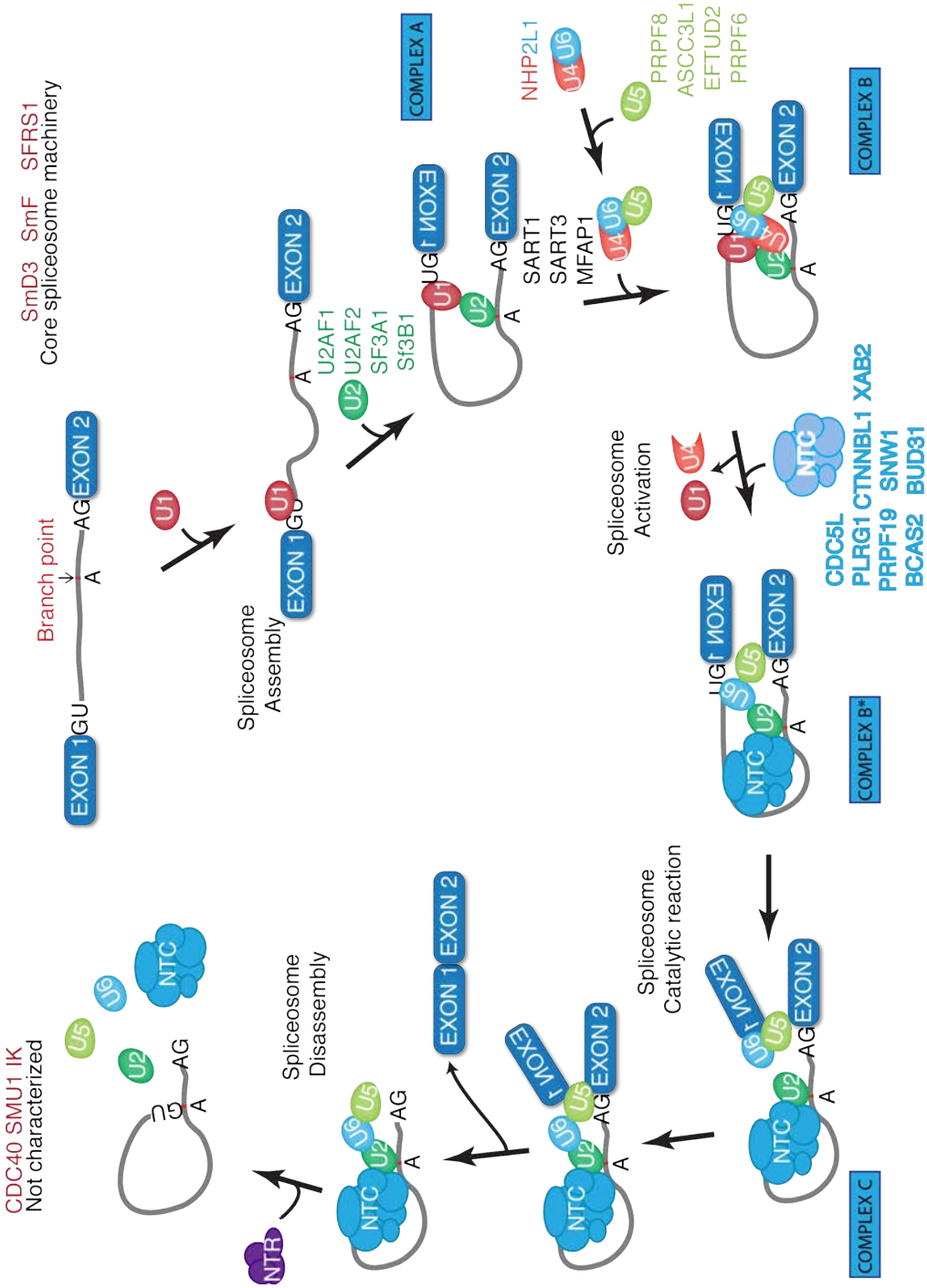

Figure 24 Schematic representation of spliceosome assembly and splicing reaction pathway highlighting spliceosome components that were identified to regulate sister chromatid cohesion

The genes that were identified to regulate sister chromatid cohesion in HeLa Kyoto cells are arranged in a colour-coded manner according to the specific part of the spliceosome assembly step that they have been implicated in (Zhou et al., 2002, Jurica and Moore, 2003, Will and Luhrmann, 2011).

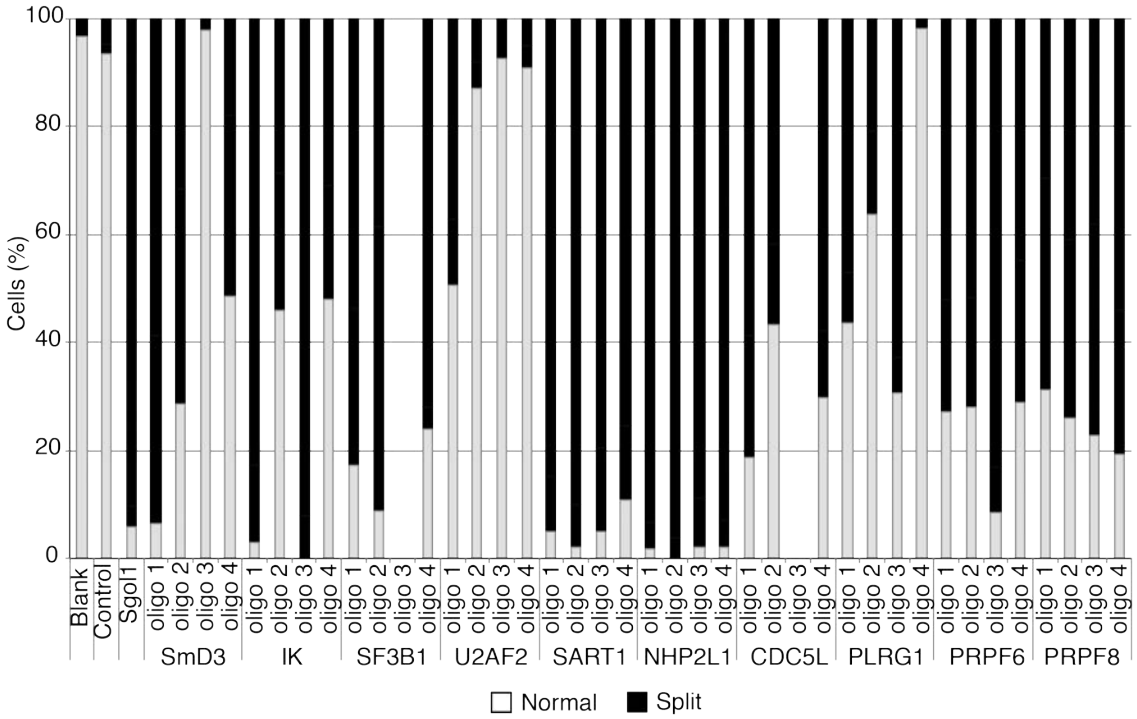

Figure 25 Deconvolution chromosome spreads of splicing factors confirm loss of sister chromatid cohesion upon their depletion

The top 10 hits from the primary chromosome spread analysis that was done using the siRNA smartpools were selected and were subjected to chromosome spread analysis with the individual siRNAs that constitute the smartpool. HeLa Kyoto cells transfected with the indicated siRNA smartpools were grown for 52 h and then treated with nocodazole (330nM) for 4 h and processed for chromosome spread analysis. Samples were scored for proportion of cells in different states of sister chromatid cohesion. SGOL1 was a positive controls for loss of sister chromatid cohesion (n> 100 cells for each condition)

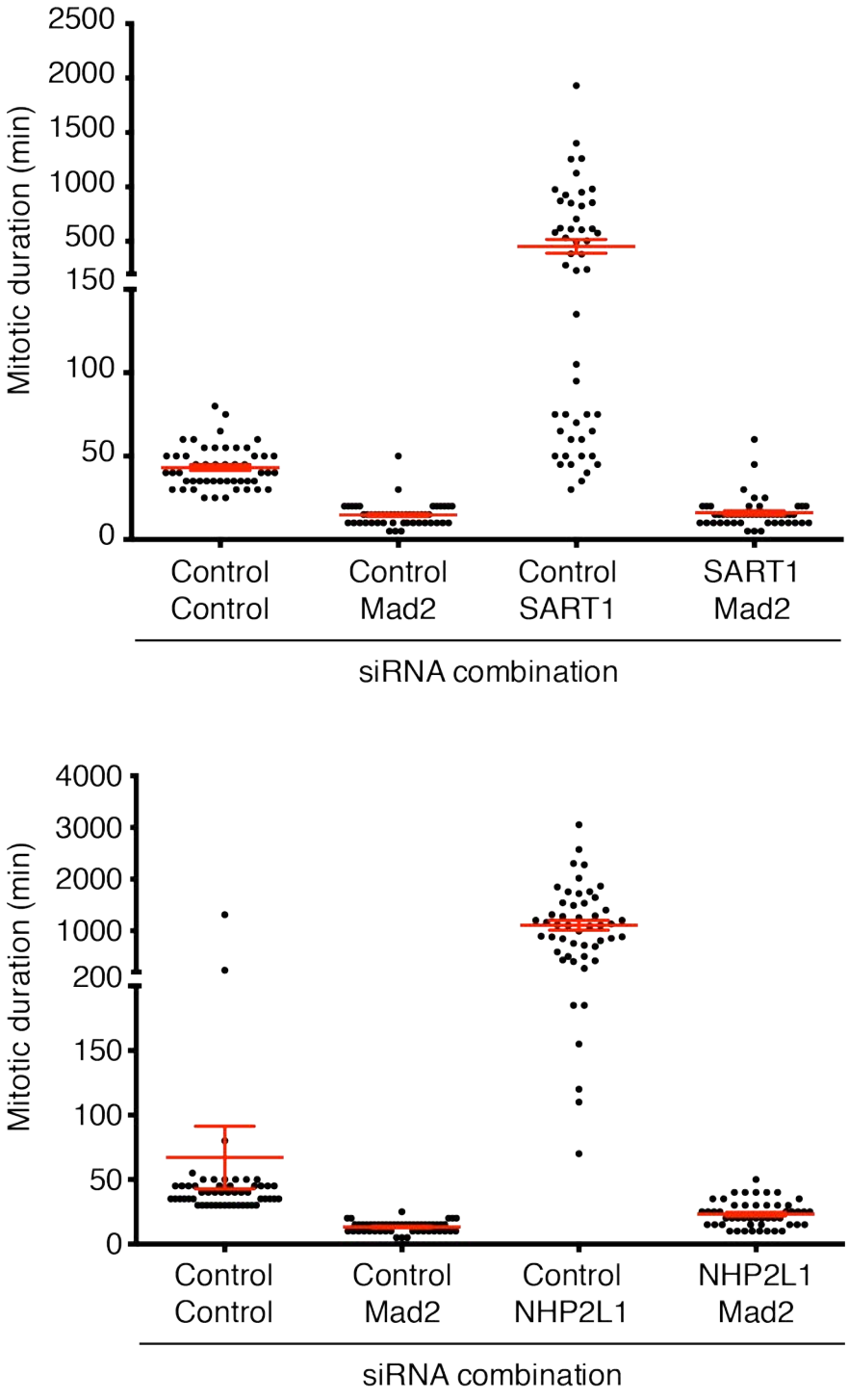

Figure 26 Depletion of SART1 and NHP2L1 results in an SAC-dependent mitotic arrest

HeLa Kyoto cells transfected with the indicated siRNA combinations were recorded using time-lapse microscopy. Mitotic duration, the time from mitotic cell rounding to anaphase onset, was determined from 24 hr post transfection. Each dot represents mitotic duration of a single cell (bars represents mean± SD)

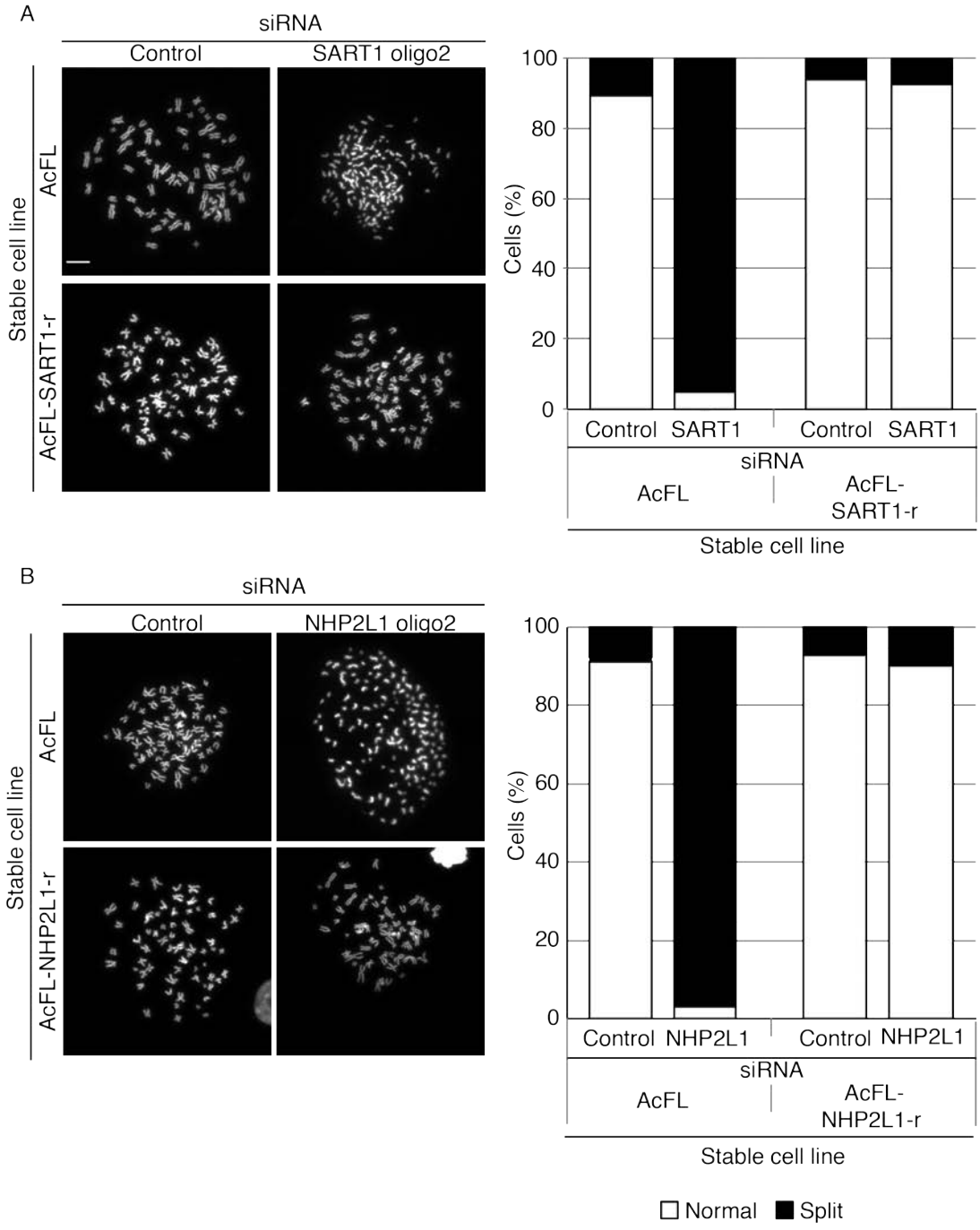

Figure 27 siRNA resistant SART1 and NHP2L1 transgenes can rescue the loss of sister chromatid cohesion caused by depletion of the endegenous counterparts

(A) Stable cell lines expressing AcFL and AcFL-tagged siRNA resistant transgene encoding SART1 (upper panel) or (B) NHP2L1 (lower panel) were transfected with the indicated siRNAs (37.5 nM). After 52 hrs, the cells were treated with nocodazole (330nM) for 4 h followed by processing for chromosome spread analysis. Images of DAPI-stained chromosome spreads from cells treated with the indicated siRNAs (left panels, scale bar = 10 μm). Samples treated as above were scored for the proportion of cells with the indicated status of sister chromatid cohesion. (n> 100 cells, bars represent mean from 3 independent experiments).

HCT116 cells

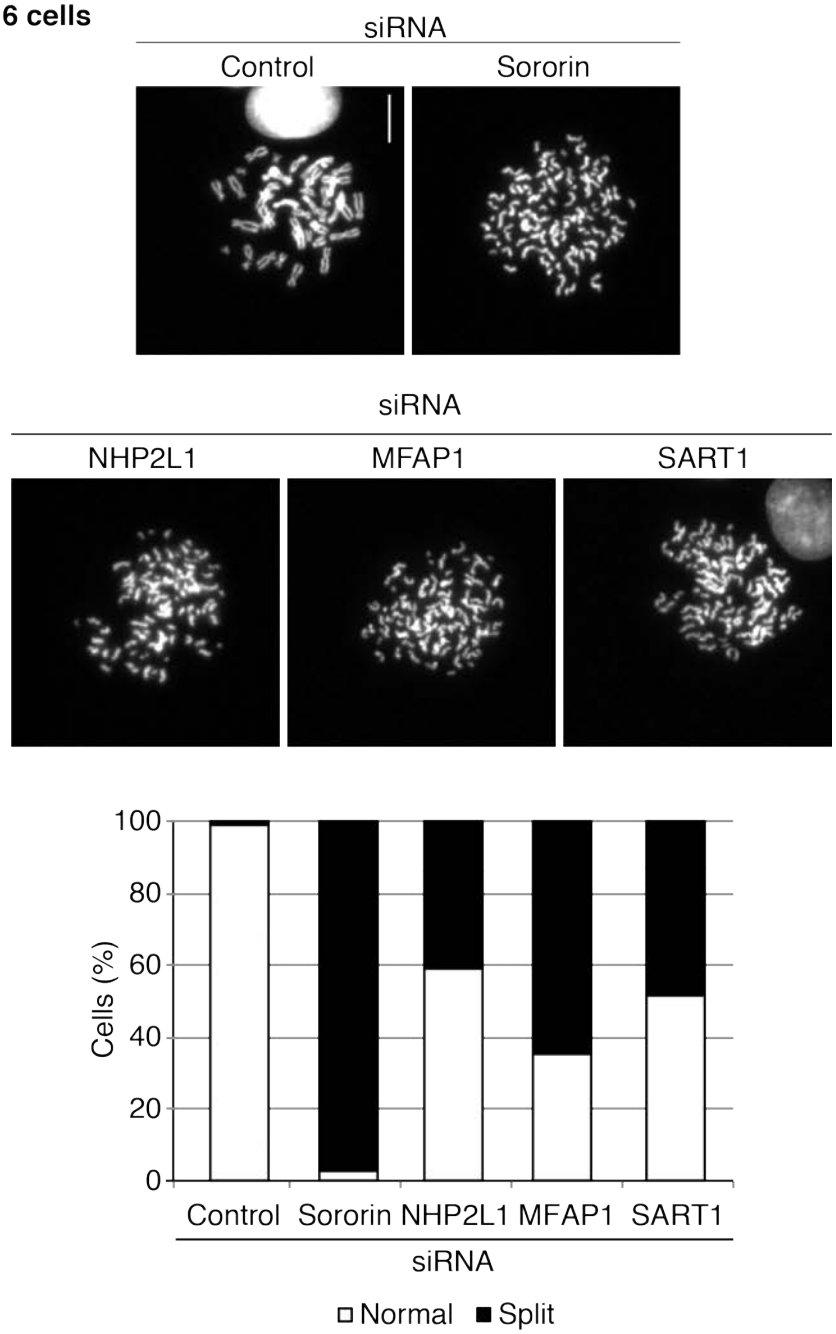

Figure 28 Depletion of splicing factors causes sister chromatid cohesion defects in HCT116 cells

HCT116 cells were transfected with the indicated siRNAs for either 24 h (Sororin and NHP2L1 siRNAs) or for 52 h (Control, MFAP1 and SART1 siRNAs) and then treated with nocodazole (330nM) for 4 h before processing for chromosome spread analysis. Spreads were scored for proportion of cells with indicated status of sister chromatid cohesion. Representative images are shown (scale bar = 10 μm, n> 100 cells, N=1).

Chapter 6. Results 4- Characterization of cohesin and sister chromatid cohesion properties upon loss of splicing factors

In the previous sections, I have described experiments that we performed in order to understand the basis behind the observation of irregular interphase nuclear morphology upon depletion of the splicing factor MFAP1 in HeLa Kyoto cells. We have found that the depletion of MFAP1 and a number of additional splicing factors leads to a premature loss of sister chromatid cohesion as revealed by chromosome spreads and mitotic FISH experiments. Further experiments were necessary to understand the effects of splicing factor depletion on the establishment and maintenance of sister chromatid cohesion and on the properties and dynamics of cohesin, the complex responsible for holding sister chromatids together. These experiments were designed to investigate the mechanistic basis for the requirements of splicing factors for sister chromatid cohesion. Pre-mRNA splicing components could influence sister chromatid cohesion through different mechanisms in a direct or indirect manner (Figure 29). First, disruption of co-transcriptional splicing could lead to faulty and stalled transcription bubbles leading to the formation of extensive RNA-DNA hybrids also known as R-loops (Helmrich et al., 2011, Skourti-Stathaki et al., 2011, Wahba et al., 2011). These R-loops might act as a physical hindrance for the establishment or maintenance of sister chromatid cohesion. A second possibility is that splicing components and complexes might have a splicing independent function in directly promoting the establishment or maintenance of sister chromatid cohesion. A third possibility is that splicing factors might indirectly influence sister chromatid cohesion by mediating the pre-mRNA processing one of multiple essential and rate-limiting cohesin subunits, thereby influencing cohesion indirectly. We sought to perform a series of experiments to test each of these possibilities.

6.1 Depletion of splicing factors results in loss of sister chromatid cohesion in interphase

In previous chromosome spread and FISH experiments, we established that cells depleted of splicing factors suffered from defective sister chromatid cohesion during mitosis. Sister chromatid cohesion is established during DNA replication in interphase (Uhlmann and Nasmyth, 1998). Thus, our mitotic experiments did not address whether cohesion was lost only as cells entered mitosis or whether sister chromatid cohesion was never established properly during S phase. Distinguishing between these possibilities could help us to narrow down possible mechanisms by which splicing proteins influence cohesion. This is possible because different sets of proteins and pathways control cohesion establishment, its maintenance through interphase and its ordered dissolution in mitosis. For instance, in vertebrate cells, Sororin is required for maintenance of sister chromatid cohesion after cohesion establishment but not earlier or during mitosis (Rankin et al., 2005, Nishiyama et al., 2010, Schmitz et al., 2007). Similarly, Sgol1 is required for protecting centromeric cohesion during early mitosis but does not seem to be crucial earlier (Nasmyth and Haering, 2009, Peters and Nishiyama, 2012). In order to scrutinize sister chromatid cohesion during interphase, we performed a FISH experiment in interphase cells using a probe that is specific for the tff1 locus on chromosome 21, a trisomic chromosome in HeLa Kyoto cells. This probe has been successfully used to investigate the state of interphase cohesion in human cells (Schmitz et al., 2007). Cells were synchronized using a single thymidine arrest initiated either at the time of siRNA transfection (SGOL1, Sororin and NHP2L1 siRNA duplexes) or 24 h post siRNA transfection (MFAP1, SART1 and CDC5L siRNA duplexes). Subsequently, cells were released from thymidine for 5 h at which point they were processed for FISH analysis. The distance between sister chromatids was determined by measuring the distance between the *tff1* FISH signal centroids for each of the three copies of chromosome 21. In control siRNA treated cells, the sister chromatid FISH signals were very close to each other and the average distance between the FISH signal centroids was 0.49 µm, in line with published observations (Nishiyama et al., 2010, Schmitz et al., 2007) (Figure 30). Depletion of SGOL1 did not affect the average distance between FISH signals in interphase. This is consistent with its mitosis-specific role in protecting centromeric sister chromatid cohesion during

prophase and prometaphase (Kitajima et al., 2004, Goulding and Earnshaw, 2005, McGuinness et al., 2005, Watanabe and Kitajima, 2005). Depletion of the cohesin stability factor Sororin on the other hand increased the distance between the dots to 0.85 µm (Figure 30). Importantly, depletion of all the splicing factors tested, namely NHP2L1, SART1 and MFAP1 resulted in a similar and significant increase in the distance between the sister chromatid signals in interphase cells (Figure 30). These results suggest that the role of splicing factors in controlling cohesion is not restricted to mitotic cells. It indicates that loss of splicing proteins abrogates sister chromatid cohesion already in interphase cells soon after DNA replication. The corollary of this interpretation is that the role of splicing factors in cohesion is unlikely to be mediated or connected to the Sgol1/PP2A pathway that protects cohesion at centromeres specifically in mitosis. The interphase FISH experiments rather point towards an important function of splicing components during the establishment or maintenance phase of sister chromatid cohesion.

6.2 Cohesin loading onto chromatin is unaffected by depletion of splicing factors

Cohesin loading in late telophase and early G1 phase represents the first essential step in the cohesin cycle (See section 1.2.4). Given that the onset of the sister chromatid cohesion loss phenotype in cells depleted of splicing factors is in interphase, we investigated the loading of cohesion onto chromatin in interphase. To do this, we used a cytological assay to quantify the amount of extraction-resistant nuclear cohesin as a proxy for the amount of cohesin associated with chromatin. This assay was successfully used to demonstrate the function of the cohesin loading complex SCC2/SCC4 (Watrin et al., 2006). The extraction step prior to fixation is essential to remove the soluble fraction of cohesin. To track the properties of cohesin we used immunofluorescence staining of the kleisin subunit Scc1. To control for subtle variations in immunofluorescence staining across different slides or within a single slide, differentially marked control and depleted cells were co-seeded on the same coverslip and assayed side-by-side. In short, HeLa Kyoto cells were transfected with siRNAs for either 18 h (Sororin and NHP2L1) or for 42 h (control, Scc4, MFAP1 and SART1). Cells were subsequently trypsinized, mixed with a HeLa Kyoto cells stably expressing H2B-mCherry in a 1:1

ratio and reseeded onto poly-L lysine coated coverslips. The cells were allowed to grow for 8 h before they were subjected to detergent extraction step, fixation and staining for SCC1. Finally, SCC1 intensity was quantified in neighbouring depleted and control H2B-mCherry-positive cells. Depletion of SCC4, an essential subunit of the cohesin (Watrin et al., 2006), severely reduced the intensity of extraction-resistant SCC1 in the nucleus (Figure 31) indicating that the assay can assess loading of cohesin complexes onto chromatin. Depletion of neither Sororin nor any of the splicing factors tested significantly reduced the staining intensity of SCC1. This result suggests that while splicing components are required for cohesion in interphase they are dispensable for cohesin loading onto chromatin.

6.3 SMC3 acetylation, a key step denoting cohesion establishment is not abrogated by the depletion of splicing factors

Following cohesin loading, the establishment of sister chromatid cohesion represents the next key event in the cohesin cycle. Thus, we decided to probe the role of the splicing factors in the establishment of cohesion. Cohesion establishment happens during DNA replication (Uhlmann and Nasmyth, 1998). One of the key steps signifying this process is the acetylation of the SMC3 subunit of cohesin (Rolef Ben-Shahar et al., 2008, Zhang et al., 2008a). An antibody that specifically detects SMC3 acetylated at K105 and K106 (Nishiyama et al., 2010) was used to measure the acetylation status of SMC3. HeLa Kyoto cells transfected with siRNAs in duplicates plates were arrested with thymidine added either 6 h after siRNA transfection (NHP2L1 and Sororin siRNAs) or 24 h after transfection (Control, ESCO1 & ESCO2, MFAP1, SART1 and CDC5L siRNAs). Cells released from thymidine were allowed to proceed through the cell cycle for 3 h before being processed for immunoblotting and flow cytometry analysis (Figure 32). Co-depletion of the two acetyl transferase paralogues ESCO1 and ESCO2 together that are responsible for SMC3 acetylation in humans (Zhang et al., 2008a, Hou and Zou, 2005) abrogated the acetylated fraction of SMC3. Depletion of the splicing factors revealed a minor reduction in SMC3 acetylation (Figure 32). Comparing the flow cytometry profiles, cells treated with siRNA duplexes targeting the splicing

factors show a slightly delayed progression through S phase compared to control or ESCO1 and ESCO2-depleted cells (Figure 32). Since SMC3 acetylation increases as cells progress from G1 to S phase, this delay may contribute to the reduction of SMC3's modification. Co-depletion of ESCO1 and ESCO2 severely compromises SMC3 acetylation but has a far less penetrant effect on sister chromatid cohesion than depletion of the splicing factors MFAP1, NHP2L1 and SART1 (data not shown). This circumstantial evidence suggests that the minor reduction in SMC3 acetylation is not causally linked to the loss of sister chromatid cohesion in cells depleted of splicing proteins.

6.4 Loss of splicing factors increases the turnover of cohesin from chromatin

Having failed to detect a major impact of splicing factors on cohesin loading and a marker for the establishment of sister chromatid cohesion, we investigated whether the depletion of splicing factors had any effect on the stability of cohesin-chromatin interactions during interphase. Experiments to characterize the interaction between cohesin and chromatin in interphase have relied on the use of a variant of fluorescence recovery after photobleaching (FRAP) technique, called inverse FRAP or iFRAP (Gerlich et al., 2006, Schmitz et al., 2007). iFRAP involves bleaching part of the GFP signal in a cell line stably expressing a cohesin subunit that is tagged with GFP and then monitoring the loss of GFP fluorescence in the unbleached area. Using this technique, it was revealed that cohesin-chromatin interactions are significantly stronger in G2 cells compared to G1 cells, reflecting the fact that cohesion establishment happens in S phase (Gerlich et al., 2006). This technique was also used to demonstrate the requirement of Sororin for maintenance of cohesion through G2 phase (Schmitz et al., 2007). For our experiments, a stable cell line expressing SMC1-EGFP was synchronized using thymidine added either at the time of siRNA transfection (Sororin siRNAs) or 24 h post siRNA transfection (MFAP1 and control siRNAs). Four h after release from thymidine, cells were treated with cycloheximide to prevent synthesis of new SMC1-EGFP. Following this, the cells were subjected to a photobleaching experiment in which SMC1-EGFP nuclear fluorescence was bleached with a laser

in half of the nucleus. In order to eliminate the contribution of soluble cohesin to the measurements, the initial photobleaching in one half of the nucleus was reiterated 5 times within 50 sec and the first post bleach frame was acquired 2 min post bleaching. This allowed for equilibration of bleached soluble SMC1-EGFP across the nuclear volume and its efficient bleaching. The difference in fluorescence intensity between the unbleached and the bleached area was measured and expressed as a ratio of the first post-bleach frame. This ratio, also known as the iFRAP ratio, was plotted over time. In control cells, the iFRAP ratio dropped gradually and a clear difference in fluorescence intensity between the bleached and unbleached area was apparent even 60 min into the experiment (Figure 33). In cells depleted of Sororin or MFAP1, the iFRAP ratio decreased rapidly with the fluorescence in the bleached and unbleached area equilibrating less than 30 min into the experiment (Figure 33). Strikingly, the loss of Sororin, a protein that antagonizes the activity of cohesin release mechanism (Nishiyama et al., 2010), and loss of the splicing component MFAP1 had a similarly penetrant effect on cohesin dynamics in vivo. This suggests that cohesin complexes dissociate from chromatin faster in cells lacking MFAP1 than in control cells. Thus, MFAP1 and possibly other splicing factors may control sister chromatid cohesion by ensuring the stable association of cohesin with chromatin. Failure to do so may explain the loss of sister chromatid cohesion observed in interphase cells following depletion of splicing proteins.

6.5 Overexpression of RNaseH1, an enzyme known to resolve R-loops, does not rescue the sister chromatid cohesion caused by depletion of splicing factors

One possibility that could explain how the loss of splicing components could hinder sister chromatid cohesion is that extensive RNA-DNA hybrids (R-loops) that might have been generated through defective or absent splicing reactions could block cohesin's ability to hold sister chromatids together. One way of testing this hypothesis was to use an enzyme that targets and removes R-loops by specifically cleaving the RNA moiety of RNA-DNA hybrids. Overexpression of RNaseH1 has been shown previously to resolve RNA-DNA hybrids (Skourti-Stathaki et al., 2011,

Cerritelli et al., 2003). Thus, we generated a stable clonal cell line expressing a GFP-tagged version of RNaseH1 that was targeted specifically to the nucleus. The transgene is expressed in 80% of the cells. We transfected control HeLa Kyoto cells and cells expressing RNase H1-EGFP with siRNAs targeting the splicing factors. Chromosome spread analysis revealed no difference in the severity of the sister chromatid cohesion loss in control cells as compared to cells expressing RNase H1 (Figure 34). These observations suggest that R-loops caused by a compromised splicing machinery are not responsible for the sister chromatid cohesion defect observed in cells lacking splicing components. A drawback of our experiments with RNase H1 and their interpretation is that we currently lack data demonstrating the efficacy of the enzyme in removing R-loops in the cell line used.

6.6 Depletion of splicing factors reduces protein levels of Sororin but not core cohesin subunits

The experiments described in the sections above indicated that the depletion of splicing factors did not affect either cohesin loading or cohesion establishment to a level commensurate with the cohesion loss phenotype observed. Our measurements of cohesin dynamics suggested that splicing components influence cohesin's association with chromatin. Next, we decided to test whether inhibition of splicing lead to reduced levels of the mature and functional form of a cohesin subunits or regulators that are indispensible for cohesin function during interphase. We transfected HeLa Kyoto cells with siRNAs targeting the splicing factors and synchronized their cell cycle using a single thymidine arrest. 5 h after release from thymidine, cells were processed for immunoblotting (fluorescent detection) with antibodies against SMC1, SMC3, SCC1/Rad21, SA2 and Sororin (Figure 35). The relative amounts of specific proteins were normalized to the levels of α-tubulin, which served as the loading control. Analysis of the band intensities revealed that there was no significant drop in protein levels of SMC1, SMC3, SCC1 or SA2 (Figure 35). However, we detected a 5-fold or higher reduction in the levels of Sororin upon depletion of all the splicing factors tested (Figure 35). This raises the possibility that the loss of splicing machinery components impacts on sister chromatid cohesion by compromising the level of the essential cohesin stabilizing

factor Sororin. The immunoblotting revealed that depletion of splicing factors led to strong drop in Sororin levels suggesting that the loss of sister chromatid cohesion upon depletion of the splicing factors is caused by loss of mature and functional Sororin. Depletion of Sororin and the splicing factors did not lead to a drop in the levels of core cohesin subunits SMC3 and SA2. SMC1 levels on the other hand increased upon depletion of the splicing factors although this was also seen in cells depleted of Sororin. Surprisingly, Scc1 levels showed a corresponding reduction compared to control cells upon depletion of the splicing factors with the depletion of Sororin also leading to a strong reduction in Scc1 levels.

6.7 Conclusion: Characterization of properties of cohesion upon loss of splicing factors

Through the experiments that I have described in this section, we have obtained a deeper understanding into the molecular mechanisms through which mediators of pre-mRNA splicing regulate sister chromatid cohesion. Depletion of splicing factors abrogated cohesion already in interphase although neither cohesin loading nor a marker for cohesion establishment was affected. Importantly, we found that the depletion of splicing factors caused an increased dissociation of cohesin from chromatin during interphase. While levels of core cohesin subunits did not diminish, levels of Sororin, a protein required for maintenance of cohesion through S–G2 phase into mitosis and the stable association of cohesin with chromatin, was significantly reduced in cells lacking splicing components. This suggests that splicing genes exert their effect on sister chromatid cohesion by regulating the levels of Sororin. Consistent with this idea, the loss of Sororin and the loss of splicing factors have similar phenotypic consequences: loss of cohesion during interphase and increased cohesin turnover on chromatin. We sought to perform more additional experiments to further test the link between splicing factors and Sororin in the next section.

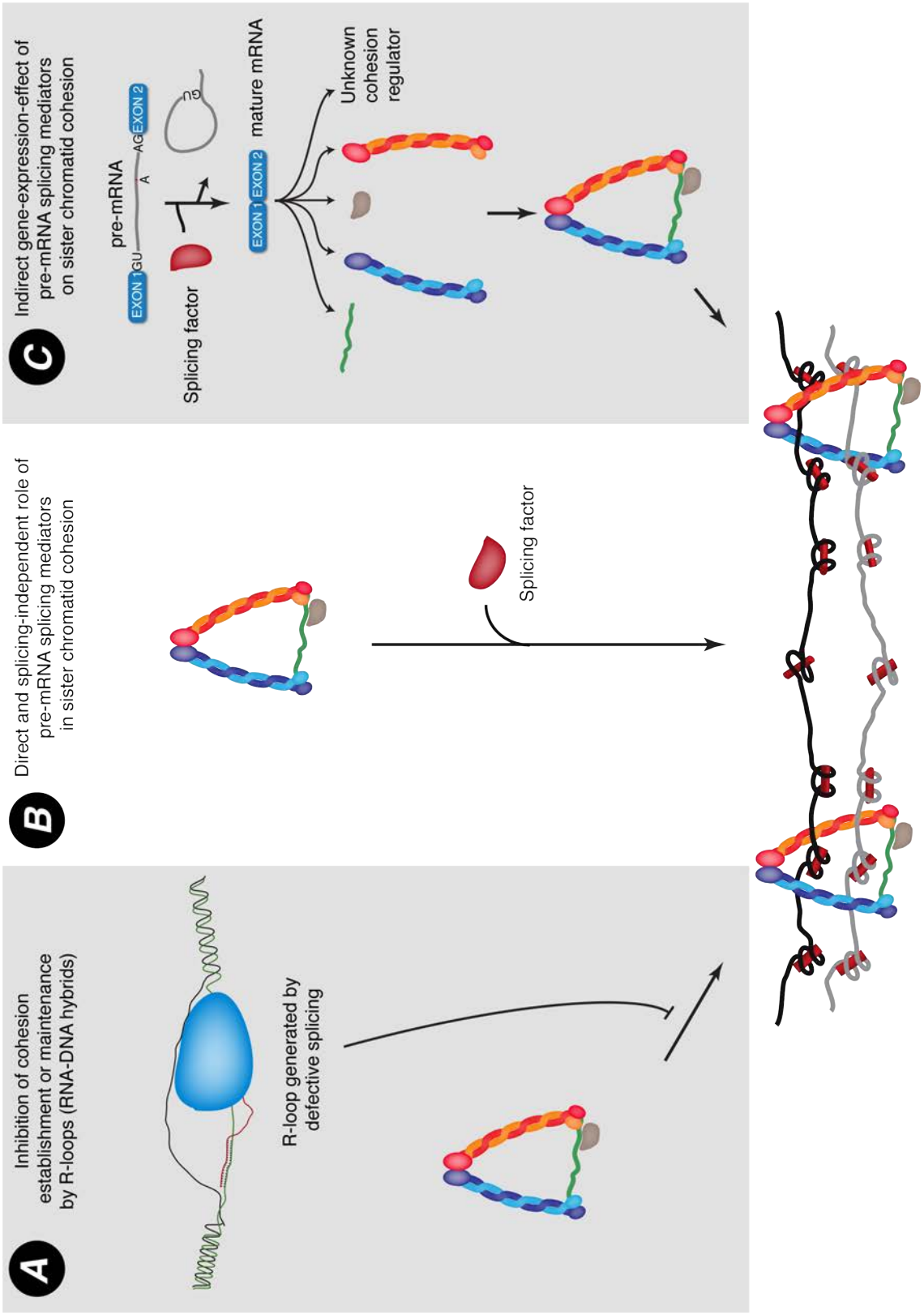

Figure 29 Schematic representation of possible mechanisms by which splicing can affect sister chromatid cohesion.

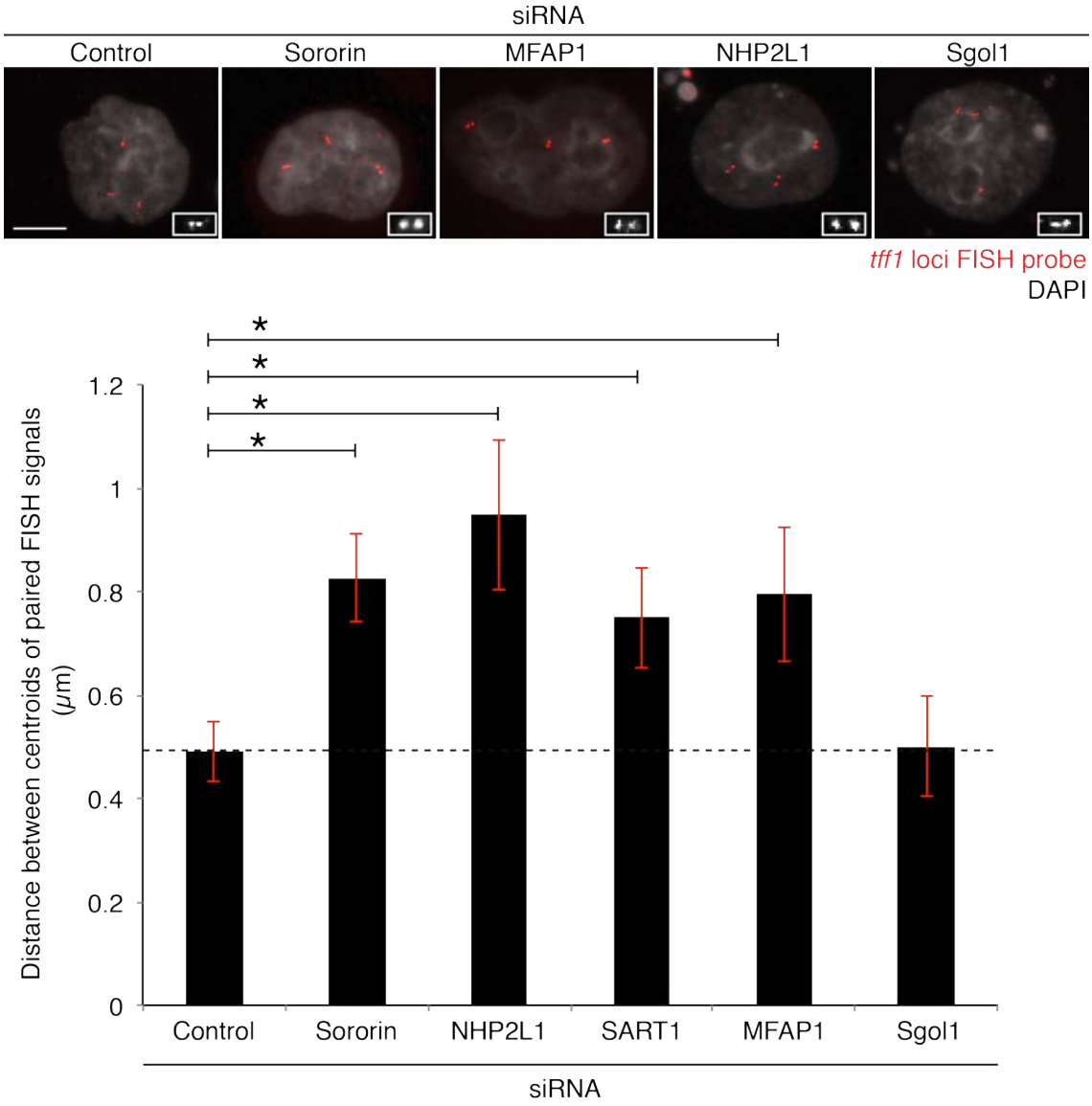

Figure 30 Depletion of splicing factors leads to an increased distance between sister chromatids in interphase

HeLa Kyoto cells were arrested in thymidine at the time of siRNA transfection (NHP2L1, Sgol1 and Sororin siRNAs) or 24 h post siRNA transfection (MFAP1, SART1, CDC5L and control siRNAs). 5 h after release from thymidine, cells were fixed, processed for fluorescence *in situ* hybridization (FISH) with a cy3-labelledprobe targeting the *tff1* loci on chromosome 21. DNA was stained with DAPI. Images of cells as treated above were acquired (upper panel, scale bar = 10μm) and the distance between the paired FISH signal centroids was determined (lower panel, n> 30 cells, N=1. Bars represent standard error of measurement at 95% confidence interval, asterisks denote a significant difference according to student's t test p< 0.01).

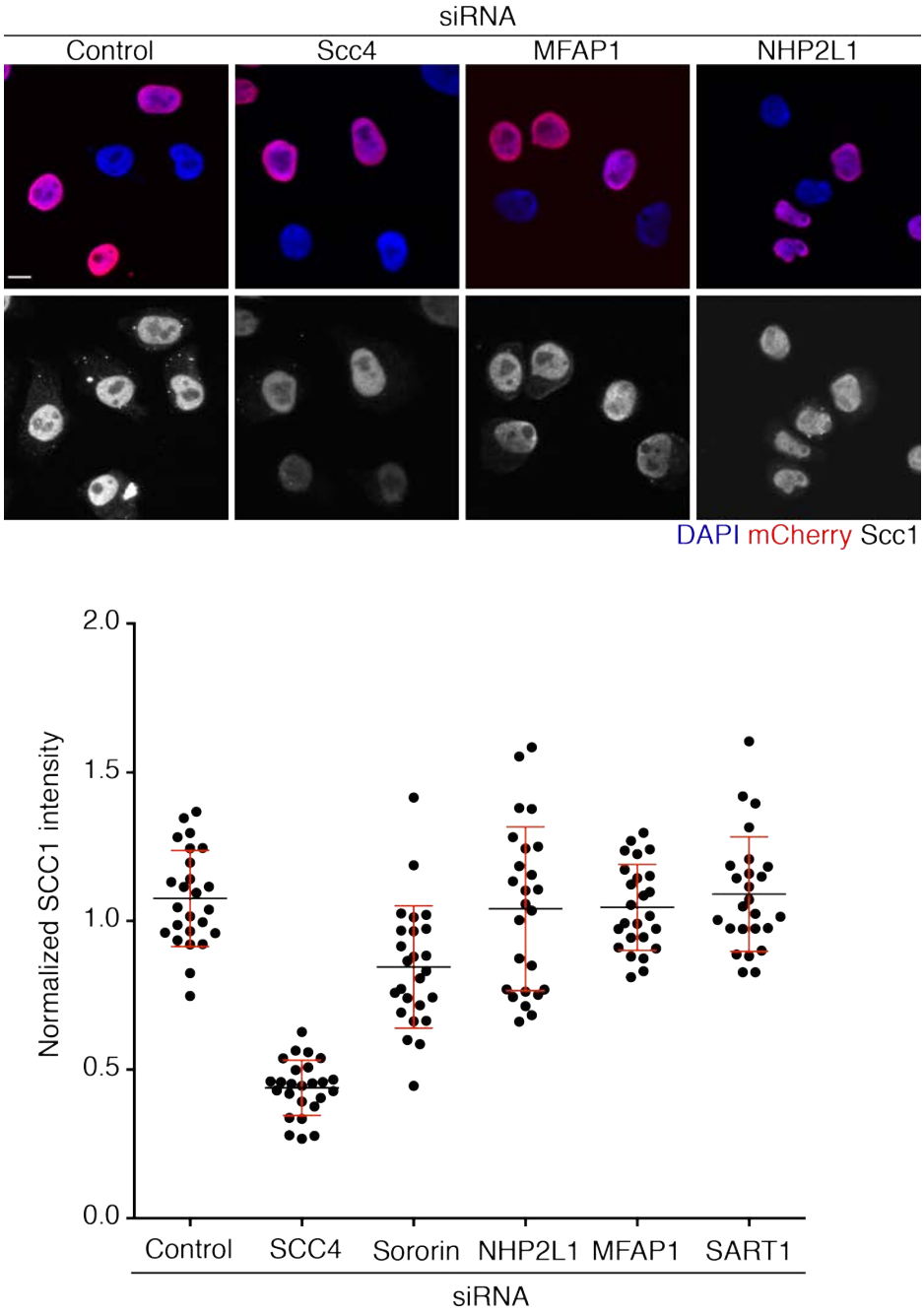

Figure 31 Splicing factors are not required for association of cohesin with chromatin

HeLa Kyoto cells were transfected with siRNAs for either 18 hrs (NHP2L1 and sororin) or for 42 h (Control, SCC4, MFAP1 and SART1 siRNAs) following which they were, mixed with HeLa Kyoto cells stably expressing H2B-mCherry, and seeded onto coverslips that were coated with poly-L-Lysine. 8 hrs later, cells were extracted (to remove the soluble fraction of cohesion), fixed and stained for Scc1 and DNA (blue). Representative images from the experiment are displayed (upper panel, Scale bar = 10 μm). Scc1 integrated fluorescence intensities of siRNA-transfected interphase cells were normalized to Scc1 integrated fluorescence intensities of neighboring untransfected interphase cells marked by H2B-mCherry (lower panel, bars represent mean ± SD; n>25 siRNA transfected cells per condition).

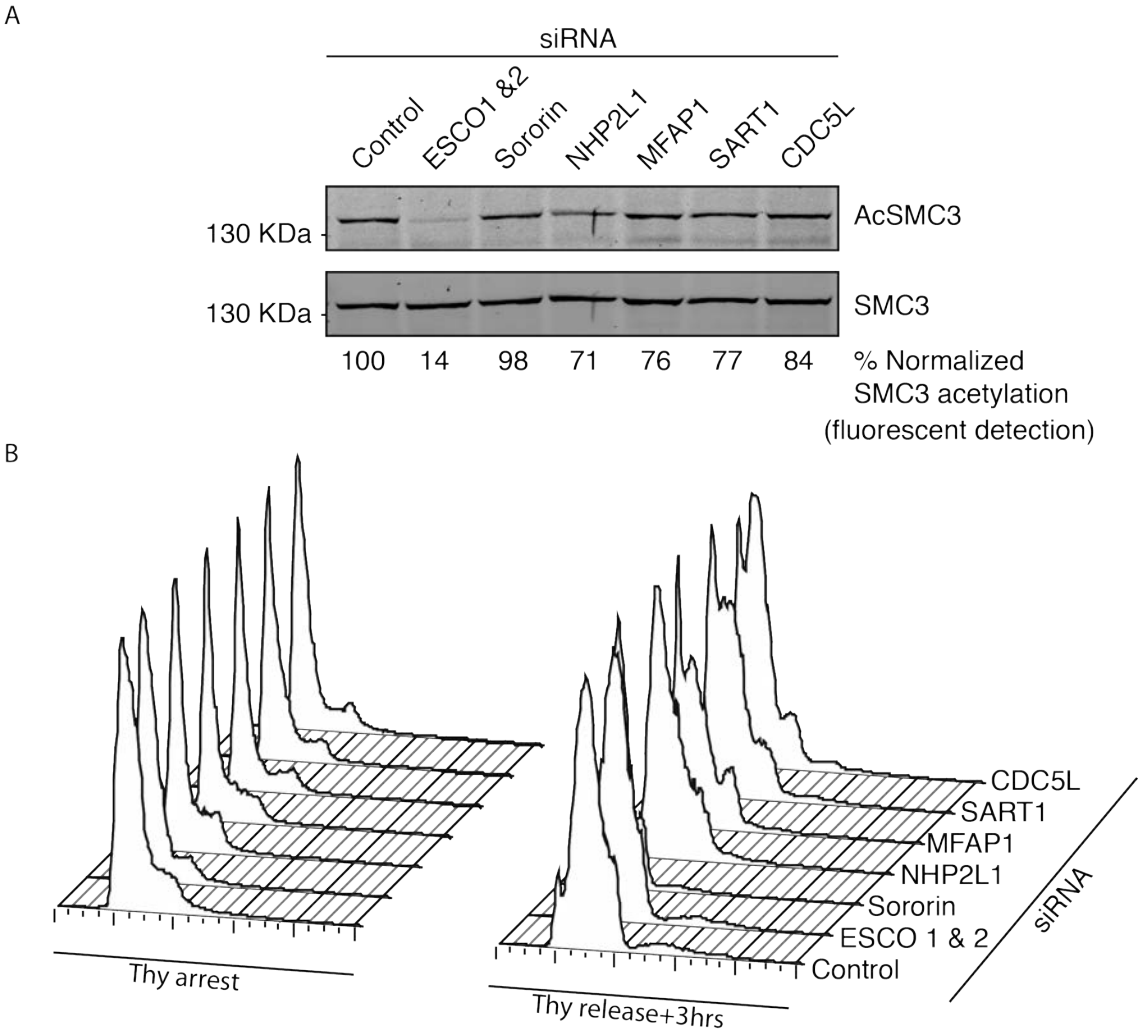

Figure 32 Acetylation of SMC3, a key marker for cohesion establishment is not severely reduced by depletion of splicing factors

(A) HeLa Kyoto cells were transfected with siRNAs (37.5 nM) for either 6 hrs (NHP2L1 and Sororin) or for 24 h (Blank, ESCO 1&2, Control, MFAP1, SART1 and CDC5L siRNAs) following which the cells were arrested in thymidine (2.5mM) for 24 h and released into DMEM. 3 hrs after release, the cells were harvested and processed for immunoblotting using AcSMC3 and SMC3 specific antibodies. (B) Concurrently, cells transfected and synchronized as above were processed for flow cytometry. Sorting was performed on a FACSCalibur (Beckton Dickinson), after staining with propidium iodide (5**µ**g/ml, 1h at 37^0 C). Cell cycle profiles analyzed using FlowJo (Tree Star softwares) were then plotted as shown.

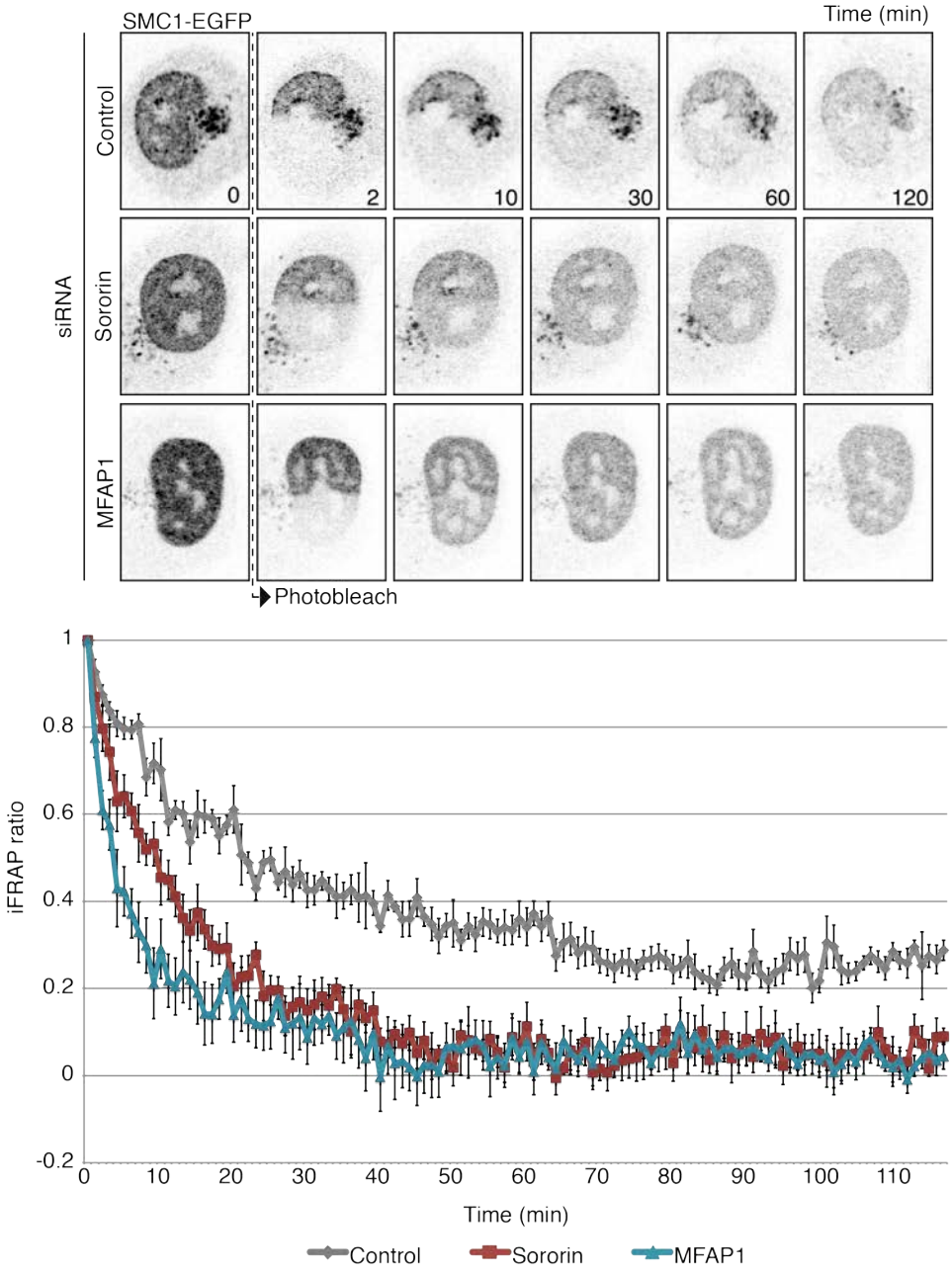

Figure 33 Inverse FRAP experiments (iFRAP) reveal enhanced dissociation of cohesin from chromatin in mFAP1-depleted cells

HeLa Kyoto cells stably expressing SMC1-EGFP were synchronized by thymidine arrest for 24 h either at the time of siRNA transfection (Sororin) or 24 h after transfection (control and MFAP1 siRNA). 5 h after release from the thymidine arrest, SMC1-EGFP fluorescence was repeatedly bleached in approximately half of the nucleus. The fluorescence intensities in the bleached and unbleached nuclear regions were followed by time-lapse microscopy with images being recorded every minute. Representative images of control Sororin and MFAP1-depleted cells are displayed. The difference in mean fluorescence intensity between bleached and unbleached nuclear regions was expressed as a ratio of the difference in fluorescence in the first post-bleach frame and plotted over time (bars represent mean ± SEM n=6 cells from 2 independent experiments).

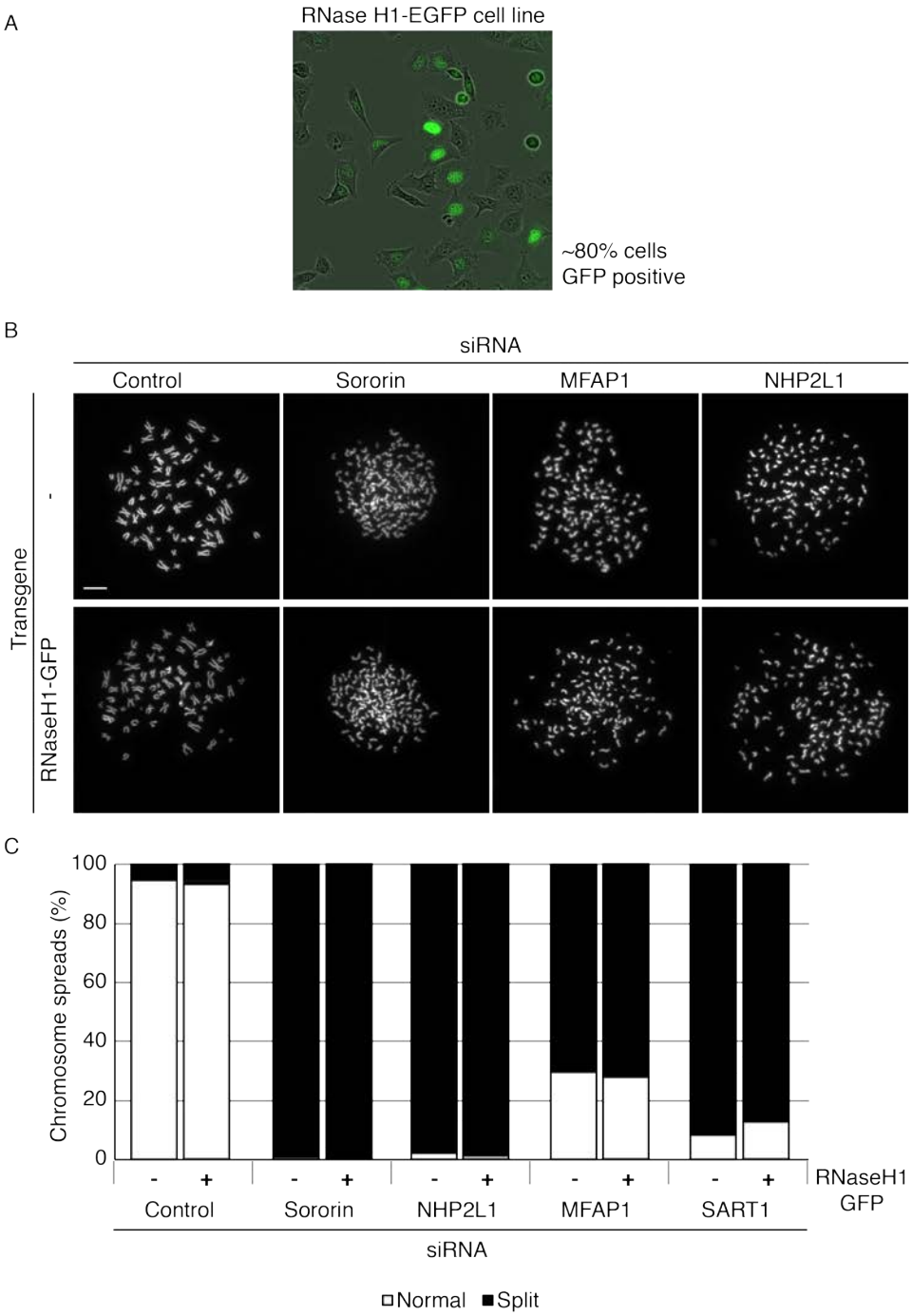

Figure 34 Overexpression of RNaseH1 does not rescue loss of sister chromatid cohesion upon depletion of splicing factors

(A) A stable cell line expressing RNaseH1-EGFP (>80% cells GFP positive) was generated. (B) This cell line and control HeLa Kyoto cells were transfected with the indicated siRNAs for 52 h and then treated with nocodazole (330nM) for 4 h before processing for chromosome spread analysis. Representative images from the assay are displayed (upper panel, scale bar = 10 μm). (C) The samples treated as above were scored for the status of sister chromatid cohesion defects and quantified as shown (lower panel, n> 100 cells, bars represent mean from 3 independent experiments).

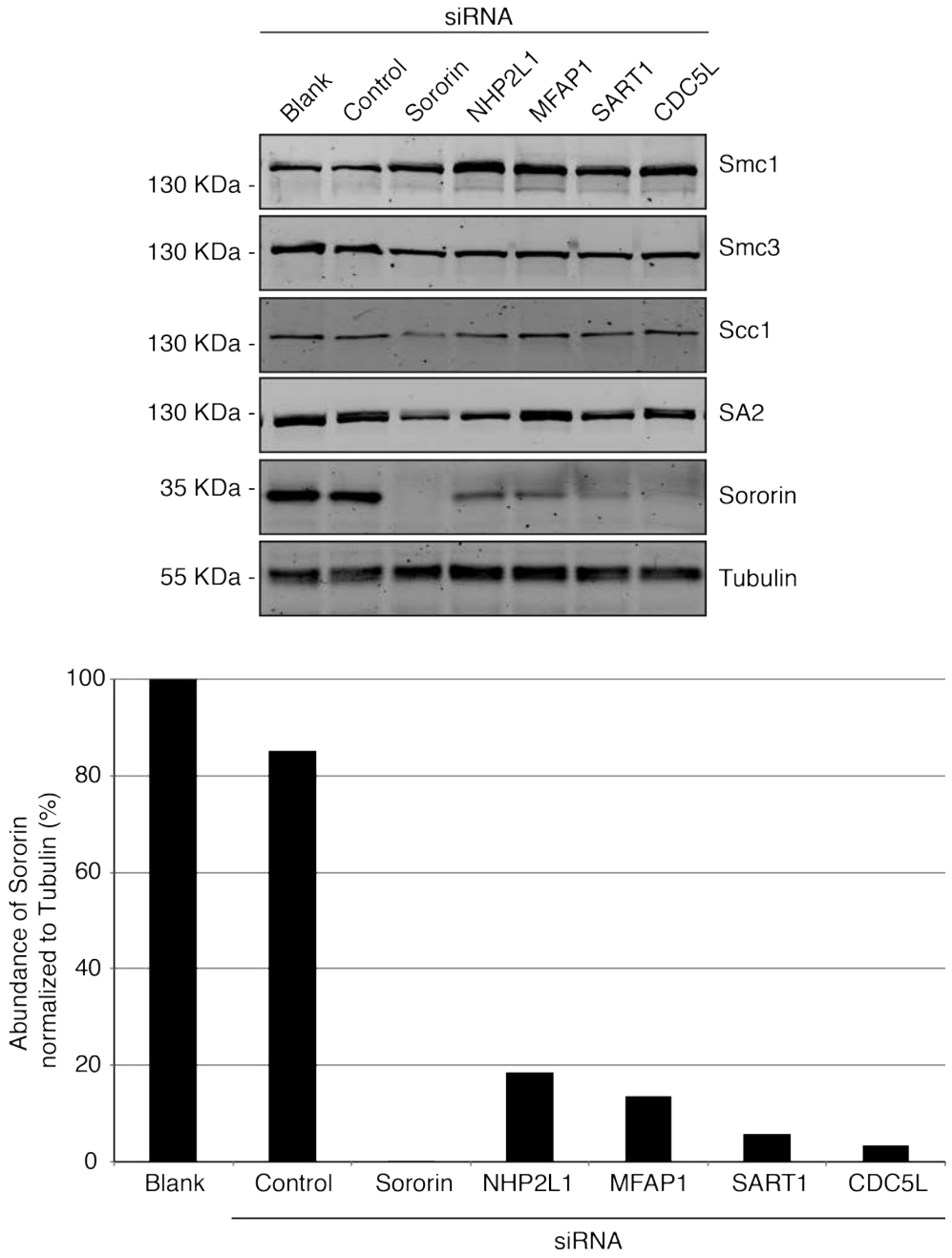

Figure 35 Depletion of splicing factors reduces protein levels of Sororin but not any other core cohesin subunit

HeLa Kyoto cells were transfected with siRNAs for either 6 h (NHP2L1 and Sororin) or for 24 h (Blank, Control, MFAP1, SART1 and CDC5L siRNAs) following which the cells were arrested in thymidine (2.5mM) for 24 h and released into DMEM. 5 h after release, the cells were harvested and processed for immunoblotting using the indicated antibodies. Secondary antibodies coupled to fluorescent tags were used and were detected using an Odyssey Imaging System. The relative protein content was normalized to the loading control α-Tubulin and the percentage of Sororin in cells treated with the indicated siRNA was plotted.

Chapter 7. Results 5- Mediators of pre-mRNA splicing regulate sister chromatid cohesion through Sororin

In the previous section, I have described experiments through which we could demonstrate that that depletion of splicing factors disrupted sister chromatid cohesion and at the same time caused a strong reduction in the levels of Sororin. We performed further experiments to test if the defect in cohesion observed was causally linked to the reduction in Sororin levels.

7.1 Pre-mRNA splicing of Sororin is perturbed upon depletion of splicing factors

Previously, I described experiments wherein we depleted splicing factors and inspected the protein levels of core cohesin subunits. We discovered that Sororin was the only protein whose levels were significantly reduced. In order to investigate whether the depletion of the splicing factors that are required for cohesion interfered with the pre-mRNA processing of Sororin, we decided to perform qRT-PCR experiments. For these experiments, HeLa Kyoto cells transfected with siRNAs targeting Sororin, NHP2L1, MFAP1, SART1 and CDC5L were released from a thymidine arrest. Five h after release, total RNA was extracted and was used to perform a reverse transcription reaction to generate the corresponding cDNAs using random hexamers as primers. A real time PCR reaction was then performed using primers that were designed as shown in Figure 36. Briefly, three sets of primers were used for Sororin, the first pair produced a product within exon 2 (to measure Sororin transcript level) the second one amplified across exon 1 and exon 2 and the third primer within intron 1. Primers within GAPDH were used as a control for the qRT-PCR reaction and the relative mRNA levels were normalized to control siRNA treated samples. Depletion of Sororin reduced Sororin mRNA levels to less than 12% when tested using exon specific primers and to about 23% using intron specific primers (Figure 36). These results validate the utility of the qRT-PCR assay to scrutinize Soririn mRNA status. In contrast to Sororin loss, depletion of all 4 splicing factors tested, resulted in a specific and substantial increase in the

amplification of the primer pair within intron 1. The increase in intron 1 signal ranged from a 2-fold to a 5-fold change. These observations suggest that depletion of splicing factors that are required for cohesion compromises splicing of Sororin pre-mRNA at least for intron 1. Failure to undergo correct splicing could lead to irregular transcription and translation resulting in a drop in the protein levels of Sororin.

7.2 A genetic complementation system for Sororin

The reduction in Sororin protein level and alteration of Sororin pre-mRNA structure raised the possibility that defective Sororin expression could represents the molecular mechanism underlying the cohesion defect in cells lacking splicing mediators. To test this possibility, we decided to use an intron-less Sororin transgene whose expression would not require pre-mRNA splicing. This transgene allowed us to test for a rescue the loss of sister chromatid cohesion in cells lacking splicing factors. As a first step towards this, we sought to establish a genetic complementation system using an AcFL-tagged Sororin cDNA that was engineered to be resistant to Sororin siRNA (Figure 37). This system allowed us to test whether the Sororin transgene was able to replace the function of the endogenous counterpart. Since stable cell lines generated by plasmid transfection strongly overexpressed the transgene, we chose lentiviral transduction with a minimal virus titre for engineering Sororin cell lines. This was necessary as over expression of Sororin at a high level could lead to an artificial stabilization of cohesin on chromatin and thereby cause by-pass suppression or other artefacts. Using lentiviral transduction, we were able to generate a cell line that expressed siRNA resistant and intron-less AcFL-Sororin at about 3-fold the endogenous level (Figure 37). Importantly, the Sororin transgene in this cell line was to completely restore normal mitotic progression and sister chromatid cohesion in cells depleted of the endogenous protein (Figure 38 and see below). We could further demonstrate that the intron-less Sororin transgene was immune to the depletion of the splicing factors whereas their endogenous counterparts were not (Figure 39). These observations suggest that the protein encoded by the engineered transgene is fully functional and that its expression is not dependent on the status of the pre-mRNA splicing machinery (Figure 39C).

7.3 Expression of the Sororin transgene cannot bypass the requirement of Scc1 and Sgol1 for sister chromatid cohesion

Having generated a transgenic complementation system for Sororin, we tested the ability of this cell line to rescue the loss of sister chromatid cohesion triggered by depletion of Sororin itself as well as of the core cohesin subunit Scc1 and the protector of centromeric cohesion SGOL1. Sororin antagonizes the cohesin-releasing anti-establishment activity of WAPL (Nishiyama et al., 2010). Depletion of SGOL1 and SCC1 served as important controls as a strong rescue of cohesion loss induced by depletion of either protein in a cell line overexpressing Sororin would indicate bypass suppression through ectopic stabilization of residual cohesin on chromatin, a phenomenon ('over-cohesion') that can also be induced by depletion of WAPL (Nishiyama et al., 2010, Peters and Nishiyama, 2012, Eichinger et al., 2013). Expression of siRNA-resistant AcFL-Sororin potently restored sister chromatid cohesion upon depletion of the endogenous counterpart (Figure 38). In contrast, expression of the transgene had only a minor impact on the severity of sister chromatid cohesion loss induced by depletion of Scc1 or Sgol1 (Figure 40). These observations suggest that the level of Sororin expression in our transgenic model cannot efficiently bypass the loss of Scc1 or Sgol1 by providing ectopic stabilization of remaining cohesin complexes. Together with the finding that the transgene is able to provide Sororin function, this observation indicates that the transgenic model is suitable for testing the hypothesis that splicing factors impact on cohesion through expression of Sororin.

7.4 Overexpression of intron-less Sororin rescues the loss of sister chromatid cohesion upon depletion of splicing factors

Having established an siRNA complementation system for Sororin and having demonstrated that the level of overexpression was low enough to prevent artefacts of Sororin over expression, we proceeded to test the ability of an intron-less Sororin

transgene to rescue the sister chromatid cohesion loss that occurs upon depletion of the splicing factors. We transfected cells expressing AcFL-Sororin-r or the AcFL tag alone with siRNAs duplexes targeting Sororin or the splicing factors MFAP1, NHP2L1, SART1 and CDC5L (Figure 41). Following transfection, cells were grown for 24 h (NHP2L1 and Sororin siRNAs), 44 h (MFAP1 and SART1 siRNAs) and 52 h (Control and CDC5L siRNAs) before being analysed by chromosome spread assays. Importantly, expression of the intron-less Sororin transgene strongly reduced the fraction of cells with split sister chromatids (Figure 41). Depending on splicing factor analysed, the defect was reduced 3 to 6-fold (Figure 41). Expression of the intron-less Sororin transgene however did not restore mitotic progression in cells depleted of splicing factors: cells were still not able to exit mitosis and eventually sustained apoptosis (data not shown). Based on these observations, we can conclude that the loss of sister chromatid cohesion in cells depleted of splicing factors is almost exclusively caused by a failure to supply sufficient Sororin protein. Thus, the main target of splicing factors in mediating sister chromatid cohesion is Sororin.

7.5 Conclusions: mediators of pre-mRNA splicing regulate sister chromatid cohesion through Sororin

In this section, I have demonstrated that depletion of selected splicing factors leads to a defect in pre-mRNA splicing of Sororin, a key regulator of sister chromatid cohesion. Since Sororin is critical for cohesion maintenance throughout interphase through to mitosis, a strong reduction in Sororin protein levels could disrupt sister chromatid cohesion in interphase cells which would eventually cause an SAC-dependent mitotic arrest as cells enter mitosis with split sister chromatids. Importantly, we have also shown that expression of an intron-less Sororin transgene can largely restore sister chromatid cohesion in cells depleted of splicing mediators. The same transgene does not rescue the loss of sister chromatid cohesion caused by depletion of other cohesin subunits. These experiments suggest that amongst cohesion regulators, Sororin is the major target of pre-mRNA splicing in the regulation of sister chromatid cohesion. Our study also reveals that the connection between sister chromatids is exquisitely sensitive to the Sororin

levels suggesting that cells have to maintain a delicate balance between the antagonizing functions of WAPL and Sororin (see discussion). Finally, the fact that Sororin transgene expression does not restore mitotic progression in cells lacking splicing factors strongly suggests that splicing contributes to the successful execution of mitosis by other as yet undefined mechanisms (see discussion).

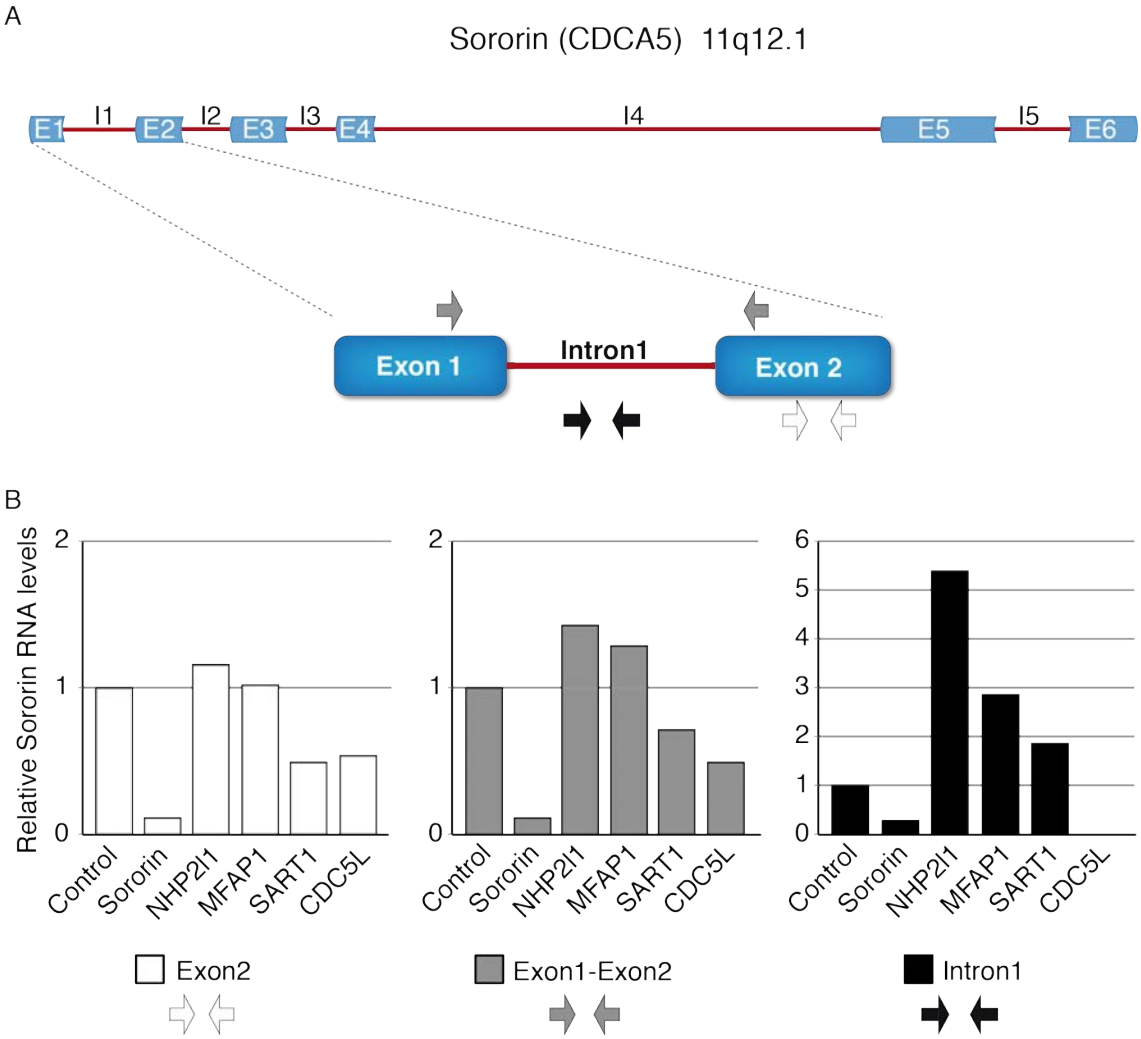

Figure 36 Sororin mRNA splicing is perturbed upon depletion of splicing factors

(A) Schematic depicting the exons and introns within the Sororin open reading frame. Sororin specific primers were chosen for qRT-PCR experiments that either amplify within exon 2 (white arrows) or across exon 1 and exon 2 (Grey arrows) or within Intron 1 (black arrows) of Sororin. (B) HeLa Kyoto cells were transfected with siRNAs for either 6 hrs (NHP2L1 and Sororin) or for 24 h (Control, MFAP1, SART1 and CDC5L siRNAs) following which the cells were arrested in thymidine (2.5mM) for 24 h and released into DMEM. 5 hrs after release, the cells were harvested and total RNA was extracted. cDNA generated from these RNA samples using random hexamers priming were processed for qRT-PCR using primers that either amplify within exon 2 (white arrows) or across exon 1 and exon 2 (Grey arrows) or within Intron 1 (black arrows) of Sororin. Quantification of relative mRNA levels by ΔΔCT method was performed as described (Section 2.6) and the data was normalized to mRNA levels in control siRNA sample Data represents average of 3 experimental repeats.

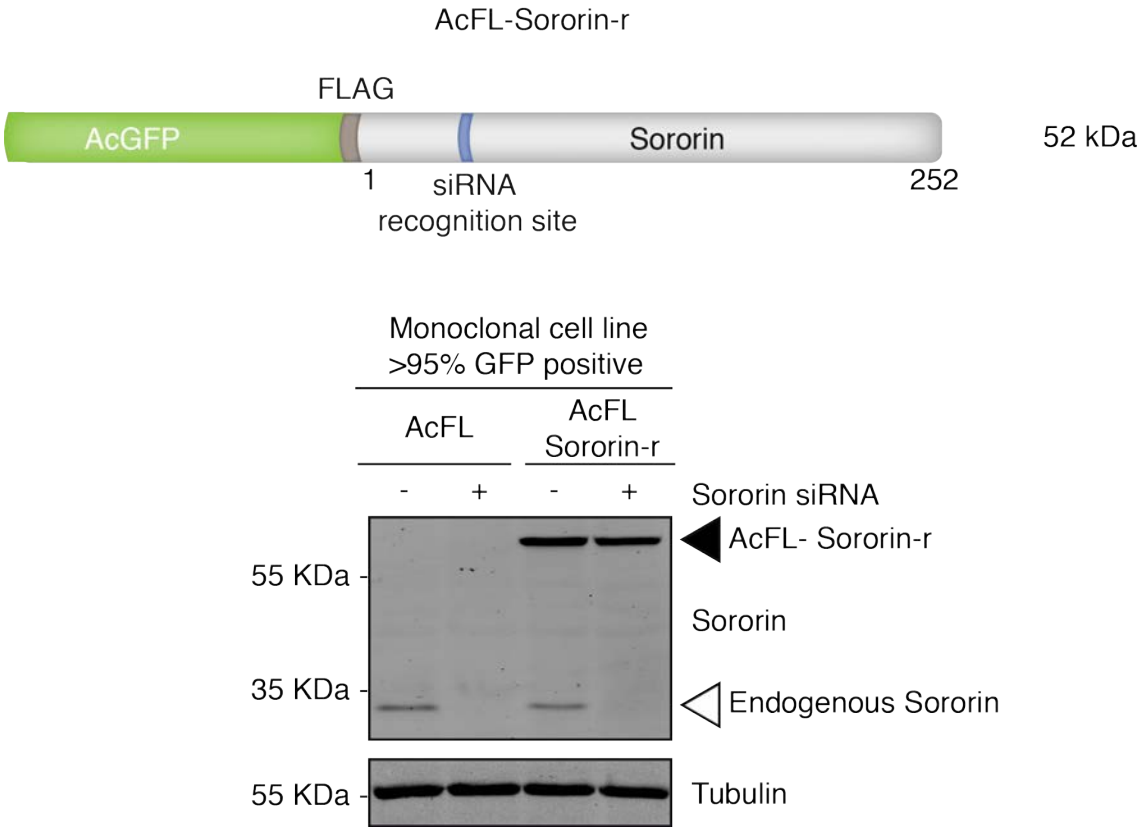

Figure 37 A genetic complementation system for Sororin

A clonal stable cell line expressing a siRNA-resistant transgenic copy of Sororin was generated by introducing silent mutations within the siRNA recognition sequence of Sororin cDNA which was tagged with AcGFP-FLAG (AcFL) at the N terminus. A lentiviral vector was generated incorporating the above-mentioned construct. Viral particles harbouring the construct were generated in 293FT cells and used to infect HeLa Kyoto cells. The clonal cell line was then generated through selection with puromycin (0.4 µg/mL). Schematic representation of the transgene (upper panel). clonal cell lines expressing either AcFL-Sororin-r or the AcFL tag alone were transfected with indicated siRNA duplexes (37.5 nM) along with thymidine (2.5mM). Cells were released after 24 h of thymidine arrest, harvested about 5 h after release and processed for immunoblotting with the indicated antibodies. Endogeneous Sororin and transgenic AcFL -Sororin-r are indicated by open and filled arrowheads respectively.

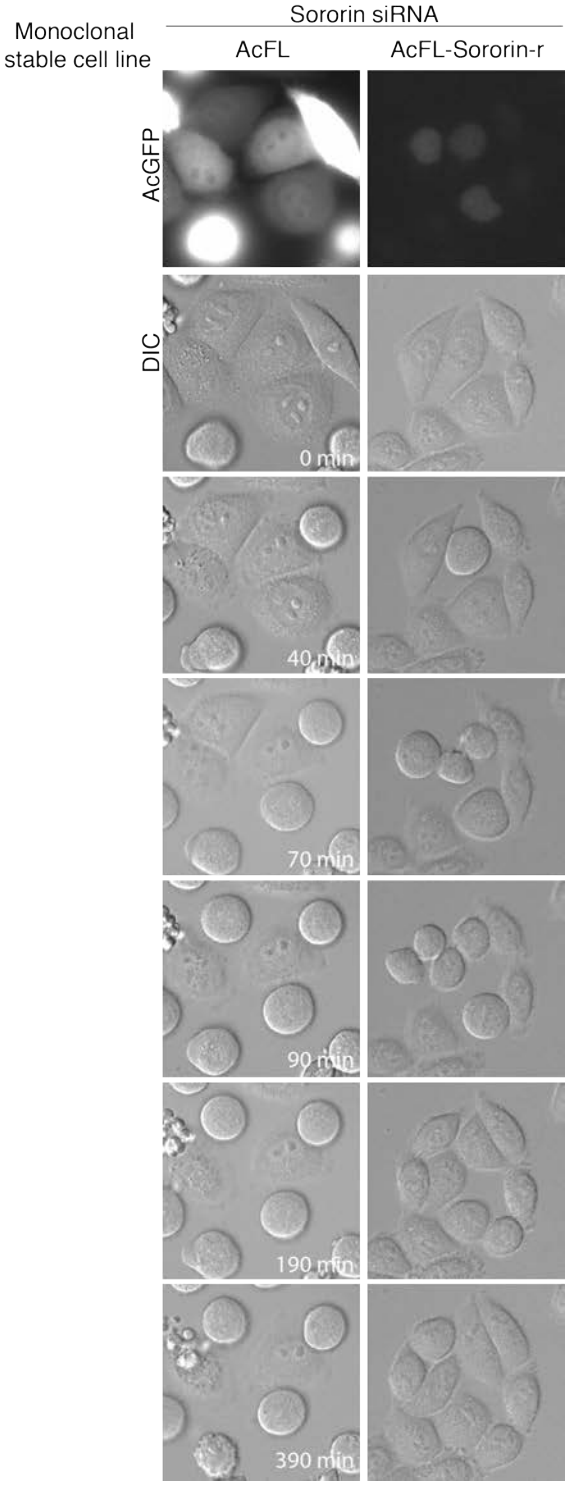

Figure 38 siRNA resistant transgenic Sororin can rescue mitotic arrest caused by depletion of endogenous Sororin

Clonal stable cell lines expressing either an AcFL tag alone or AcFL-Sororin-r were transfected with Sororin siRNA duplexes (37.5 nM) and were subjected to time-lapse microscopy 16 h post siRNA transfection. Images were acquired at 40X magnification with an interval of 10 min between acquisitions. Representative images from the two conditions that were imaged are shown.

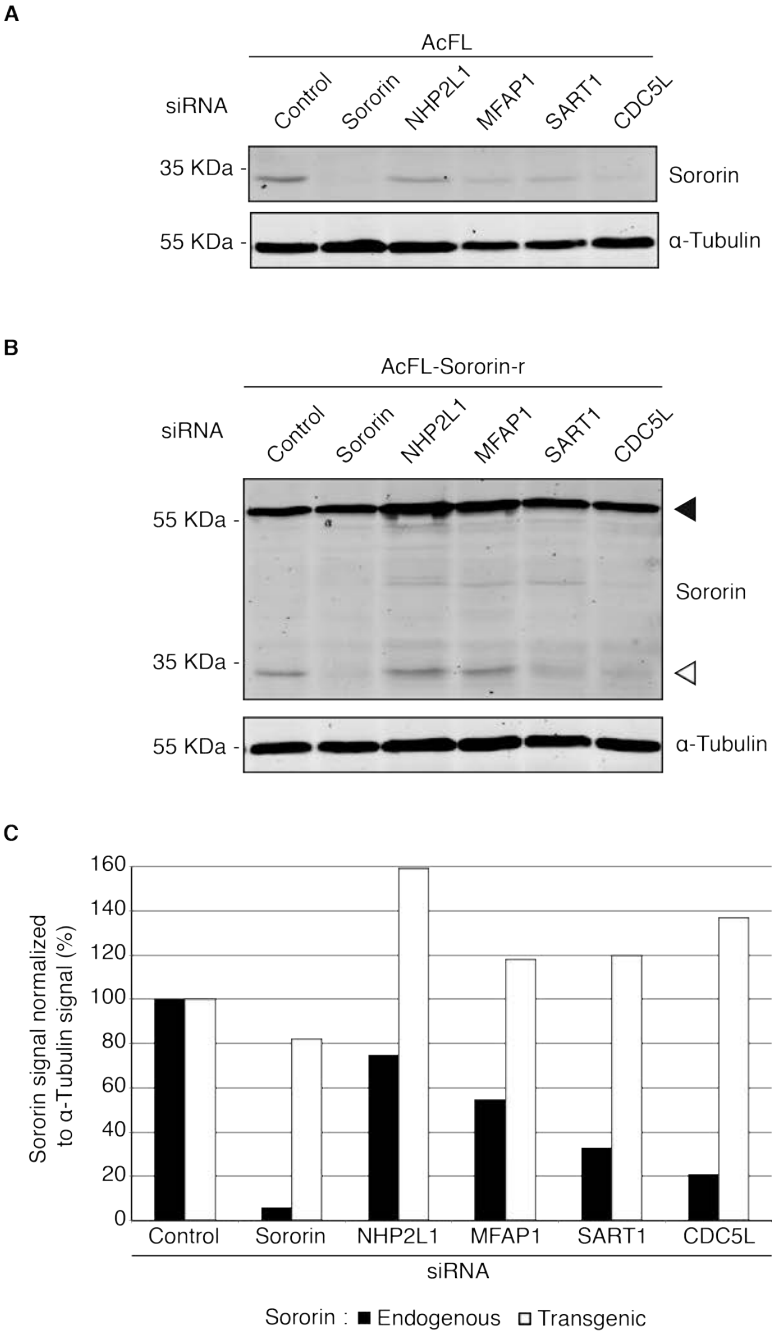

Figure 39 Depletion of splicing factors affects the levels of endogenous Sororin but not the transgenic intron-less Sororin

Clonal stable cell lines expressing either (A) an AcFL tag alone or (B) AcFL-Sororin-r were transfected with siRNAs for either 6 h (NHP2L1 and Sororin) or for 24 h (Control, MFAP1, SART1 and CDC5L siRNAs) following which the cells were arrested in 2.5 mM thymidine for 24 h and then released into DMEM. 5 h after release, the cells were harvested and processed for immunoblotting (fluorescent detection) using the indicated antibodies. Secondary antibodies coupled to fluorescent tags were used and detected using an Odyssey Imaging System. (C) The relative protein content from the immunoblot (B) was normalized to the loading control tubulin and the percentage of either endogenous (black arrowhead in immunoblot) or transgenic intron-less (white arrowhead) Sororin protein in cells treated with the indicated siRNAs was plotted.

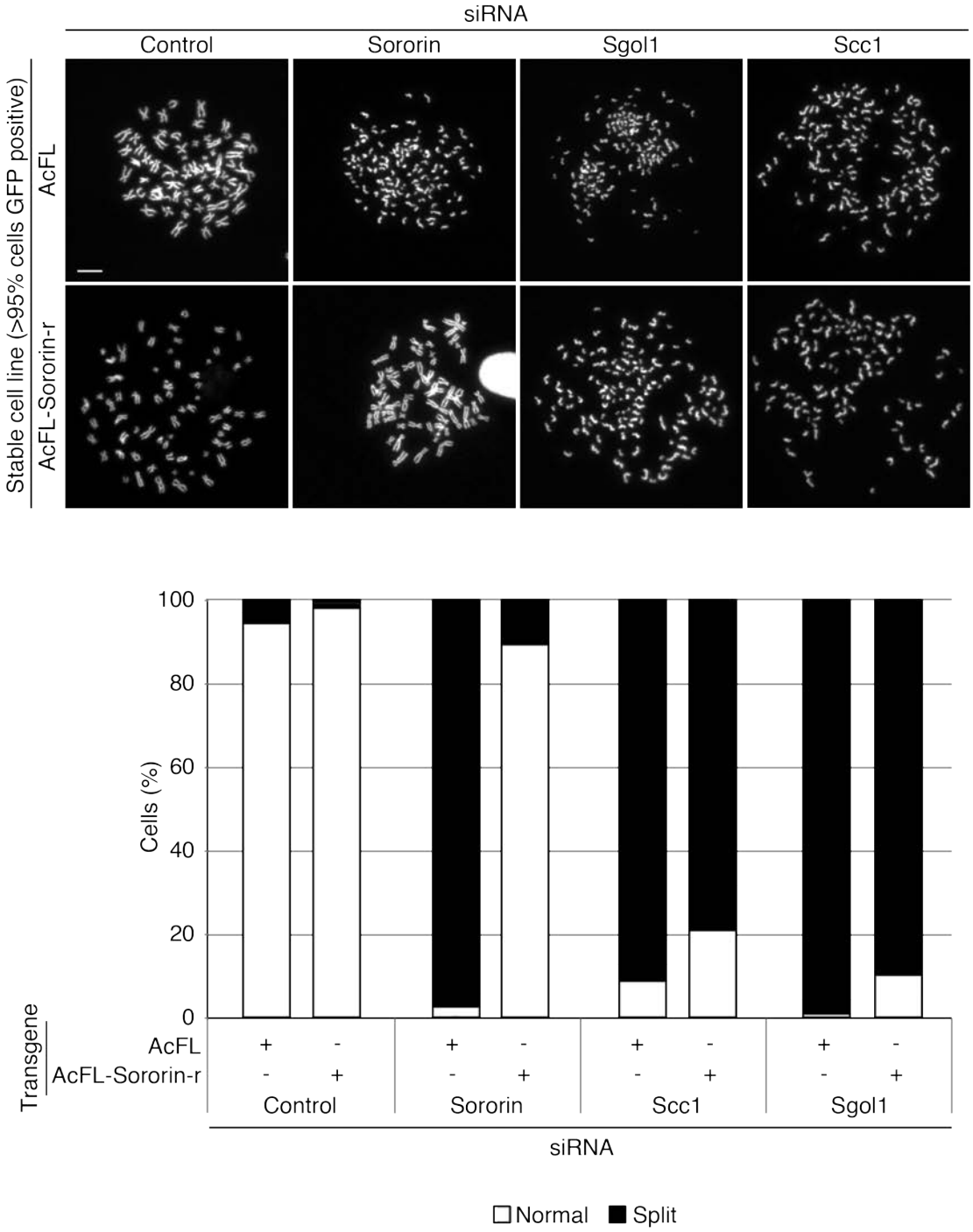

Figure 40 Transgenic expression of siRNA-resistant Sororin does not efficiently compensate for loss of Scc1 or Sgol1

Stable cell lines expressing either the AcFL tag alone or siRNA resistant AcFL-Sororin-r were transfected with the indicated siRNAs (37.5 nM) and were grown for 24 h (Sororin and Sgol1 siRNAs) or 44 h (Control siRNA) or 52 h (Scc1 siRNA). Subsequently, cells were treated with nocodazole (330nM) for 4 h and processed for chromosome spread analysis. Images of chromosome spreads from cells treated with the indicated siRNAs (upper panel, scale bar = 10 μm). Samples treated as above were scored for proportion of cells in different states of sister chromatid cohesion. (lower panels, n> 100 cells, bars represent mean from 3 independent experiments).

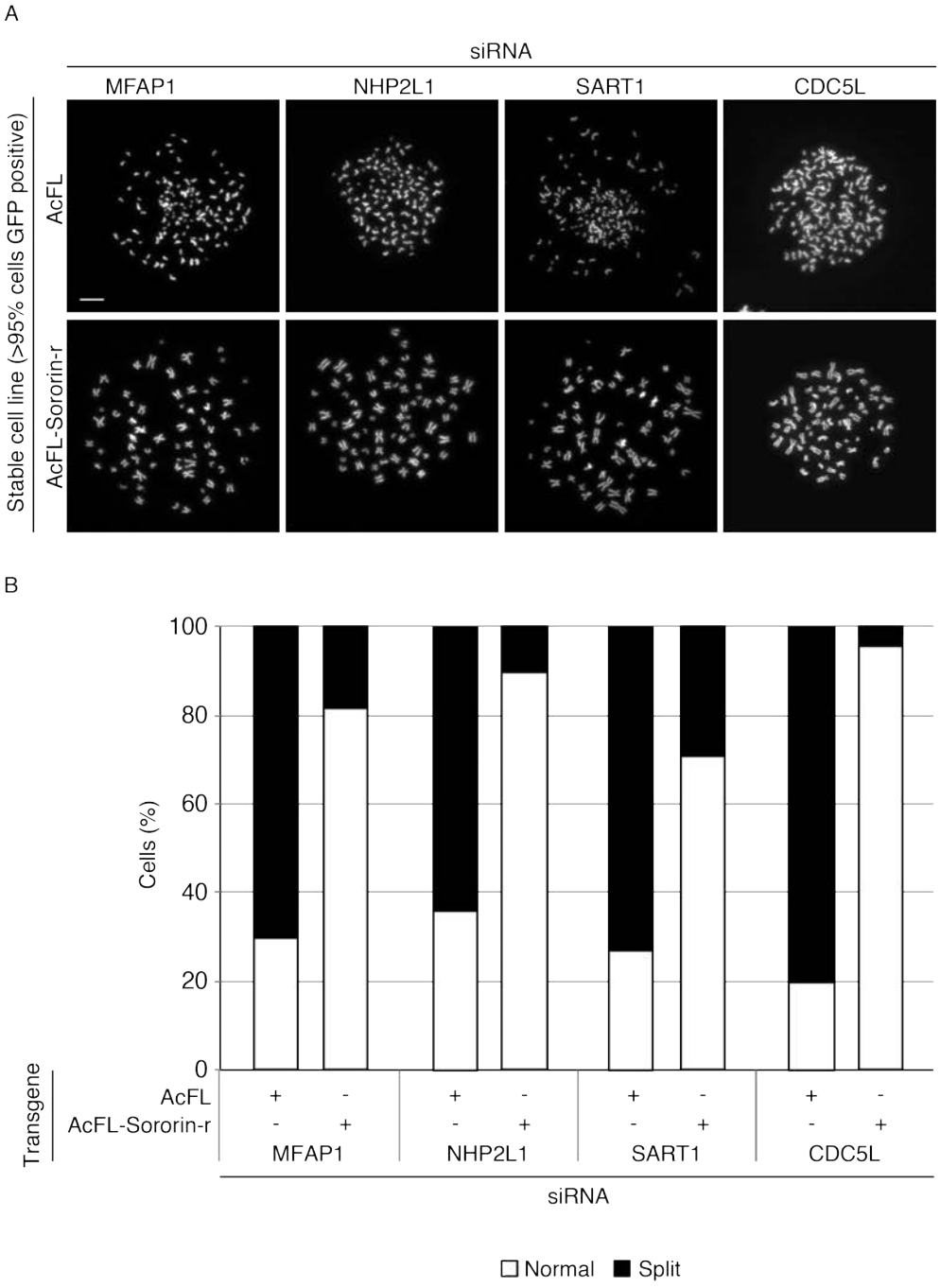

Figure 41 Expression of intron-less Sororin potently suppresses sister chromatid cohesion loss caused by depletion of splicing factors

Stable cell lines expressing either the AcFL tag alone or AcFL-Sororin-r were transfected with the indicated siRNAs (37.5 nM) and were grown for 24 hrs (NHP2L1 siRNA) or 44 h (Control, MFAP1 and SART1 siRNAs) or 52 h (CDC5L siRNA). Subsequently, cells were treated with nocodazole (330nM) for 4 h and processed for chromosome spread analysis. (A) Images of chromosome spreads from cells treated with the indicated siRNAs (scale bar = 10 μm). (B) Samples treated as above were scored for the status of sister chromatid cohesion. (n> 100 cells, bars represent mean from 3 independent experiments).

Chapter 8. Discussion

8.1 Off-target effects, the bane of functional genomic screens

The main aim of my project was to identify novel regulators of mitosis and cytokinesis using previously published genome-wide RNAi (Kittler et al., 2007, Mukherji et al., 2006, Neumann et al., 2010) and proteomic datasets (Skop et al., 2004) as an enriched source of candidate genes. Of the 718 genes chosen for the screen, the overlap among the different screens was less than 10%. Though at first glance, the lack of overlap amongst the screens is surprising, it is worth noting that the above-mentioned screens used different siRNA reagents, vastly dissimilar readouts and most importantly unique criteria to discern whether a particular gene was a hit. Another important factor that could explain the lack of correspondence between the screens is the existence of off-target effects mediated by the siRNA reducing the mRNA levels of intended as well as unintended targets. While one of the genome-wide siRNA screens used endonuclease-prepared siRNAs (esiRNAs) that are transcribed *in vitro* from DNA templates, effectively leading to a mixture of multiple siRNAs targeting each gene (Kittler et al., 2007), the other screens used individual siRNAs for the primary screen followed by validation with multiple siRNAs. It has been noted that using 'pools' of siRNAs targeting a particular gene rather than individual siRNA increases from 80% to 95%, the probability of knockdown of the target mRNA to <1/3 of its level (Echeverri and Perrimon, 2006). Off-target effects can be elicited by partial or complete homology between the seed region of the siRNA (nucleotides 2-8 of the antisense strand) and an unintended target mRNA leading to non-specific mRNA degradation (Birmingham et al., 2006, Jackson et al., 2003). Additionally siRNAs have been known to function through the miRNA pathway causing translational inhibition of non-specific targets (Doench et al., 2003, Scacheri et al., 2004).

In our screen workflow, we sought to perform the primary screen with siGENOME SMARTpools of 4 individual siRNAs against each gene. This increases the probability of target mRNA knockdown and reduces the effective concentration of the individual siRNA used. Additionally, it being a demonstrably efficient methodology to combat off-target effects, we performed downstream deconvolution screens to test the ability of individual siRNAs that constitute the pools to reproduce

the phenotype we obtained with the pools. Subsequent to the deconvolution analysis, we performed depletion experiments for selected genes with siRNAs from multiple manufacturers targeting a different stretch of sequence within each gene. This was done in order to increase the confidence about the conclusions drawn from the primary and the deconvolution screens. In summary, we decided to pursue an initial three-pronged system of assessing the hits from the primary screen before performing further assays.

In our primary siRNA screen with SMARTpools, we observed that the negative controls scored less than 8% while the positive controls scored upwards of 80% in terms of percentage nuclear abnormalities. Of the 50 hits chosen from the primary screen for further analysis, only 7 (as shown in Table 7) could reproducibly replicate the phenotype of the corresponding SMARTpool in at least two out of the four siRNA duplexes (See Table 7). This suggests that ~90% of the hits from the screen are probably due to off-target effects mediated by one of the four siRNAs that constitute the pool. This brings us to question why we were able to only detect such a meagre number of genuine hits while having started with an enriched dataset of cell cycle regulatory genes. Firstly, the cut-off in phenotypic assays that was used to classify an siRNA target as a hit was not the same in the different screens and in some cases was as low as the negative controls in our screen. Secondly, the use of automated readouts as necessitated by high throughput screens themselves could have contributed to the detection of false positives. Thirdly, it is possible that the siRNA duplexes, transfection protocol and duration of siRNA treatment that we used for our screen may not have been sufficient to reduce the protein levels of many candidate genes to levels that would have resulted in a discernible phenotype. Last but not least, given that about 90% of the top hits from our screen are likely off-target effect hits, it is possible that a vast majority of the hits from genome-wide screens suffer from the same problem.

From our primary siRNA screen, depletion of a gene named ARL5A led to a penetrant cytokinesis failure and persistence of abnormal tubulin bridges between interphase cells (Figure 13). However, further examination revealed that the phenotype was reproduced in only 2 out of 6 siRNAs tested although all six siRNA duplexes could significantly reduce the mRNA levels of ARL5A. This combined with the demonstrated off-target activity of the siRNAs against CEP55 suggested that

the cytokinesis defect observed in cells transfected with siRNAs targeting ARL5A were most likely caused by an off-target effect on CEP55.

Another hit to emerge from our siRNA screen was MFAP1, a known regulator of the tri-snRNP complex of the spliceosome. Contrary to ARL5A, the interphase nuclear morphology phenotype caused by MFAP1 SMARTpools in the primary screen was reproducibly observed in all 4 out of the 4 siRNAs tested (Figure 15). RT-PCR experiments with MFAP1 specific primers and immunoblotting experiments with MFAP1 specific antibody revealed the reduction of MFAP1 mRNA and the protein levels respectively upon transfection with MFAP1 siRNA duplexes.

The gold standard among strategies to winnow out off-target effects from genuine hits is phenotypic rescue by using a genetic complementation system. In this system, a cell line that stably expresses a transgenic copy of the gene concerned with silent mutations in the siRNA recognition sequence is generated. The immunity of this transgenic construct to the siRNA, as assessed by its ability to rescue the phenotype caused by the siRNA is a test of the genuineness of a particular hit. It is however critical to perform and interpret these complementation experiments carefully as failure to express the transgene at near physiological levels can lead to false 'rescues' (Hübner et al., 2009). A cell line stably expressing an siRNA resistant transgene of MFAP1 at near endogenous levels could potently suppress the interphase nuclear morphology defect (Figure 16). The specificity of MFAP1 specific siRNAs and the interesting interphase nuclear phenotype encouraged us to probe in more detail the role of MFAP1 in maintaining nuclear morphology.

Our experience working with hits from the screen such as ARL5A, MFAP1 and others suggests that a majority of hits emerging from siRNA screens suffer from the problem of off target effects and that robust downstream analyses such as performing depletion experiments with multiple siRNA duplexes and the use of a genetic complementation system together serve to separate the wheat from the chaff in terms of novel hits from siRNA screens. The pitfalls with siRNAs and the inherent off-target effects associated with them necessitate the development of better gene targeting approaches. Highly efficient genome editing approaches like the CRISPR/CAS system (Wang et al., 2009, Cong et al., 2013) holds much

promise and in the future, siRNA-based studies should be supplemented with such techniques.

8.2 Depletion of pre-mRNA splicing mediators leads to the loss of sister chromatid cohesion and cell division failure

After having established a causative link between the observed interphase nuclear morphology phenotype and the loss of MFAP1 protein, we sought to understand the molecular basis underlying this phenomenon. We could demonstrate that MFAP1-depleted cells arrested in mitosis in a spindle assembly checkpoint (SAC) dependent manner. Furthermore, mitotic chromosome spreads and FISH experiments revealed that MFAP1-depleted cells exhibited premature sister chromatid cohesion loss. We hypothesised that the lack of cohesion between sister chromatids in these cells could be the underlying cause behind their inability to align their chromosomes at the metaphase plate and to execute mitosis successfully.

Using a mass spectrometry dataset of spliceosome components (Zhou et al., 2002) and the MitoCheck phenotypic profile database (http://www.mitocheck.org), we identified 33 pre-mRNA splicing genes whose depletion led to abnormal mitosis and cell death. Remarkably, we could show that the depletion of 30 out of the 33 genes by siRNA duplexes led to a premature loss of sister chromatid cohesion. For the depletion of many splicing factors, the severity of the sister chromatid cohesion defect was comparable to the loss of a core cohesin function, such as depletion of the ring subunit SCC1. We sought to understand the molecular basis behind the unusual link between pre-mRNA splicing and sister chromatid cohesion. Crucially, we could show that depletion of four distinct splicing factors namely MFAP1, NHP2L1, CDC5L and SART1 resulted in a loss of sister chromatid cohesion in interphase soon after DNA replication already in S-phase that is different from the mitosis specific loss of sister chromatid cohesion that cells sustain upon loss of Sgol1, a well-known regulator of centromeric cohesion in mitosis (Kitajima et al., 2004, McGuinness et al., 2005, Watanabe and Kitajima, 2005).

8.3 Loss of pre-mRNA splicing factors perturb the levels of Sororin, a protein required for sister chromatid cohesion

In order to decipher the molecular mechanism by which pre-mRNA splicing factors control sister chromatid cohesion, we pursued several distinct possibilities. Defects in viability caused by the depletion of a splicing factor ASF/SF2 in chicken DT40 cells were shown to be rescued by expressing RNaseH1 in these cells (Li and Manley, 2005). Based on this we hypothesised that R-loops (RNA-DNA hybrids) that might be generated by faulty co-transcriptional splicing processes could act as a physical hindrance for the cohesin ring to encircle chromatin. Since expression of the enzymes RNaseH1 is known to remove the RNA component of the R-loops, we tested if expression of RNaseH1 could rescue the loss of sister chromatid cohesion upon the depletion of the splicing factors. We observed no change in the proportion of cells that exhibited split sisters in cells that express RNaseH1 or not. One caveat of our experiments using transgenic RNase H1 is that we have no evidence as yet to demonstrate that the RNaseH1 is functional in the cells when we deplete the pre-mRNA splicing factors. Nevertheless, the very same RNaseH1-EGFP construct that we used to generate the transgenic cell line has been successfully used to resolve R-loops in the past (Cerritelli et al., 2003, Skourti-Stathaki et al., 2011).

Depletion of the splicing factors did not measurably affect the loading of cohesin onto chromatin. However, it resulted in an increased dissociation of cohesin from chromatin as demonstrated by iFRAP experiments (Figure 33). As a next step, we hypothesised an indirect and gene expression-mediated role of pre-mRNA splicing factors in sister chromatid cohesion. The idea was that the inhibition of pre-mRNA splicing led to a defect in cohesin maintenance during interphase through a perturbation in the protein levels of either the core cohesin subunits, SMC1, SMC3, SCC1 and SA2 or of Sororin, a protein required for cohesion maintenance in post-replicative cells. Through immunoblotting experiments, we observed that the levels of Sororin dropped 5-fold or higher upon depletion of the splicing factors suggesting that it was the primary target of the pre-mRNA splicing factors among the proteins regulating sister chromatid cohesion. We also observed smaller perturbations in the levels of SMC1, SCC1 and SA2 although this was evident in cells depleted of Sororin as well. We do not yet know if the fluctuation in the levels of the core cohesin subunits contributes to the loss of sister chromatid cohesion upon

depletion of the splicing factors and more interestingly upon depletion of Sororin. We hypothesise that the depletion of pre-mRNA splicing factors results in reduced maintenance of cohesin on chromatin because of lack of availability of Sororin.

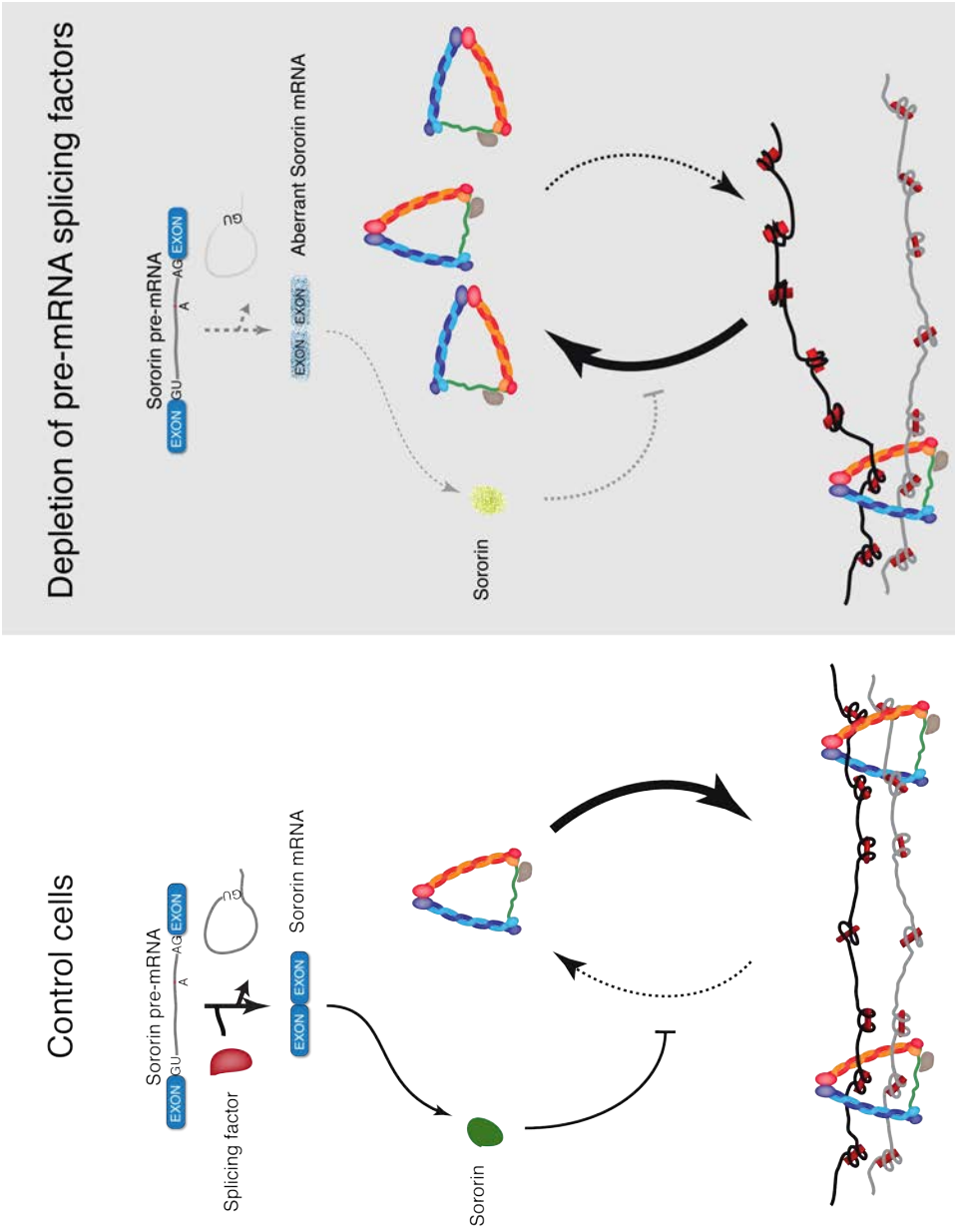

Figure 42 Model for Sororin-mediated regulation of sister chromatid cohesion by effectors of pre-mRNA splicing
In control cells, pre-mRNA splicing of Sororin ensures the presence of functional Sororin protein at the S-phase of every cell cycle. Upon depletion of pre-mRNA splicing factors, levels of Sororin protein drops steeply as there is no new Sororin protein being producedd to replenish the ones that are degraded during the G1-phase of every cell cycle. The lack of Sororin, a factor necessary for cohesion maintenance leads to a a reduced association between cohesin and chromatin and thereby to a premature loss of sister chromatid cohesion.

In addition to measuring the protein levels of mature Sororin, we performed RT-PCR experiments using Sororin specific primers that either amplify within intron 1 or across exon 1 and exon 2. We observed that depletion of splicing factors led to a 2-5-fold increase in the presence of the intron compared to the control although levels of exon1-2 either stayed the same or reduced by 1 fold. This suggests that pre-mRNA splicing of Sororin is defective upon depletion of the splicing factors. This raises the possibility that lack of pre-mRNA splicing of Sororin could lead to the production of an erroneous truncated Sororin protein. Interestingly, intron 1 does not contain an in-frame stop codon although it introduces a frame shift that leads to a premature stop codon in exon 3 irrespective of the splicing status of intron 2. This suggests that an erroneous and non-functional Sororin protein that is made up of just exon1-intron1-exon2-intron2-exon3 or exon1-intron1-exon2-exon3 might be produced. Since the Sororin antibody that we have, was raised against a stretch of amino acids in the N terminus of the protein, it is possible that this non-functional Sororin protein might still be detectable in samples where pre-mRNA splicing is affected. We are currently pursuing this idea. It is also worth mentioning that we only use primers specific for intron 1 for the RT-PCR experiment. In the near future, we will expand this analysis to detect the levels of the other 4 introns in Sororin upon depletion of the splicing factors.

Having demonstrated a steep fall in the levels of mature and functional Sororin protein and a perturbation in the pre-mRNA splicing status of Sororin mRNA in cells transfected with siRNAs against the splicing factors, the logical step forward was to determine if supplying an intron-less transgene of Sororin could rescue the sister chromatid cohesion in cells depleted of the splicing factors. We observed that a cell line expressing an intron-less Sororin transgene could rescue the loss of sister chromatid cohesion that was caused by the depletion of the splicing factors. However, the mitotic arrest persisted even in the presence of the intron-less Sororin. Since the expression of an intron-less transgene of Sororin only rescues the loss of sister chromatid cohesion but not mitotic progression, leaving cells transfected with siRNAs against the splicing factors for prolonged duration in mitosis could lead to an artificial loss of sister chromatid cohesion caused by cohesion fatigue (Daum et al., 2011, Stevens et al., 2011). This suggests cohesion fatigue may contribute to the fact that we only observe an incomplete (yet strong)

rescue in sister chromatid cohesion by expressing an intron-less Sororin transgene. Changing the timing of cell growth and mitotic arrest prior to performing chromosome spreads can address this possibility.

The intron-less Sororin rescue experiment firstly reveals that the loss of sister chromatid cohesion that is caused by the depletion of the splicing factors is most likely caused by a precipitous drop in Sororin levels. Secondly, it tells us that the loss of pre-mRNA splicing factors affects the execution of mitosis not just through a Sororin dependent loss of sister chromatid cohesion but also through an as yet unknown mechanism. Kathleen Gould and colleagues demonstrated the requirement of pre-mRNA splicing of α-tubulin for the proper functioning of the mitotic spindle in yeast cells (Burns et al., 2002). Taken together with our observation that the mitotic arrest triggered in cells depleted of the splicing factors is dependent on the spindle assembly checkpoint, it is possible that in addition to the loss of sister chromatid cohesion mediated through Sororin, defects in pre-mRNA splicing could affect the formation of the mitotic spindle in mammalian cells. This could be through pre-mRNA splicing of a number of possible targets such as α or β-tubulin isoforms, centrosomal components etc. In addition to the mitotic spindle, it is also possible that depletion of pre-mRNA splicing components could cause mis-splicing of targets that are critical for mitotic exit such as components of the APC/C, mitotic phosphatases, components of the kinetochore etc. The SAC dependence of the mitotic arrest however suggests a reduced probability for the target of the pre-mRNA splicing machinery to be mitotic phosphatases or a component of the APC/C although this possibility cannot be completely ruled out. Further work is necessary to uncover the other potential targets of the pre-mRNA splicing machinery to understand the molecular mechanisms behind the mitotic arrest triggered in cells defective in pre-mRNA splicing.

It is interesting that Sororin is one of the primary targets of the splicing machinery in regulating sister chromatid cohesion, why might this be the case? About 90% of the cohesin complexes are removed intact without the need for separase mediated cleavage through the prophase pathway (Peters et al., 2008). This ensures that a steady supply of cohesin ring complexes abound in the cell thereby rendering the core subunits refractory to the loss of pre-mRNA splicing. Sororin on the other hand, is degraded at the end of every cell cycle through APC/C^{Cdh1} mediated proteasomal

degradation at G_1-phase (Rankin et al., 2005, Wu et al., 2011, Peters and Nishiyama, 2012, Zhang and Pati, 2012) thereby necessitates renewed Sororin translation and possibly transcription of Sororin mRNA for production of mature Sororin protein at every S-phase of the cell cycle. We hypothesize that this opens up Sororin to defects in pre-mRNA splicing errors. Given the delicate balance maintained by the cohesion-maintaining activity of Sororin and the anti-establishment effect mediated by WAPL, it is conceivable that any perturbations in the relative amounts of these proteins impacts sister chromatid cohesion dramatically. Thus, Sororin while being an indispensable factor for cohesion maintenance, is also a protein whose levels fluctuate through cell cycle thereby possibly creating a strict dependence on gene expression competence. This hypothesis makes a testable prediction that the critical factor behind the premature loss of sister chromatid cohesion upon depletion of the splicing factors is that the anti-establishment effect of WAPL is relatively unchecked by the drop in levels of Sororin. Therefore, its stands to suggest that, removing the anti-establishment effect by depleting WAPL should make the cells immune to not only loss of Sororin as has been demonstrated before (Nishiyama et al., 2010) but also to loss of pre-mRNA splicing regulators. Secondly, the need for transcription and post-transcriptional processing of Sororin mRNA at every cell cycle happens because of the APC/C^{Cdh1} mediated degradation of Sororin in the G1-phase of the cell cycle. Is it possible to prevent this degradation of Sororin? Previously it has been shown that the KEN box domain in Sororin makes it a target for APC/C^{Cdh1} mediated degradation (Rankin et al., 2005). To date it is not known why Sororin has to be degraded at the end of mitosis. It is thought that the presence of Sororin before replication could create cohesion artefacts that might have unforeseen consequences on sister chromatid cohesion and thereby for DNA damage repair processes (Peters and Nishiyama, 2012, Zhang et al., 2011, Rankin et al., 2005, Rankin, 2005). However, it is known that Sororin binding to cohesin requires DNA replication and SMC3 acetylation that happen only in S-phase. Thus Sororin cannot cause cohesion artefacts before S-phase and there seems to be no requirement for it to be degraded by the APC/C. Even though there is an indication that mutating the KEN box domain of Sororin, rendering it resistant to APC/C^{Cdh1} mediated degradation affects cell growth, this idea has never been reportedly tested (Rankin, 2005, Zhang and Pati, 2012). It is therefore possible to test if the absence of

Sororin pre-mRNA splicing caused by the depletion of splicing factors, can be offset by preventing the degradation of Sororin by either mutating the KEN box domain or by depleting Cdh1 from cells. We will test these ideas in the lab in the near future.

8.4 Are mitotic defects the primary effect of pre-mRNA processing defects?

A number of recent reports suggest that perturbing pre-mRNA processing pathways through siRNA based depletion results in a protracted mitotic arrest, some accompanied by a premature loss of sister chromatid cohesion (Yamazaki et al., 2010, Matsunaga et al., 2012, Hofmann et al., 2010). Additionally a number of pre-mRNA processing components have been identified as regulators of the cell cycle in the genome-wide siRNA screens for novel regulators of the cell cycle(Neumann et al., 2010, Kittler et al., 2007). Also, it was shown a while ago, that a temperature sensitive mutant of Cdc5 in fission yeast was defective in pre-mRNA splicing of α-tubulin and resulted in defects in mitosis. Furthermore, these defects in nuclear division could be ameliorated by the removal of the single intron from α-tubulin although the cells still suffered from the global loss of splicing (Burns et al., 2002). This raises the interesting question as to why a defect in the pre-mRNA processing pathways manifests primarily through defects in mitosis. Though it is currently not known if and why this might be the case, we have made some observations that could shed some light into this phenomenon. We have observed that inhibiting global splicing in human cells by using spliceostatin A, a potent inhibitor of pre-mRNA splicing (Kaida et al., 2007, Roybal and Jurica, 2010) at concentrations (50-250 nM) that are known to inhibit pre-mRNA splicing, prevents mitotic entry in HeLa cells (Data not shown). Reducing the spliceostain A concentration to less than 2 nM led to a mitotic arrest that was not accompanied by defects in sister chromatid cohesion. It thus raises the possibility that differential sensitivity amongst targets for the requirement of pre-mRNA processing pathways is reflected as varied phenotypes within cells. This suggests that pharmacologically inhibiting pre-mRNA splicing globally can lead to an arrest in cell cycle progression in interphase whereas a less potent mode of splicing inhibition by siRNA mediated

depletion of some spliceosome components allows cell cycle progression but inhibits successful mitosis by affecting either sister chromatid cohesion, the mitotic spindle, mitotic exit components or all or some of them. This hypothesis could be tested perhaps by imposing a gradient of splicing competence in cells by using different concentrations of global splicing inhibitors and assessing the functionality or the pre-mRNA splicing status of specific mitotic target proteins using RNA-Seq experiments.

The experiments with spliceostatin A also raises the possibility that using concentrations of spliceostatin A that prevent mitotic entry can still affect sister chromatid cohesion in interphase cells. We are testing this hypothesis by performing FISH experiments in interphase cells to test for the status of sister chromatid cohesion upon treatment with different doses of spliceostatin A.

8.5 SF3B1 mutations in hematopoietic malignancies; A connection to sister chromatid cohesion and cohesin turnover on chromatin?

Through our chromosome spread analysis for spliceosome components, we have observed that one of the splicing factors whose depletion by siRNA causes a dramatic loss of sister chromatid cohesion during mitosis is SF3B1. SF3B1 is a component of the U2 snRNP complex that is required for the assembly of the pre-spliceosomal E complex. Recently, SF3B1 has emerged as one of the most frequently mutated genes in Chronic Lymphocytic Leukemia (CLL) patients, ahead of even the tumour suppressor TP53 (Wang et al., 2011, Rossi et al., 2012, Quesada et al., 2012, Landau and Wu, 2013). Somatic SF3B1 mutations were also detected at high frequency in individuals affected by myelodyplastic syndrome (MDS), reaching 65% penetrance in MDS with ringed sideroblasts, a variant of MDS (Papaemmanuil et al., 2011, Yoshida et al., 2011). The most frequent recurrent mutation in CLL and MDS patients is K700E (more than 50% of cases). The recurrent nature of somatic SF3B1 mutations in MDS and CLL strongly suggest that these mutations act as key driver events in these diseases. Despite the overwhelming association of SF3B1 mutations with myeloid neoplasms and leukemias, the mechanisms by which these mutations contribute to pathogenesis at the cellular level and the specific targets of SF3B1 that are perturbed remain

unclear. Our finding that SF3B1 is essential for sister chromatid cohesion raises the possibility that mutations in SF3B1 could contribute to CLL and MDS pathology by affecting the turnover of cohesin on chromatin. In addition to SF3B1, Depletion of another pre-mRNA splicing factor, U2AF1 which is also mutated in MDS (Yoshida et al., 2011), also severely impairs sister chromatid cohesion. We will test the above-mentioned hypothesis by determining the properties of cohesin and the state of sister chromatid cohesion in cells carrying the SF3B1 disease mutation K700E. In addition to using a HeLa cell line expressing a transgenic copy of SF3B1 with the K700E mutation, we plan to assess the state of sister chromatid cohesion in peripheral blood mononuclear fractions of CLL patients carrying the K700E mutation (provided by Dr. Elías Campo and Dr. Carlos López-Otín, Univ. of Barcelona Hospital Clinic and Univ. of Oviedo, Spain). Based on our finding that the expression of an intron-less transgene of Sororin can rescue the sister chromatid cohesion loss caused by depletion of a number of splicing factors, we will test whether expression of this transgene can restore cohesin-related cellular or molecular defects in SF3B1-K700E models.

8.6 Other novel hits from the siRNA screen beyond MFAP1

In order to facilitate downstream analysis, we used an arbitrary cut-off of 23% nuclear abnormalities in the primary screen to shortlist genes for further analysis. However, further experiments demonstrated that low scoring genes based on the readout that we used in the primary screen, might have a much more potent impact on mitosis than revealed by nuclear abnormalities observed in interphase. Illustratively, while MFAP1 registered a score only of 23% nuclear abnormalities in the primary screen, downstream experiments revealed that depletion of MFAP1 resulted in almost all cells failing to undergo successful mitosis with more than 75-90% of cells suffering from premature loss of sister chromatid cohesion. The discrepancy between phenotypic penetrance in interphase versus mitosis is probably caused by the loss of severely defective and arrested mitotic cells by apoptosis. The use of live cell imaging as primary screen readout could have ameliorated this problem. These considerations warrant the further investigation of seemingly low scoring hits (below 23% nuclear abnormalities) from our primary

screen. Gene depletions in this category might potentially have far stronger consequences for mitosis than is revealed by the interphase readout. This will be pursued in the lab in the future with a special emphasis on the mitotic index measurements upon knockdown of specific genes.

Reference List

ADACHI, Y., KOKUBU, A., EBE, M., NAGAO, K. & YANAGIDA, M. 2008. Cut1/separase-dependent roles of multiple phosphorylation of fission yeast cohesion subunit Rad21 in post-replicative damage repair and mitosis. *Cell Cycle,* 7**,** 765-76.

ADAMS, R. R., WHEATLEY, S. P., GOULDSWORTHY, A. M., KANDELS-LEWIS, S. E., CARMENA, M., SMYTHE, C., GERLOFF, D. L. & EARNSHAW, W. C. 2000. INCENP binds the Aurora-related kinase AIRK2 and is required to target it to chromosomes, the central spindle and cleavage furrow. *Curr Biol,* 10**,** 1075-8.

AGOSTINIS, P., DERUA, R., SARNO, S., GORIS, J. & MERLEVEDE, W. 1992. Specificity of the polycation-stimulated (type-2A) and ATP,Mg-dependent (type-1) protein phosphatases toward substrates phosphorylated by P34cdc2 kinase. *Eur J Biochem,* 205**,** 241-8.

AJUH, P., KUSTER, B., PANOV, K., ZOMERDIJK, J. C., MANN, M. & LAMOND, A. I. 2000. Functional analysis of the human CDC5L complex and identification of its components by mass spectrometry. *EMBO J,* 19**,** 6569-81.

AJUH, P., SLEEMAN, J., CHUSAINOW, J. & LAMOND, A. I. 2001. A direct interaction between the carboxyl-terminal region of CDC5L and the WD40 domain of PLRG1 is essential for pre-mRNA splicing. *J Biol Chem,* 276**,** 42370-81.

ANDERSEN, D. S. & TAPON, N. 2008. Drosophila MFAP1 is required for pre-mRNA processing and G2/M progression. *J Biol Chem,* 283**,** 31256-67.

ANDERSON, D. E., LOSADA, A., ERICKSON, H. P. & HIRANO, T. 2002. Condensin and cohesin display different arm conformations with characteristic hinge angles. *J Cell Biol,* 156**,** 419-24.

ANGELL, R. 1995. Mechanism of chromosome nondisjunction in human oocytes. *Prog Clin Biol Res,* 393**,** 13-26.

ARUMUGAM, P., GRUBER, S., TANAKA, K., HAERING, C. H., MECHTLER, K. & NASMYTH, K. 2003. ATP hydrolysis is required for cohesin's association with chromosomes. *Curr Biol,* 13**,** 1941-53.

ARUMUGAM, P., NISHINO, T., HAERING, C. H., GRUBER, S. & NASMYTH, K. 2006. Cohesin's ATPase activity is stimulated by the C-terminal Winged-Helix domain of its kleisin subunit. *Curr Biol,* 16**,** 1998-2008.

AXTON, J. M., DOMBRADI, V., COHEN, P. T. & GLOVER, D. M. 1990. One of the protein phosphatase 1 isoenzymes in Drosophila is essential for mitosis. *Cell,* 63**,** 33-46.

BALASUBRAMANIAN, M. K., SRINIVASAN, R., HUANG, Y. & NG, K. H. 2012. Comparing contractile apparatus-driven cytokinesis mechanisms across kingdoms. *Cytoskeleton (Hoboken),* 69**,** 942-56.

BANNISTER, L. A., REINHOLDT, L. G., MUNROE, R. J. & SCHIMENTI, J. C. 2004. Positional cloning and characterization of mouse mei8, a disrupted allelle of the meiotic cohesin Rec8. *Genesis,* 40**,** 184-94.

BARBER, T. D., MCMANUS, K., YUEN, K. W., REIS, M., PARMIGIANI, G., SHEN, D., BARRETT, I., NOUHI, Y., SPENCER, F., MARKOWITZ, S., VELCULESCU, V. E., KINZLER, K. W., VOGELSTEIN, B., LENGAUER, C. & HIETER, P. 2008. Chromatid cohesion defects may underlie chromosome instability in human colorectal cancers. *Proc Natl Acad Sci U S A,* 105**,** 3443-8.

BARR, A. R. & GERGELY, F. 2007. Aurora-A: the maker and breaker of spindle poles. *J Cell Sci,* 120**,** 2987-96.
BARR, F. A. 2002. Inheritance of the endoplasmic reticulum and Golgi apparatus. *Curr Opin Cell Biol,* 14**,** 496-9.
BARR, F. A. & GRUNEBERG, U. 2007. Cytokinesis: placing and making the final cut. *Cell,* 131**,** 847-60.
BARR, F. A., SILLJE, H. H. & NIGG, E. A. 2004. Polo-like kinases and the orchestration of cell division. *Nat Rev Mol Cell Biol,* 5**,** 429-40.
BARTELS, C., KLATT, C., LUHRMANN, R. & FABRIZIO, P. 2002. The ribosomal translocase homologue Snu114p is involved in unwinding U4/U6 RNA during activation of the spliceosome. *EMBO Rep,* 3**,** 875-80.
BASTOS, R. N. & BARR, F. A. 2010. Plk1 negatively regulates Cep55 recruitment to the midbody to ensure orderly abscission. *J Cell Biol,* 191**,** 751-60.
BECKOUET, F., HU, B., ROIG, M. B., SUTANI, T., KOMATA, M., ULUOCAK, P., KATIS, V. L., SHIRAHIGE, K. & NASMYTH, K. 2010. An Smc3 acetylation cycle is essential for establishment of sister chromatid cohesion. *Mol Cell,* 39**,** 689-99.
BEHZADNIA, N., GOLAS, M. M., HARTMUTH, K., SANDER, B., KASTNER, B., DECKERT, J., DUBE, P., WILL, C. L., URLAUB, H., STARK, H. & LUHRMANN, R. 2007. Composition and three-dimensional EM structure of double affinity-purified, human prespliceosomal A complexes. *EMBO J,* 26**,** 1737-48.
BERGLUND, J. A., ABOVICH, N. & ROSBASH, M. 1998. A cooperative interaction between U2AF65 and mBBP/SF1 facilitates branchpoint region recognition. *Genes Dev,* 12**,** 858-67.
BERGLUND, J. A., CHUA, K., ABOVICH, N., REED, R. & ROSBASH, M. 1997. The splicing factor BBP interacts specifically with the pre-mRNA branchpoint sequence UACUAAC. *Cell,* 89**,** 781-7.
BIRMINGHAM, A., ANDERSON, E. M., REYNOLDS, A., ILSLEY-TYREE, D., LEAKE, D., FEDOROV, Y., BASKERVILLE, S., MAKSIMOVA, E., ROBINSON, K., KARPILOW, J., MARSHALL, W. S. & KHVOROVA, A. 2006. 3' UTR seed matches, but not overall identity, are associated with RNAi off-targets. *Nat Methods,* 3**,** 199-204.
BLAT, Y. & KLECKNER, N. 1999. Cohesins bind to preferential sites along yeast chromosome III, with differential regulation along arms versus the centric region. *Cell,* 98**,** 249-59.
BLOOM, J. & CROSS, F. R. 2007. Multiple levels of cyclin specificity in cell-cycle control. *Nat Rev Mol Cell Biol,* 8**,** 149-60.
BONNAL, S. & VALCARCEL, J. 2008. Molecular biology: spliceosome meets telomerase. *Nature,* 456**,** 879-80.
BONNAL, S., VIGEVANI, L. & VALCARCEL, J. 2012. The spliceosome as a target of novel antitumour drugs. *Nat Rev Drug Discov,* 11**,** 847-59.
BORGES, V., LEHANE, C., LOPEZ-SERRA, L., FLYNN, H., SKEHEL, M., ROLEF BEN-SHAHAR, T. & UHLMANN, F. 2010. Hos1 deacetylates Smc3 to close the cohesin acetylation cycle. *Mol Cell,* 39**,** 677-88.
BRENNAN, I. M., PETERS, U., KAPOOR, T. M. & STRAIGHT, A. F. 2007. Polo-like kinase controls vertebrate spindle elongation and cytokinesis. *PLoS One,* 2**,** e409.
BRIESE, M., ESMAEILI, B. & SATTELLE, D. B. 2005. Is spinal muscular atrophy the result of defects in motor neuron processes? *Bioessays,* 27**,** 946-57.
BRITO, D. A. & RIEDER, C. L. 2006. Mitotic checkpoint slippage in humans occurs via cyclin B destruction in the presence of an active checkpoint. *Curr Biol,* 16**,** 1194-200.

BUHEITEL, J. & STEMMANN, O. 2013. Prophase pathway-dependent removal of cohesin from human chromosomes requires opening of the Smc3-Scc1 gate. *EMBO J,* 32**,** 666-76.

BURKARD, M. E., MACIEJOWSKI, J., RODRIGUEZ-BRAVO, V., REPKA, M., LOWERY, D. M., CLAUSER, K. R., ZHANG, C., SHOKAT, K. M., CARR, S. A., YAFFE, M. B. & JALLEPALLI, P. V. 2009. Plk1 self-organization and priming phosphorylation of HsCYK-4 at the spindle midzone regulate the onset of division in human cells. *PLoS Biol,* 7**,** e1000111.

BURKARD, M. E., RANDALL, C. L., LAROCHELLE, S., ZHANG, C., SHOKAT, K. M., FISHER, R. P. & JALLEPALLI, P. V. 2007. Chemical genetics reveals the requirement for Polo-like kinase 1 activity in positioning RhoA and triggering cytokinesis in human cells. *Proc Natl Acad Sci U S A,* 104**,** 4383-8.

BURNS, C. G., OHI, R., MEHTA, S., O'TOOLE, E. T., WINEY, M., CLARK, T. A., SUGNET, C. W., ARES, M., JR. & GOULD, K. L. 2002. Removal of a single alpha-tubulin gene intron suppresses cell cycle arrest phenotypes of splicing factor mutations in Saccharomyces cerevisiae. *Mol Cell Biol,* 22**,** 801-15.

C, B. J. 1974. HeLa (for Henrietta Lacks). *Science,* 184**,** 1268.

CAMPBELL, C. S. & DESAI, A. 2013. Tension sensing by Aurora B kinase is independent of survivin-based centromere localization. *Nature,* 497**,** 118-21.

CANUDAS, S. & SMITH, S. 2009. Differential regulation of telomere and centromere cohesion by the Scc3 homologues SA1 and SA2, respectively, in human cells. *J Cell Biol,* 187**,** 165-73.

CAPUTI, M. & ZAHLER, A. M. 2002. SR proteins and hnRNP H regulate the splicing of the HIV-1 tev-specific exon 6D. *EMBO J,* 21**,** 845-55.

CARLTON, J. G., CABALLE, A., AGROMAYOR, M., KLOC, M. & MARTIN-SERRANO, J. 2012. ESCRT-III governs the Aurora B-mediated abscission checkpoint through CHMP4C. *Science,* 336**,** 220-5.

CARMENA, M. & EARNSHAW, W. C. 2003. The cellular geography of aurora kinases. *Nat Rev Mol Cell Biol,* 4**,** 842-54.

CARMENA, M., RUCHAUD, S. & EARNSHAW, W. C. 2009. Making the Auroras glow: regulation of Aurora A and B kinase function by interacting proteins. *Curr Opin Cell Biol,* 21**,** 796-805.

CARMENA, M., WHEELOCK, M., FUNABIKI, H. & EARNSHAW, W. C. 2012. The chromosomal passenger complex (CPC): from easy rider to the godfather of mitosis. *Nat Rev Mol Cell Biol,* 13**,** 789-803.

CERRITELLI, S. M., FROLOVA, E. G., FENG, C., GRINBERG, A., LOVE, P. E. & CROUCH, R. J. 2003. Failure to produce mitochondrial DNA results in embryonic lethality in Rnaseh1 null mice. *Mol Cell,* 11**,** 807-15.

CHAKAROVA, C. F., HIMS, M. M., BOLZ, H., ABU-SAFIEH, L., PATEL, R. J., PAPAIOANNOU, M. G., INGLEHEARN, C. F., KEEN, T. J., WILLIS, C., MOORE, A. T., ROSENBERG, T., WEBSTER, A. R., BIRD, A. C., GAL, A., HUNT, D., VITHANA, E. N. & BHATTACHARYA, S. S. 2002. Mutations in HPRP3, a third member of pre-mRNA splicing factor genes, implicated in autosomal dominant retinitis pigmentosa. *Hum Mol Genet,* 11**,** 87-92.

CHAN, K. L., ROIG, M. B., HU, B., BECKOUET, F., METSON, J. & NASMYTH, K. 2012. Cohesin's DNA exit gate is distinct from its entrance gate and is regulated by acetylation. *Cell,* 150**,** 961-74.

CHAPMAN, J. R., TAYLOR, M. R. & BOULTON, S. J. 2012. Playing the end game: DNA double-strand break repair pathway choice. *Mol Cell,* 47**,** 497-510.

CHATTERJEE, A., ZAKIAN, S., HU, X. W. & SINGLETON, M. R. 2013. Structural insights into the regulation of cohesion establishment by Wpl1. *EMBO J,* 32**,** 677-87.

CHEESEMAN, I. M., ANDERSON, S., JWA, M., GREEN, E. M., KANG, J., YATES, J. R., 3RD, CHAN, C. S., DRUBIN, D. G. & BARNES, G. 2002. Phospho-regulation of kinetochore-microtubule attachments by the Aurora kinase Ipl1p. *Cell,* 111**,** 163-72.

CHEESEMAN, I. M. & DESAI, A. 2008. Molecular architecture of the kinetochore-microtubule interface. *Nat Rev Mol Cell Biol,* 9**,** 33-46.

CHEN, L. L., SABRIPOUR, M., WU, E. F., PRIETO, V. G., FULLER, G. N. & FRAZIER, M. L. 2005. A mutation-created novel intra-exonic pre-mRNA splice site causes constitutive activation of KIT in human gastrointestinal stromal tumors. *Oncogene,* 24**,** 4271-80.

CHOI, J., CHEN, J., SCHREIBER, S. L. & CLARDY, J. 1996. Structure of the FKBP12-rapamycin complex interacting with the binding domain of human FRAP. *Science,* 273**,** 239-42.

CIOSK, R., SHIRAYAMA, M., SHEVCHENKO, A., TANAKA, T., TOTH, A., SHEVCHENKO, A. & NASMYTH, K. 2000. Cohesin's binding to chromosomes depends on a separate complex consisting of Scc2 and Scc4 proteins. *Mol Cell,* 5**,** 243-54.

CIOSK, R., ZACHARIAE, W., MICHAELIS, C., SHEVCHENKO, A., MANN, M. & NASMYTH, K. 1998. An ESP1/PDS1 complex regulates loss of sister chromatid cohesion at the metaphase to anaphase transition in yeast. *Cell,* 93**,** 1067-76.

CLUTE, P. & PINES, J. 1999. Temporal and spatial control of cyclin B1 destruction in metaphase. *Nat Cell Biol,* 1**,** 82-7.

COLLETTE, K. S., PETTY, E. L., GOLENBERG, N., BEMBENEK, J. N. & CSANKOVSZKI, G. 2011. Different roles for Aurora B in condensin targeting during mitosis and meiosis. *J Cell Sci,* 124**,** 3684-94.

CONG, L., RAN, F. A., COX, D., LIN, S., BARRETTO, R., HABIB, N., HSU, P. D., WU, X., JIANG, W., MARRAFFINI, L. A. & ZHANG, F. 2013. Multiplex genome engineering using CRISPR/Cas systems. *Science,* 339**,** 819-23.

CONRAD, C. & GERLICH, D. W. 2010. Automated microscopy for high-content RNAi screening. *The Journal of Cell Biology,* 188**,** 453-461.

CORTES-LEDESMA, F. & AGUILERA, A. 2006. Double-strand breaks arising by replication through a nick are repaired by cohesin-dependent sister-chromatid exchange. *EMBO Rep,* 7**,** 919-26.

DAHAN, O. & KUPIEC, M. 2004. The Saccharomyces cerevisiae gene CDC40/PRP17 controls cell cycle progression through splicing of the ANC1 gene. *Nucleic Acids Res,* 32**,** 2529-40.

DAUM, J. R., POTAPOVA, T. A., SIVAKUMAR, S., DANIEL, J. J., FLYNN, J. N., RANKIN, S. & GORBSKY, G. J. 2011. Cohesion fatigue induces chromatid separation in cells delayed at metaphase. *Curr Biol,* 21**,** 1018-24.

DE SOUZA, C. P., ELLEM, K. A. & GABRIELLI, B. G. 2000. Centrosomal and cytoplasmic Cdc2/cyclin B1 activation precedes nuclear mitotic events. *Exp Cell Res,* 257**,** 11-21.

DEARDORFF, M. A., BANDO, M., NAKATO, R., WATRIN, E., ITOH, T., MINAMINO, M., SAITOH, K., KOMATA, M., KATOU, Y., CLARK, D., COLE, K. E., DE BAERE, E., DECROOS, C., DI DONATO, N., ERNST, S., FRANCEY, L. J., GYFTODIMOU, Y., HIRASHIMA, K., HULLINGS, M., ISHIKAWA, Y., JAULIN, C., KAUR, M., KIYONO, T., LOMBARDI, P. M., MAGNAGHI-JAULIN, L., MORTIER, G. R., NOZAKI, N., PETERSEN, M. B., SEIMIYA, H., SIU, V. M., SUZUKI, Y., TAKAGAKI, K., WILDE, J. J., WILLEMS, P. J., PRIGENT, C., GILLESSEN-KAESBACH, G., CHRISTIANSON, D. W., KAISER, F. J., JACKSON, L. G., HIROTA, T., KRANTZ, I. D. & SHIRAHIGE, K. 2012. HDAC8 mutations in Cornelia de Lange syndrome affect the cohesin acetylation cycle. *Nature,* 489**,** 313-7.

DEARDORFF, M. A., KAUR, M., YAEGER, D., RAMPURIA, A., KOROLEV, S., PIE, J., GIL-RODRIGUEZ, C., ARNEDO, M., LOEYS, B., KLINE, A. D., WILSON, M., LILLQUIST, K., SIU, V., RAMOS, F. J., MUSIO, A., JACKSON, L. S., DORSETT, D. & KRANTZ, I. D. 2007. Mutations in cohesin complex members SMC3 and SMC1A cause a mild variant of cornelia de Lange syndrome with predominant mental retardation. *Am J Hum Genet,* 80**,** 485-94.

DECKERT, J., HARTMUTH, K., BOEHRINGER, D., BEHZADNIA, N., WILL, C. L., KASTNER, B., STARK, H., URLAUB, H. & LUHRMANN, R. 2006. Protein composition and electron microscopy structure of affinity-purified human spliceosomal B complexes isolated under physiological conditions. *Mol Cell Biol,* 26**,** 5528-43.

DEPHOURE, N., ZHOU, C., VILLEN, J., BEAUSOLEIL, S. A., BAKALARSKI, C. E., ELLEDGE, S. J. & GYGI, S. P. 2008. A quantitative atlas of mitotic phosphorylation. *Proc Natl Acad Sci U S A,* 105**,** 10762-7.

DOENCH, J. G., PETERSEN, C. P. & SHARP, P. A. 2003. siRNAs can function as miRNAs. *Genes Dev,* 17**,** 438-42.

DONZE, D., ADAMS, C. R., RINE, J. & KAMAKAKA, R. T. 1999. The boundaries of the silenced HMR domain in Saccharomyces cerevisiae. *Genes Dev,* 13**,** 698-708.

DORSETT, D. 2007. Roles of the sister chromatid cohesion apparatus in gene expression, development, and human syndromes. *Chromosoma,* 116**,** 1-13.

DORSETT, D. & KRANTZ, I. D. 2009. On the molecular etiology of Cornelia de Lange syndrome. *Ann N Y Acad Sci,* 1151**,** 22-37.

DREIER, M. R., BEKIER, M. E., 2ND & TAYLOR, W. R. 2011. Regulation of sororin by Cdk1-mediated phosphorylation. *J Cell Sci,* 124**,** 2976-87.

ECHEVERRI, C. J. & PERRIMON, N. 2006. High-throughput RNAi screening in cultured cells: a user's guide. *Nature Reviews Genetics,* 7**,** 373-384.

EGGERT, U. S., KIGER, A. A., RICHTER, C., PERLMAN, Z. E., PERRIMON, N., MITCHISON, T. J. & FIELD, C. M. 2004. Parallel Chemical Genetic and Genome-Wide RNAi Screens Identify Cytokinesis Inhibitors and Targets. *PLoS Biology,* 2**,** e379.

EICHINGER, C. S., KURZE, A., OLIVEIRA, R. A. & NASMYTH, K. 2013. Disengaging the Smc3/kleisin interface releases cohesin from Drosophila chromosomes during interphase and mitosis. *EMBO J,* 32**,** 656-65.

ELIA, A. E., CANTLEY, L. C. & YAFFE, M. B. 2003. Proteomic screen finds pSer/pThr-binding domain localizing Plk1 to mitotic substrates. *Science,* 299**,** 1228-31.

ELLERMEIER, C. & SMITH, G. R. 2005. Cohesins are required for meiotic DNA breakage and recombination in Schizosaccharomyces pombe. *Proc Natl Acad Sci U S A,* 102**,** 10952-7.

ERFLE, H., NEUMANN, B., LIEBEL, U., ROGERS, P., HELD, M., WALTER, T., ELLENBERG, J. & PEPPERKOK, R. 2007. Reverse transfection on cell arrays for high content screening microscopy. *Nature Protocols,* 2**,** 392-399.

ERRICO, A., COSENTINO, C., RIVERA, T., LOSADA, A., SCHWOB, E., HUNT, T. & COSTANZO, V. 2009. Tipin/Tim1/And1 protein complex promotes Pol alpha chromatin binding and sister chromatid cohesion. *EMBO J,* 28**,** 3681-92.

EVANS, T., ROSENTHAL, E. T., YOUNGBLOM, J., DISTEL, D. & HUNT, T. 1983. Cyclin: a protein specified by maternal mRNA in sea urchin eggs that is destroyed at each cleavage division. *Cell,* 33**,** 389-96.

EYTAN, E., MOSHE, Y., BRAUNSTEIN, I. & HERSHKO, A. 2006. Roles of the anaphase-promoting complex/cyclosome and of its activator Cdc20 in functional substrate binding. *Proc Natl Acad Sci U S A,* 103**,** 2081-6.

FABBRO, M., ZHOU, B.-B., TAKAHASHI, M., SARCEVIC, B., LAL, P., GRAHAM, M. E., GABRIELLI, B. G., ROBINSON, P. J., NIGG, E. A. & ONO, Y. 2005. Cdk1/Erk2- and Plk1-Dependent Phosphorylation of a Centrosome Protein,

Cep55, Is Required for Its Recruitment to Midbody and Cytokinesis. *Developmental Cell,* 9**,** 477-488.
FABRIZIO, P., DANNENBERG, J., DUBE, P., KASTNER, B., STARK, H., URLAUB, H. & LUHRMANN, R. 2009. The evolutionarily conserved core design of the catalytic activation step of the yeast spliceosome. *Mol Cell,* 36**,** 593-608.
FLEMMING, W. 1882. Zellsubstanz, kern und Zellteilung. *Leipzig: Verlag von F.C.W. Vogel*.
FOX-WALSH, K. L., DOU, Y., LAM, B. J., HUNG, S. P., BALDI, P. F. & HERTEL, K. J. 2005. The architecture of pre-mRNAs affects mechanisms of splice-site pairing. *Proc Natl Acad Sci U S A,* 102**,** 16176-81.
FULLER, B. G., LAMPSON, M. A., FOLEY, E. A., ROSASCO-NITCHER, S., LE, K. V., TOBELMANN, P., BRAUTIGAN, D. L., STUKENBERG, P. T. & KAPOOR, T. M. 2008. Midzone activation of aurora B in anaphase produces an intracellular phosphorylation gradient. *Nature,* 453**,** 1132-6.
FUNABIKI, H., YAMANO, H., KUMADA, K., NAGAO, K., HUNT, T. & YANAGIDA, M. 1996. Cut2 proteolysis required for sister-chromatid seperation in fission yeast. *Nature,* 381**,** 438-41.
GANDHI, R., GILLESPIE, P. J. & HIRANO, T. 2006. Human Wapl is a cohesin-binding protein that promotes sister-chromatid resolution in mitotic prophase. *Curr Biol,* 16**,** 2406-17.
GAVET, O. & PINES, J. 2010. Progressive activation of CyclinB1-Cdk1 coordinates entry to mitosis. *Dev Cell,* 18**,** 533-43.
GERHART, J., WU, M. & KIRSCHNER, M. 1984. Cell cycle dynamics of an M-phase-specific cytoplasmic factor in Xenopus laevis oocytes and eggs. *J Cell Biol,* 98**,** 1247-55.
GERLICH, D., KOCH, B., DUPEUX, F., PETERS, J. M. & ELLENBERG, J. 2006. Live-cell imaging reveals a stable cohesin-chromatin interaction after but not before DNA replication. *Curr Biol,* 16**,** 1571-8.
GERMAN, J. 1979. Roberts' syndrome. I. Cytological evidence for a disturbance in chromatid pairing. *Clin Genet,* 16**,** 441-7.
GHARBI-AYACHI, A., LABBE, J. C., BURGESS, A., VIGNERON, S., STRUB, J. M., BRIOUDES, E., VAN-DORSSELAER, A., CASTRO, A. & LORCA, T. 2010. The substrate of Greatwall kinase, Arpp19, controls mitosis by inhibiting protein phosphatase 2A. *Science,* 330**,** 1673-7.
GHIGNA, C., GIORDANO, S., SHEN, H., BENVENUTO, F., CASTIGLIONI, F., COMOGLIO, P. M., GREEN, M. R., RIVA, S. & BIAMONTI, G. 2005. Cell motility is controlled by SF2/ASF through alternative splicing of the Ron protooncogene. *Mol Cell,* 20**,** 881-90.
GILLESPIE, P. J. & HIRANO, T. 2004. Scc2 couples replication licensing to sister chromatid cohesion in Xenopus egg extracts. *Curr Biol,* 14**,** 1598-603.
GILLILAND, W. D. & HAWLEY, R. S. 2005. Cohesin and the maternal age effect. *Cell,* 123**,** 371-3.
GIMENEZ-ABIAN, J. F., SUMARA, I., HIROTA, T., HAUF, S., GERLICH, D., DE LA TORRE, C., ELLENBERG, J. & PETERS, J. M. 2004. Regulation of sister chromatid cohesion between chromosome arms. *Curr Biol,* 14**,** 1187-93.
GIORGI, C. & MOORE, M. J. 2007. The nuclear nurture and cytoplasmic nature of localized mRNPs. *Semin Cell Dev Biol,* 18**,** 186-93.
GLOTZER, M. 2005. The molecular requirements for cytokinesis. *Science,* 307**,** 1735-1739.
GLOTZER, M. 2009. The 3Ms of central spindle assembly: microtubules, motors and MAPs. *Nat Rev Mol Cell Biol,* 10**,** 9-20.

GLOVER, D. M., LEIBOWITZ, M. H., MCLEAN, D. A. & PARRY, H. 1995. Mutations in aurora prevent centrosome separation leading to the formation of monopolar spindles. *Cell,* 81**,** 95-105.

GOLAN, A., YUDKOVSKY, Y. & HERSHKO, A. 2002. The cyclin-ubiquitin ligase activity of cyclosome/APC is jointly activated by protein kinases Cdk1-cyclin B and Plk. *J Biol Chem,* 277**,** 15552-7.

GORR, I. H., BOOS, D. & STEMMANN, O. 2005. Mutual inhibition of separase and Cdk1 by two-step complex formation. *Mol Cell,* 19**,** 135-41.

GOTTIFREDI, V. & PRIVES, C. 2005. The S phase checkpoint: when the crowd meets at the fork. *Semin Cell Dev Biol,* 16**,** 355-68.

GOULDING, S. E. & EARNSHAW, W. C. 2005. Shugoshin: a centromeric guardian senses tension. *Bioessays,* 27**,** 588-91.

GRAUBERT, T. A., SHEN, D., DING, L., OKEYO-OWUOR, T., LUNN, C. L., SHAO, J., KRYSIAK, K., HARRIS, C. C., KOBOLDT, D. C., LARSON, D. E., MCLELLAN, M. D., DOOLING, D. J., ABBOTT, R. M., FULTON, R. S., SCHMIDT, H., KALICKI-VEIZER, J., O'LAUGHLIN, M., GRILLOT, M., BATY, J., HEATH, S., FRATER, J. L., NASIM, T., LINK, D. C., TOMASSON, M. H., WESTERVELT, P., DIPERSIO, J. F., MARDIS, E. R., LEY, T. J., WILSON, R. K. & WALTER, M. J. 2012. Recurrent mutations in the U2AF1 splicing factor in myelodysplastic syndromes. *Nat Genet,* 44**,** 53-7.

GRAVELEY, B. R. 2000. Sorting out the complexity of SR protein functions. *RNA,* 6**,** 1197-211.

GREEN, R. A., PALUCH, E. & OEGEMA, K. 2012. Cytokinesis in animal cells. *Annu Rev Cell Dev Biol,* 28**,** 29-58.

GROTE, M., WOLF, E., WILL, C. L., LEMM, I., AGAFONOV, D. E., SCHOMBURG, A., FISCHLE, W., URLAUB, H. & LUHRMANN, R. 2010. Molecular architecture of the human Prp19/CDC5L complex. *Mol Cell Biol,* 30**,** 2105-19.

GRUBER, S., ARUMUGAM, P., KATOU, Y., KUGLITSCH, D., HELMHART, W., SHIRAHIGE, K. & NASMYTH, K. 2006. Evidence that loading of cohesin onto chromosomes involves opening of its SMC hinge. *Cell,* 127**,** 523-37.

GRUBER, S., HAERING, C. H. & NASMYTH, K. 2003. Chromosomal cohesin forms a ring. *Cell,* 112**,** 765-77.

GRUNEBERG, U., NEEF, R., HONDA, R., NIGG, E. A. & BARR, F. A. 2004. Relocation of Aurora B from centromeres to the central spindle at the metaphase to anaphase transition requires MKlp2. *J Cell Biol,* 166**,** 167-72.

GUACCI, V., HOGAN, E. & KOSHLAND, D. 1994. Chromosome condensation and sister chromatid pairing in budding yeast. *J Cell Biol,* 125**,** 517-30.

GUACCI, V., KOSHLAND, D. & STRUNNIKOV, A. 1997. A direct link between sister chromatid cohesion and chromosome condensation revealed through the analysis of MCD1 in S. cerevisiae. *Cell,* 91**,** 47-57.

GUIZETTI, J. & GERLICH, D. W. 2010. Cytokinetic abscission in animal cells. *Semin Cell Dev Biol,* 21**,** 909-16.

GULLEROVA, M. & PROUDFOOT, N. J. 2008. Cohesin complex promotes transcriptional termination between convergent genes in S. pombe. *Cell,* 132**,** 983-95.

GUTTINGER, S., LAURELL, E. & KUTAY, U. 2009. Orchestrating nuclear envelope disassembly and reassembly during mitosis. *Nat Rev Mol Cell Biol,* 10**,** 178-91.

HAERING, C. H., FARCAS, A. M., ARUMUGAM, P., METSON, J. & NASMYTH, K. 2008. The cohesin ring concatenates sister DNA molecules. *Nature,* 454**,** 297-301.

HAERING, C. H., LOWE, J., HOCHWAGEN, A. & NASMYTH, K. 2002. Molecular architecture of SMC proteins and the yeast cohesin complex. *Mol Cell,* 9**,** 773-88.

HAERING, C. H., SCHOFFNEGGER, D., NISHINO, T., HELMHART, W., NASMYTH, K. & LOWE, J. 2004. Structure and stability of cohesin's Smc1-kleisin interaction. *Mol Cell,* 15**,** 951-64.

HAGTING, A., DEN ELZEN, N., VODERMAIER, H. C., WAIZENEGGER, I. C., PETERS, J. M. & PINES, J. 2002. Human securin proteolysis is controlled by the spindle checkpoint and reveals when the APC/C switches from activation by Cdc20 to Cdh1. *J Cell Biol,* 157**,** 1125-37.

HARPER, J. W., ADAMI, G. R., WEI, N., KEYOMARSI, K. & ELLEDGE, S. J. 1993. The p21 Cdk-interacting protein Cip1 is a potent inhibitor of G1 cyclin-dependent kinases. *Cell,* 75**,** 805-16.

HARRISON, J. C. & HABER, J. E. 2006. Surviving the breakup: the DNA damage checkpoint. *Annu Rev Genet,* 40**,** 209-35.

HARTMUTH, K., URLAUB, H., VORNLOCHER, H. P., WILL, C. L., GENTZEL, M., WILM, M. & LUHRMANN, R. 2002. Protein composition of human prespliceosomes isolated by a tobramycin affinity-selection method. *Proc Natl Acad Sci U S A,* 99**,** 16719-24.

HARTWELL, L. H. & WEINERT, T. A. 1989. Checkpoints: controls that ensure the order of cell cycle events. *Science,* 246**,** 629-34.

HASSOLD, T. & HUNT, P. 2001. To err (meiotically) is human: the genesis of human aneuploidy. *Nat Rev Genet,* 2**,** 280-91.

HASTINGS, M. L., RESTA, N., TRAUM, D., STELLA, A., GUANTI, G. & KRAINER, A. R. 2005. An LKB1 AT-AC intron mutation causes Peutz-Jeghers syndrome via splicing at noncanonical cryptic splice sites. *Nat Struct Mol Biol,* 12**,** 54-9.

HAUF, S., COLE, R. W., LATERRA, S., ZIMMER, C., SCHNAPP, G., WALTER, R., HECKEL, A., VAN MEEL, J., RIEDER, C. L. & PETERS, J. M. 2003. The small molecule Hesperadin reveals a role for Aurora B in correcting kinetochore-microtubule attachment and in maintaining the spindle assembly checkpoint. *J Cell Biol,* 161**,** 281-94.

HAUF, S., ROITINGER, E., KOCH, B., DITTRICH, C. M., MECHTLER, K. & PETERS, J. M. 2005. Dissociation of cohesin from chromosome arms and loss of arm cohesion during early mitosis depends on phosphorylation of SA2. *PLoS Biol,* 3**,** e69.

HAUF, S., WAIZENEGGER, I. C. & PETERS, J. M. 2001. Cohesin cleavage by separase required for anaphase and cytokinesis in human cells. *Science,* 293**,** 1320-3.

HEIDINGER-PAULI, J. M., UNAL, E., GUACCI, V. & KOSHLAND, D. 2008. The kleisin subunit of cohesin dictates damage-induced cohesion. *Mol Cell,* 31**,** 47-56.

HEIDINGER-PAULI, J. M., UNAL, E. & KOSHLAND, D. 2009. Distinct targets of the Eco1 acetyltransferase modulate cohesion in S phase and in response to DNA damage. *Mol Cell,* 34**,** 311-21.

HELMRICH, A., BALLARINO, M. & TORA, L. 2011. Collisions between replication and transcription complexes cause common fragile site instability at the longest human genes. *Mol Cell,* 44**,** 966-77.

HEROLD, N., WILL, C. L., WOLF, E., KASTNER, B., URLAUB, H. & LUHRMANN, R. 2009. Conservation of the protein composition and electron microscopy structure of Drosophila melanogaster and human spliceosomal complexes. *Mol Cell Biol,* 29**,** 281-301.

HERRMANN, J. & OPITZ, J. M. 1977. The SC phocomelia and the Roberts syndrome: nosologic aspects. *Eur J Pediatr,* 125**,** 117-34.

HIRANO, T. & MITCHISON, T. J. 1994. A heterodimeric coiled-coil protein required for mitotic chromosome condensation in vitro. *Cell,* 79**,** 449-58.

HODGES, C. A., REVENKOVA, E., JESSBERGER, R., HASSOLD, T. J. & HUNT, P. A. 2005. SMC1beta-deficient female mice provide evidence that cohesins are a missing link in age-related nondisjunction. *Nat Genet,* 37**,** 1351-5.

HOFFMAN, B. E. & GRABOWSKI, P. J. 1992. U1 snRNP targets an essential splicing factor, U2AF65, to the 3' splice site by a network of interactions spanning the exon. *Genes Dev,* 6**,** 2554-68.

HOFFMANN, I., CLARKE, P. R., MARCOTE, M. J., KARSENTI, E. & DRAETTA, G. 1993. Phosphorylation and activation of human cdc25-C by cdc2--cyclin B and its involvement in the self-amplification of MPF at mitosis. *EMBO J,* 12**,** 53-63.

HOFMANN, J. C., HUSEDZINOVIC, A. & GRUSS, O. J. 2010. The function of spliceosome components in open mitosis. *Nucleus,* 1**,** 447-59.

HOLT, L. J., TUCH, B. B., VILLEN, J., JOHNSON, A. D., GYGI, S. P. & MORGAN, D. O. 2009. Global analysis of Cdk1 substrate phosphorylation sites provides insights into evolution. *Science,* 325**,** 1682-6.

HORNIG, N. C., KNOWLES, P. P., MCDONALD, N. Q. & UHLMANN, F. 2002. The dual mechanism of separase regulation by securin. *Curr Biol,* 12**,** 973-82.

HORSFIELD, J. A., ANAGNOSTOU, S. H., HU, J. K., CHO, K. H., GEISLER, R., LIESCHKE, G., CROSIER, K. E. & CROSIER, P. S. 2007. Cohesin-dependent regulation of Runx genes. *Development,* 134**,** 2639-49.

HOU, F. & ZOU, H. 2005. Two human orthologues of Eco1/Ctf7 acetyltransferases are both required for proper sister-chromatid cohesion. *Mol Biol Cell,* 16**,** 3908-18.

HOUSE, A. E. & LYNCH, K. W. 2006. An exonic splicing silencer represses spliceosome assembly after ATP-dependent exon recognition. *Nat Struct Mol Biol,* 13**,** 937-44.

HU, B., ITOH, T., MISHRA, A., KATOH, Y., CHAN, K. L., UPCHER, W., GODLEE, C., ROIG, M. B., SHIRAHIGE, K. & NASMYTH, K. 2011. ATP hydrolysis is required for relocating cohesin from sites occupied by its Scc2/4 loading complex. *Curr Biol,* 21**,** 12-24.

HÜBNER, N. C., WANG, L. H.-C., KAULICH, M., DESCOMBES, P., POSER, I. & NIGG, E. A. 2009. Re-examination of siRNA specificity questions role of PICH and Tao1 in the spindle checkpoint and identifies Mad2 as a sensitive target for small RNAs. *Chromosoma,* 119**,** 149-165.

HUNT, P. & HASSOLD, T. 2010. Female meiosis: coming unglued with age. *Curr Biol,* 20**,** R699-702.

IVANOV, D. & NASMYTH, K. 2005. A topological interaction between cohesin rings and a circular minichromosome. *Cell,* 122**,** 849-60.

IVANOV, D. & NASMYTH, K. 2007. A physical assay for sister chromatid cohesion in vitro. *Mol Cell,* 27**,** 300-10.

IVANOV, D., SCHLEIFFER, A., EISENHABER, F., MECHTLER, K., HAERING, C. H. & NASMYTH, K. 2002. Eco1 is a novel acetyltransferase that can acetylate proteins involved in cohesion. *Curr Biol,* 12**,** 323-8.

IZUMI, T., WALKER, D. H. & MALLER, J. L. 1992. Periodic changes in phosphorylation of the Xenopus cdc25 phosphatase regulate its activity. *Mol Biol Cell,* 3**,** 927-39.

JACKSON, A. L., BARTZ, S. R., SCHELTER, J., KOBAYASHI, S. V., BURCHARD, J., MAO, M., LI, B., CAVET, G. & LINSLEY, P. S. 2003. Expression profiling reveals off-target gene regulation by RNAi. *Nat Biotechnol,* 21**,** 635-7.

JACKSON, L., KLINE, A. D., BARR, M. A. & KOCH, S. 1993. de Lange syndrome: a clinical review of 310 individuals. *Am J Med Genet,* 47**,** 940-6.

JASPERSEN, S. L., CHARLES, J. F. & MORGAN, D. O. 1999. Inhibitory phosphorylation of the APC regulator Hct1 is controlled by the kinase Cdc28 and the phosphatase Cdc14. *Curr Biol,* 9**,** 227-36.

JEFFREY, P. D., RUSSO, A. A., POLYAK, K., GIBBS, E., HURWITZ, J., MASSAGUE, J. & PAVLETICH, N. P. 1995. Mechanism of CDK activation revealed by the structure of a cyclinA-CDK2 complex. *Nature,* 376**,** 313-20.

JONES, R. M. & PETERMANN, E. 2012. Replication fork dynamics and the DNA damage response. *Biochem J,* 443**,** 13-26.

JURICA, M. S. 2008. Detailed close-ups and the big picture of spliceosomes. *Curr Opin Struct Biol,* 18**,** 315-20.

JURICA, M. S., LICKLIDER, L. J., GYGI, S. R., GRIGORIEFF, N. & MOORE, M. J. 2002. Purification and characterization of native spliceosomes suitable for three-dimensional structural analysis. *RNA,* 8**,** 426-39.

JURICA, M. S. & MOORE, M. J. 2003. Pre-mRNA splicing: awash in a sea of proteins. *Mol Cell,* 12**,** 5-14.

KAGEY, M. H., NEWMAN, J. J., BILODEAU, S., ZHAN, Y., ORLANDO, D. A., VAN BERKUM, N. L., EBMEIER, C. C., GOOSSENS, J., RAHL, P. B., LEVINE, S. S., TAATJES, D. J., DEKKER, J. & YOUNG, R. A. 2010. Mediator and cohesin connect gene expression and chromatin architecture. *Nature,* 467**,** 430-5.

KAIDA, D., MOTOYOSHI, H., TASHIRO, E., NOJIMA, T., HAGIWARA, M., ISHIGAMI, K., WATANABE, H., KITAHARA, T., YOSHIDA, T., NAKAJIMA, H., TANI, T., HORINOUCHI, S. & YOSHIDA, M. 2007. Spliceostatin A targets SF3b and inhibits both splicing and nuclear retention of pre-mRNA. *Nat Chem Biol,* 3**,** 576-83.

KAITNA, S., MENDOZA, M., JANTSCH-PLUNGER, V. & GLOTZER, M. 2000. Incenp and an aurora-like kinase form a complex essential for chromosome segregation and efficient completion of cytokinesis. *Curr Biol,* 10**,** 1172-81.

KAMATH, R. S., FRASER, A. G., DONG, Y., POULIN, G., DURBIN, R., GOTTA, M., KANAPIN, A., LE BOT, N., MORENO, S., SOHRMANN, M., WELCHMAN, D. P., ZIPPERLEN, P. & AHRINGER, J. 2003. Systematic functional analysis of the Caenorhabditis elegans genome using RNAi. *Nature,* 421**,** 231-7.

KARNI, R., DE STANCHINA, E., LOWE, S. W., SINHA, R., MU, D. & KRAINER, A. R. 2007. The gene encoding the splicing factor SF2/ASF is a proto-oncogene. *Nat Struct Mol Biol,* 14**,** 185-93.

KIM, S. T., XU, B. & KASTAN, M. B. 2002. Involvement of the cohesin protein, Smc1, in Atm-dependent and independent responses to DNA damage. *Genes Dev,* 16**,** 560-70.

KITAGAWA, M., HIGASHI, H., JUNG, H. K., SUZUKI-TAKAHASHI, I., IKEDA, M., TAMAI, K., KATO, J., SEGAWA, K., YOSHIDA, E., NISHIMURA, S. & TAYA, Y. 1996. The consensus motif for phosphorylation by cyclin D1-Cdk4 is different from that for phosphorylation by cyclin A/E-Cdk2. *EMBO J,* 15**,** 7060-9.

KITAJIMA, T. S., KAWASHIMA, S. A. & WATANABE, Y. 2004. The conserved kinetochore protein shugoshin protects centromeric cohesion during meiosis. *Nature,* 427**,** 510-7.

KITAJIMA, T. S., SAKUNO, T., ISHIGURO, K., IEMURA, S., NATSUME, T., KAWASHIMA, S. A. & WATANABE, Y. 2006. Shugoshin collaborates with protein phosphatase 2A to protect cohesin. *Nature,* 441**,** 46-52.

KITTLER, R., PELLETIER, L., HENINGER, A.-K., SLABICKI, M., THEIS, M., MIROSLAW, L., POSER, I., LAWO, S., GRABNER, H., KOZAK, K., WAGNER, J., SURENDRANATH, V., RICHTER, C., BOWEN, W., JACKSON, A. L., HABERMANN, B., HYMAN, A. A. & BUCHHOLZ, F. 2007. Genome-scale RNAi profiling of cell division in human tissue culture cells. *Nature Cell Biology,* 9**,** 1401-1412.

KITTLER, R., PUTZ, G., PELLETIER, L., POSER, I., HENINGER, A. K., DRECHSEL, D., FISCHER, S., KONSTANTINOVA, I., HABERMANN, B., GRABNER, H., YASPO, M. L., HIMMELBAUER, H., KORN, B., NEUGEBAUER, K.,

PISABARRO, M. T. & BUCHHOLZ, F. 2004. An endoribonuclease-prepared siRNA screen in human cells identifies genes essential for cell division. *Nature,* 432**,** 1036-40.

KLEIN, F., MAHR, P., GALOVA, M., BUONOMO, S. B., MICHAELIS, C., NAIRZ, K. & NASMYTH, K. 1999. A central role for cohesins in sister chromatid cohesion, formation of axial elements, and recombination during yeast meiosis. *Cell,* 98**,** 91-103.

KOIVOMAGI, M., VALK, E., VENTA, R., IOFIK, A., LEPIKU, M., MORGAN, D. O. & LOOG, M. 2011. Dynamics of Cdk1 substrate specificity during the cell cycle. *Mol Cell,* 42**,** 610-23.

KOSHLAND, D. & HARTWELL, L. H. 1987. The structure of sister minichromosome DNA before anaphase in Saccharomyces cerevisiae. *Science,* 238**,** 1713-6.

KOTANI, S., TANAKA, H., YASUDA, H. & TODOKORO, K. 1999. Regulation of APC activity by phosphorylation and regulatory factors. *J Cell Biol,* 146**,** 791-800.

KRAFT, C., HERZOG, F., GIEFFERS, C., MECHTLER, K., HAGTING, A., PINES, J. & PETERS, J. M. 2003. Mitotic regulation of the human anaphase-promoting complex by phosphorylation. *EMBO J,* 22**,** 6598-609.

KRAFT, C., VODERMAIER, H. C., MAURER-STROH, S., EISENHABER, F. & PETERS, J. M. 2005. The WD40 propeller domain of Cdh1 functions as a destruction box receptor for APC/C substrates. *Mol Cell,* 18**,** 543-53.

KRAMER, E. R., SCHEURINGER, N., PODTELEJNIKOV, A. V., MANN, M. & PETERS, J. M. 2000. Mitotic regulation of the APC activator proteins CDC20 and CDH1. *Mol Biol Cell,* 11**,** 1555-69.

KRANTZ, I. D., MCCALLUM, J., DESCIPIO, C., KAUR, M., GILLIS, L. A., YAEGER, D., JUKOFSKY, L., WASSERMAN, N., BOTTANI, A., MORRIS, C. A., NOWACZYK, M. J., TORIELLO, H., BAMSHAD, M. J., CAREY, J. C., RAPPAPORT, E., KAWAUCHI, S., LANDER, A. D., CALOF, A. L., LI, H. H., DEVOTO, M. & JACKSON, L. G. 2004. Cornelia de Lange syndrome is caused by mutations in NIPBL, the human homolog of Drosophila melanogaster Nipped-B. *Nat Genet,* 36**,** 631-5.

KUENG, S., HEGEMANN, B., PETERS, B. H., LIPP, J. J., SCHLEIFFER, A., MECHTLER, K. & PETERS, J. M. 2006. Wapl controls the dynamic association of cohesin with chromatin. *Cell,* 127**,** 955-67.

LAFONT, A. L., SONG, J. & RANKIN, S. 2010. Sororin cooperates with the acetyltransferase Eco2 to ensure DNA replication-dependent sister chromatid cohesion. *Proc Natl Acad Sci U S A,* 107**,** 20364-9.

LAMMER, C., WAGERER, S., SAFFRICH, R., MERTENS, D., ANSORGE, W. & HOFFMANN, I. 1998. The cdc25B phosphatase is essential for the G2/M phase transition in human cells. *J Cell Sci,* 111 (Pt 16)**,** 2445-53.

LANDAU, D. A. & WU, C. J. 2013. Chronic lymphocytic leukemia: molecular heterogeneity revealed by high-throughput genomics. *Genome Med,* 5**,** 47.

LANDEIRA, D., BART, J. M., VAN TYNE, D. & NAVARRO, M. 2009. Cohesin regulates VSG monoallelic expression in trypanosomes. *J Cell Biol,* 186**,** 243-54.

LANDER, E. S., LINTON, L. M., BIRREN, B., NUSBAUM, C., ZODY, M. C., BALDWIN, J., DEVON, K., DEWAR, K., DOYLE, M., FITZHUGH, W., FUNKE, R., GAGE, D., HARRIS, K., HEAFORD, A., HOWLAND, J., KANN, L., LEHOCZKY, J., LEVINE, R., MCEWAN, P., MCKERNAN, K., MELDRIM, J., MESIROV, J. P., MIRANDA, C., MORRIS, W., NAYLOR, J., RAYMOND, C., ROSETTI, M., SANTOS, R., SHERIDAN, A., SOUGNEZ, C., STANGE-THOMANN, N., STOJANOVIC, N., SUBRAMANIAN, A., WYMAN, D., ROGERS, J., SULSTON, J., AINSCOUGH, R., BECK, S., BENTLEY, D., BURTON, J., CLEE, C., CARTER, N., COULSON, A., DEADMAN, R., DELOUKAS, P., DUNHAM, A., DUNHAM, I., DURBIN, R., FRENCH, L., GRAFHAM, D., GREGORY, S.,

HUBBARD, T., HUMPHRAY, S., HUNT, A., JONES, M., LLOYD, C., MCMURRAY, A., MATTHEWS, L., MERCER, S., MILNE, S., MULLIKIN, J. C., MUNGALL, A., PLUMB, R., ROSS, M., SHOWNKEEN, R., SIMS, S., WATERSTON, R. H., WILSON, R. K., HILLIER, L. W., MCPHERSON, J. D., MARRA, M. A., MARDIS, E. R., FULTON, L. A., CHINWALLA, A. T., PEPIN, K. H., GISH, W. R., CHISSOE, S. L., WENDL, M. C., DELEHAUNTY, K. D., MINER, T. L., DELEHAUNTY, A., KRAMER, J. B., COOK, L. L., FULTON, R. S., JOHNSON, D. L., MINX, P. J., CLIFTON, S. W., HAWKINS, T., BRANSCOMB, E., PREDKI, P., RICHARDSON, P., WENNING, S., SLEZAK, T., DOGGETT, N., CHENG, J. F., OLSEN, A., LUCAS, S., ELKIN, C., UBERBACHER, E., FRAZIER, M., et al. 2001. Initial sequencing and analysis of the human genome. *Nature,* 409**,** 860-921.

LANE, H. A. & NIGG, E. A. 1996. Antibody microinjection reveals an essential role for human polo-like kinase 1 (Plk1) in the functional maturation of mitotic centrosomes. *J Cell Biol,* 135**,** 1701-13.

LE HIR, H., IZAURRALDE, E., MAQUAT, L. E. & MOORE, M. J. 2000. The spliceosome deposits multiple proteins 20-24 nucleotides upstream of mRNA exon-exon junctions. *EMBO J,* 19**,** 6860-9.

LE HIR, H. & SERAPHIN, B. 2008. EJCs at the heart of translational control. *Cell,* 133**,** 213-6.

LEE, H. H., ELIA, N., GHIRLANDO, R., LIPPINCOTT-SCHWARTZ, J. & HURLEY, J. H. 2008. Midbody targeting of the ESCRT machinery by a noncanonical coiled coil in CEP55. *Science,* 322**,** 576-80.

LEE, M. G. & NURSE, P. 1987. Complementation used to clone a human homologue of the fission yeast cell cycle control gene cdc2. *Nature,* 327**,** 31-5.

LENART, P., PETRONCZKI, M., STEEGMAIER, M., DI FIORE, B., LIPP, J. J., HOFFMANN, M., RETTIG, W. J., KRAUT, N. & PETERS, J. M. 2007. The small-molecule inhibitor BI 2536 reveals novel insights into mitotic roles of polo-like kinase 1. *Curr Biol,* 17**,** 304-15.

LENGRONNE, A., KATOU, Y., MORI, S., YOKOBAYASHI, S., KELLY, G. P., ITOH, T., WATANABE, Y., SHIRAHIGE, K. & UHLMANN, F. 2004. Cohesin relocation from sites of chromosomal loading to places of convergent transcription. *Nature,* 430**,** 573-8.

LI, X. & MANLEY, J. L. 2005. Inactivation of the SR protein splicing factor ASF/SF2 results in genomic instability. *Cell,* 122**,** 365-78.

LINDON, C. & PINES, J. 2004. Ordered proteolysis in anaphase inactivates Plk1 to contribute to proper mitotic exit in human cells. *J Cell Biol,* 164**,** 233-41.

LIPP, J. J., HIROTA, T., POSER, I. & PETERS, J. M. 2007. Aurora B controls the association of condensin I but not condensin II with mitotic chromosomes. *J Cell Sci,* 120**,** 1245-55.

LIU, F., ROTHBLUM-OVIATT, C., RYAN, C. E. & PIWNICA-WORMS, H. 1999. Overproduction of human Myt1 kinase induces a G2 cell cycle delay by interfering with the intracellular trafficking of Cdc2-cyclin B1 complexes. *Mol Cell Biol,* 19**,** 5113-23.

LIU, H., RANKIN, S. & YU, H. 2012. Phosphorylation-enabled binding of SGO1-PP2A to cohesin protects sororin and centromeric cohesion during mitosis. *Nat Cell Biol,* 15**,** 40-9.

LIU, J. & KRANTZ, I. D. 2009. Cornelia de Lange syndrome, cohesin, and beyond. *Clin Genet,* 76**,** 303-14.

LLANO, E., HERRAN, Y., GARCIA-TUNON, I., GUTIERREZ-CABALLERO, C., DE ALAVA, E., BARBERO, J. L., SCHIMENTI, J., DE ROOIJ, D. G., SANCHEZ-MARTIN, M. & PENDAS, A. M. 2012. Meiotic cohesin complexes are essential for the formation of the axial element in mice. *J Cell Biol,* 197**,** 877-85.

LONG, J. C. & CACERES, J. F. 2009. The SR protein family of splicing factors: master regulators of gene expression. *Biochem J,* 417**,** 15-27.
LOOG, M. & MORGAN, D. O. 2005. Cyclin specificity in the phosphorylation of cyclin-dependent kinase substrates. *Nature,* 434**,** 104-8.
LOPEZ-BIGAS, N., AUDIT, B., OUZOUNIS, C., PARRA, G. & GUIGO, R. 2005. Are splicing mutations the most frequent cause of hereditary disease? *FEBS Lett,* 579**,** 1900-3.
LOSADA, A., HIRANO, M. & HIRANO, T. 1998. Identification of Xenopus SMC protein complexes required for sister chromatid cohesion. *Genes Dev,* 12**,** 1986-97.
LOSADA, A., HIRANO, M. & HIRANO, T. 2002. Cohesin release is required for sister chromatid resolution, but not for condensin-mediated compaction, at the onset of mitosis. *Genes Dev,* 16**,** 3004-16.
LOSADA, A., YOKOCHI, T., KOBAYASHI, R. & HIRANO, T. 2000. Identification and characterization of SA/Scc3p subunits in the Xenopus and human cohesin complexes. *J Cell Biol,* 150**,** 405-16.
LOWE, M. & BARR, F. A. 2007. Inheritance and biogenesis of organelles in the secretory pathway. *Nat Rev Mol Cell Biol,* 8**,** 429-39.
LOWE, M., RABOUILLE, C., NAKAMURA, N., WATSON, R., JACKMAN, M., JAMSA, E., RAHMAN, D., PAPPIN, D. J. & WARREN, G. 1998. Cdc2 kinase directly phosphorylates the cis-Golgi matrix protein GM130 and is required for Golgi fragmentation in mitosis. *Cell,* 94**,** 783-93.
LUKAS, C., SORENSEN, C. S., KRAMER, E., SANTONI-RUGIU, E., LINDENEG, C., PETERS, J. M., BARTEK, J. & LUKAS, J. 1999. Accumulation of cyclin B1 requires E2F and cyclin-A-dependent rearrangement of the anaphase-promoting complex. *Nature,* 401**,** 815-8.
MACUREK, L., LINDQVIST, A., LIM, D., LAMPSON, M. A., KLOMPMAKER, R., FREIRE, R., CLOUIN, C., TAYLOR, S. S., YAFFE, M. B. & MEDEMA, R. H. 2008. Polo-like kinase-1 is activated by aurora A to promote checkpoint recovery. *Nature,* 455**,** 119-23.
MAILAND, N., PODTELEJNIKOV, A. V., GROTH, A., MANN, M., BARTEK, J. & LUKAS, J. 2002. Regulation of G(2)/M events by Cdc25A through phosphorylation-dependent modulation of its stability. *EMBO J,* 21**,** 5911-20.
MAJUMDER, P., GOMEZ, J. A., CHADWICK, B. P. & BOSS, J. M. 2008. The insulator factor CTCF controls MHC class II gene expression and is required for the formation of long-distance chromatin interactions. *J Exp Med,* 205**,** 785-98.
MAKAROV, E. M., MAKAROVA, O. V., URLAUB, H., GENTZEL, M., WILL, C. L., WILM, M. & LUHRMANN, R. 2002. Small nuclear ribonucleoprotein remodeling during catalytic activation of the spliceosome. *Science,* 298**,** 2205-8.
MAKAROVA, O. V., MAKAROV, E. M., LIU, S., VORNLOCHER, H. P. & LUHRMANN, R. 2002. Protein 61K, encoded by a gene (PRPF31) linked to autosomal dominant retinitis pigmentosa, is required for U4/U6*U5 tri-snRNP formation and pre-mRNA splicing. *EMBO J,* 21**,** 1148-57.
MAKAROVA, O. V., MAKAROV, E. M. & LUHRMANN, R. 2001. The 65 and 110 kDa SR-related proteins of the U4/U6.U5 tri-snRNP are essential for the assembly of mature spliceosomes. *EMBO J,* 20**,** 2553-63.
MAKAROVA, O. V., MAKAROV, E. M., URLAUB, H., WILL, C. L., GENTZEL, M., WILM, M. & LUHRMANN, R. 2004. A subset of human 35S U5 proteins, including Prp19, function prior to catalytic step 1 of splicing. *EMBO J,* 23**,** 2381-91.
MANCHADO, E., GUILLAMOT, M., DE CARCER, G., EGUREN, M., TRICKEY, M., GARCIA-HIGUERA, I., MORENO, S., YAMANO, H., CANAMERO, M. & MALUMBRES, M. 2010. Targeting mitotic exit leads to tumor regression in vivo:

Modulation by Cdk1, Mastl, and the PP2A/B55alpha,delta phosphatase. *Cancer Cell,* 18**,** 641-54.
MANNINI, L., LIU, J., KRANTZ, I. D. & MUSIO, A. 2010a. Spectrum and consequences of SMC1A mutations: the unexpected involvement of a core component of cohesin in human disease. *Hum Mutat,* 31**,** 5-10.
MANNINI, L., MENGA, S. & MUSIO, A. 2010b. The expanding universe of cohesin functions: a new genome stability caretaker involved in human disease and cancer. *Hum Mutat,* 31**,** 623-30.
MARTINEZ-CONTRERAS, R., CLOUTIER, P., SHKRETA, L., FISETTE, J. F., REVIL, T. & CHABOT, B. 2007. hnRNP proteins and splicing control. *Adv Exp Med Biol,* 623**,** 123-47.
MARUMOTO, T., ZHANG, D. & SAYA, H. 2005. Aurora-A - a guardian of poles. *Nat Rev Cancer,* 5**,** 42-50.
MASAI, H., MATSUMOTO, S., YOU, Z., YOSHIZAWA-SUGATA, N. & ODA, M. 2010. Eukaryotic chromosome DNA replication: where, when, and how? *Annu Rev Biochem,* 79**,** 89-130.
MASUDA, S., DAS, R., CHENG, H., HURT, E., DORMAN, N. & REED, R. 2005. Recruitment of the human TREX complex to mRNA during splicing. *Genes Dev,* 19**,** 1512-7.
MASUI, Y. 1982. Oscillatory activity of maturation promoting factor (MPF) in extracts of Rana pipiens eggs. *J Exp Zool,* 224**,** 389-99.
MASUI, Y. & MARKERT, C. L. 1971. Cytoplasmic control of nuclear behavior during meiotic maturation of frog oocytes. *J Exp Zool,* 177**,** 129-45.
MATSUNAGA, S., TAKATA, H., MORIMOTO, A., HAYASHIHARA, K., HIGASHI, T., AKATSUCHI, K., MIZUSAWA, E., YAMAKAWA, M., ASHIDA, M., MATSUNAGA, T. M., AZUMA, T., UCHIYAMA, S. & FUKUI, K. 2012. RBMX: a regulator for maintenance and centromeric protection of sister chromatid cohesion. *Cell Rep,* 1**,** 299-308.
MATTHEWS, H. K., DELABRE, U., ROHN, J. L., GUCK, J., KUNDA, P. & BAUM, B. 2012. Changes in Ect2 localization couple actomyosin-dependent cell shape changes to mitotic progression. *Dev Cell,* 23**,** 371-83.
MATULIENE, J. & KURIYAMA, R. 2002. Kinesin-like protein CHO1 is required for the formation of midbody matrix and the completion of cytokinesis in mammalian cells. *Mol Biol Cell,* 13**,** 1832-45.
MC INTYRE, J., MULLER, E. G., WEITZER, S., SNYDSMAN, B. E., DAVIS, T. N. & UHLMANN, F. 2007. In vivo analysis of cohesin architecture using FRET in the budding yeast Saccharomyces cerevisiae. *EMBO J,* 26**,** 3783-93.
MCCRACKEN, S., LONGMAN, D., MARCON, E., MOENS, P., DOWNEY, M., NICKERSON, J. A., JESSBERGER, R., WILDE, A., CACERES, J. F., EMILI, A. & BLENCOWE, B. J. 2005. Proteomic analysis of SRm160-containing complexes reveals a conserved association with cohesin. *J Biol Chem,* 280**,** 42227-36.
MCDONALD, W. H., OHI, R., SMELKOVA, N., FRENDEWEY, D. & GOULD, K. L. 1999. Myb-related fission yeast cdc5p is a component of a 40S snRNP-containing complex and is essential for pre-mRNA splicing. *Mol Cell Biol,* 19**,** 5352-62.
MCGOWAN, C. H. & RUSSELL, P. 1993. Human Wee1 kinase inhibits cell division by phosphorylating p34cdc2 exclusively on Tyr15. *EMBO J,* 12**,** 75-85.
MCGUINNESS, B. E., HIROTA, T., KUDO, N. R., PETERS, J. M. & NASMYTH, K. 2005. Shugoshin prevents dissociation of cohesin from centromeres during mitosis in vertebrate cells. *PLoS Biol,* 3**,** e86.
MCKIE, A. B., MCHALE, J. C., KEEN, T. J., TARTTELIN, E. E., GOLIATH, R., VAN LITH-VERHOEVEN, J. J., GREENBERG, J., RAMESAR, R. S., HOYNG, C. B.,

CREMERS, F. P., MACKEY, D. A., BHATTACHARYA, S. S., BIRD, A. C., MARKHAM, A. F. & INGLEHEARN, C. F. 2001. Mutations in the pre-mRNA splicing factor gene PRPC8 in autosomal dominant retinitis pigmentosa (RP13). *Hum Mol Genet,* 10**,** 1555-62.

MEGEE, P. C., MISTROT, C., GUACCI, V. & KOSHLAND, D. 1999. The centromeric sister chromatid cohesion site directs Mcd1p binding to adjacent sequences. *Mol Cell,* 4**,** 445-50.

MEGGENDORFER, M., ROLLER, A., HAFERLACH, T., EDER, C., DICKER, F., GROSSMANN, V., KOHLMANN, A., ALPERMANN, T., YOSHIDA, K., OGAWA, S., KOEFFLER, H. P., KERN, W., HAFERLACH, C. & SCHNITTGER, S. 2012. SRSF2 mutations in 275 cases with chronic myelomonocytic leukemia (CMML). *Blood,* 120**,** 3080-8.

MENDOZA, M., NORDEN, C., DURRER, K., RAUTER, H., UHLMANN, F. & BARRAL, Y. 2009. A mechanism for chromosome segregation sensing by the NoCut checkpoint. *Nature Cell Biology,* 11**,** 477-483.

MICHAELIS, C., CIOSK, R. & NASMYTH, K. 1997. Cohesins: chromosomal proteins that prevent premature separation of sister chromatids. *Cell,* 91**,** 35-45.

MISULOVIN, Z., SCHWARTZ, Y. B., LI, X. Y., KAHN, T. G., GAUSE, M., MACARTHUR, S., FAY, J. C., EISEN, M. B., PIRROTTA, V., BIGGIN, M. D. & DORSETT, D. 2008. Association of cohesin and Nipped-B with transcriptionally active regions of the Drosophila melanogaster genome. *Chromosoma,* 117**,** 89-102.

MITCHISON, T. J. & SALMON, E. D. 2001. Mitosis: a history of division. *Nat Cell Biol,* 3**,** E17-21.

MOCCIARO, A., BERDOUGO, E., ZENG, K., BLACK, E., VAGNARELLI, P., EARNSHAW, W., GILLESPIE, D., JALLEPALLI, P. & SCHIEBEL, E. 2010. Vertebrate cells genetically deficient for Cdc14A or Cdc14B retain DNA damage checkpoint proficiency but are impaired in DNA repair. *J Cell Biol,* 189**,** 631-9.

MOCHIDA, S., MASLEN, S. L., SKEHEL, M. & HUNT, T. 2010. Greatwall phosphorylates an inhibitor of protein phosphatase 2A that is essential for mitosis. *Science,* 330**,** 1670-3.

MOORE, M. J. & SHARP, P. A. 1993. Evidence for two active sites in the spliceosome provided by stereochemistry of pre-mRNA splicing. *Nature,* 365**,** 364-8.

MORDES, D., LUO, X., KAR, A., KUO, D., XU, L., FUSHIMI, K., YU, G., STERNBERG, P., JR. & WU, J. Y. 2006. Pre-mRNA splicing and retinitis pigmentosa. *Mol Vis,* 12**,** 1259-71.

MORGAN, D. O. 1995. Principles of CDK regulation. *Nature,* 374**,** 131-4.

MOSER, S. C. & SWEDLOW, J. R. 2011. How to be a mitotic chromosome. *Chromosome Res,* 19**,** 307-19.

MUELLER, P. R., COLEMAN, T. R., KUMAGAI, A. & DUNPHY, W. G. 1995. Myt1: a membrane-associated inhibitory kinase that phosphorylates Cdc2 on both threonine-14 and tyrosine-15. *Science,* 270**,** 86-90.

MUKHERJI, M., BELL, R., SUPEKOVA, L., WANG, Y., ORTH, A. P., BATALOV, S., MIRAGLIA, L., HUESKEN, D., LANGE, J., MARTIN, C., SAHASRABUDHE, S., REINHARDT, M., NATT, F., HALL, J., MICKANIN, C., LABOW, M., CHANDA, S. K., CHO, C. Y. & SCHULTZ, P. G. 2006. Genome-wide functional analysis of human cell-cycle regulators. *Proceedings of the National Academy of Sciences,* 103**,** 14819-14824.

MUSACCHIO, A. & SALMON, E. D. 2007. The spindle-assembly checkpoint in space and time. *Nat Rev Mol Cell Biol,* 8**,** 379-93.

MUSIO, A., SELICORNI, A., FOCARELLI, M. L., GERVASINI, C., MILANI, D., RUSSO, S., VEZZONI, P. & LARIZZA, L. 2006. X-linked Cornelia de Lange syndrome owing to SMC1L1 mutations. *Nat Genet,* 38**,** 528-30.

NAKAJIMA, H., TOYOSHIMA-MORIMOTO, F., TANIGUCHI, E. & NISHIDA, E. 2003. Identification of a consensus motif for Plk (Polo-like kinase) phosphorylation reveals Myt1 as a Plk1 substrate. *J Biol Chem,* 278**,** 25277-80.

NAKAYAMA, K. & NAKAYAMA, K. 1998. Cip/Kip cyclin-dependent kinase inhibitors: brakes of the cell cycle engine during development. *Bioessays,* 20**,** 1020-9.

NARLA, G., DIFEO, A., REEVES, H. L., SCHAID, D. J., HIRSHFELD, J., HOD, E., KATZ, A., ISAACS, W. B., HEBBRING, S., KOMIYA, A., MCDONNELL, S. K., WILEY, K. E., JACOBSEN, S. J., ISAACS, S. D., WALSH, P. C., ZHENG, S. L., CHANG, B. L., FRIEDRICHSEN, D. M., STANFORD, J. L., OSTRANDER, E. A., CHINNAIYAN, A. M., RUBIN, M. A., XU, J., THIBODEAU, S. N., FRIEDMAN, S. L. & MARTIGNETTI, J. A. 2005. A germline DNA polymorphism enhances alternative splicing of the KLF6 tumor suppressor gene and is associated with increased prostate cancer risk. *Cancer Res,* 65**,** 1213-22.

NASMYTH, K. & HAERING, C. H. 2009. Cohesin: its roles and mechanisms. *Annu Rev Genet,* 43**,** 525-58.

NATIVIO, R., WENDT, K. S., ITO, Y., HUDDLESTON, J. E., URIBE-LEWIS, S., WOODFINE, K., KRUEGER, C., REIK, W., PETERS, J. M. & MURRELL, A. 2009. Cohesin is required for higher-order chromatin conformation at the imprinted IGF2-H19 locus. *PLoS Genet,* 5**,** e1000739.

NEEF, R., GRUNEBERG, U., KOPAJTICH, R., LI, X., NIGG, E. A., SILLJE, H. & BARR, F. A. 2007. Choice of Plk1 docking partners during mitosis and cytokinesis is controlled by the activation state of Cdk1. *Nat Cell Biol,* 9**,** 436-44.

NEUBAUER, G., KING, A., RAPPSILBER, J., CALVIO, C., WATSON, M., AJUH, P., SLEEMAN, J., LAMOND, A. & MANN, M. 1998. Mass spectrometry and EST-database searching allows characterization of the multi-protein spliceosome complex. *Nat Genet,* 20**,** 46-50.

NEUMANN, B., HELD, M., LIEBEL, U., ERFLE, H., ROGERS, P., PEPPERKOK, R. & ELLENBERG, J. 2006. High-throughput RNAi screening by time-lapse imaging of live human cells. *Nat Methods,* 3**,** 385-90.

NEUMANN, B., WALTER, T., HÉRICHÉ, J.-K., BULKESCHER, J., ERFLE, H., CONRAD, C., ROGERS, P., POSER, I., HELD, M., LIEBEL, U., CETIN, C., SIECKMANN, F., PAU, G., KABBE, R., WÜNSCHE, A., SATAGOPAM, V., SCHMITZ, M. H. A., CHAPUIS, C., GERLICH, D. W., SCHNEIDER, R., EILS, R., HUBER, W., PETERS, J.-M., HYMAN, A. A., DURBIN, R., PEPPERKOK, R. & ELLENBERG, J. 2010. Phenotypic profiling of the human genome by time-lapse microscopy reveals cell division genes. *Nature,* 464**,** 721-727.

NIGG, E. A., BLANGY, A. & LANE, H. A. 1996. Dynamic changes in nuclear architecture during mitosis: on the role of protein phosphorylation in spindle assembly and chromosome segregation. *Exp Cell Res,* 229**,** 174-80.

NIIYA, F., XIE, X., LEE, K. S., INOUE, H. & MIKI, T. 2005. Inhibition of cyclin-dependent kinase 1 induces cytokinesis without chromosome segregation in an ECT2 and MgcRacGAP-dependent manner. *J Biol Chem,* 280**,** 36502-9.

NILSEN, T. W. 2003. The spliceosome: the most complex macromolecular machine in the cell? *Bioessays,* 25**,** 1147-9.

NILSEN, T. W. & GRAVELEY, B. R. 2010. Expansion of the eukaryotic proteome by alternative splicing. *Nature,* 463**,** 457-63.

NISHIYAMA, T., LADURNER, R., SCHMITZ, J., KREIDL, E., SCHLEIFFER, A., BHASKARA, V., BANDO, M., SHIRAHIGE, K., HYMAN, A. A., MECHTLER, K. & PETERS, J. M. 2010. Sororin mediates sister chromatid cohesion by antagonizing Wapl. *Cell,* 143**,** 737-49.

NISHIYAMA, T., SYKORA, M. M., HUIS IN 'T VELD, P. J., MECHTLER, K. & PETERS, J. M. 2013. Aurora B and Cdk1 mediate Wapl activation and release of

acetylated cohesin from chromosomes by phosphorylating Sororin. *Proc Natl Acad Sci U S A,* 110**,** 13404-9.

NORDEN, C., MENDOZA, M., DOBBELAERE, J., KOTWALIWALE, C. V., BIGGINS, S. & BARRAL, Y. 2006. The NoCut pathway links completion of cytokinesis to spindle midzone function to prevent chromosome breakage. *Cell,* 125**,** 85-98.

NURSE, P. 1990. Universal control mechanism regulating onset of M-phase. *Nature,* 344**,** 503-8.

OHI, M. D., LINK, A. J., REN, L., JENNINGS, J. L., MCDONALD, W. H. & GOULD, K. L. 2002. Proteomics analysis reveals stable multiprotein complexes in both fission and budding yeasts containing Myb-related Cdc5p/Cef1p, novel pre-mRNA splicing factors, and snRNAs. *Mol Cell Biol,* 22**,** 2011-24.

OHI, R., MCCOLLUM, D., HIRANI, B., DEN HAESE, G. J., ZHANG, X., BURKE, J. D., TURNER, K. & GOULD, K. L. 1994. The Schizosaccharomyces pombe cdc5+ gene encodes an essential protein with homology to c-Myb. *EMBO J,* 13**,** 471-83.

OHLSSON, R., BARTKUHN, M. & RENKAWITZ, R. 2010. CTCF shapes chromatin by multiple mechanisms: the impact of 20 years of CTCF research on understanding the workings of chromatin. *Chromosoma,* 119**,** 351-60.

OIKAWA, K., AKIYOSHI, A., TANAKA, M., TAKANASHI, M., NISHI, H., ISAKA, K., KISEKI, H., IDEI, T., TSUKAHARA, Y., HASHIMURA, N., MUKAI, K. & KURODA, M. 2008. Expression of various types of alternatively spliced WAPL transcripts in human cervical epithelia. *Gene,* 423**,** 57-62.

OIKAWA, K., OHBAYASHI, T., KIYONO, T., NISHI, H., ISAKA, K., UMEZAWA, A., KURODA, M. & MUKAI, K. 2004. Expression of a novel human gene, human wings apart-like (hWAPL), is associated with cervical carcinogenesis and tumor progression. *Cancer Res,* 64**,** 3545-9.

OLIVEIRA, R. A., HAMILTON, R. S., PAULI, A., DAVIS, I. & NASMYTH, K. 2010. Cohesin cleavage and Cdk inhibition trigger formation of daughter nuclei. *Nat Cell Biol,* 12**,** 185-92.

OSHIMORI, N., OHSUGI, M. & YAMAMOTO, T. 2006. The Plk1 target Kizuna stabilizes mitotic centrosomes to ensure spindle bipolarity. *Nat Cell Biol,* 8**,** 1095-101.

PACHECO, T. R., MOITA, L. F., GOMES, A. Q., HACOHEN, N. & CARMO-FONSECA, M. 2006. RNA interference knockdown of hU2AF35 impairs cell cycle progression and modulates alternative splicing of Cdc25 transcripts. *Mol Biol Cell,* 17**,** 4187-99.

PAGANI, F., RAPONI, M. & BARALLE, F. E. 2005. Synonymous mutations in CFTR exon 12 affect splicing and are not neutral in evolution. *Proc Natl Acad Sci U S A,* 102**,** 6368-72.

PAPAEMMANUIL, E., CAZZOLA, M., BOULTWOOD, J., MALCOVATI, L., VYAS, P., BOWEN, D., PELLAGATTI, A., WAINSCOAT, J. S., HELLSTROM-LINDBERG, E., GAMBACORTI-PASSERINI, C., GODFREY, A. L., RAPADO, I., CVEJIC, A., RANCE, R., MCGEE, C., ELLIS, P., MUDIE, L. J., STEPHENS, P. J., MCLAREN, S., MASSIE, C. E., TARPEY, P. S., VARELA, I., NIK-ZAINAL, S., DAVIES, H. R., SHLIEN, A., JONES, D., RAINE, K., HINTON, J., BUTLER, A. P., TEAGUE, J. W., BAXTER, E. J., SCORE, J., GALLI, A., DELLA PORTA, M. G., TRAVAGLINO, E., GROVES, M., TAURO, S., MUNSHI, N. C., ANDERSON, K. C., EL-NAGGAR, A., FISCHER, A., MUSTONEN, V., WARREN, A. J., CROSS, N. C., GREEN, A. R., FUTREAL, P. A., STRATTON, M. R., CAMPBELL, P. J. & CHRONIC MYELOID DISORDERS WORKING GROUP OF THE INTERNATIONAL CANCER GENOME, C. 2011. Somatic SF3B1 mutation in myelodysplasia with ring sideroblasts. *N Engl J Med,* 365**,** 1384-95.

PARELHO, V., HADJUR, S., SPIVAKOV, M., LELEU, M., SAUER, S., GREGSON, H. C., JARMUZ, A., CANZONETTA, C., WEBSTER, Z., NESTEROVA, T., COBB, B. S., YOKOMORI, K., DILLON, N., ARAGON, L., FISHER, A. G. & MERKENSCHLAGER, M. 2008. Cohesins functionally associate with CTCF on mammalian chromosome arms. *Cell,* 132**,** 422-33.

PATEL, A. A. & STEITZ, J. A. 2003. Splicing double: insights from the second spliceosome. *Nat Rev Mol Cell Biol,* 4**,** 960-70.

PAULI, A., ALTHOFF, F., OLIVEIRA, R. A., HEIDMANN, S., SCHULDINER, O., LEHNER, C. F., DICKSON, B. J. & NASMYTH, K. 2008. Cell-type-specific TEV protease cleavage reveals cohesin functions in Drosophila neurons. *Dev Cell,* 14**,** 239-51.

PELLESTOR, F., ANDREO, B., ANAHORY, T. & HAMAMAH, S. 2006. The occurrence of aneuploidy in human: lessons from the cytogenetic studies of human oocytes. *Eur J Med Genet,* 49**,** 103-16.

PELLESTOR, F., ANDREO, B., ARNAL, F., HUMEAU, C. & DEMAILLE, J. 2003. Maternal aging and chromosomal abnormalities: new data drawn from in vitro unfertilized human oocytes. *Hum Genet,* 112**,** 195-203.

PEREZ DE CASTRO, I., DE CARCER, G., MONTOYA, G. & MALUMBRES, M. 2008. Emerging cancer therapeutic opportunities by inhibiting mitotic kinases. *Curr Opin Pharmacol,* 8**,** 375-83.

PETERS, J. M. 2012. The many functions of cohesin--different rings to rule them all? *EMBO J,* 31**,** 2061-3.

PETERS, J. M. & NISHIYAMA, T. 2012. Sister chromatid cohesion. *Cold Spring Harb Perspect Biol,* 4.

PETERS, J. M., TEDESCHI, A. & SCHMITZ, J. 2008. The cohesin complex and its roles in chromosome biology. *Genes Dev,* 22**,** 3089-114.

PETRONCZKI, M., GLOTZER, M., KRAUT, N. & PETERS, J. M. 2007. Polo-like kinase 1 triggers the initiation of cytokinesis in human cells by promoting recruitment of the RhoGEF Ect2 to the central spindle. *Dev Cell,* 12**,** 713-25.

PETRONCZKI, M., LENART, P. & PETERS, J. M. 2008. Polo on the Rise-from Mitotic Entry to Cytokinesis with Plk1. *Dev Cell,* 14**,** 646-59.

PETRONCZKI, M., SIOMOS, M. F. & NASMYTH, K. 2003. Un menage a quatre: the molecular biology of chromosome segregation in meiosis. *Cell,* 112**,** 423-40.

PETTIGREW, C., WAYTE, N., LOVELOCK, P. K., TAVTIGIAN, S. V., CHENEVIX-TRENCH, G., SPURDLE, A. B. & BROWN, M. A. 2005. Evolutionary conservation analysis increases the colocalization of predicted exonic splicing enhancers in the BRCA1 gene with missense sequence changes and in-frame deletions, but not polymorphisms. *Breast Cancer Res,* 7**,** R929-39.

PFLEGER, C. M. & KIRSCHNER, M. W. 2000. The KEN box: an APC recognition signal distinct from the D box targeted by Cdh1. *Genes Dev,* 14**,** 655-65.

PINES, J. 2011. Cubism and the cell cycle: the many faces of the APC/C. *Nat Rev Mol Cell Biol,* 12**,** 427-38.

PIWNICA-WORMS, H., ATHERTON-FESSLER, S., LEE, M. S., OGG, S., SWENSON, K. I. & PARKER, L. L. 1991. p107wee1 is a serine/threonine and tyrosine kinase that promotes the tyrosine phosphorylation of the cyclin/p34cdc2 complex. *Cold Spring Harb Symp Quant Biol,* 56**,** 567-76.

POTAPOVA, T. A., DAUM, J. R., PITTMAN, B. D., HUDSON, J. R., JONES, T. N., SATINOVER, D. L., STUKENBERG, P. T. & GORBSKY, G. J. 2006. The reversibility of mitotic exit in vertebrate cells. *Nature,* 440**,** 954-8.

POTTS, P. R., PORTEUS, M. H. & YU, H. 2006. Human SMC5/6 complex promotes sister chromatid homologous recombination by recruiting the SMC1/3 cohesin complex to double-strand breaks. *EMBO J,* 25**,** 3377-88.

PREISINGER, C. & BARR, F. A. 2005. Kinases regulating Golgi apparatus structure and function. *Biochem Soc Symp*, 15-30.

QIAN, Y. W., ERIKSON, E., LI, C. & MALLER, J. L. 1998. Activated polo-like kinase Plx1 is required at multiple points during mitosis in Xenopus laevis. *Mol Cell Biol,* 18, 4262-71.

QUESADA, V., CONDE, L., VILLAMOR, N., ORDONEZ, G. R., JARES, P., BASSAGANYAS, L., RAMSAY, A. J., BEA, S., PINYOL, M., MARTINEZ-TRILLOS, A., LOPEZ-GUERRA, M., COLOMER, D., NAVARRO, A., BAUMANN, T., AYMERICH, M., ROZMAN, M., DELGADO, J., GINE, E., HERNANDEZ, J. M., GONZALEZ-DIAZ, M., PUENTE, D. A., VELASCO, G., FREIJE, J. M., TUBIO, J. M., ROYO, R., GELPI, J. L., OROZCO, M., PISANO, D. G., ZAMORA, J., VAZQUEZ, M., VALENCIA, A., HIMMELBAUER, H., BAYES, M., HEATH, S., GUT, M., GUT, I., ESTIVILL, X., LOPEZ-GUILLERMO, A., PUENTE, X. S., CAMPO, E. & LOPEZ-OTIN, C. 2012. Exome sequencing identifies recurrent mutations of the splicing factor SF3B1 gene in chronic lymphocytic leukemia. *Nat Genet,* 44, 47-52.

RANKIN, S. 2005. Sororin, the cell cycle and sister chromatid cohesion. *Cell Cycle,* 4, 1039-42.

RANKIN, S., AYAD, N. G. & KIRSCHNER, M. W. 2005. Sororin, a substrate of the anaphase-promoting complex, is required for sister chromatid cohesion in vertebrates. *Mol Cell,* 18, 185-200.

RAO, P. N. & JOHNSON, R. T. 1970. Mammalian cell fusion: studies on the regulation of DNA synthesis and mitosis. *Nature,* 225, 159-64.

RAPPSILBER, J., RYDER, U., LAMOND, A. I. & MANN, M. 2002. Large-scale proteomic analysis of the human spliceosome. *Genome Res,* 12, 1231-45.

REBER, A., LEHNER, C. F. & JACOBS, H. W. 2006. Terminal mitoses require negative regulation of Fzr/Cdh1 by Cyclin A, preventing premature degradation of mitotic cyclins and String/Cdc25. *Development,* 133, 3201-11.

REED, R. 2000. Mechanisms of fidelity in pre-mRNA splicing. *Curr Opin Cell Biol,* 12, 340-5.

REED, R. & CHENG, H. 2005. TREX, SR proteins and export of mRNA. *Curr Opin Cell Biol,* 17, 269-73.

REMESEIRO, S., CUADRADO, A., GOMEZ-LOPEZ, G., PISANO, D. G. & LOSADA, A. 2012. A unique role of cohesin-SA1 in gene regulation and development. *EMBO J,* 31, 2090-102.

REMESEIRO, S., CUADRADO, A. & LOSADA, A. 2013. Cohesin in development and disease. *Development,* 140, 3715-8.

RIEDEL, C. G., KATIS, V. L., KATOU, Y., MORI, S., ITOH, T., HELMHART, W., GALOVA, M., PETRONCZKI, M., GREGAN, J., CETIN, B., MUDRAK, I., OGRIS, E., MECHTLER, K., PELLETIER, L., BUCHHOLZ, F., SHIRAHIGE, K. & NASMYTH, K. 2006. Protein phosphatase 2A protects centromeric sister chromatid cohesion during meiosis I. *Nature,* 441, 53-61.

RINO, J. & CARMO-FONSECA, M. 2009. The spliceosome: a self-organized macromolecular machine in the nucleus? *Trends Cell Biol,* 19, 375-84.

ROBBERSON, B. L., COTE, G. J. & BERGET, S. M. 1990. Exon definition may facilitate splice site selection in RNAs with multiple exons. *Mol Cell Biol,* 10, 84-94.

ROLEF BEN-SHAHAR, T., HEEGER, S., LEHANE, C., EAST, P., FLYNN, H., SKEHEL, M. & UHLMANN, F. 2008. Eco1-dependent cohesin acetylation during establishment of sister chromatid cohesion. *Science,* 321, 563-6.

ROLLINS, R. A., KOROM, M., AULNER, N., MARTENS, A. & DORSETT, D. 2004. Drosophila nipped-B protein supports sister chromatid cohesion and opposes

the stromalin/Scc3 cohesion factor to facilitate long-range activation of the cut gene. *Mol Cell Biol,* 24**,** 3100-11.

ROSSI, D., RASI, S., SPINA, V., FANGAZIO, M., MONTI, S., GRECO, M., CIARDULLO, C., FAMA, R., CRESTA, S., BRUSCAGGIN, A., LAURENTI, L., MARTINI, M., MUSTO, P., FORCONI, F., MARASCA, R., LAROCCA, L. M., FOA, R. & GAIDANO, G. 2012. Different impact of NOTCH1 and SF3B1 mutations on the risk of chronic lymphocytic leukemia transformation to Richter syndrome. *Br J Haematol,* 158**,** 426-9.

ROWLAND, B. D., ROIG, M. B., NISHINO, T., KURZE, A., ULUOCAK, P., MISHRA, A., BECKOUET, F., UNDERWOOD, P., METSON, J., IMRE, R., MECHTLER, K., KATIS, V. L. & NASMYTH, K. 2009. Building sister chromatid cohesion: smc3 acetylation counteracts an antiestablishment activity. *Mol Cell,* 33**,** 763-74.

ROY, M., XU, Q. & LEE, C. 2005. Evidence that public database records for many cancer-associated genes reflect a splice form found in tumors and lack normal splice forms. *Nucleic Acids Res,* 33**,** 5026-33.

ROYBAL, G. A. & JURICA, M. S. 2010. Spliceostatin A inhibits spliceosome assembly subsequent to prespliceosome formation. *Nucleic Acids Res,* 38**,** 6664-72.

RUBIO, E. D., REISS, D. J., WELCSH, P. L., DISTECHE, C. M., FILIPPOVA, G. N., BALIGA, N. S., AEBERSOLD, R., RANISH, J. A. & KRUMM, A. 2008. CTCF physically links cohesin to chromatin. *Proc Natl Acad Sci U S A,* 105**,** 8309-14.

RUCHAUD, S., CARMENA, M. & EARNSHAW, W. C. 2007. Chromosomal passengers: conducting cell division. *Nature Reviews Molecular Cell Biology,* 8**,** 798-812.

RUSAN, N. M., FAGERSTROM, C. J., YVON, A. M. & WADSWORTH, P. 2001. Cell cycle-dependent changes in microtubule dynamics in living cells expressing green fluorescent protein-alpha tubulin. *Mol Biol Cell,* 12**,** 971-80.

RYU, B., KIM, D. S., DELUCA, A. M. & ALANI, R. M. 2007. Comprehensive expression profiling of tumor cell lines identifies molecular signatures of melanoma progression. *PLoS One,* 2**,** e594.

SAITO, R. M., PERREAULT, A., PEACH, B., SATTERLEE, J. S. & VAN DEN HEUVEL, S. 2004. The CDC-14 phosphatase controls developmental cell-cycle arrest in C. elegans. *Nat Cell Biol,* 6**,** 777-83.

SALIC, A., WATERS, J. C. & MITCHISON, T. J. 2004. Vertebrate shugoshin links sister centromere cohesion and kinetochore microtubule stability in mitosis. *Cell,* 118**,** 567-78.

SANTAMARIA, A., NEEF, R., EBERSPACHER, U., EIS, K., HUSEMANN, M., MUMBERG, D., PRECHTL, S., SCHULZE, V., SIEMEISTER, G., WORTMANN, L., BARR, F. A. & NIGG, E. A. 2007. Use of the novel Plk1 inhibitor ZK-thiazolidinone to elucidate functions of Plk1 in early and late stages of mitosis. *Mol Biol Cell,* 18**,** 4024-36.

SCACHERI, P. C., ROZENBLATT-ROSEN, O., CAPLEN, N. J., WOLFSBERG, T. G., UMAYAM, L., LEE, J. C., HUGHES, C. M., SHANMUGAM, K. S., BHATTACHARJEE, A., MEYERSON, M. & COLLINS, F. S. 2004. Short interfering RNAs can induce unexpected and divergent changes in the levels of untargeted proteins in mammalian cells. *Proc Natl Acad Sci U S A,* 101**,** 1892-7.

SCHLEIFFER, A., KAITNA, S., MAURER-STROH, S., GLOTZER, M., NASMYTH, K. & EISENHABER, F. 2003. Kleisins: a superfamily of bacterial and eukaryotic SMC protein partners. *Mol Cell,* 11**,** 571-5.

SCHMIDT, C. K., BROOKES, N. & UHLMANN, F. 2009. Conserved features of cohesin binding along fission yeast chromosomes. *Genome Biol,* 10**,** R52.

SCHMIDT, D., SCHWALIE, P. C., ROSS-INNES, C. S., HURTADO, A., BROWN, G. D., CARROLL, J. S., FLICEK, P. & ODOM, D. T. 2010. A CTCF-independent role for cohesin in tissue-specific transcription. *Genome Res,* 20**,** 578-88.

SCHMITZ, J., WATRIN, E., LENART, P., MECHTLER, K. & PETERS, J. M. 2007. Sororin is required for stable binding of cohesin to chromatin and for sister chromatid cohesion in interphase. *Curr Biol,* 17**,** 630-6.

SCHMITZ, M. H. A., HELD, M., JANSSENS, V., HUTCHINS, J. R. A., HUDECZ, O., IVANOVA, E., GORIS, J., TRINKLE-MULCAHY, L., LAMOND, A. I., POSER, I., HYMAN, A. A., MECHTLER, K., PETERS, J.-M. & GERLICH, D. W. 2010. Live-cell imaging RNAi screen identifies PP2A–B55α and importin-β1 as key mitotic exit regulators in human cells. *Nature Cell Biology,* 12**,** 886-893.

SCHNEIDER, B. L., YANG, Q. H. & FUTCHER, A. B. 1996. Linkage of replication to start by the Cdk inhibitor Sic1. *Science,* 272**,** 560-2.

SCHNEIDER, M., WILL, C. L., ANOKHINA, M., TAZI, J., URLAUB, H. & LUHRMANN, R. 2010. Exon definition complexes contain the tri-snRNP and can be directly converted into B-like precatalytic splicing complexes. *Mol Cell,* 38**,** 223-35.

SCHULDINER, O., BERDNIK, D., LEVY, J. M., WU, J. S., LUGINBUHL, D., GONTANG, A. C. & LUO, L. 2008. piggyBac-based mosaic screen identifies a postmitotic function for cohesin in regulating developmental axon pruning. *Dev Cell,* 14**,** 227-38.

SCHULE, B., OVIEDO, A., JOHNSTON, K., PAI, S. & FRANCKE, U. 2005. Inactivating mutations in ESCO2 cause SC phocomelia and Roberts syndrome: no phenotype-genotype correlation. *Am J Hum Genet,* 77**,** 1117-28.

SCHUMACHER, J. M., GOLDEN, A. & DONOVAN, P. J. 1998. AIR-2: An Aurora/Ipl1-related protein kinase associated with chromosomes and midbody microtubules is required for polar body extrusion and cytokinesis in Caenorhabditis elegans embryos. *J Cell Biol,* 143**,** 1635-46.

SEITAN, V. C., BANKS, P., LAVAL, S., MAJID, N. A., DORSETT, D., RANA, A., SMITH, J., BATEMAN, A., KRPIC, S., HOSTERT, A., ROLLINS, R. A., ERDJUMENT-BROMAGE, H., TEMPST, P., BENARD, C. Y., HEKIMI, S., NEWBURY, S. F. & STRACHAN, T. 2006. Metazoan Scc4 homologs link sister chromatid cohesion to cell and axon migration guidance. *PLoS Biol,* 4**,** e242.

SHARMA, S., KOHLSTAEDT, L. A., DAMIANOV, A., RIO, D. C. & BLACK, D. L. 2008. Polypyrimidine tract binding protein controls the transition from exon definition to an intron defined spliceosome. *Nat Struct Mol Biol,* 15**,** 183-91.

SHTEINBERG, M., PROTOPOPOV, Y., LISTOVSKY, T., BRANDEIS, M. & HERSHKO, A. 1999. Phosphorylation of the cyclosome is required for its stimulation by Fizzy/cdc20. *Biochem Biophys Res Commun,* 260**,** 193-8.

SJOBLOM, T., JONES, S., WOOD, L. D., PARSONS, D. W., LIN, J., BARBER, T. D., MANDELKER, D., LEARY, R. J., PTAK, J., SILLIMAN, N., SZABO, S., BUCKHAULTS, P., FARRELL, C., MEEH, P., MARKOWITZ, S. D., WILLIS, J., DAWSON, D., WILLSON, J. K., GAZDAR, A. F., HARTIGAN, J., WU, L., LIU, C., PARMIGIANI, G., PARK, B. H., BACHMAN, K. E., PAPADOPOULOS, N., VOGELSTEIN, B., KINZLER, K. W. & VELCULESCU, V. E. 2006. The consensus coding sequences of human breast and colorectal cancers. *Science,* 314**,** 268-74.

SJOGREN, C. & NASMYTH, K. 2001. Sister chromatid cohesion is required for postreplicative double-strand break repair in Saccharomyces cerevisiae. *Curr Biol,* 11**,** 991-5.

SKOP, A. R., LIU, H., YATES, J., 3RD, MEYER, B. J. & HEALD, R. 2004. Dissection of the mammalian midbody proteome reveals conserved cytokinesis mechanisms. *Science,* 305**,** 61-6.

SKOTHEIM, R. I. & NEES, M. 2007. Alternative splicing in cancer: noise, functional, or systematic? *Int J Biochem Cell Biol,* 39**,** 1432-49.

SKOURTI-STATHAKI, K., PROUDFOOT, N. J. & GROMAK, N. 2011. Human senataxin resolves RNA/DNA hybrids formed at transcriptional pause sites to promote Xrn2-dependent termination. *Mol Cell,* 42**,** 794-805.

SMITH, C. W. & VALCARCEL, J. 2000. Alternative pre-mRNA splicing: the logic of combinatorial control. *Trends Biochem Sci,* 25**,** 381-8.

SMITH, D. J., QUERY, C. C. & KONARSKA, M. M. 2008. "Nought may endure but mutability": spliceosome dynamics and the regulation of splicing. *Mol Cell,* 30**,** 657-66.

SMITH, P. C., KARPOWICH, N., MILLEN, L., MOODY, J. E., ROSEN, J., THOMAS, P. J. & HUNT, J. F. 2002. ATP binding to the motor domain from an ABC transporter drives formation of a nucleotide sandwich dimer. *Mol Cell,* 10**,** 139-49.

SOLOMON, D. A., KIM, T., DIAZ-MARTINEZ, L. A., FAIR, J., ELKAHLOUN, A. G., HARRIS, B. T., TORETSKY, J. A., ROSENBERG, S. A., SHUKLA, N., LADANYI, M., SAMUELS, Y., JAMES, C. D., YU, H., KIM, J. S. & WALDMAN, T. 2011. Mutational inactivation of STAG2 causes aneuploidy in human cancer. *Science,* 333**,** 1039-43.

SONG, J., LAFONT, A., CHEN, J., WU, F. M., SHIRAHIGE, K. & RANKIN, S. 2012. Cohesin acetylation promotes sister chromatid cohesion only in association with the replication machinery. *J Biol Chem,* 287**,** 34325-36.

SONNICHSEN, B., KOSKI, L. B., WALSH, A., MARSCHALL, P., NEUMANN, B., BREHM, M., ALLEAUME, A. M., ARTELT, J., BETTENCOURT, P., CASSIN, E., HEWITSON, M., HOLZ, C., KHAN, M., LAZIK, S., MARTIN, C., NITZSCHE, B., RUER, M., STAMFORD, J., WINZI, M., HEINKEL, R., RODER, M., FINELL, J., HANTSCH, H., JONES, S. J., JONES, M., PIANO, F., GUNSALUS, K. C., OEGEMA, K., GONCZY, P., COULSON, A., HYMAN, A. A. & ECHEVERRI, C. J. 2005. Full-genome RNAi profiling of early embryogenesis in Caenorhabditis elegans. *Nature,* 434**,** 462-9.

SONODA, E., MATSUSAKA, T., MORRISON, C., VAGNARELLI, P., HOSHI, O., USHIKI, T., NOJIMA, K., FUKAGAWA, T., WAIZENEGGER, I. C., PETERS, J. M., EARNSHAW, W. C. & TAKEDA, S. 2001. Scc1/Rad21/Mcd1 is required for sister chromatid cohesion and kinetochore function in vertebrate cells. *Dev Cell,* 1**,** 759-70.

SPLINTER, E., HEATH, H., KOOREN, J., PALSTRA, R. J., KLOUS, P., GROSVELD, F., GALJART, N. & DE LAAT, W. 2006. CTCF mediates long-range chromatin looping and local histone modification in the beta-globin locus. *Genes Dev,* 20**,** 2349-54.

SREBROW, A. & KORNBLIHTT, A. R. 2006. The connection between splicing and cancer. *J Cell Sci,* 119**,** 2635-41.

STEDMAN, W., KANG, H., LIN, S., KISSIL, J. L., BARTOLOMEI, M. S. & LIEBERMAN, P. M. 2008. Cohesins localize with CTCF at the KSHV latency control region and at cellular c-myc and H19/Igf2 insulators. *EMBO J,* 27**,** 654-66.

STEGMEIER, F. & AMON, A. 2004. Closing mitosis: the functions of the Cdc14 phosphatase and its regulation. *Annu Rev Genet,* 38**,** 203-32.

STEIGEMANN, P., WURZENBERGER, C., SCHMITZ, M. H., HELD, M., GUIZETTI, J., MAAR, S. & GERLICH, D. W. 2009. Aurora B-mediated abscission checkpoint protects against tetraploidization. *Cell,* 136**,** 473-84.

STEMMANN, O., ZOU, H., GERBER, S. A., GYGI, S. P. & KIRSCHNER, M. W. 2001. Dual inhibition of sister chromatid separation at metaphase. *Cell,* 107**,** 715-26.

STENSON, P. D., BALL, E. V., MORT, M., PHILLIPS, A. D., SHIEL, J. A., THOMAS, N. S., ABEYSINGHE, S., KRAWCZAK, M. & COOPER, D. N. 2003. Human Gene Mutation Database (HGMD): 2003 update. *Hum Mutat,* 21**,** 577-81.

STERNER, D. A., CARLO, T. & BERGET, S. M. 1996. Architectural limits on split genes. *Proc Natl Acad Sci U S A,* 93**,** 15081-5.
STEVENS, D., GASSMANN, R., OEGEMA, K. & DESAI, A. 2011. Uncoordinated loss of chromatid cohesion is a common outcome of extended metaphase arrest. *PLoS One,* 6**,** e22969.
STEVENS, S. W., RYAN, D. E., GE, H. Y., MOORE, R. E., YOUNG, M. K., LEE, T. D. & ABELSON, J. 2002. Composition and functional characterization of the yeast spliceosomal penta-snRNP. *Mol Cell,* 9**,** 31-44.
STRASSER, K., MASUDA, S., MASON, P., PFANNSTIEL, J., OPPIZZI, M., RODRIGUEZ-NAVARRO, S., RONDON, A. G., AGUILERA, A., STRUHL, K., REED, R. & HURT, E. 2002. TREX is a conserved complex coupling transcription with messenger RNA export. *Nature,* 417**,** 304-8.
STRAUSFELD, U., FERNANDEZ, A., CAPONY, J. P., GIRARD, F., LAUTREDOU, N., DERANCOURT, J., LABBE, J. C. & LAMB, N. J. 1994. Activation of p34cdc2 protein kinase by microinjection of human cdc25C into mammalian cells. Requirement for prior phosphorylation of cdc25C by p34cdc2 on sites phosphorylated at mitosis. *J Biol Chem,* 269**,** 5989-6000.
STROM, L., KARLSSON, C., LINDROOS, H. B., WEDAHL, S., KATOU, Y., SHIRAHIGE, K. & SJOGREN, C. 2007. Postreplicative formation of cohesion is required for repair and induced by a single DNA break. *Science,* 317**,** 242-5.
STROM, L., LINDROOS, H. B., SHIRAHIGE, K. & SJOGREN, C. 2004. Postreplicative recruitment of cohesin to double-strand breaks is required for DNA repair. *Mol Cell,* 16**,** 1003-15.
STROM, L. & SJOGREN, C. 2005. DNA damage-induced cohesion. *Cell Cycle,* 4**,** 536-9.
STROM, L. & SJOGREN, C. 2007. Chromosome segregation and double-strand break repair - a complex connection. *Curr Opin Cell Biol,* 19**,** 344-9.
SU, K. C., TAKAKI, T. & PETRONCZKI, M. 2011. Targeting of the RhoGEF Ect2 to the equatorial membrane controls cleavage furrow formation during cytokinesis. *Dev Cell,* 21**,** 1104-15.
SUMARA, I., GIMENEZ-ABIAN, J. F., GERLICH, D., HIROTA, T., KRAFT, C., DE LA TORRE, C., ELLENBERG, J. & PETERS, J. M. 2004. Roles of polo-like kinase 1 in the assembly of functional mitotic spindles. *Curr Biol,* 14**,** 1712-22.
SUMARA, I., VORLAUFER, E., GIEFFERS, C., PETERS, B. H. & PETERS, J. M. 2000. Characterization of vertebrate cohesin complexes and their regulation in prophase. *J Cell Biol,* 151**,** 749-62.
SUMARA, I., VORLAUFER, E., STUKENBERG, P. T., KELM, O., REDEMANN, N., NIGG, E. A. & PETERS, J. M. 2002. The dissociation of cohesin from chromosomes in prophase is regulated by Polo-like kinase. *Mol Cell,* 9**,** 515-25.
SUN, Y., KUCEJ, M., FAN, H. Y., YU, H., SUN, Q. Y. & ZOU, H. 2009. Separase is recruited to mitotic chromosomes to dissolve sister chromatid cohesion in a DNA-dependent manner. *Cell,* 137**,** 123-32.
SUNKEL, C. E. & GLOVER, D. M. 1988. polo, a mitotic mutant of Drosophila displaying abnormal spindle poles. *J Cell Sci,* 89 (Pt 1)**,** 25-38.
SUTANI, T., KAWAGUCHI, T., KANNO, R., ITOH, T. & SHIRAHIGE, K. 2009. Budding yeast Wpl1(Rad61)-Pds5 complex counteracts sister chromatid cohesion-establishing reaction. *Curr Biol,* 19**,** 492-7.
SUTTERLIN, C., LIN, C. Y., FENG, Y., FERRIS, D. K., ERIKSON, R. L. & MALHOTRA, V. 2001. Polo-like kinase is required for the fragmentation of pericentriolar Golgi stacks during mitosis. *Proc Natl Acad Sci U S A,* 98**,** 9128-32.
SWEDLOW, J. R., COTTA-RAMUSINO, C. & ELLEDGE, S. J. 2010. Cell biology forum: Genome-wide view of mitosis. *Nature,* 464**,** 684-5.

TAKAHASHI, T. S., YIU, P., CHOU, M. F., GYGI, S. & WALTER, J. C. 2004. Recruitment of Xenopus Scc2 and cohesin to chromatin requires the pre-replication complex. *Nat Cell Biol,* 6**,** 991-6.
TALLURI, S. & DICK, F. A. 2012. Regulation of transcription and chromatin structure by pRB: here, there and everywhere. *Cell Cycle,* 11**,** 3189-98.
TAMKUN, J. W., KAHN, R. A., KISSINGER, M., BRIZUELA, B. J., RULKA, C., SCOTT, M. P. & KENNISON, J. A. 1991. The arflike gene encodes an essential GTP-binding protein in Drosophila. *Proc Natl Acad Sci U S A,* 88**,** 3120-4.
TAN, S. Y. & BROWN, J. 2006. Rudolph Virchow (1821-1902): "pope of pathology". *Singapore Med J,* 47**,** 567-8.
TANACKOVIC, G., RANSIJN, A., THIBAULT, P., ABOU ELELA, S., KLINCK, R., BERSON, E. L., CHABOT, B. & RIVOLTA, C. 2011. PRPF mutations are associated with generalized defects in spliceosome formation and pre-mRNA splicing in patients with retinitis pigmentosa. *Hum Mol Genet,* 20**,** 2116-30.
TANAKA, K., HAO, Z., KAI, M. & OKAYAMA, H. 2001. Establishment and maintenance of sister chromatid cohesion in fission yeast by a unique mechanism. *EMBO J,* 20**,** 5779-90.
TANAKA, S. & ARAKI, H. 2010. Regulation of the initiation step of DNA replication by cyclin-dependent kinases. *Chromosoma,* 119**,** 565-74.
TANAKA, T., COSMA, M. P., WIRTH, K. & NASMYTH, K. 1999. Identification of cohesin association sites at centromeres and along chromosome arms. *Cell,* 98**,** 847-58.
TANAKA, T., FUCHS, J., LOIDL, J. & NASMYTH, K. 2000. Cohesin ensures bipolar attachment of microtubules to sister centromeres and resists their precocious separation. *Nat Cell Biol,* 2**,** 492-9.
TANAKA, T. U., RACHIDI, N., JANKE, C., PEREIRA, G., GALOVA, M., SCHIEBEL, E., STARK, M. J. & NASMYTH, K. 2002. Evidence that the Ipl1-Sli15 (Aurora kinase-INCENP) complex promotes chromosome bi-orientation by altering kinetochore-spindle pole connections. *Cell,* 108**,** 317-29.
TANENBAUM, M. E. & MEDEMA, R. H. 2010. Mechanisms of centrosome separation and bipolar spindle assembly. *Dev Cell,* 19**,** 797-806.
TANG, Z., SHU, H., QI, W., MAHMOOD, N. A., MUMBY, M. C. & YU, H. 2006. PP2A is required for centromeric localization of Sgo1 and proper chromosome segregation. *Dev Cell,* 10**,** 575-85.
TANGE, T. O., NOTT, A. & MOORE, M. J. 2004. The ever-increasing complexities of the exon junction complex. *Curr Opin Cell Biol,* 16**,** 279-84.
TERRET, M. E., SHERWOOD, R., RAHMAN, S., QIN, J. & JALLEPALLI, P. V. 2009. Cohesin acetylation speeds the replication fork. *Nature,* 462**,** 231-4.
TOMKINS, D., HUNTER, A. & ROBERTS, M. 1979. Cytogenetic findings in Roberts-SC phocomelia syndrome(s). *Am J Med Genet,* 4**,** 17-26.
TOMKINS, D. J. & SISKEN, J. E. 1984. Abnormalities in the cell-division cycle in Roberts syndrome fibroblasts: a cellular basis for the phenotypic characteristics? *Am J Hum Genet,* 36**,** 1332-40.
TONKIN, E. T., WANG, T. J., LISGO, S., BAMSHAD, M. J. & STRACHAN, T. 2004. NIPBL, encoding a homolog of fungal Scc2-type sister chromatid cohesion proteins and fly Nipped-B, is mutated in Cornelia de Lange syndrome. *Nat Genet,* 36**,** 636-41.
TOTH, A., CIOSK, R., UHLMANN, F., GALOVA, M., SCHLEIFFER, A. & NASMYTH, K. 1999. Yeast cohesin complex requires a conserved protein, Eco1p(Ctf7), to establish cohesion between sister chromatids during DNA replication. *Genes Dev,* 13**,** 320-33.
TOTH, A., RABITSCH, K. P., GALOVA, M., SCHLEIFFER, A., BUONOMO, S. B. & NASMYTH, K. 2000. Functional genomics identifies monopolin: a kinetochore

protein required for segregation of homologs during meiosis i. *Cell,* 103**,** 1155-68.
UBERSAX, J. A., WOODBURY, E. L., QUANG, P. N., PARAZ, M., BLETHROW, J. D., SHAH, K., SHOKAT, K. M. & MORGAN, D. O. 2003. Targets of the cyclin-dependent kinase Cdk1. *Nature,* 425**,** 859-64.
UHLMANN, F., LOTTSPEICH, F. & NASMYTH, K. 1999. Sister-chromatid separation at anaphase onset is promoted by cleavage of the cohesin subunit Scc1. *Nature,* 400**,** 37-42.
UHLMANN, F. & NASMYTH, K. 1998. Cohesion between sister chromatids must be established during DNA replication. *Curr Biol,* 8**,** 1095-101.
UHLMANN, F., WERNIC, D., POUPART, M. A., KOONIN, E. V. & NASMYTH, K. 2000. Cleavage of cohesin by the CD clan protease separin triggers anaphase in yeast. *Cell,* 103**,** 375-86.
UNAL, E., HEIDINGER-PAULI, J. M., KIM, W., GUACCI, V., ONN, I., GYGI, S. P. & KOSHLAND, D. E. 2008. A molecular determinant for the establishment of sister chromatid cohesion. *Science,* 321**,** 566-9.
UNAL, E., HEIDINGER-PAULI, J. M. & KOSHLAND, D. 2007. DNA double-strand breaks trigger genome-wide sister-chromatid cohesion through Eco1 (Ctf7). *Science,* 317**,** 245-8.
VALADKHAN, S. 2007. The spliceosome: caught in a web of shifting interactions. *Curr Opin Struct Biol,* 17**,** 310-5.
VAN DEN BERG, D. J. & FRANCKE, U. 1993. Sensitivity of Roberts syndrome cells to gamma radiation, mitomycin C, and protein synthesis inhibitors. *Somat Cell Mol Genet,* 19**,** 377-92.
VAN HEEMST, D., JAMES, F., POGGELER, S., BERTEAUX-LECELLIER, V. & ZICKLER, D. 1999. Spo76p is a conserved chromosome morphogenesis protein that links the mitotic and meiotic programs. *Cell,* 98**,** 261-71.
VAZQUEZ-NOVELLE, M. D. & PETRONCZKI, M. 2010. Relocation of the chromosomal passenger complex prevents mitotic checkpoint engagement at anaphase. *Curr Biol,* 20**,** 1402-7.
VEGA, H., WAISFISZ, Q., GORDILLO, M., SAKAI, N., YANAGIHARA, I., YAMADA, M., VAN GOSLIGA, D., KAYSERILI, H., XU, C., OZONO, K., JABS, E. W., INUI, K. & JOENJE, H. 2005. Roberts syndrome is caused by mutations in ESCO2, a human homolog of yeast ECO1 that is essential for the establishment of sister chromatid cohesion. *Nat Genet,* 37**,** 468-70.
VENABLES, J. P. 2006. Unbalanced alternative splicing and its significance in cancer. *Bioessays,* 28**,** 378-86.
VERMA, R., ANNAN, R. S., HUDDLESTON, M. J., CARR, S. A., REYNARD, G. & DESHAIES, R. J. 1997. Phosphorylation of Sic1p by G1 Cdk required for its degradation and entry into S phase. *Science,* 278**,** 455-60.
VISCONTE, V., MAKISHIMA, H., MACIEJEWSKI, J. P. & TIU, R. V. 2012. Emerging roles of the spliceosomal machinery in myelodysplastic syndromes and other hematological disorders. *Leukemia,* 26**,** 2447-54.
VITHANA, E. N., ABU-SAFIEH, L., ALLEN, M. J., CAREY, A., PAPAIOANNOU, M., CHAKAROVA, C., AL-MAGHTHEH, M., EBENEZER, N. D., WILLIS, C., MOORE, A. T., BIRD, A. C., HUNT, D. M. & BHATTACHARYA, S. S. 2001. A human homolog of yeast pre-mRNA splicing gene, PRP31, underlies autosomal dominant retinitis pigmentosa on chromosome 19q13.4 (RP11). *Mol Cell,* 8**,** 375-81.
WAHBA, L., AMON, J. D., KOSHLAND, D. & VUICA-ROSS, M. 2011. RNase H and multiple RNA biogenesis factors cooperate to prevent RNA:DNA hybrids from generating genome instability. *Mol Cell,* 44**,** 978-88.

WAHL, M. C., WILL, C. L. & LUHRMANN, R. 2009. The spliceosome: design principles of a dynamic RNP machine. *Cell,* 136**,** 701-18.
WAIZENEGGER, I., GIMENEZ-ABIAN, J. F., WERNIC, D. & PETERS, J. M. 2002. Regulation of human separase by securin binding and autocleavage. *Curr Biol,* 12**,** 1368-78.
WAIZENEGGER, I. C., HAUF, S., MEINKE, A. & PETERS, J. M. 2000. Two distinct pathways remove mammalian cohesin from chromosome arms in prophase and from centromeres in anaphase. *Cell,* 103**,** 399-410.
WANG, G. S. & COOPER, T. A. 2007. Splicing in disease: disruption of the splicing code and the decoding machinery. *Nat Rev Genet,* 8**,** 749-61.
WANG, H. H., ISAACS, F. J., CARR, P. A., SUN, Z. Z., XU, G., FOREST, C. R. & CHURCH, G. M. 2009. Programming cells by multiplex genome engineering and accelerated evolution. *Nature,* 460**,** 894-8.
WANG, L., LAWRENCE, M. S., WAN, Y., STOJANOV, P., SOUGNEZ, C., STEVENSON, K., WERNER, L., SIVACHENKO, A., DELUCA, D. S., ZHANG, L., ZHANG, W., VARTANOV, A. R., FERNANDES, S. M., GOLDSTEIN, N. R., FOLCO, E. G., CIBULSKIS, K., TESAR, B., SIEVERS, Q. L., SHEFLER, E., GABRIEL, S., HACOHEN, N., REED, R., MEYERSON, M., GOLUB, T. R., LANDER, E. S., NEUBERG, D., BROWN, J. R., GETZ, G. & WU, C. J. 2011. SF3B1 and other novel cancer genes in chronic lymphocytic leukemia. *N Engl J Med,* 365**,** 2497-506.
WANG, X. & DAI, W. 2005. Shugoshin, a guardian for sister chromatid segregation. *Exp Cell Res,* 310**,** 1-9.
WANG, Z. & BURGE, C. B. 2008. Splicing regulation: from a parts list of regulatory elements to an integrated splicing code. *RNA,* 14**,** 802-13.
WANG, Z. X., SHI, L., LIU, J. F., AN, X. M., CHANG, W. R. & LIANG, D. C. 2005. 2.0 A crystal structure of human ARL5-GDP3'P, a novel member of the small GTP-binding proteins. *Biochem Biophys Res Commun,* 332**,** 640-5.
WARD, A. J. & COOPER, T. A. 2010. The pathobiology of splicing. *J Pathol,* 220**,** 152-63.
WATANABE, N., BROOME, M. & HUNTER, T. 1995. Regulation of the human WEE1Hu CDK tyrosine 15-kinase during the cell cycle. *EMBO J,* 14**,** 1878-91.
WATANABE, Y. & KITAJIMA, T. S. 2005. Shugoshin protects cohesin complexes at centromeres. *Philos Trans R Soc Lond B Biol Sci,* 360**,** 515-21, discussion 521.
WATANABE, Y. & NURSE, P. 1999. Cohesin Rec8 is required for reductional chromosome segregation at meiosis. *Nature,* 400**,** 461-4.
WATRIN, E. & PETERS, J. M. 2006. Cohesin and DNA damage repair. *Exp Cell Res,* 312**,** 2687-93.
WATRIN, E. & PETERS, J. M. 2009. The cohesin complex is required for the DNA damage-induced G2/M checkpoint in mammalian cells. *EMBO J,* 28**,** 2625-35.
WATRIN, E., SCHLEIFFER, A., TANAKA, K., EISENHABER, F., NASMYTH, K. & PETERS, J. M. 2006. Human Scc4 is required for cohesin binding to chromatin, sister-chromatid cohesion, and mitotic progression. *Curr Biol,* 16**,** 863-74.
WEINBERG, R. A. 1995. The retinoblastoma protein and cell cycle control. *Cell,* 81**,** 323-30.
WEITZER, S., LEHANE, C. & UHLMANN, F. 2003. A model for ATP hydrolysis-dependent binding of cohesin to DNA. *Curr Biol,* 13**,** 1930-40.
WELLS, N. J., WATANABE, N., TOKUSUMI, T., JIANG, W., VERDECIA, M. A. & HUNTER, T. 1999. The C-terminal domain of the Cdc2 inhibitory kinase Myt1 interacts with Cdc2 complexes and is required for inhibition of G(2)/M progression. *J Cell Sci,* 112 (Pt 19)**,** 3361-71.
WENDT, K. S., YOSHIDA, K., ITOH, T., BANDO, M., KOCH, B., SCHIRGHUBER, E., TSUTSUMI, S., NAGAE, G., ISHIHARA, K., MISHIRO, T., YAHATA, K.,

IMAMOTO, F., ABURATANI, H., NAKAO, M., IMAMOTO, N., MAESHIMA, K., SHIRAHIGE, K. & PETERS, J. M. 2008. Cohesin mediates transcriptional insulation by CCCTC-binding factor. *Nature,* 451**,** 796-801.

WHEATLEY, S. P., HINCHCLIFFE, E. H., GLOTZER, M., HYMAN, A. A., SLUDER, G. & WANG, Y. 1997. CDK1 inactivation regulates anaphase spindle dynamics and cytokinesis in vivo. *J Cell Biol,* 138**,** 385-93.

WILL, C. L. & LUHRMANN, R. 2011. Spliceosome structure and function. *Cold Spring Harb Perspect Biol,* 3.

WILLIAMS, B. C., GARRETT-ENGELE, C. M., LI, Z., WILLIAMS, E. V., ROSENMAN, E. D. & GOLDBERG, M. L. 2003. Two putative acetyltransferases, san and deco, are required for establishing sister chromatid cohesion in Drosophila. *Curr Biol,* 13**,** 2025-36.

WINER, J., JUNG, C. K., SHACKEL, I. & WILLIAMS, P. M. 1999. Development and validation of real-time quantitative reverse transcriptase-polymerase chain reaction for monitoring gene expression in cardiac myocytes in vitro. *Anal Biochem,* 270**,** 41-9.

WINKLER, C., EGGERT, C., GRADL, D., MEISTER, G., GIEGERICH, M., WEDLICH, D., LAGGERBAUER, B. & FISCHER, U. 2005. Reduced U snRNP assembly causes motor axon degeneration in an animal model for spinal muscular atrophy. *Genes Dev,* 19**,** 2320-30.

WOLSTENHOLME, J. & ANGELL, R. R. 2000. Maternal age and trisomy--a unifying mechanism of formation. *Chromosoma,* 109**,** 435-8.

WU, F. M., NGUYEN, J. V. & RANKIN, S. 2011. A conserved motif at the C terminus of sororin is required for sister chromatid cohesion. *J Biol Chem,* 286**,** 3579-86.

WU, J. Q., GUO, J. Y., TANG, W., YANG, C. S., FREEL, C. D., CHEN, C., NAIRN, A. C. & KORNBLUTH, S. 2009. PP1-mediated dephosphorylation of phosphoproteins at mitotic exit is controlled by inhibitor-1 and PP1 phosphorylation. *Nat Cell Biol,* 11**,** 644-51.

WURZENBERGER, C. & GERLICH, D. W. 2011. Phosphatases: providing safe passage through mitotic exit. *Nat Rev Mol Cell Biol,* 12**,** 469-82.

XIAO, X., WANG, Z., JANG, M. & BURGE, C. B. 2007. Coevolutionary networks of splicing cis-regulatory elements. *Proc Natl Acad Sci U S A,* 104**,** 18583-8.

XIONG, B., LU, S. & GERTON, J. L. 2010. Hos1 is a lysine deacetylase for the Smc3 subunit of cohesin. *Curr Biol,* 20**,** 1660-5.

XU, H., BEASLEY, M. D., WARREN, W. D., VAN DER HORST, G. T. & MCKAY, M. J. 2005. Absence of mouse REC8 cohesin promotes synapsis of sister chromatids in meiosis. *Dev Cell,* 8**,** 949-61.

YAMAZAKI, T., FUJIWARA, N., YUKINAGA, H., EBISUYA, M., SHIKI, T., KURIHARA, T., KIOKA, N., KAMBE, T., NAGAO, M., NISHIDA, E. & MASUDA, S. 2010. The closely related RNA helicases, UAP56 and URH49, preferentially form distinct mRNA export machineries and coordinately regulate mitotic progression. *Mol Biol Cell,* 21**,** 2953-65.

YOSHIDA, K., SANADA, M., SHIRAISHI, Y., NOWAK, D., NAGATA, Y., YAMAMOTO, R., SATO, Y., SATO-OTSUBO, A., KON, A., NAGASAKI, M., CHALKIDIS, G., SUZUKI, Y., SHIOSAKA, M., KAWAHATA, R., YAMAGUCHI, T., OTSU, M., OBARA, N., SAKATA-YANAGIMOTO, M., ISHIYAMA, K., MORI, H., NOLTE, F., HOFMANN, W. K., MIYAWAKI, S., SUGANO, S., HAFERLACH, C., KOEFFLER, H. P., SHIH, L. Y., HAFERLACH, T., CHIBA, S., NAKAUCHI, H., MIYANO, S. & OGAWA, S. 2011. Frequent pathway mutations of splicing machinery in myelodysplasia. *Nature,* 478**,** 64-9.

ZACHARIAE, W., SCHWAB, M., NASMYTH, K. & SEUFERT, W. 1998. Control of cyclin ubiquitination by CDK-regulated binding of Hct1 to the anaphase promoting complex. *Science,* 282**,** 1721-4.

ZACHARIAS, H. 2001. Key word: chromosome. *Chromosome Res,* 9**,** 345-55.
ZENG, K., BASTOS, R. N., BARR, F. A. & GRUNEBERG, U. 2010. Protein phosphatase 6 regulates mitotic spindle formation by controlling the T-loop phosphorylation state of Aurora A bound to its activator TPX2. *J Cell Biol,* 191**,** 1315-32.
ZHANG, J., SHI, X., LI, Y., KIM, B. J., JIA, J., HUANG, Z., YANG, T., FU, X., JUNG, S. Y., WANG, Y., ZHANG, P., KIM, S. T., PAN, X. & QIN, J. 2008a. Acetylation of Smc3 by Eco1 is required for S phase sister chromatid cohesion in both human and yeast. *Mol Cell,* 31**,** 143-51.
ZHANG, N., GE, G., MEYER, R., SETHI, S., BASU, D., PRADHAN, S., ZHAO, Y. J., LI, X. N., CAI, W. W., EL-NAGGAR, A. K., BALADANDAYUTHAPANI, V., KITTRELL, F. S., RAO, P. H., MEDINA, D. & PATI, D. 2008b. Overexpression of Separase induces aneuploidy and mammary tumorigenesis. *Proc Natl Acad Sci U S A,* 105**,** 13033-8.
ZHANG, N., PANIGRAHI, A. K., MAO, Q. & PATI, D. 2011. Interaction of Sororin protein with polo-like kinase 1 mediates resolution of chromosomal arm cohesion. *J Biol Chem,* 286**,** 41826-37.
ZHANG, N. & PATI, D. 2012. Sororin is a master regulator of sister chromatid cohesion and separation. *Cell Cycle,* 11**,** 2073-83.
ZHAO, W. M. 2006. Cep55, a Microtubule-bundling Protein, Associates with Centralspindlin to Control the Midbody Integrity and Cell Abscission during Cytokinesis. *Molecular Biology of the Cell,* 17**,** 3881-3896.
ZHAO, W. M., SEKI, A. & FANG, G. 2006. Cep55, a microtubule-bundling protein, associates with centralspindlin to control the midbody integrity and cell abscission during cytokinesis. *Mol Biol Cell,* 17**,** 3881-96.
ZHOU, Z., LICKLIDER, L. J., GYGI, S. P. & REED, R. 2002. Comprehensive proteomic analysis of the human spliceosome. *Nature,* 419**,** 182-5.

Appendix

The full list of candidate genes, the details of the Dharmacon siRNA smartpools used to target them and the percentage nuclear abnormalities that the siRNA duplexes elicit in cells is shown in the table below.

Plate	Well	Pool Catalog Number	Gene Symbol	GENE ID	Gene Accession	% nuclear abnormalities
Plate 1	A04	M-015921-01	ABC1	63897	NM_022070	3.06
Plate 1	A05	M-011320-01	ABLIM1	3983	NM_006720	2.96
Plate 1	A06	M-013586-01	ABTB1	80325	NM_172028	5.42
Plate 8	A03	M-009002-00	ACAD9	28976	NM_014049	8.90
Plate 8	A06	M-004929-02	ACVR1C	130399	NM_001111033	14.20
Plate 8	G08	M-013315-01	AD-017	55830	NM_152932	9.12
Plate 1	A09	M-005757-01	ADAM19	8728	NM_023038	10.00
Plate 1	A10	M-004525-00	ADAM33	80332	NM_025220	10.03
Plate 2	A04	M-015673-01	AF15Q14	57082	NM_144508	24.50
Plate 8	A07	M-008696-00	AGXT2L1	64850	NM_031279	6.01
Plate 1	A12	M-010232-00	AKAP12	9590	NM_005100	41.00
Plate 1	B03	M-011954-02	AKAP5	9495	NM_004857	3.13
Plate 1	B04	M-004041-02	AKR1C4	1109	NM_001818	8.04
Plate 1	B05	M-003002-02	AKT3	10000	NM_005465	5.04
Plate 1	B06	M-008379-02	ALDH9A1	223	NM_000696	6.12
Plate 8	A08	M-009026-01	ALOX15B	247	NM_001141	6.70
Plate 1	B08	M-010174-01	AMPD3	272	NM_001025389	4.25
Plate 9	F08	M-011206-01	ANG	283	NM_001097577	11.28
Plate 1	B09	M-008417-02	ANK2	287	NM_020977	5.08
Plate 1	B11	M-013755-00	ANKRD2	26287	NM_020349	8.00
Plate 1	B12	M-016466-00	ANKRD5	63926	NM_022096	4.31
Plate 1	C03	M-020957-01	ANKRD7	56311	NM_019644	1.85
Plate 8	A09	M-006838-03	ANLN	54443	NM_018685	**82.92**
Plate 1	G12	M-006838-03	ANLN	54443	NM_018685	**88.50**
Plate 1	C04	M-011212-00	ANXA11	311	NM_001157	6.48
Plate 1	C05	M-011209-01	ANXA5	308	NM_001154	4.77
Plate 1	C06	M-011210-01	ANXA6	309	NM_004033	13.24
Plate 1	C07	M-010760-01	ANXA7	310	NM_001156	16.52
Plate 1	C08	M-019183-01	AP1G1	164	NM_001128	1.82
Plate 1	C09	M-008170-01	AP2M1	1173	NM_001025205	2.78
Plate 1	C10	M-008335-01	ARHGAP17	55114	NM_018054	5.21
Plate 8	A10	M-010360-00	ARHGEF11	9826	NM_014784	17.24
Plate 8	A11	M-012083-01	ARL4A	10124	NM_212460	24.13
Plate 8	A12	M-012408-01	ARL5	26225	NM_177985	22.64
Plate 8	A04	M-020372-01	ARP3BETA	57180	NM_001040135	9.27
Plate 8	B03	M-012081-00	ARPC2	10109	NM_005731	4.20
Plate 8	A05	M-019043-01	ARPM2	140625	NM_080431	10.97
Plate 8	B04	M-013180-00	ASB12	142689	NM_130388	3.85
Plate 3	C11	M-016064-01	ASPRV1	151516	NM_152792	10.77

Plate 1	D03	M-003326-08	AURKB	9212	NM_004217	**74.49**
Plate 10	A10	M-003326-08	AURKB	9212	NM_004217	**78.53**
Plate 9	C11	M-003326-08	AURKB	9212	NM_004217	**80.97**
Plate 1	D04	M-005432-00	AVPR2	554	NM_000054	5.16
Plate 8	B05	M-019319-01	B3GTL	145173	NM_194318	8.96
Plate 1	A08	M-008243-02	BAF53A	86	NM_177989	11.53
Plate 1	D06	M-003873-02	BARD1	580	NM_000465	8.71
Plate 1	D09	M-020487-01	BAZ2B	29994	NM_013450	6.36
Plate 10	A06	M-013536-00	BBP	83941	NM_032027	5.94
Plate 8	B06	M-012708-00	BCAS2	10286	NM_005872	11.71
Plate 1	D10	M-004386-01	BFAR	51283	NM_016561	3.99
Plate 1	D12	M-011219-01	BMP2	650	NM_001200	10.47
Plate 1	E03	M-004933-04	BMPR1A	657	NM_004329	3.93
Plate 8	B07	M-015957-00	BTBD14A	138151	NM_144653	6.80
Plate 1	E04	M-019161-01	BTN3A2	11118	NM_007047	5.81
Plate 1	E08	M-014732-00	C10ORF45	83641	NM_031453	6.81
Plate 1	E09	M-018851-02	C10ORF53	282966	NM_001042427	5.94
Plate 10	A03	M-013900-02	C10ORF61	26123	NM_015631	6.59
Plate 1	E10	M-014035-01	C11ORF24	53838	NM_022338	2.80
Plate 10	C05	M-017741-00	C13ORF22	10208	NM_005800	15.71
Plate 1	E12	M-012952-01	C13ORF23	80209	NM_170719	8.86
Plate 7	E11	M-015254-01	C14ORF150	112840	NM_080666	21.24
Plate 8	B11	M-007044-00	C14ORF4	64207	NM_024496	10.00
Plate 1	F03	M-018521-01	C14ORF54	161142	NM_173526	3.79
Plate 1	F04	M-020807-00	C14ORF94	54930	NM_017815	15.48
Plate 1	F05	M-015917-01	C18ORF24	220134	NM_145060	21.71
Plate 8	B12	M-023865-01	C19ORF7	23211	NM_015168	6.83
Plate 8	C03	M-020490-00	C1GALT1	56913	NM_020156	8.17
Plate 8	C06	M-033644-00	C1orf178	440603	NM_001010922	6.67
Plate 1	F10	M-017146-01	C1QTNF2	114898	NM_031908	9.84
Plate 1	F11	M-013787-01	C20ORF77	58490	NM_021215	14.20
Plate 2	G10	M-019909-00	C21ORF5	9980	NM_005128	5.35
Plate 1	F12	M-020812-01	C21ORF91	54149	NM_001100421	11.91
Plate 1	G03	M-018422-01	C2ORF17	79137	NM_024293	4.26
Plate 1	G04	M-013862-00	C2ORF25	27249	NM_015702	5.25
Plate 1	G05	M-010273-01	C3F	10162	NM_005768	11.99
Plate 1	G07	M-011122-01	C4B	721	NM_001002029	3.82
Plate 1	G08	M-025105-01	C6ORF110	55362	NM_018426	4.14
Plate 1	G09	M-027225-01	C6ORF167	253714	NM_198468	13.24
Plate 1	G10	M-015508-01	C6ORF51	112495	NM_138408	14.90
Plate 6	C06	M-016343-00	C8ORF20	80346	NM_025232	7.91
Plate 10	C09	M-016561-01	C9ORF112	92715	NM_138778	6.19
Plate 1	H03	M-014311-01	C9ORF16	79095	NM_024112	12.75
Plate 1	H05	M-003634-01	CA12	771	NM_001218	3.32
Plate 1	H06	M-018982-00	CABP7	164633	NM_182527	4.13
Plate 1	H07	M-012519-01	CACNG4	27092	NM_014405	46.71
Plate 1	H09	M-008197-01	CALR	811	NM_004343	8.29
Plate 1	H10	M-004940-00	CAMK1	8536	NM_003656	6.07
Plate 1	H11	M-004943-04	CAMK2B	816	NM_172084	34.56

Plate 2	A03	M-003636-03	CANX	821	NM_001024649	8.06
Plate 8	C10	M-012212-01	CAPZA1	829	NM_006135	8.67
Plate 5	B12	M-004398-00	CARD4	10392	NM_006092	13.11
Plate 2	A05	M-003465-03	CASP2	835	NM_032983	5.73
Plate 8	C11	M-009561-02	CBX7	23492	NM_175709	13.23
Plate 2	A07	M-014775-01	CCDC8	83987	NM_032040	12.78
Plate 8	C12	M-020279-00	CCDC9	26093	NM_015603	8.92
Plate 2	A12	M-020147-00	CCT4	10575	NM_006430	4.65
Plate 9	C06	M-004687-02	CDC2L1	984	NM_033487	26.84
Plate 2	B03	M-011237-00	CDC5L	988	NM_001253	32.11
Plate 2	B04	M-003233-03	CDC6	990	NM_001254	10.60
Plate 2	B05	M-003238-02	CDK4	1019	NM_000075	3.18
Plate 2	B06	M-003242-02	CDK8	1024	NM_001260	4.97
Plate 2	B07	M-004797-01	CDKL2	8999	NM_003948	3.96
Plate 2	B08	M-004799-03	CDKL5	6792	NM_001037343	6.29
Plate 2	B09	M-003248-01	CDT1	81620	NM_030928	12.57
Plate 2	B10	M-008755-01	CDYL2	124359	NM_152342	5.75
Plate 2	B11	M-003252-02	CENPE	1062	NM_001813	19.24
Plate 2	C04	M-032250-01	CEP192	55125	NM_032142	17.57
Plate 2	C03	M-006893-01	**CEP55**	55165	NM_018131	**86.13**
Plate 7	F10	M-020317-00	CGI-127	51646	NM_016061	6.60
Plate 6	E03	M-020992-01	CGI-49	51097	NM_016002	6.56
Plate 3	B11	M-021013-01	CGI-90	51115	NM_016033	6.69
Plate 7	D11	M-021018-01	CGI-94	51118	NM_016037	7.84
Plate 2	C05	M-015779-01	CHRDL1	91851	NM_145234	8.01
Plate 8	D04	M-006139-01	CHRNA5	1138	NM_000745	9.55
Plate 8	D05	M-004613-00	CIT	11113	NM_007174	**86.90**
Plate 4	A07	M-004613-00	CIT	11113	NM_007174	**93.98**
Plate 8	D06	M-017099-02	CKAP2	26586	NM_018204	15.71
Plate 2	C06	M-006847-02	CKAP5	9793	NM_014756	**78.43**
Plate 2	C07	M-007678-00	CKS2	1164	NM_001827	6.85
Plate 2	C08	M-006831-01	CLASP1	23332	NM_015282	3.40
Plate 2	C09	M-006157-02	CLCNKB	1188	NM_000085	17.63
Plate 2	C10	M-012294-01	CLDN16	10686	NM_006580	8.79
Plate 2	C12	M-004800-01	CLK1	1195	NM_004071	8.90
Plate 8	D11	M-007856-00	CNTFR	1271	NM_001842	6.19
Plate 2	D03	M-009725-01	CNTNAP1	8506	NM_003632	7.50
Plate 2	D04	M-015904-00	COG7	91949	NM_153603	5.12
Plate 2	D05	M-011009-01	COL10A1	1300	NM_000493	7.37
Plate 2	D06	M-011835-01	COPA	1314	NM_004371	11.88
Plate 2	D09	M-017940-00	COPB	1315	NM_016451	11.90
Plate 2	D10	M-010493-01	CORO1B	57175	NM_001018070	22.68
Plate 8	D12	M-017331-00	CORO1C	23603	NM_014325	41.25
Plate 2	D11	M-013104-00	COTL1	23406	NM_021149	14.06
Plate 2	D12	M-013179-00	COX7A2L	9167	NM_004718	4.67
Plate 8	E03	M-005819-02	CPA5	93979	NM_080385	3.10
Plate 2	E03	M-008754-00	CRABP1	1381	NM_004378	7.44
Plate 8	E04	M-004412-01	CRADD	8738	NM_003805	6.30
Plate 2	E04	M-019757-01	CRISP2	7180	NM_003296	4.28

Plate 2	E05	M-017044-02	CRYGN	155051	NM_144727	8.07
Plate 2	E06	M-003110-02	CSK	1445	NM_004383	4.36
Plate 2	E07	M-019940-02	CSN3	1448	NM_005212	9.88
Plate 2	E08	M-007679-00	CSNK2B	1460	NM_001320	11.85
Plate 2	E09	M-020003-01	CTDSPL	10217	NM_005808	14.15
Plate 2	E10	M-016267-02	CTLA4	1493	NM_001037631	7.74
Plate 2	E11	M-017535-00	CTNNBL1	56259	NM_030877	10.43
Plate 2	E12	M-012572-01	CTNND1	1500	NM_001085469	19.23
Plate 8	E05	M-005833-01	CTRC	11330	NM_007272	3.72
Plate 8	E06	M-005834-00	CTRL	1506	NM_001907	5.23
Plate 2	F03	M-004086-01	CUL1	8454	NM_003592	48.39
Plate 6	A10	M-015828-01	CX40.1	219770	NM_153368	8.00
Plate 2	F05	M-016697-01	CYC1	1537	NM_001916	16.67
Plate 8	E07	M-008736-00	CYP2C19	1557	NM_000769	7.67
Plate 2	F07	M-011841-01	DBN1	1627	NM_004395	8.02
Plate 2	F09	M-004269-02	DCLRE1C	64421	NM_022487	7.06
Plate 2	F10	M-012874-00	DCTN1	1639	NM_004082	5.10
Plate 2	F11	M-012218-00	DCTN2	10540	NM_006400	3.81
Plate 8	E08	M-010397-01	DDX24	57062	NM_020414	4.64
Plate 2	F12	M-009333-00	DGAT2	84649	NM_032564	21.05
Plate 8	E10	M-006717-01	DGKI	9162	NM_004717	4.13
Plate 8	E11	M-006670-01	DHPS	1725	NM_013407	23.44
Plate 2	G03	M-010506-02	DHX8	1659	NM_004941	21.19
Plate 2	A10	M-014708-01	DKFZP434K1172	83446	NM_031290	9.14
Plate 2	A06	M-019301-02	DKFZP434O0527	255101	NM_152389	7.69
Plate 2	G04	M-014787-00	DKFZP434P0316	84074	NM_032134	6.27
Plate 3	A08	M-013812-01	DKFZP547C176	55531	NM_018712	7.03
Plate 2	G05	M-020539-01	DKFZP564C186	26155	NM_015658	7.44
Plate 10	D09	M-019325-00	DKFZP686L1814	132660	NM_194282	16.23
Plate 4	E06	M-019325-00	DKFZP686L1814	132660	NM_194282	23.72
Plate 7	G11	M-016535-01	DKFZP761B128	144348	NM_152437	9.35
Plate 1	C11	M-017365-00	DKFZP761H079	200894	NM_144996	5.65
Plate 4	G08	M-018560-01	DKFZP761N1114	148808	NM_181644	63.33
Plate 8	E12	M-015059-01	DMRTC1	63947	NM_033053	5.98
Plate 2	G06	M-005281-02	DNCL1	8655	NM_003746	8.81
Plate 2	G07	M-012092-01	DNM1L	10059	NM_005690	8.64
Plate 2	G08	M-019915-00	DOCK2	1794	NM_004946	4.53
Plate 2	G09	M-014040-00	DOCK9	23348	NM_015296	6.01
Plate 2	G11	M-008343-00	DPEP3	64180	NM_022357	36.14
Plate 2	G12	M-005477-01	DRD1	1812	NM_000794	6.80
Plate 9	F03	M-020467-02	DSCR1L2	11123	NM_013441	3.56
Plate 2	H04	M-007892-01	DUSP19	142679	NM_080876	1.96
Plate 2	H05	M-003568-01	DUSP8	1850	NM_004420	12.66

Plate 2	H06	M-006828-02	DYNC1H1	1778	NM_001376	3.65
Plate 2	H07	M-004730-03	DYRK2	8445	NM_003583	5.92
Plate 7	B07	M-011023-01	DYT1	1861	NM_000113	10.30
Plate 2	H08	M-006450-00	ECT2	1894	NM_018098	**99.34**
		M-006450-00	ECT2	1894	NM_018098	**99.34**
Plate 2	H11	M-004012-02	EEA1	8411	NM_003566	7.42
Plate 8	F04	M-015668-00	EGFL7	51162	NM_016215	4.81
Plate 3	A03	M-004276-02	EGLN1	54583	NM_022051	5.36
Plate 3	A04	M-004277-00	EGLN2	112398	NM_053046	9.78
Plate 3	A05	M-019022-02	EHD1	10938	NM_006795	4.19
Plate 3	A06	M-004883-03	EIF2AK3	9451	NM_004836	5.79
Plate 8	F05	M-005864-02	ELA3B	23436	NM_007352	5.56
Plate 3	A07	M-015640-02	ELAC2	60528	NM_018127	9.46
Plate 3	A09	M-021932-02	ENAH	55740	NM_018212	2.57
Plate 8	D03	M-008893-01	ENC1	8507	NM_003633	4.10
Plate 3	A10	M-009805-01	ENPP5	59084	NM_021572	9.17
Plate 9	A12	M-010663-01	EPLIN	51474	NM_016357	3.29
Plate 3	A11	M-012670-01	ERH	2079	NM_004450	5.69
Plate 4	F09	M-004807-02	ERK8	225689	NM_139021	5.16
Plate 3	B04	M-005491-01	F2RL2	2151	NM_004101	3.50
Plate 7	A12	M-014908-00	FAM11A	84548	NM_032508	14.15
Plate 3	B09	M-020870-00	FAM38A	9780	NM_014745	21.24
Plate 3	B12	M-011033-01	FANCC	2176	NM_000136	6.29
Plate 8	F08	M-013991-01	FANCE	2178	NM_021922	12.06
Plate 8	F09	M-015068-01	FATE1	89885	NM_033085	10.09
Plate 8	F10	M-017621-00	FBLN5	10516	NM_006329	9.02
Plate 3	C04	M-012423-02	FBXL3P	26223	NM_012159	7.09
Plate 7	H10		FBXO5			94.77
Plate 5	A05	M-013584-01	FER1L3	26509	NM_133337	17.63
Plate 8	F12	M-013145-01	FGF12	2257	NM_021032	10.86
Plate 3	C06	M-003132-04	FGFR2	2263	NM_000141	4.29
Plate 8	G03	M-009426-01	FKBP6	8468	NM_003602	5.02
Plate 3	C07	M-018143-01	FLJ10276	55108	NM_018045	5.45
Plate 6	G10	M-018144-00	FLJ10379	55133	NM_018079	11.94
Plate 3	C03	M-022320-01	FLJ10719	55215	NM_018193	3.61
Plate 9	E12	M-020984-00	FLJ11016	55285	NM_018301	2.33
Plate 6	C12	M-021241-01	FLJ11164	55316	NM_018346	5.59
Plate 1	G11	M-021056-00	FLJ11267	56260	NM_019607	3.19
Plate 4	G04	M-008447-02	FLJ12847	79648	NM_024596	5.00
Plate 2	B12	M-014577-02	FLJ13111	80152	NM_025082	11.66
Plate 7	G12	M-014417-01	FLJ13841	79755	NM_024702	18.73
Plate 5	D06	M-018156-00	FLJ14001	79730	NM_024677	5.61
Plate 3	B08	M-015007-00	FLJ14668	84908	NM_032822	13.86
Plate 7	B11	M-009655-02	FLJ20244	55621	NM_017722	17.30
Plate 1	H04	M-020707-01	FLJ20245	54863	NM_017723	14.97
Plate 3	C08	M-018096-01	FLJ20397	54919	NM_017802	6.36
Plate 8	C04	M-020836-01	FLJ20508	54955	NM_017850	7.36
Plate 3	B06	M-014365-01	FLJ21103	79607	NM_024556	7.19

Plate 3	C09	M-016327-00	FLJ22318	64777	NM_022762	5.20
Plate 6	F03	M-005321-00	FLJ23356	84197	NM_032237	12.35
Plate 3	C10	M-018406-00	FLJ23657	152816	NM_178497	5.35
Plate 2	F04	M-017083-00	FLJ25444	254158	NM_152761	22.63
Plate 10	D03	M-016739-00	FLJ25476	149076	NM_152493	8.98
Plate 8	B10	M-018954-01	FLJ25773	283598	NM_182560	26.69
Plate 1	A11	M-008134-00	FLJ30473	150209	NM_144704	13.00
Plate 3	G11	M-015913-01	FLJ30678	139324	NM_144657	5.42
Plate 10	C12	M-016831-01	FLJ30726	124961	NM_153018	8.23
Plate 10	D06	M-007122-01	FLJ31295	121274	NM_152320	5.66
Plate 3	E09	M-015840-01	FLJ31978	144423	NM_144669	5.66
Plate 1	E05	M-017181-00	FLJ32001	163882	NM_152609	7.40
Plate 5	B04	M-004052-02	FLJ32685	152110	NM_152534	3.95
Plate 1	F08	M-019223-01	FLJ32940	126859	NM_182766	6.99
Plate 3	C12	M-016597-00	FLJ33008	145748	NM_152449	5.85
Plate 2	A08	M-016956-01	FLJ33084	149483	NM_152500	20.76
Plate 4	D05	M-017970-01	FLJ33207	339855	NM_178554	7.95
Plate 10	C08	M-016825-01	FLJ33817	124997	NM_152348	8.50
Plate 8	C08	M-015548-00	FLJ35725	152992	NM_152544	12.74
Plate 5	C08	M-016639-00	FLJ35773	162387	NM_152599	2.35
Plate 3	B10	M-016939-00	FLJ35782	170062	NM_152631	5.60
Plate 8	H08	M-018861-00	FLJ35834	154865	NM_178827	4.62
Plate 2	A11	M-015467-00	FLJ38159	220388	NM_152723	8.04
Plate 1	B10	M-016498-01	FLJ38335	162282	NM_153228	15.88
Plate 1	F07	M-027230-01	FLJ41131	284325	NM_198476	16.45
Plate 1	F06	M-027257-01	FLJ45778	374872	NM_198532	6.11
Plate 3	D04	M-010636-00	FLOT1	10211	NM_005803	5.18
Plate 8	G04	M-004110-00	FOSL2	2355	NM_005253	6.25
Plate 2	F06	M-005498-02	FY	2532	NM_002036	7.50
Plate 8	G05	M-003962-01	FZD8	8325	NM_031866	10.23
Plate 3	D05	M-006178-01	GABRR1	2569	NM_002042	10.93
Plate 7	F06	M-017496-02	GAGED3	9502	NM_130777	11.21
Plate 3	D06	M-014197-00	GALNT5	11227	NM_014568	6.38
Plate 3	D09	M-004141-01	GALR3	8484	NM_003614	4.60
Plate 3	D10	M-011665-00	GAS1	2619	NM_002048	7.30
Plate 7	F09	M-005280-00	GAS41	8089	NM_006530	7.89
Plate 8	G06	M-012040-01	GDF9	2661	NM_005260	8.64
Plate 3	D11	M-011286-01	GDI1	2664	NM_001493	4.25
Plate 3	D12	M-008717-00	GEM	2669	NM_005261	6.89
Plate 3	E03	M-013342-01	GIMAP5	55340	NM_018384	6.94
Plate 3	E04	M-019997-02	GIPC1	10755	NM_202494	6.85
Plate 3	E05	M-017368-01	GJA5	2702	NM_181703	11.00
Plate 8	G07	M-017887-01	GJB1	2705	NM_001097642	12.74
Plate 3	E06	M-019948-02	GJB3	2707	NM_001005752	3.79
Plate 3	E07	M-018750-00	GJE1	349149	NM_181538	7.83
Plate 3	E08	M-012634-01	GLRX	2745	NM_002064	2.83
Plate 3	E10	M-008561-00	GNA14	9630	NM_004297	8.43
Plate 3	E11	M-003897-00	GNAI2	2771	NM_002070	6.30
Plate 3	E12	M-010825-02	GNAS	2778	NM_001077488	3.83

Plate 3	F03	M-017241-00	GNB2	2783	NM_005273	7.26
Plate 3	F04	M-006876-01	GNB2L1	10399	NM_006098	10.90
Plate 3	F05	M-012699-01	GNG5	2787	NM_005274	4.53
Plate 3	F06	M-006413-01	GOLPH3L	55204	NM_018178	4.94
Plate 3	F07	M-013510-00	GORASP1	64689	NM_031899	3.42
Plate 3	F08	M-019045-01	GORASP2	26003	NM_015530	5.50
Plate 3	F09	M-010980-02	GOSR2	9570	NM_054022	6.43
Plate 3	F10	M-016826-00	GPATC1	55094	NM_018025	4.89
Plate 3	F11	M-005553-01	GPR19	2842	NM_006143	27.43
Plate 3	C05	M-005572-00	GPR41	2865	NM_005304	5.39
Plate 3	F12	M-005581-02	GPR55	9290	NM_005683	5.88
Plate 3	G03	M-005591-02	GPR68	8111	NM_003485	8.96
Plate 3	G05	M-009445-01	GPX5	2880	NM_003996	5.59
Plate 3	G06	M-004626-01	GRK5	2869	NM_005308	5.75
Plate 8	G09	M-017321-01	GTPBP1	9567	NM_004286	5.23
Plate 3	G07	M-006733-00	GUCY1B3	2983	NM_000857	17.81
Plate 8	G10	M-005888-02	GZMA	3001	NM_006144	8.24
Plate 3	G08	M-016696-00	HAVCR2	84868	NM_032782	7.57
Plate 3	G09	M-012168-01	HAX1	10456	NM_001018837	7.67
Plate 9	A06	M-007025-00	HCA127	55906	NM_018684	12.91
Plate 3	G10	M-019953-01	HCFC1	3054	NM_005334	4.34
Plate 6	D11	M-016834-01	HCNGP	29115	NM_013260	17.45
Plate 3	G12	M-011049-01	HEXA	3073	NM_000520	5.62
Plate 3	H03	M-013018-00	HHIP	64399	NM_022475	6.62
Plate 6	B08	M-021212-02	HHL	9910	NM_001035230	7.37
Plate 2	F08	M-016867-01	HIP-55	28988	NM_001014436	14.88
Plate 3	H04	M-009431-01	HIP2	3093	NM_001111113	7.10
Plate 3	H06	M-013126-00	HIST1H2AJ	8331	NM_021066	7.21
Plate 3	H07	M-019163-02	HIST3H2A	92815	NM_033445	4.00
Plate 8	G11	M-013228-02	HLA-DQA1	3117	NM_002122	9.87
Plate 5	D04	M-008848-00	HMP19	51617	NM_015980	23.99
Plate 8	G12	M-008488-01	HNMT	3176	NM_001024074	7.45
Plate 3	H08	M-016845-01	HOOK1	51361	NM_015888	7.93
Plate 3	H09	M-012911-00	HOXD1	3231	NM_024501	9.88
Plate 3	H10	M-020867-01	HP1-BP74	50809	NM_016287	7.74
Plate 6	A03	M-010102-01	HRMT1L2	3276	NM_198318	12.01
Plate 6	A05	M-007773-00	HRMT1L6	55170	NM_018137	5.37
Plate 3	H11	M-008140-02	HSD17B7	51478	NM_016371	8.55
Plate 3	H12	M-021084-01	HSPA14	51182	NM_016299	4.40
Plate 4	A03	M-008198-02	HSPA5	3309	NM_005347	7.76
Plate 8	H03	M-004287-01	HSPBAP1	79663	NM_024610	11.88
Plate 2	A09	M-020558-01	HSPC009	28958	NM_001040431	6.85
Plate 4	H12	M-021196-01	HSPC242	51537	NM_001003704	5.80
Plate 1	E07	M-017892-00	HT021	57415	NM_020685	7.72
Plate 4	A04	M-016762-01	HTF9C	27037	NM_182984	14.24
Plate 8	H04	M-005642-03	HTR5A	3361	NM_024012	12.99
Plate 4	A05	M-012014-00	IBSP	3381	NM_004967	6.56
Plate 4	A06	M-013217-01	IFNK	56832	NM_020124	14.61
Plate 8	H05	M-012638-00	IFNW1	3467	NM_002177	4.89

Plate 8	H06	M-012190-01	IK	3550	NM_006083	12.89
Plate 7	H11		IKIP			10.26
Plate 8	H07	M-007990-01	IL4R	3566	NM_001008699	6.75
Plate 4	A08	M-006823-01	INCENP	3619	NM_020238	**97.40**
Plate 8	H09	M-006823-01	INCENP	3619	NM_020238	**97.92**
Plate 4	A09	M-011701-02	INHBA	3624	NM_002192	5.47
Plate 4	A10	M-003302-01	IRAK4	51135	NM_016123	3.70
Plate 4	A11	M-004506-00	ITGB1	3688	NM_002211	6.52
Plate 4	A12	M-009841-00	ITSN2	50618	NM_006277	18.24
Plate 8	H10	M-017187-00	JAG2	3714	NM_002226	5.52
Plate 4	B03	M-003145-02	JAK1	3716	NM_002227	7.89
Plate 4	B04	M-011708-00	JUP	3728	NM_002230	13.21
Plate 7	H12		KALRN			6.73
Plate 8	H11	M-008846-01	KCNAB3	9196	NM_004732	5.30
Plate 8	H12	M-006251-00	KCNJ6	3763	NM_002240	7.40
Plate 4	B06	M-009140-01	KCNK18	338567	NM_181840	8.18
Plate 9	A03	M-006264-01	KCNK5	8645	NM_003740	8.28
Plate 4	B07	M-006265-00	KCNK6	9424	NM_004823	8.50
Plate 4	B08	M-004461-01	KCNN4	3783	NM_002250	4.73
Plate 4	B09	M-027333-00	KCNT2	343450	NM_198503	4.04
Plate 9	A04	M-017862-00	KCTD13	253980	NM_178863	5.66
Plate 4	B10	M-021199-01	KCTD5	54442	NM_018992	15.99
Plate 4	B11	M-012453-00	KEAP1	9817	NM_012289	13.91
Plate 7	C05	M-014094-01	KIAA0153	23170	NM_015140	14.01
Plate 4	B12	M-022485-01	KIAA0350	23274	NM_015226	19.38
Plate 4	C03	M-026188-01	KIAA0368	23392	NM_001080398	10.71
Plate 3	H05	M-004786-00	KIAA0377	9677	NM_014659	10.70
Plate 7	F12	M-006919-01	KIAA0478	9923	NM_014870	24.16
Plate 9	A05	M-021259-00	KIAA0649	9858	NM_014811	10.29
Plate 4	C04	M-025319-01	KIAA0895	23366	NM_001100425	7.30
Plate 1	B07	M-021515-01	KIAA1163	57463	NM_020703	6.69
Plate 5	E10	M-023583-02	KIAA1268	54625	NM_017554	6.65
Plate 1	D05	M-023331-01	KIAA1447	57597	NM_001080519	7.42
Plate 3	G04	M-015158-01	KIAA1893	114787	NM_052899	8.76
Plate 4	C05	M-008252-01	KIF12	113220	NM_138424	13.49
Plate 9	A09	M-004959-02	KIF2	3796	NM_004520	7.84
Plate 9	A08	M-004957-01	KIF20A	10112	NM_005733	**99.38**
Plate 4	C06	M-004957-01	KIF20A	10112	NM_005733	**99.39**
Plate 4	C07	M-004962-00	KIF22	3835	NM_007317	6.07
Plate 10	D10	M-004956-01	KIF23	9493	NM_004856	**98.10**
Plate 4	C08	M-004956-01	KIF23	9493	NM_004856	**100.00**
Plate 4	C09	M-004955-01	KIF2C	11004	NM_006845	14.58
Plate 4	C10	M-008867-00	KIF5B	3799	NM_004521	7.88
Plate 4	C11	M-004958-02	KIFC1	3833	NM_002263	18.01
Plate 4	C12	M-008338-02	KIFC3	3801	NM_005550	13.29
Plate 4	D03	M-014218-02	KLC2	64837	NM_022822	5.71
Plate 4	D04	M-005906-01	KLK1	3816	NM_002257	4.64
Plate 9	A10	M-018761-01	KRT25D	162605	NM_181535	4.30
Plate 4	D06	M-017231-00	LAD1	3898	NM_005558	9.66

Plate 7	B08	M-013913-00	LAP1B	26092	NM_015602	5.66
Plate 4	D10	M-019015-00	LCE1B	353132	NM_178349	15.16
Plate 4	D09	M-003151-02	LCK	3932	NM_001042771	4.08
Plate 9	A11	M-033067-00	LCN9	392399	NM_001001676	5.28
Plate 4	D11	M-011718-01	LGALS1	3956	NM_002305	16.03
Plate 9	F12	M-005615-01	LGR8	122042	NM_130806	4.43
Plate 4	D12	M-031935-01	LIMD1	8994	NM_014240	14.84
Plate 4	E03	M-007730-02	LIMK1	3984	NM_002314	3.46
Plate 4	E04	M-011999-01	LIMS1	3987	NM_004987	9.90
Plate 4	E05	M-018918-01	LIN9	286826	NM_173083	12.05
Plate 4	E07	M-004978-01	LMNA	4000	NM_005572	12.54
Plate 4	E08	M-005270-01	LMNB1	4001	NM_005573	5.45
Plate 7	F05	M-023639-01	LOC126374	126374	NM_001080436	8.04
Plate 8	D10	M-018979-01	LOC134147	134147	NM_138809	6.18
Plate 5	C06	M-025360-01	LOC136242	136242	NM_001008270	9.66
Plate 6	H08	M-007346-00	LOC136306	136306	NM_174959	65.05
Plate 7	F07	M-032755-01	LOC139604	139604	NM_001099921	3.91
Plate 8	F06	M-018737-01	LOC144347	144347	NM_181709	54.57
Plate 10	D08	M-007139-02	LOC146542	146542	NM_001024683	7.57
Plate 10	D12	M-010460-01	LOC146909	146909	NM_001080443	7.06
Plate 4	E09	M-023794-01	LOC147645	147645	XM_085831	8.85
Plate 9	C07	M-031931-00	LOC161247	161247	NM_203402	67.90
Plate 7	D03	M-017807-00	LOC167127	167127	NM_174914	15.49
Plate 9	A07	M-031748-00	LOC284058	284058	NM_015443	12.50
Plate 3	D03	M-024742-01	LOC340152	340152	NM_207360	17.98
Plate 8	F11	M-022374-01	LOC343413	343413	NM_001004310	2.62
Plate 9	C05	M-034898-00	LOC492311	492311	NM_001007189	7.63
Plate 8	B09	M-015521-01	LOC90668	90668	NM_138360	7.35
Plate 8	E09	M-016878-01	LOC91614	91614	NM_001077242	13.49
Plate 7	A11	M-015539-01	LOC92305	92305	NM_138385	12.20
Plate 4	E10	M-008021-00	LOXL3	84695	NM_032603	6.05
Plate 9	B03	M-004721-01	LRP1	4035	NM_002332	9.72
Plate 9	B04	M-027194-01	LRP4	4038	NM_002334	6.93
Plate 4	E11	M-003844-02	LRP5	4041	NM_002335	7.14
Plate 4	E12	M-180353-00	LRTM2	654429	NM_001039029	12.35
Plate 4	F03	M-019866-01	LY86	9450	NM_004271	10.78
Plate 4	F04	M-008388-01	LYPLAL1	127018	NM_138794	14.59
Plate 4	F05	M-010611-01	M6PR	4074	NM_002355	6.91
Plate 4	F06	M-011327-00	MAGOH	4116	NM_002370	8.55
Plate 9	B05	M-009369-01	MAOA	4128	NM_000240	7.29
Plate 4	F10	M-003572-02	MAP2K1IP1	8649	NM_021970	5.79
Plate 4	F07	M-003966-05	MAP2K5	5607	NM_002757	13.86
Plate 4	F08	M-003587-01	MAP4K2	5871	NM_004579	4.46
Plate 9	B06	M-004020-03	MASTL	84930	NM_032844	4.61
Plate 4	F11	M-005659-02	MC3R	4159	NM_019888	20.79
Plate 4	F12	M-005661-00	MC5R	4161	NM_005913	18.18
Plate 4	G03	M-004570-00	MCP	4179	NM_002389	8.92
Plate 7	D06	M-021121-01	MDS032	55850	NM_018467	8.75
Plate 4	G05	M-014896-01	MEGF11	84465	NM_032445	6.82

Plate 4	G07	M-020071-01	MFAP1	4236	NM_005926	24.63
Plate 4	G06	M-012177-01	MFI2	4241	NM_033316	6.18
Plate 4	G09	M-012503-01	MGAT4B	11282	NM_014275	12.82
Plate 1	E11	M-014628-01	MGC10946	80763	NM_030572	9.24
Plate 4	G10	M-014850-00	MGC11061	84272	NM_032312	8.68
Plate 4	G11	M-014974-00	MGC13125	84811	NM_032725	7.00
Plate 4	G12	M-010186-01	MGC15763	92106	NM_138381	14.44
Plate 7	G05	M-015908-00	MGC17986	163071	NM_153608	10.70
Plate 4	H03	M-015142-01	MGC20398	91603	NM_052857	7.74
Plate 10	B10	M-016109-01	MGC20470	143630	NM_145053	8.71
Plate 3	B07	M-018738-01	MGC21688	131408	NM_144635	19.24
Plate 8	C09	M-016181-01	MGC22793	221908	NM_145030	5.42
Plate 9	C12	M-003978-02	MGC24137	143503	NM_152430	3.27
Plate 5	C09	M-017069-00	MGC26647	219557	NM_152706	5.90
Plate 4	H04	M-014261-00	MGC3036	65999	NM_023942	38.26
Plate 8	F07	M-015721-01	MGC33371	143684	NM_144664	5.26
Plate 6	C11	M-014848-01	MGC4189	84268	NM_001033002	36.76
Plate 2	H12	M-014958-00	MGC4266	84766	NM_032680	11.31
Plate 3	B05	M-019315-01	MGC45871	359845	NM_182705	12.42
Plate 4	H05	M-014312-01	MGC4707	79096	NM_001003678	29.82
Plate 8	C07	M-018640-01	MGC52423	149466	NM_182517	8.06
Plate 1	H12	M-005349-02	MGC8407	79012	NM_024046	16.62
Plate 8	C05	M-015087-00	MGC9084	92342	NM_033418	9.24
Plate 1	F09	M-014303-00	MGC955	79078	NM_024097	7.21
Plate 9	B07	M-009403-01	MGLL	11343	NM_001003794	11.73
Plate 4	H06	M-024432-01	MICAL3	57553	NM_015241	9.65
Plate 4	H07	M-019104-02	MKLN1	4289	NM_013255	9.25
Plate 4	H08	M-010580-02	MLL5	55904	NM_018682	4.55
Plate 4	H09	M-005954-01	MMP12	4321	NM_002426	12.12
Plate 4	H10	M-012214-01	MS4A1	931	NM_021950	12.20
Plate 4	H11	M-011732-02	MSN	4478	NM_002444	11.37
Plate 9	B08	M-013953-01	MTBP	27085	NM_022045	4.23
Plate 9	B09	M-004769-01	MYD88	4615	NM_002468	6.51
Plate 5	A03	M-007668-01	MYH9	4627	NM_002473	10.97
Plate 5	A04	M-006355-00	MYO6	4646	NM_004999	6.40
Plate 5	A06	M-015642-00	MYOZ1	58529	NM_021245	9.63
Plate 5	A07	M-014800-00	MYST1	84148	NM_032188	8.98
Plate 9	B10	M-008648-01	NAGS	162417	NM_153006	8.31
Plate 5	A09	M-019107-02	NCOA6	23054	NM_014071	9.51
Plate 5	A10	M-020145-02	NCOR2	9612	NM_001077261	8.56
Plate 9	B11	M-012675-01	NDUFB10	4716	NM_004548	9.27
Plate 5	A11	M-019815-01	NDUFS3	4722	NM_004551	10.10
Plate 5	A12	M-008306-00	NEDD1	121441	NM_152905	24.04
Plate 5	B03	M-007178-02	NEDD4	4734	NM_006154	6.51
Plate 9	B12	M-007187-02	NEDD4L	23327	NM_015277	15.08
Plate 9	C03	M-018345-01	NEGR1	257194	NM_173808	7.69
Plate 5	B05	M-004867-02	NEK3	4752	NM_152720	4.55
Plate 5	B06	M-011092-00	NEU1	4758	NM_000434	7.82
Plate 5	B07	M-016715-00	NEURL	9148	NM_004210	35.90
Plate 5	B08	M-004766-01	NFKBIE	4794	NM_004556	5.21

Plate 5	B09	M-019900-01	NHP2L1	4809	NM_001003796	35.20
Plate 5	B10	M-011489-00	NIPSNAP1	8508	NM_003634	10.51
Plate 5	B11	M-009835-02	NKTR	4820	NM_005385	4.00
Plate 5	C03	M-018267-01	NLRC5	84166	NM_032206	6.23
Plate 9	C04	M-008951-01	NMNAT1	64802	NM_022787	3.83
Plate 5	C04	M-012059-00	NOG	9241	NM_005450	6.05
Plate 1	E06	M-016554-00	NOR1	127700	NM_145047	10.45
Plate 5	C05	M-010194-00	NOX4	50507	NM_016931	3.95
Plate 5	C10	M-015737-01	NPM1	4869	NM_001037738	5.03
Plate 9	C08	M-012347-00	NPM3	10360	NM_006993	8.54
Plate 5	C11	M-003429-00	NR5A1	2516	NM_004959	4.56
Plate 5	C12	M-013871-00	NRIP3	56675	NM_020645	5.69
Plate 5	D03	M-009401-01	NSF	4905	NM_006178	4.06
Plate 5	D09	M-003161-02	NTRK3	4916	NM_002530	6.41
Plate 5	D10	M-011980-00	NUP214	8021	NM_005085	5.84
Plate 5	D11	M-012132-00	NUTF2	10204	NM_005796	11.46
Plate 5	D12	M-024101-01	ODZ3	55714	NM_001080477	6.91
Plate 5	E03	M-005147-03	OGG1	4968	NM_016827	7.07
Plate 9	C09	M-012783-00	OIP5	11339	NM_007280	6.40
Plate 9	C10	M-017475-02	OPRS1	10280	NM_147157	8.18
Plate 6	F06	M-017475-02	OPRS1	10280	NM_147157	19.52
Plate 6	A11	M-023248-01	OR4D1	26689	NM_012374	13.86
Plate 5	E04	M-030003-00	OR51T1	401665	NM_001004759	17.48
Plate 5	E05	M-030022-02	OR52E4	390081	NM_001005165	7.21
Plate 5	E06	M-010528-00	OSM	5008	NM_020530	6.15
Plate 9	D03	M-005690-01	P2RY10	27334	NM_198333	26.51
Plate 1	D11	M-018580-00	P5326	83638	NM_031450	24.18
Plate 5	E07	M-010027-02	PAEP	5047	NM_002571	9.57
Plate 5	E08	M-010330-02	PAFAH1B1	5048	NM_000430	15.29
Plate 9	D04	M-019597-01	PALM	5064	NM_001040134	11.76
Plate 5	E09	M-005130-02	PAPPA	5069	NM_002581	16.72
Plate 5	E12	M-011349-00	PCDH8	5100	NM_002590	9.42
Plate 5	E11	M-032620-01	PCLO	27445	NM_014510	16.15
Plate 9	D05	M-007648-01	PDE4B	5142	NM_001037339	5.08
Plate 5	F03	M-007649-02	PDE4C	5143	NM_001098818	22.70
Plate 9	D09	M-005019-00	PDK1	5163	NM_002610	3.32
Plate 5	F04	M-005020-00	PDK2	5164	NM_002611	25.89
Plate 5	F05	M-013081-01	PDLIM7	9260	NM_213636	8.50
Plate 9	D06	M-003017-02	PDPK1	5170	NM_031268	18.39
Plate 5	F06	M-017120-01	PDXP	57026	NM_020315	3.86
Plate 9	D10	M-014911-00	PDZK4	57595	NM_032512	12.25
Plate 5	F07	M-006545-00	PEX10	5192	NM_002617	5.57
Plate 5	F08	M-012591-02	PEX13	5194	NM_002618	2.99
Plate 5	F09	M-020445-02	PHACTR2	9749	NM_001100166	16.67
Plate 9	D11	M-016904-01	PHPT1	29085	NM_014172	7.59
Plate 5	F10	M-004004-03	PICALM	8301	NM_001008660	16.41
Plate 9	D12	M-006777-03	PIK4CB	5298	NM_002651	10.76
Plate 10	B09	M-003291-03	PIN1	5300	NM_006221	13.88
Plate 10	E03	M-004030-02	PINK1	65018	NM_032409	7.38

Plate 5	F11	M-004904-00	PIP	5304	NM_002652	16.14
Plate 5	F12	M-004535-00	PIP5K2C	79837	NM_024779	9.57
Plate 5	G03	M-006916-00	PJA2	9867	NM_014819	2.62
Plate 5	G04	M-008274-02	PLCB2	5330	NM_004573	4.19
Plate 5	G05	M-004201-01	PLCE1	51196	NM_016341	3.92
Plate 5	G06	M-003945-03	PLEC1	5339	NM_201378	8.17
Plate 5	G07	M-003257-02	PLK3	1263	NM_004073	7.08
Plate 9	E03	M-019593-01	PLRG1	5356	NM_002669	7.02
Plate 5	G08	M-031971-01	PLXNA1	5361	NM_032242	12.27
Plate 5	G09	M-006547-01	PML	5371	NM_033247	10.03
Plate 5	G10	M-011886-00	PNUTL2	5414	NM_004574	6.71
Plate 5	G11	M-012649-00	POLG	5428	NM_002693	8.85
Plate 5	G12	M-016449-00	POP5	51367	NM_015918	8.15
Plate 9	E04	M-019690-01	POU2F2	5452	NM_002698	4.13
Plate 5	H04	M-011500-00	PPAP2C	8612	NM_003712	12.50
Plate 5	H05	M-008907-00	PPIH	10465	NM_006347	12.01
Plate 5	H06	M-016820-00	PPIL5	122769	NM_152329	6.58
Plate 5	H07	M-008679-01	PPM1L	151742	NM_139245	8.81
Plate 5	H03	M-008927-01	PPP1CA	5499	NM_206873	5.97
Plate 5	H08	M-008685-00	PPP1CB	5500	NM_002709	6.83
Plate 5	H09	M-011340-01	PPP1R12A	4659	NM_002480	11.99
Plate 5	H10	M-004824-01	PPP2R2A	5520	NM_002717	5.79
Plate 5	H11	M-003022-02	PPP2R2B	5521	NM_181676	9.55
Plate 9	E05	M-009259-00	PPP5C	5536	NM_006247	6.61
Plate 5	H12	M-009935-01	PPP6C	5537	NM_002721	17.97
Plate 4	B05	M-019491-00	PRC1	9055	NM_003981	**96.22**
Plate 10	D07	M-019491-00	PRC1	9055	NM_003981	**97.14**
Plate 9	E06	M-017949-00	PRG2	5553	NM_002728	35.46
Plate 9	E07	M-023495-01	PRICKLE2	166336	NM_198859	6.31
Plate 9	E08	M-007675-00	PRKAB1	5564	NM_006253	8.74
Plate 7	F03	M-005362-01	PRKWNK1	65125	NM_018979	10.13
Plate 9	E09	M-006017-02	PRTN3	5657	NM_002777	9.69
Plate 6	A06	M-005709-00	PTAFR	5724	NM_000952	4.44
Plate 1	A07	M-008999-02	PTE2B	122970	NM_152331	9.64
Plate 6	A07	M-005712-00	PTGER2	5732	NM_000956	5.60
Plate 6	A08	M-004557-01	PTGS2	5743	NM_000963	6.69
Plate 10	D11	M-008584-00	PTPDC1	138639	NM_152422	8.31
Plate 6	A12	M-019214-00	RAB22A	57403	NM_020673	13.62
Plate 6	B03	M-008828-01	RAB24	53917	NM_130781	6.40
Plate 6	B04	M-008933-02	RAB37	326624	NM_175738	16.77
Plate 6	B05	M-008539-01	RAB4A	5867	NM_004578	10.75
Plate 6	B06	M-010388-00	RAB7	7879	NM_004637	13.68
Plate 6	B07	M-003905-00	RAB8A	4218	NM_005370	5.36
Plate 6	B09	M-007262-01	RABGGTB	5876	NM_004582	9.43
Plate 6	B11	M-007741-01	RAC2	5880	NM_002872	6.98
Plate 9	E10	M-008650-00	RACGAP1	29127	NM_013277	**97.72**
Plate 6	B10	M-008650-00	RACGAP1	29127	NM_013277	**99.69**
		M-008650-00	RACGAP1	29127	NM_013277	**99.69**
Plate 2	H03	M-020543-00	RAMP	51514	NM_016448	7.56

Plate 6	B12	M-007676-01	RAPGEF3	10411	NM_006105	15.17
Plate 9	E11	M-031911-00	RASL11A	387496	NM_206827	11.24
Plate 6	C03	M-017623-02	RBBP9	10741	NM_006606	8.70
Plate 6	C04	M-009065-00	RBM10	8241	NM_005676	12.89
Plate 6	D04	M-009065-00	RBM10	8241	NM_005676	14.29
Plate 2	H10	M-016635-00	RCD-8	23644	NM_014329	21.93
Plate 9	F04	M-017962-01	RCN3	57333	NM_020650	5.69
Plate 9	F05	M-010008-02	RDH10	157506	NM_172037	3.32
Plate 6	C05	M-003629-00	RDH11	51109	NM_016026	12.05
Plate 7	E10	M-014614-00	REC14	80349	NM_025234	8.47
Plate 6	C07	M-013796-00	RGMA	56963	NM_020211	3.95
Plate 9	F06	M-009419-00	RGS11	8786	NM_003834	4.61
Plate 9	F07	M-006027-00	RHBDL1	9028	NM_003961	7.27
Plate 6	C08	M-008340-01	RHOT2	89941	NM_138769	11.25
			RISC NTC			6.56
Plate 9	F09	M-021381-01	RNASE4	6038	NM_194431	4.64
Plate 9	F10	M-006980-00	RNF141	50862	NM_016422	10.87
Plate 6	C09	M-024565-01	RNF215	200312	NM_001017981	9.72
Plate 5	C07	M-021562-03	RP13-15M17.2	199953	NM_001010866	6.65
Plate 6	C10	M-003753-03	RP6-213H19.1	51765	NM_001042452	18.98
Plate 6	A09	M-015749-01	RPA1	6117	NM_002945	23.10
Plate 9	F11	M-004663-02	RPS6KA2	6196	NM_001006932	13.16
Plate 2	C11	M-005294-00	RSN	6249	NM_002956	10.53
Plate 6	D03	M-019212-01	RSU1	6251	NM_152724	7.31
Plate 6	D05	M-006293-01	RYR2	6262	NM_001035	17.39
Plate 6	D06	M-011766-01	S100A10	6281	NM_002966	4.96
Plate 6	D09	M-012191-00	S100A2	6273	NM_005978	6.75
Plate 6	D10	M-013463-03	S100A6	6277	NM_014624	6.81
Plate 6	D12	M-017283-01	SART1	9092	NM_005146	14.78
Plate 8	F03	M-013644-01	SART2	29940	NM_001080976	6.42
Plate 1	C12	M-011772-01	SCA2	6311	NM_002973	5.06
Plate 6	E04	M-012290-00	SCGB1D1	10648	NM_006552	20.40
Plate 6	E05	M-003705-01	SCGB2A2	4250	NM_002411	9.45
Plate 6	E06	M-006296-02	SCN11A	11280	NM_014139	5.51
Plate 9	G03	M-020909-00	SCN1B	6324	NM_001037	12.66
Plate 9	G04	M-006500-03	SCN5A	6331	NM_001099405	10.66
Plate 6	E07	M-005373-01	SCYL1	57410	NM_001048218	6.33
Plate 6	E08	M-018964-01	SDK1	221935	NM_001079653	7.64
Plate 6	E09	M-017396-00	SDK2	54549	NM_019064	61.22
Plate 9	G05	M-009582-00	SEC23A	10484	NM_006364	11.46
Plate 6	E10	M-009592-01	SEC23B	10483	NM_032986	7.26
Plate 6	E11	M-014166-00	SEC31L1	22872	NM_014933	2.87
Plate 3	A12	M-013312-01	SEC3L1	55763	NM_178237	11.33
Plate 3	B03	M-019010-01	SEC6L1	11336	NM_007277	4.15
Plate 6	E12	M-007289-02	SEMA4B	10509	NM_198925	13.74
Plate 9	G06	M-012062-01	SEPP1	6414	NM_005410	5.99
Plate 9	G07	M-007724-01	SH2D4A	63898	NM_022071	9.48
Plate 6	F04	M-015810-02	SH3GLB2	56904	NM_020145	8.19

			SI NTC			7.71
Plate 9	G08	M-015154-00	SIGLEC11	114132	NM_052884	5.44
Plate 1	H08	M-012521-01	SIP	27101	NM_001007214	3.32
Plate 9	G09	M-017524-00	SIPA1	6494	NM_006747	9.09
Plate 6	A04	M-015817-02	SKB1	10419	NM_006109	8.72
Plate 8	D09	M-017179-00	SKD3	81570	NM_030813	5.96
Plate 6	F07	M-019583-01	SLAMF1	6504	NM_003037	4.58
Plate 9	G10	M-007446-01	SLC22A12	116085	NM_144585	5.97
Plate 9	G11	M-007486-03	SLC25A5	292	NM_001152	5.44
Plate 6	F08	M-007529-01	SLC30A8	169026	NM_173851	4.73
Plate 9	G12	M-010705-01	SLC35D2	11046	NM_007001	6.75
Plate 9	H03	M-007557-01	SLC37A4	2542	NM_001467	9.69
Plate 9	H04	M-007590-02	SLC5A2	6524	NM_003041	4.90
Plate 6	F09	M-007591-01	SLC5A3	6526	NM_006933	6.71
Plate 6	F10	M-007435-00	SLCO4A1	28231	NM_016354	20.74
Plate 6	F11	M-003850-02	SLK	9748	NM_014720	9.20
Plate 9	H05	M-006836-01	SMC2L1	10592	NM_006444	3.96
Plate 6	F12	M-017440-00	SMTN	6525	NM_006932	8.71
Plate 6	G03	M-021129-01	SMU1	55234	NM_018225	33.55
Plate 6	F05	M-017521-01	SN	6614	NM_023068	12.06
Plate 6	G04	M-010056-01	SNFT	55509	NM_018664	46.69
Plate 6	G05	M-016821-00	SNRPG	6637	NM_003096	50.89
Plate 6	G06	M-011520-00	SNX4	8723	NM_003794	3.93
Plate 6	G08	M-012983-01	SON	6651	NM_032195	49.22
Plate 9	H06	M-016807-00	SPAG4L	140732	NM_080675	13.29
Plate 9	H07	M-031850-01	SPATC1	375686	NM_198572	6.56
Plate 6	G07	M-020897-02	SPCS2	9789	NM_014752	3.44
Plate 9	H08	M-012558-01	SPP1	6696	NM_000582	5.53
Plate 6	G09	M-015457-00	SPRY4	81848	NM_030964	19.94
Plate 9	H09	M-017767-01	SRP14	6727	NM_003134	8.68
Plate 10	A11	M-006563-02	SSA1	6737	NM_003141	6.46
Plate 6	G11	M-003712-02	ST14	6768	NM_021978	7.98
Plate 9	H10	M-008402-01	ST6GAL2	84620	NM_032528	2.08
Plate 6	G12	M-011894-01	STAU	6780	NM_017454	25.49
Plate 6	H03	M-005383-02	STK33	65975	NM_030906	22.36
Plate 6	H04	M-004875-02	STK39	27347	NM_013233	11.52
Plate 6	H05	M-019572-02	STRN	6801	NM_003162	20.47
Plate 6	H06	M-009602-02	STS	412	NM_000351	6.64
Plate 6	H07	M-012655-02	SYP	6855	NM_003179	11.61
Plate 9	H11	M-019166-01	SYT8	90019	NM_138567	7.37
Plate 6	H09	M-005736-01	TAAR1	134864	NM_138327	37.38
Plate 6	H10	M-005739-01	TAS1R2	80834	NM_152232	24.72
Plate 9	H12	M-014409-00	TBC1D17	79735	NM_024682	9.01
Plate 6	H11	M-012152-00	TBL1X	6907	NM_005647	10.83
Plate 6	H12	M-003780-02	TDG	6996	NM_003211	3.75
Plate 7	A03	M-008506-00	TDO2	6999	NM_005651	3.88
Plate 7	A06	M-019966-01	TFIP11	24144	NM_012143	6.37
Plate 7	A07	M-003929-02	TGFBR1	7046	NM_004612	7.58
Plate 7	A08	M-017078-00	THEG	51298	NM_016585	20.96
Plate 7	A04	M-019488-01	TIMELESS	8914	NM_003920	4.58

Plate 10	A04	M-013948-03	TIPARP	25976	NM_015508	13.64
Plate 1	A03	M-009932-02	TJP2	9414	NM_201629	4.08
Plate 7	A09	M-009932-02	TJP2	9414	NM_201629	6.69
Plate 7	A10	M-008086-01	TLR1	7096	NM_003263	15.97
Plate 10	A05	M-005120-03	TLR2	7097	NM_003264	7.34
Plate 10	A09	M-021501-00	TLT4	285852	NM_198153	18.11
Plate 7	B03	M-009919-00	TNFAIP3	7128	NM_006290	7.35
Plate 10	A07	M-014328-00	TNIP2	79155	NM_024309	8.31
Plate 7	B04	M-004740-01	TNKS	8658	NM_003747	5.88
Plate 10	A08	M-015315-00	TNP2	7142	NM_005425	20.30
Plate 7	B05	M-011308-01	TNPO1	3842	NM_153188	7.42
Plate 7	B06	M-015878-01	TOMM22	56993	NM_020243	6.38
Plate 7	B09	M-014203-00	TOR1B	27348	NM_014506	5.73
Plate 7	B10	M-007093-01	TRIM63	84676	NM_032588	13.35
Plate 10	A12	M-006109-01	TRPA1	8989	NM_007332	5.96
Plate 10	B03	M-006509-01	TRPC3	7222	NM_003305	4.53
Plate 7	B12	M-006518-03	TRPV1	7442	NM_018727	9.73
Plate 7	C03	M-013879-00	TRUB2	26995	NM_015679	2.43
Plate 7	C04	M-009055-01	TSP50	29122	NM_013270	2.80
Plate 10	B04	M-028592-01	TSPYL1	7259	NM_003309	26.44
Plate 1	G06	M-014389-02	TTMP	79669	NM_024616	2.39
Plate 7	C06	M-010685-02	TTYH2	94015	NM_052869	5.10
Plate 10	B05	M-025280-01	TTYH3	80727	NM_025250	15.84
Plate 7	C07	M-008779-01	TUBA1	7277	NM_006000	35.24
Plate 7	C08	M-008265-01	TUBB2	10383	NM_006088	17.28
Plate 7	C09	M-006791-01	TXNDC3	51314	NM_016616	10.56
Plate 7	C10	M-008361-00	TXNL4	10907	NM_006701	6.73
Plate 10	B06	M-004348-01	UBE2M	9040	NM_003969	9.15
Plate 7	C11	M-013566-00	UBQLN2	29978	NM_013444	3.87
Plate 10	B11	M-004062-01	UCK1	83549	NM_031432	6.60
Plate 10	B12	M-011418-02	UCN	7349	NM_003353	6.11
Plate 7	C12	M-007638-01	UCP3	7352	NM_022803	8.43
Plate 7	D04	M-018039-00	UNC93A	54346	NM_018974	7.08
Plate 7	D05	M-027236-01	UNQ3033	284415	NM_198481	5.87
Plate 8	B08	M-032544-00	UNQ3112	399967	NM_212555	10.14
Plate 7	A05	M-027221-01	UNQ9391	203074	NM_198464	5.61
Plate 10	C03	M-006061-02	USP1	7398	NM_001017416	5.52
Plate 7	D09	M-006077-01	USP29	57663	NM_020903	8.50
Plate 7	D10	M-021294-03	USP30	84749	NM_032663	4.58
Plate 10	C04	M-021192-00	USP52	9924	NM_014871	18.50
Plate 10	C06	M-012326-02	UTS2	10911	NM_006786	12.43
Plate 10	C07	M-012497-00	VAMP1	6843	NM_014231	7.87
Plate 7	D12	M-021382-01	VAPA	9218	NM_194434	6.60
Plate 7	E03	M-009288-01	VCL	7414	NM_003373	4.98
Plate 7	E04	M-013581-01	VCX	26609	NM_013452	9.47
Plate 7	E05	M-010894-00	VPS35	55737	NM_018206	3.35
Plate 7	E06	M-004683-02	VRK1	7443	NM_003384	4.76
Plate 7	E07	M-004684-02	VRK2	7444	NM_006296	8.10
Plate 7	E08	M-016716-01	VTI1A	143187	NM_145206	8.78

Plate 5	D05	M-013551-01	WBSCR20C	260294	NM_001039487	14.43
Plate 7	E09	M-013375-00	WDR5B	54554	NM_019069	9.43
Plate 7	E12	M-010564-02	WFDC2	10406	NM_006103	7.91
Plate 7	F04	M-005031-02	WNK4	65266	NM_032387	7.19
Plate 10	C10	M-008659-03	WNT4	54361	NM_030761	5.93
Plate 2	H09	M-008044-01	XEDAR	60401	NM_021783	6.96
Plate 7	F08	M-003030-02	XPO1	7514	NM_003400	11.86
Plate 7	F11	M-021226-01	ZBED4	9889	NM_014838	10.84
Plate 10	C11	M-014903-00	ZC3HDC8	84524	NM_032494	9.32
Plate 7	H04	M-021470-01	ZFP29	54993	NM_001007072	7.35
Plate 7	G03	M-017752-01	ZFP42	132625	NM_174900	7.40
Plate 7	G04	M-017676-01	ZHX2	22882	NM_014943	3.28
Plate 7	G06	M-021350-00	ZNF189	7743	NM_003452	8.86
Plate 5	A08	M-006578-02	ZNF42	7593	NM_003422	12.13
Plate 7	G07	M-025188-01	ZNF479	90827	NM_033273	8.04
Plate 7	H05	M-014327-00	ZNF495	79149	NM_024303	3.87
Plate 10	D04	M-018086-00	ZNF511	118472	NM_145806	5.97
Plate 7	G08	M-016106-00	ZNF549	256051	NM_153263	2.13
Plate 10	D05	M-015888-00	ZNF561	93134	NM_152289	3.69
Plate 7	G09	M-017929-00	ZNF575	284346	NM_174945	5.61
Plate 7	G10	M-016640-01	ZNF579	163033	NM_152600	11.27
Plate 7	H03	M-019562-01	ZNF85	7639	NM_003429	4.52

Genes that are known to be part of the spliceosome assembly and pre-mRNA splicing pathway and whose depletion leads to mitotic defects were identified through the MitoCheck database (See section 5.1) and chromosome spread analysis was carried out in HeLa cells depleted of these genes using the SMARTpool siRNAs as listed below. Positive and negative controls used in the chromosome spread analysis are shaded in grey.

No.	Well	Pool Catalog Number	Gene Symbol	GENE ID	Gene Accession
1	A01	M-019085-00	SNRPD3	6634	NM_004175
2	A02	M-019575-01	SNRPF	6636	NM_003095
3	A03	M-018672-01	SFRS1	6426	NM_006924
4	A04	M-012380-01	U2AF2	11338	NM_001012478
5	A05	M-012325-01	U2AF1	7307	NM_001025203
6	A06	M-020061-02	SF3B1	23451	NM_001005526
7	A07	M-016051-01	SF3A1	10291	NM_001005409
8	A08	M-012252-02	PRPF8	10594	NM_006445
9	A09	M-014161-00	SNRNP200	23020	NM_014014
10	A10	M-019851-00	EFTUD2	9343	NM_004247
11	A11	M-012821-01	PRPF6	24148	NM_012469
12	A12	M-019900-01	NHP2L1	4809	NM_001003796
13	B01	M-017283-01	SART1	9092	NM_005146
14	B02	M-013447-01	SART3	9733	NM_014706
15	B03	M-020071-01	MFAP1	4236	NM_005926

16	B04	M-011237-00	CDC5L	988	NM_001253
17	B05	M-019593-01	PLRG1	5356	NM_002669
18	B06	M-004668-02	PRPF19	27339	NM_014502
19	B07	M-012708-00	BCAS2	10286	NM_005872
20	B08	M-017535-00	CTNNBL1	56259	NM_030877
21	B09	M-012446-00	SNW1	22938	NM_012245
22	B10	M-018665-00	BUD31	8896	NM_003910
23	B11	M-004914-01	XAB2	56949	NM_020196
24	B12	M-017191-01	SLU7	10569	NM_006425
25	C01	M-013213-00	CDC40	51362	NM_015891
26	C02	M-021129-01	SMU1	55234	NM_018225
27	C03	M-012190-01	IK	3550	NM_006083
28	C04	M-015475-01	SGOL1	151648	NM_001012413
29	C05	M-003271-01	MAD2L1	4085	NM_002358
30	C06	M-006832-01	RAD21	5885	NM_006265
31	C07	M-006833-00	SMC1A	8243	NM_006306
32	C08	M-017813-00	LSM2	57819	NM_021177
33	C09	M-017025-00	LSM4	25804	NM_012321
34	C10	M-011327-00	MAGOH	4116	NM_002370
35	C11	M-011965-00	RBM39	9584	NM_004902
36	C12	M-022214-01	AQR	9716	NM_014691
37	D01	M-014879-01	THOC3	84321	NM_032361